MEDICAL LIBRARY

APR 5 '49

JOURNAL OF THE NATIONAL CANCER INSTITUTE

CONTENTS

DISTRIBUTION STUDIES IN MICE FOLLOWING THE INTRAVENOUS INJECTION OF DIETHYL β-IODOETHYL AMINE HYDROCHLORIDE PREPARED WITH RADIOACTIVE IODINE. *Arnold M. Seligman, Alexander M. Rutenburg,* and *Orrie M. Friedman*..... 261

FIBROIDS IN A GUINEA PIG (FAMILY 13) AFTER PARTIAL CASTRATION. *E. M. Nadel*..... 271

MASCULINIZING OVARIAN TUMOR OF ADRENAL TYPE. *Edward J. Mortell.* 277

SOME OBSERVATIONS ON THE NORMAL AND PATHOLOGIC ANATOMY OF THE KIDNEY OF THE MOUSE. *Thelma B. Dunn*..... 285

ALDOLASE IN THE SERUM AND TISSUES OF TUMOR-BEARING ANIMALS. *John A. Sibley* and *Albert L. Lehninger*..... 303

CYTOLOGICAL STUDIES ON THE NATURE OF THE CYTOPLASMIC PARTICULATES IN THE CLOUDMAN S91 MOUSE MELANOMA, THE DERIVED ALGIRE S91A PARTIALLY AMELANOTIC MELANOMA, AND THE HARDING-PASSEY MOUSE MELANOMA. *M. W. Woods, H. G. duBuy, Dean Burk,* and *Marie L. Hesselbach*..... 311

Contents continued on page 2

VOLUME 9 February 1949 NUMBER 4

FEDERAL SECURITY AGENCY
Public Health Service

CONTENTS—Continued

ENZYMATIC ACTIVITIES OF ISOLATED AMELANOTIC AND MELANOTIC GRANULES OF MOUSE MELANOMAS AND A SUGGESTED RELATIONSHIP TO MITOCHONDRIA. *H. G. duBuy, M. W. Woods, Dean Burk,* and *Mary D. Lackey* 325

PHYSICOCHEMICAL STUDIES OF REVERSIBLE AND IRREVERSIBLE COMPLEXES OF COBALT, HISTIDINE, AND MOLECULAR OXYGEN. *John Z. Hearon, Dean Burk,* and *Arthur L. Schade* 337

FEDERAL SECURITY AGENCY Public Health Service

JOURNAL OF THE NATIONAL CANCER INSTITUTE

VOLUME 9 FEBRUARY 1949 NUMBER 4

DISTRIBUTION STUDIES IN MICE FOLLOWING THE INTRAVENOUS INJECTION OF DIETHYL β-IODOETHYL AMINE HYDROCHLORIDE PREPARED WITH RADIOACTIVE IODINE [1] [2]

By ARNOLD M. SELIGMAN, *assistant professor of surgery*, ALEXANDER M. RUTENBURG, *assistant resident in surgery*, and ORRIE M. FRIEDMAN, *research fellow in chemistry, Kirstein Laboratory for Surgical Research, Beth Israel Hospital, Boston, the Department of Surgery, Harvard Medical School, and the Chemical Laboratory, Harvard University*

INTRODUCTION

The nitrogen mustards (β-chloroethyl amines) have been shown to serve as valuable therapeutic adjuncts in the palliation of Hodgkin's disease, chronic leukemia, malignant lymphoma, and anaplastic bronchogenic carcinoma (*1–5*). Because of the pronounced chemical reactivity of the mustards, it may be questioned whether the β-chloroethyl amines reach neoplastic tissue as such, or whether a reaction product of the mustard with some constituent of the blood is responsible for the cytotoxic effects observed following injection.

In the view now generally held, the first step in the reaction of the mustards is cyclization to ethylene immonium compounds and loss of halogen in ionic form (*6–9*). The positively charged cyclic immonium ion then reacts rapidly with a wide variety of inorganic and organic substances that may be present (*6*, *10*, *11*). A clue to the behavior of the mustards in vivo would be provided by a comparison of the distribution after intravenous injection of a mustard, which contains radioactive halogen in the β-ethyl position, with the distribution of radioactive ionic halide. If the distribution of radioactivity in the tissues, rate of its disappearance from the blood, and rate of appearance in the urine were the same following the injection of mustard which contains radioactive halogen as that following the injection of radioactive halide ion, one could assume that the first step of the reaction of mustard, which results in loss of halogen, had occurred promptly and completely. Retention of radioactivity in any tissue for longer periods than those observed after injection of radioactive halogen and prolonged rate of excretion of radioactive halogen would indicate that some halogen-containing mustard (and therefore uncyclized mustard) had reached the tissues intact through the circulation.

For this study, it was considered preferable to select a simple nitrogen mustard, i. e., one containing a single β-iodoethyl group. This compound was prepared by replacement of chlorine in the corresponding chloroethyl amine with radioactive iodine by treatment of the base in anhydrous acetone with radioactive sodium iodide. The amine was then precipitated from benzene as the hydrochloride salt.

The preparation of radioactive diethyl β-iodoethyl amine hydrochloride and the comparison of the distribution of radioactivity in the tissues of normal and tumor-bearing mice following injection of this mustard, with the distribution of radioactivity following injection of radioactive sodium iodide, form the basis of this report.

[1] Received for publication July 17, 1948.

[2] This investigation was supported by a research grant from the National Cancer Institute of the National Institutes of Health, Public Health Service, Federal Security Agency.

819164—49——1

EXPERIMENTAL PROCEDURE

Diethyl β-Radioiodoethyl Amine Hydrochloride ($I^{131}NM$)

Diethyl β-chloroethyl amine hydrochloride was prepared according to Gough and King (*12*) from diethyl β-hydroxy ethyl amine (24 gm.) and thionyl chloride (48 gm.) in chloroform (240 cc.), and crystallized from alcohol-ether; melting point 203°–205°. A cold aqueous solution of this amine hydrochloride (22 gm.) was treated with 3.4 gm. of sodium hydroxide. The free base was quickly extracted with 100 cc. of ether in three portions, and the combined extracts were dried over anhydrous sodium sulfate and stored in the cold. This stock solution was used in subsequent preparations.

An aliquot (43 mg. in 0.65 cc.) was warmed on the steam bath to remove the ether. The oil that remained was dissolved in 5 cc. of reagent acetone, and a solution of 50 mg. of radioactive sodium iodide [3] in 5 cc. of acetone was added. The mixture was warmed on the steam bath for 8 minutes, when the precipitation of sodium chloride was complete and practically all the acetone had evaporated.

Dry benzene (10 cc.) was added to precipitate any excess sodium iodide, and the reaction mixture was filtered. Hydrogen chloride was bubbled into the filtrate for 3 minutes. The amine hydrochloride precipitated after the solution was concentrated by heating on the steam bath and was obtained as fine white crystals, melting point 166°–167°. The yield was 60 mg. (70 percent based on sodium iodide). A sample of nonradioactive product prepared for analysis by repeated crystallization from alcohol-benzene was obtained as fine white needles, melting point 173°–174°. Analysis: Calculated for $C_6H_{15}NICl$: C,27.32; H,5.73; found: C,27.05; H,5.90.

[3] This was prepared by dissolving 50 mg. of sodium iodide in an aqueous solution containing 1 millicurie of carrier-free I^{131} as the sodium salt and evaporating at 37° C. to dryness. Carrier-free I^{131} was obtained from the chain-reacting pile at Oak Ridge, Tenn.

Acute Toxicity [4]

The acute toxicity of diethyl β-iodoethyl amine hydrochloride (INM) upon intraperitoneal injection in mice was compared with that of diethyl β-chloroethyl amine hydrochloride and with the more toxic methyl-bis(β-chloroethyl) amine hydrochloride, the nitrogen mustard which is used clinically (table 1). The amine hydrochlorides were dissolved in saline immediately before injection and given in a volume of 0.1 cc. to stock albino mice weighing about 25 gm. All deaths within 10 days were considered acute. On a molecular basis methyl-bis(β-chloroethyl) amine hydrochloride appears to be about 30–40 times more toxic than INM. However, INM is about twice as toxic as its chloro analog on a molecular basis and roughly the same on a weight basis.

The toxicity of INM was doubled upon intravenous injection in mice (table 2). The injection in 0.25-cc. volume required 6–8 seconds.

[4] With the technical assistance of Myron Milden.

Table 1.—*Comparison of the toxicity of 3 nitrogen mustards following intraperitoneal injection in mice*

Formula	Molecular weight	Dose per 20-gm. mouse		Number of mice used	Number of deaths for each day after injection										Average weight loss	Mortality within 10 days
					1	2	3	4	5	6	7	8	9	10		
		Mg.	*Moles × 10⁻⁶*												*Grams*	*Percent*
Diethyl β-iodoethyl amine hydrochloride.	263	2.0	7.6	16	0	0	0	0	1	0	0	0	0	0	3	
		2.3	8.9	6	1	1	0	0	0	0	0	0	0	0	0	
		2.4	9.0	6	0	1	0	0	0	0	2	0	0	0	6	
		3.0	11.0	6	2	0	1	0	0	0	0	0	0	0		
		3.2	12.0	6	2	1	1	0	0	0	0	0	0	0		
Diethyl β-chloroethyl amine hydrochloride.	171	1.5	8.9	6	0	0	0	0	0	0	0	0	0	0	2	
		1.8	11.0	6	0	0	1	0	0	0	0	0	0	0	7	
		2.4	14.0	6	0	1	0	0	0	0	1	0	0	0	2	
		2.9	17.0	6	3	0	1	0	1	1						
		3.2	19.0	6	5	0	0	0	0	1						
Methyl-bis(β-chloroethyl) amine hydrochloride.	191	.034	.18	6	0	0	0	0	0	0	0	0	0	0	4	
		.062	.32	10	0	0	0	1	0	1	1	0	0	0		
		.064	.33	5	0	0	0	0	0	0	0	2	0	0		
		.075	.39	11	0	0	0	0	0	0	1	1	2	0	3	
		.080	.42	6	0	0	0	0	1	0	0	0	0	0	6	
		.11	.56	6	0	0	0	0	0	1	2	2	0	0		
		.21	1.1	6	0	1	1	2	0	0	2					
		.33	1.7	6	0	1	1	3	0	0	1					

TABLE 2.—*Toxicity of diethyl β-iodoethyl amine hydrochloride following intravenous injection in mice*

Number of mice	Dose per 20-gm. mouse		Mortality within 10 days
	Milligrams	*Moles × 10⁻⁶*	*Percent*
10	0.8	3.0	0
10	1.6	6.1	0
10	2.4	9.1	100
10	3.2	12.0	100

PREPARATION OF MATERIAL FOR INJECTION

Both radioactive $I^{131}NM$ and NaI^{131} were dissolved in 0.85-percent saline, and each dose was given intravenously via a tail vein in a volume of 0.25 cc. Each injection took about 5 seconds, and for each experiment all injections were completed within 10 minutes after preparation of the solution. The dose of $I^{131}NM$ was 1.0 mg. (4 mg./cubic centimeter), and the pH of the solution was found to be 4.6. Ten minutes later the pH was unchanged, but after 3 hours the pH was 4.2. In the control experiments with NaI^{131}, an equivalent amount of iodine was given, i.e., 0.48 mg. of iodine or 0.57 mg. of NaI with an estimated activity of about 15 microcuries.[5]

PREPARATION OF TISSUES FOR RADIOACTIVITY MEASUREMENT (*13*)

Both normal stock albino mice (20–25 gm.) and Swiss mice (18–23 gm.) with 6-day-old sarcoma 37 growing in the subcutaneous space of the flank were used.

At fixed intervals following injection of the radioactive material, the mice were killed by decapitation, arterial blood was collected in a tube containing dry heparin, and 0.25 cc. of the blood was transferred with a tuberculin syringe and needle to an aluminum cup for radioactivity measurement.

Following exanguination, aliquots of organs and tissues were removed in thin slices, wiped dry of all excess blood, and rapidly weighed with a torsion balance. This procedure in exsanguinated animals reduced the blood content of each tissue to a minimum (*14*, *15*). Whenever possible 200 mg. of each tissue was taken. When the weight of an organ was less than 200 mg., it was taken in toto and the radioactivity expressed on a 200-mg.-weight basis. In the case of thyroid gland, which averaged 4–6 mg., and two–three mesenteric lymph nodes which weighed about 6 mg., the radioactivity was not calculated for 200 mg. of tissue.

In one experiment, blood was obtained from three mice each at three time intervals after injection of $I^{131}NM$, and the pooled blood specimens were immediately separated into cells and plasma by centrifugation. The hematocrit was determined, and radioactivity measurements were made on 0.25 cc. each of whole blood, unwashed blood cells, and plasma.

The tissues were placed in aluminum cups (1.2 cm. in diameter) and evaporated for 48 hours at 37° C. to dryness. The dry weight of 200 mg. of wet tissues (blood 0.25 cc.) of each of nine mice is given in table 3. Although the dry weights of the various tissues were not constant and therefore introduced error in radioactivity measurement due to differences in self-absorption of beta rays, the dry weight of the same tissue in different mice was remarkably uniform. Corrections in radioactivity for variations in dry weight, therefore, were not made, since the dry weight of any given tissue obtained wet varied little from mouse to mouse and gave sufficient accuracy in comparing the changes in radioactivity of any given tissue with time.

TABLE 3.—*Dry weights of 200 mg. of wet tissues of each of 9 mice*

Liver	Blood [1]	Kidney	Muscle	Lungs	Intestine	Spleen	Tumor
Mg.	*Mg.*	*Mg.*	*Mg.*	*Mg.*	*Mg.*	*Mg.*	*Mg.*
64	62	54	51	45	45	46	37
65	58	53	52	49	52	48	35
66	60	54	50	49	45	45	41
66	65	53	52	44	48	45	42
65	68	51	50	45	50	47	38
67	60	51	54	52	52	46	39
64	62	52	53	48	43	47	38
64	62	54	53	48	47	42	36
66	62	53	52	46	46	46	36
[2] 65	[2] 62	[2] 53	[2] 52	[2] 47	[2] 48	[2] 46	[2] 38

[1] Measured as 0.25 cc.
[2] Average weight.

Urine samples were collected at intervals in some of the experiments (0.1–0.5 cc.), and in separate experiments urine was collected for 24 hours by ligature obstruction of the penile urethra of male mice (0.8–1.2 cc.). Several mice were used for each experiment because ligatures caused slough or were removed by some of the mice. These mice with urinary obstruction were not used for any other determinations. The urine was removed from the bladder through the opened

[5] NaI^{131} solution was prepared by dissolving 11.4 mg. of sodium iodide in 4.5 cc. of saline, and 300 microcuries of the sodium salt of carrier-free I^{131} in 0.5 cc. of water was added.

peritoneal cavity with a tuberculin syringe and transferred directly to aluminum cups for evaporation.

Standards were prepared by two hundredfold to four hundredfold dilution with saline of 0.25 cc. of the solution used for injection. A 0.25-cc. portion of this solution was evaporated with 0.25 cc. of normal mouse blood in order to approximate the dry weight of the other samples. Separate standards were prepared with normal mouse urine for measurement of radioactivity of urine.

Radioactivity measurements were made on a Tracerlab autoscaler with a Victoreen-Geiger tube (bell type with end mica window weighing 4 mg. per square centimeter). The tube and samples were shielded with 1.5 inches of lead. All specimens were at least 20 times background.

Calculations

All radioactivity measurements were calculated for 200 mg. of tissue in a 23-gm. mouse. In the case of blood, although 0.25 cc. was actually measured in order to conform more closely to the dry weight of other tissues, the activity was calculated for 0.20 cc. In proportioning the tissue radioactivity to a standard mouse weighing 23 gm., it was assumed that the radioactivity per unit weight of tissue would be inversely proportional to the weight of the animal following injection of a constant quantity of radioactive substance.

Assuming the blood volume of each mouse to be 10 percent of the body weight, the radioactivity of the blood and tissue samples was calculated in percent of the activity of 0.2 cc. of blood circulating at zero time, from the following equation:

$$\text{Radioactivity of tissue sample in percent of activity of blood at zero time} = \frac{\text{Radioactivity of sample} \times \text{circulating blood volume (2.3 cc.)} \times 100}{\text{Radioactivity of standard} \times \text{dilution factor} \times \text{volume of blood sample (0.2 cc.)}} = \frac{\text{Radioactivity of sample} \times 1{,}150}{\text{Radioactivity of standard} \times \text{dilution factor}} \quad (1)$$

The activities of thyroid gland and of mesenteric lymph nodes were calculated as radioactivity of the total organ (less than 200 mg.) in terms of percent of radioactivity of 0.2 cc. of blood circulating at zero time, from the same equation. The radioactivity of urine was expressed in percent of the total radioactivity which was injected per mouse.

RESULTS

Distribution of Radioactivity in Mouse Tissues Following Injection of $I^{131}NM$ and NaI^{131}

The data for two experiments with each radioactive substance in normal and tumor-bearing mice are presented in table 4 and figures 1–5.

In both normal and tumor-bearing mice, the disappearance of radioactivity from the circulating blood was rapid in the first 2 hours following injection of both $I^{131}NM$ and NaI^{131}. In 15 minutes, the level of radioactivity was 15–20 percent, and in 2 hours less than 5 percent of the activity at zero time. After 4 hours, the blood levels of radioactivity for $I^{131}NM$ and NaI^{131} differed. In the mice which received NaI^{131} there was almost complete disappearance of circulating radioactivity from the fourth to the eighth hours, while in mice which received $I^{131}NM$, circulating radioactivity at the fourth hour was 3 percent and at the eighth hour 1–3 percent of that at zero time (fig. 1). By the sixteenth hour (shown only in table 4), the mice which received $I^{131}NM$ still had 0.2–0.3 percent of the activity at zero time.

Partition of radioactivity between blood cells and plasma was determined for pooled samples of blood taken at 4.7, 8.5, and 10 hours after injection of $I^{131}NM$ (table 5). This was not done in the case of mice injected with NaI^{131} because too little radioactivity persisted in the blood at these time intervals. The high cellular content of radioactivity is consistent with the hypothesis that uncyclized mustard gained entrance to the cells. The blood cell activities given are too low and the plasma activities too high because of differences in dry weight of 0.25 cc. of each as compared with whole blood. The blood cell activities as measured may have been 3–8 percent too high because the cells were not washed.

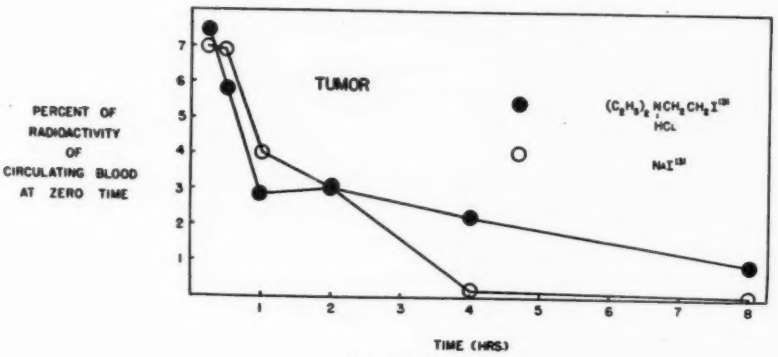

FIGURE 1.

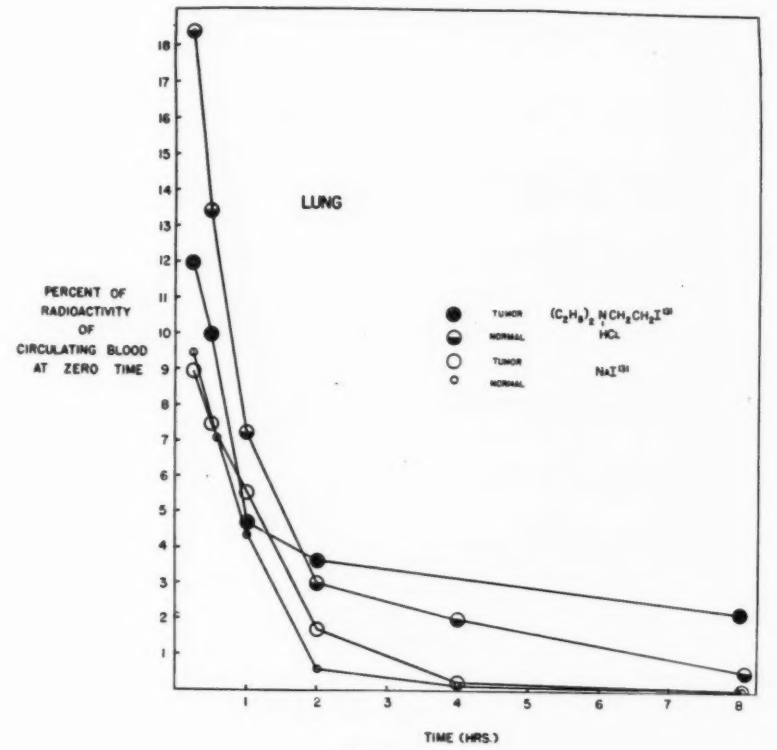

FIGURE 2.

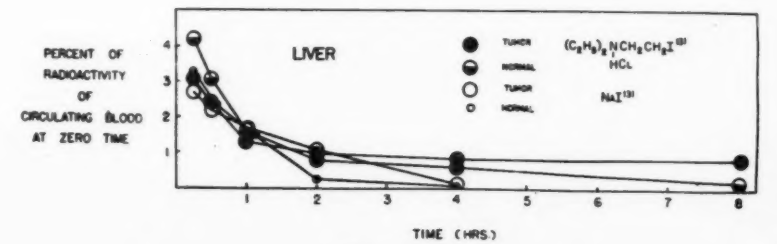

FIGURE 3.

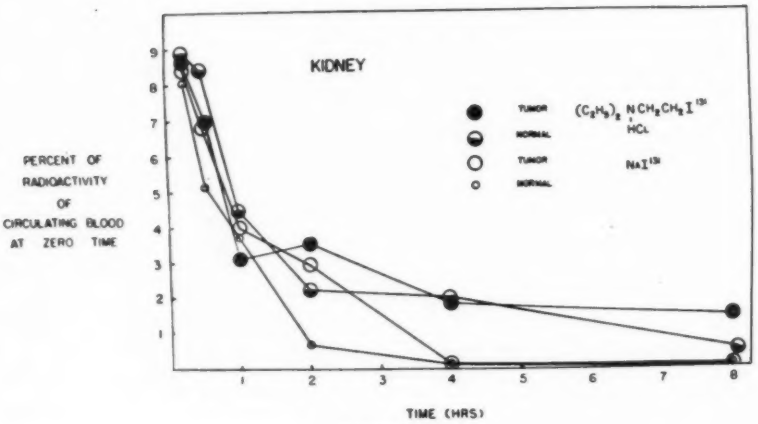

FIGURE 4.

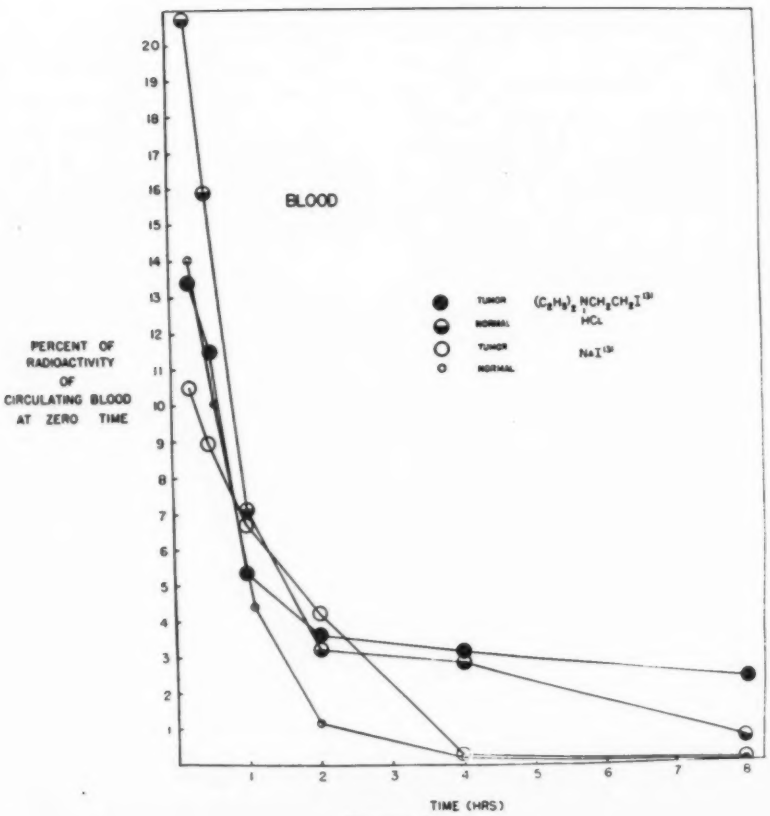

FIGURE 5.

TABLE 4.—*Radioactivity of 200 mg. of blood and tissues of each of 2 groups of 9 normal mice and 9 Swiss mice with sarcoma 37, expressed in percent of the radioactivity of blood at zero time, measured at intervals after injection of $I^{131}NM$ and NaI^{131}*

NORMAL MICE

	$I^{131}NM$									NaI^{131}								
	Time in hours									Time in hours								
	0.25	0.5	1	2	4	8.1	17.5	24	49	0.25	0.58	1	2	4	8	16	24	48
Blood	20.8	15.9	7.1	3.2	2.7	0.7	0.3	0.3	0.1	14.0	10.0	4.4	1.1	0.2	0.02	0.01	0	0
Lung	18.4	13.4	7.2	3.0	2.0	.5	.2	.2	.08	9.4	7.1	4.3	.6	.2	.02	.02	.01	0
Liver	4.2	3.1	1.6	.8	.6	.1	.2	.1	.06	3.3	2.3	1.5	.3	.04	.02	.01	0	0
Kidney	8.9	8.4	4.4	2.2	2.0	.4	.2	.1	.07	8.1	5.2	1.9	.4	.05	.01	.01	0	0
Spleen	5.9	5.3	2.9	1.4	1.0	.3	.4	.1	.04	4.3	3.1	1.9	.4	.05	.01	.01	0	0
Muscle	2.0	1.6	.9	.5	.3	.1	.03	.03	.1	1.8	.9	.6	.2	.02	0	.01	0	0
Intestine	4.8	4.4	2.3	1.7	.7	.2	.1	.08	.1	4.3	2.9	4.6	.3	.1	.02	.01	0	0
Thyroid [1]	.2	.9	1.1	.04	.04	.05	0	0	0	.5	.1	.1	.1	0	0	0	0	0
Mesenteric lymph nodes [1]	.9	.6	.2	.2	.2	.2	0	.05	0	.5	.3	.2	.03	0	0	0	0	0

SWISS MICE WITH SARCOMA 37

	0.25	0.55	1	2	4	8	15.5	24	49	0.25	0.50	1	2	4	8	16	24	48
Blood	13.4	11.5	5.3	3.6	3.1	2.4	0.2	0.2	0	10.5	8.9	6.7	4.2	0.3	0.1	0.04	0.03	0
Lung	11.9	9.9	4.7	3.6	.....	2.2	.2	.2	0	8.9	7.4	5.5	1.8	.2	.06	.02	0	0
Liver	3.1	2.4	1.3	.9	.8	.8	.05	.05	0	2.7	2.2	1.7	1.1	.1	.02	0	0	0
Kidney	8.7	7.0	3.1	3.5	1.9	1.4	.1	.1	0	8.4	6.9	4.0	2.9	.2	.04	0	0	0
Tumor	7.5	5.8	2.8	3.0	2.2	.9	.1	.1	0	7.0	6.9	4.1	3.0	.2	.03	0	0	0
Spleen	4.9	3.7	1.6	2.3	1.6	1.0	.2	.2	0	4.6	3.9	2.9	1.5	.4	0	0	0	0
Muscle	1.5	1.4	.6	.8	.5	.3	.04	.06	0	.....	.....	.....	.....	.....	.....	.....	.....	.....
Intestine	3.6	3.1	2.3	1.6	1.0	.6	.1	.1	0	.....	.....	.....	.....	.....	.....	.....	.....	.....
Thyroid [1]	.8	.4	.2	.5	.1	.1	0	0	0	.....	.....	.....	.....	.....	.....	.....	.....	.....
Mesenteric lymph nodes [1]	.5	.3	.1	.2	.1	.1	0	0	0	.....	.....	.....	.....	.....	.....	.....	.....	.....

[1] Radioactivity of thyroid and mesenteric lymph nodes is given for the total weight of tissue examined (about 6 mg.) and can be converted to that of 200 mg. by multiplying the activity given in the table by 33.

TABLE 5.—*Partition of radioactivity in blood cells and plasma after injection of $I^{131}NM$*

Time after injection (in hours)	Radioactivity in percent of whole blood as measured		
	Blood cells	Plasma	Calculated for whole blood
	Percent	*Percent*	*Percent*
4.7	23	90	113
8.5	39	93	132
10	33	85	118

Among the tissues examined, the greatest concentration of radioactivity was found in the thyroid gland, lungs, and mesenteric lymph nodes. Although the specific radioactivity of thyroid was highest, the total activity localized in the thyroid was relatively insignificant. The larger the quantity of carrier iodine used, the smaller the proportion of the dose accumulated by the thyroid (*16*). Therefore the thyroids in these experiments were saturated by a small fraction of the large dose of iodine (0.48 mg.) made available to each mouse. The high concentration of radioactivity in the lungs soon after $I^{131}NM$ injection as compared with that after NaI^{131} injection was more striking in the case of lung than for other tissues (compare fig. 2 with figs. 3, 4, and 5). The rate of disappearance of radioactivity from the lung was similar to that of the circulating blood (figs. 1 and 2). Four hours after injection of NaI^{131} very little radioactivity was found in any of the tissues, including sarcoma 37 (table 4). Four hours after injection of $I^{131}NM$, the radioactivity in blood and lung was 2–3 percent, in kidney and tumor 1–2 percent, and in liver 0.5–1 percent of that in the same weight of blood at zero time. This difference persisted for many hours.

The radioactivity of the thyroid gland increased during the first hour after injection of $I^{131}NM$, reflecting the rate of liberation of ionic iodine from the compound (table 4, normal mice). This phenomenon was not observed in Swiss mice with tumors or after injection of NaI^{131} in normal mice.

There was rapid urinary excretion of radioactivity, presumably in the form of iodide, following injection of $I^{131}NM$ and NaI^{131} (table 6). Very little radioactivity appeared in the urine after 24 hours in the case of injected $I^{131}NM$, or after 8 hours in the case of NaI^{131} (tables 6 and 7). This suggests either delayed liberation of ionic iodine from a portion of the $I^{131}NM$ injected or delayed diffusion of ionic iodine out of cells.

TABLE 6.—*Percent of total administered radioactivity found in mouse urine*[1] *collected at intervals after injection of* $I^{131}NM$ *and* NaI^{131}

Time interval (in hours)	Radioactivity injected					
	$I^{131}NM$ in normal mice				$I^{131}NM$ in tumor-bearing mice	NaI^{131} in normal mice
	Percent	*Percent*	*Percent*	*Percent*	*Percent*	*Percent*
¼	10.8	13.0	18.0	.....	0	5.2
½	7.4	17.4	10.6	.....	23.4	6.7
1	10.6	19.5	.....	.....	34.6	13.7
2	6.0	13.5	9.3	16.3	18.5	5.0
4	.....	.....	3.8	9.0	13.0	2.8
8	.....	2.3	.....	5.4	7.4	.2
16	.....	.....	.....	1.2	1.5	.06
24	.....	.....	.....	.9	1.4	.08
48	.....	.....	.....	.01	0	.01

[1] Urine specimens collected at specific intervals were representative samples of the urine at the particular time and did not constitute necessarily the total output from one interval to the next.

TABLE 7.—*Percent of total administered radioactivity found in urine collected for periods by urethral obstruction*[1] *after injection of* $I^{131}NM$ *and* NaI^{131} *in normal mice*

Period of urine collection (in hours)	Radioactivity injected	
	$I^{131}NM$	NaI^{131}
	Percent	*Percent*
0–16	[2] 9.3	18.4
½–24	14.3	.....
18–38	.7	.2
20–48	.....	.4
24–48	.2	.....

[1] The data are subject to the error of possible suppression of urinary secretion produced by acute urinary obstruction.
[2] The mouse died between the twelfth and sixteenth hours.

DISCUSSION

The chemical and pharmacological activity of the nitrogen mustards stems from the ability of the β-chloroethyl amine groups to cyclize in polar solvents with the formation of the ethylene immonium ion and halide ion. The cyclic product has a high order of chemical activity (particularly in alkaline solution), for it is a powerful alkylating agent and readily reacts with innumerable compounds which possess a variety of functional groups (*6, 10, 11*). Aqueous solutions of the hydrochloride salt are sufficiently acid to prevent cyclization of the mustards during the brief period required for their preparation and injection. Once injected, the pH, temperature, and chemical content of the plasma are such as to favor rapid cyclization. These considerations have raised the question whether the nitrogen mustards are able to reach tumor tissue unaltered after intravenous injection.

For the preliminary experiments which constitute this report, a simple mustard (single β-iodoethyl group) was selected to avoid complication in interpretations, which would be introduced by serial cyclization of additional β-iodoethyl groups. It is claimed that at least two β-chloroethyl groups in mustards are necessary in order to induce leukopenia in animals (*17*). The toxicity of diethyl β-chloroethyl amine was found to be about one-fortieth and $I^{131}NM$ about one-thirtieth that of methyl-bis(β-chloroethyl) amine on a molecular basis. Methyl-bis(β-chloroethyl) amine has been reported to be 50 times as toxic for mice as diethyl β-chloroethyl amine based on the comparison of the LD_{50} (*17, 18*).

The rapid disappearance of radioactivity from the circulating blood and the rapid appearance of radioactivity in the urine following injection of both NaI^{131} and $I^{131}NM$ indicate that a large fraction of the mustard cyclizes and liberates radioactive iodide ion promptly. The high concentration of radioactivity in pulmonary tissue is consistent with the fact that it is the first tissue reached by mustard following intravenous injection and is exposed to the total dose before the tissues are reached through the arterial circuit. The persistence of a definite but small amount of radioactivity in the circulating blood, tissues, and tumor, observed 4–8 hours following $I^{131}NM$ injection, was not observed after NaI^{131} injection. Further evidences of delayed liberation of ionic iodine are afforded by the observation of prolonged excretion of radioactivity in small amounts after $I^{131}NM$ injection and from the finding of one-third of the radioactivity of the blood located in the blood cells. These facts suggest that a definite but small fraction of the mustard base reached the tissue cells intact and penetrated these cells in uncyclized, lipoid-soluble form. Cyclization with liberation of iodide ion may have been slowed in the cells, or diffusion of iodide ion out of the cells may have been delayed. These experiments indicate only the minimum amount of the reactive form of nitrogen mustard which reached tissue cells, because some of the immonium ion (which is not radioactive) may have reached the same locus, and because some of the iodide ion liberated within the cell may have diffused out.

It has been postulated that the action of the amine mustards is due to their ability to inhibit vital enzyme systems (*2*). Since this would require intracellular retention of at least part of

the administered mustard, the suggestive findings that some $I^{131}NM$ penetrates tissue cells lend support to this hypothesis. Therefore, it is not necessary to hypothesize that the cytotoxic effects of the amine mustards are due to reaction products of the mustard with blood constituents.

These preliminary distribution studies suggest further that whatever specificity for certain neoplastic tissue mustards have shown is due more to the fact that higher concentrations reach those tissues than to any inherent specific toxicity for the neoplastic cells. Thus lung, blood, and lymphoid neoplasms should be affected, whereas other tumors should not. This is borne out by clinical observations. A similar study is in progress with radioactive methyl-bis(β-iodoethyl) amine.

SUMMARY

Diethyl β-radioiodoethyl amine ($I^{131}NM$) was prepared from the chloro derivative by treatment in anhydrous acetone with radioactive sodium iodide (I^{131}). A molecular equivalent was found to be about one-thirtieth as toxic for mice as methyl-bis(β-chloroethyl) amine.

A comparison of the rate of disappearance from the blood and tissues and the appearance in the urine of radioactivity following intravenous injection of $I^{131}NM$ and NaI^{131} indicated that most of the mustard was rapidly cyclized to the immonium ion with loss of iodide ion, but that a small portion reached the tissues intact and penetrated the cells.

The highest concentration of radioactivity due to $I^{131}NM$ was noted in blood, lung, and lymph nodes. This distribution conforms to the locus of clinical activity of the mustards. Lower concentration of radioactivity was noted in kidney, liver, and sarcoma 37 growing in the subcutaneous space.

REFERENCES

(1) Spurr, C. L., Jacobson, L. O., Smith, T. R., and Barron, E. S. G.: The clinical application of methyl-bis(β-chloroethyl) amine hydrochloride to the treatment of lymphomas and allied dyscrasias. *In* Approaches to Tumor Chemotherapy, pp. 306–318. Science Press Printing Co., Lancaster, Pa. (1947).

(2) Karnofsky, D. A., Craver, L. F., Rhoads, C. P., and Abels, J. C.: An evaluation of methyl-bis(β-chloroethyl) amine hydrochloride and tris(β-chloroethyl) amine hydrochloride (nitrogen mustards) in the treatment of lymphomas, leukemia and allied diseases. *In* Approaches to Tumor Chemotherapy, pp. 319–337. Science Press Printing Co., Lancaster, Pa. (1947).

(3) Goodman, L. S., Wintrobe, M. M., McLennan, M. T., Dameshek, W., Goodman, M. J., and Gilman, A.: Use of methyl-bis(β-chloroethyl) amine hydrochloride and tris(β-chloroethyl) amine hydrochloride (nitrogen mustards) in the therapy of Hodgkin's disease, lymphosarcoma, leukemia and certain allied and miscellaneous diseases. *In* Approaches to Tumor Chemotherapy, pp. 338–346. Science Press Printing Co., Lancaster, Pa. (1947).

(4) Wintrobe, M. M., McLennan, M. T., and Huguley, C. M.: Clinical experiences with nitrogen mustard therapy. *In* Approaches to Tumor Chemotherapy, pp. 347–357. Science Press Printing Co., Lancaster, Pa. (1947).

(5) Rhoads, C. P.: Nitrogen mustards in the treatment of neoplastic disease. J. A. M. A. 131: 656–658 (1946).

(6) Gilman, A., and Philips, F. S.: The biological action and therapeutic applications of the (β-chlorethyl) amines and sulfides. Science 103: 409–415 (1946).

(7) Golumbic, C., Fruton, J. S., and Bergmann, M.: Chemical reactions of the nitrogen mustard gases. I. The transformations of methyl-bis(β-chloroethyl) amine in water. J. Org. Chem. 11: 518–535 (1946).

(8) Golumbic, C., and Bergmann, M.: Chemical reactions of the nitrogen mustard gases. II. The composition of aged unbuffered solutions of methyl-bis(β-chloroethyl) amine. J. Org. Chem. 11: 536–542 (1946).

(9) Golumbic, C., Stahmann, M. A., and Bergmann, M.: Chemical reaction of the nitrogen mustard gases. IV. The transformations of tris(β-chloroethyl) amine in water. J. Org. Chem. 11: 550–558 (1946).

(10) Fruton, J. S., Stein, W. H., and Bergmann, M.: Chemical reaction of the nitrogen mustard gases. V. The reactions of the nitrogen mustard gases with protein constituents. J. Org. Chem. 11: 559–570 (1946).

819164—49——2

(*11*) Fruton, J. S., Stein, W. H., Stahmann, M. A., and Golumbic, C.: Chemical reaction of the nitrogen mustard gases. VI. The reactions of the nitrogen mustard gases with chemical compounds of biological interest. J. Org. Chem. 11: 571–580 (1946).

(*12*) Gough, G. A. C., and King, H.: Trypanosidal action and chemical composition. VIII. Derivatives of β-amino ethyl and γ-amino propyl arsinic acids. J. Chem. Soc., pp. 2426–2447 (1928).

(*13*) Seligman, A. M., Shear, M. J., Leiter, J., and Sweet, B.: Chemical alteration of polysaccharide from *Serratia marcescens*. I. Tumor-necrotizing polysaccharide tagged with radioactive iodine. J. Nat. Cancer Inst. 9: 13–18 (1948).

(*14*) Fine, J. and Seligman, A. M.: Traumatic shock. An experimental study including evidence against the capillary leakage hypothesis. Ann. Surg. 118: 238–255 (1943).

(*15*) Gibson, J. G., Seligman, A. M., Peacock, W. C., Aub, J. C., Fine, J., and Evans, R. D.: The distribution of red cells and plasma in large and minute vessels of the normal dog, determined by radioactive isotopes of iron and iodine. J. Clin. Investigation 25: 848–857 (1946).

(*16*) Astwood, E. B., and Stanley, M. M.: Use of radioactive iodine in the study of thyroid function in man. West. J. Surg. 55: 625–639 (1947).

(*17*) Anslow, W. P., Karnofsky, D. A., Jager, B. V., and Smith, H. W.: The toxicity and pharmacological action of the nitrogen mustards and certain related compounds. J. Pharm. & Exper. Therap. 91: 224–235 (1947).

(*18*) Philips, F. S., and Gilman, A: The relation between chemical constitution and biological action of the nitrogen mustards. *In* Approaches to Tumor Chemotherapy, pp. 285–292. Science Press Printing Co., Lancaster, Pa. (1947).

FIBROIDS IN A GUINEA PIG (FAMILY 13) AFTER PARTIAL CASTRATION [1]

By ELI. M. NADEL, M. D.,[2] *National Cancer Institute, National Institutes of Health, Public Health Service, Federal Security Agency*

INTRODUCTION

Fibroid tumors have been induced in the guinea pig by continuous stimulation with estrogenic preparations (*1*). In the female, they have been found in the wall of the uterus, stomach, and intestine and in the pancreas, spleen, and parietal peritoneum. Since a higher incidence of these tumors developed in castrated as compared with noncastrated female guinea pigs following such treatment, Lipschütz postulated that the corpus luteum hormone produced by the normal adult ovary was antagonistic to the oncogenic action of estrogen. The prevention of fibroid-tumor production by the simultaneous injection of corpus luteum hormone and estrogens into castrated female guinea pigs provides strong support for this postulate (*2*).

Lipschütz found that fibroid tumors did not develop in female guinea pigs which were subjected to the endogenous estrogenic stimulation resulting after ovarian fragmentation, i. e., partial castration (*2*). It is of especial interest that corpora lutea were regularly demonstrated in the ovarian fragment remaining after partial castration (*3*).

There is here reported the development of fibroids in a female guinea pig inadvertently subjected to ovarian fragmentation rather than complete castration. In this case, no corpus luteum was found in the remaining ovarian fragment. The possibility is suggested that endogenous hyperestrinism unopposed by corpus luteum hormone may induce fibroids in guinea pigs.

EXPERIMENTAL PROCEDURE

A 21-day-old female guinea pig (family 13) was partially castrated. It was returned to maternal feeding until weaned at 32 days when it was placed on a diet of Purina rabbit pellets and wet cabbage.

OBSERVATIONS

The vagina opened at 30 days and except for three occasions of 5–7 days each remained open until the animal died 6 months later. Each closure was immediately preceded by the appearance of blood at the vaginal orifice. During the 6-month period, the nipples gradually enlarged. The animal died at night within 8 hours following examination. When last examined, slight abdominal pressure forced approximately 1 cc. of blood from the vaginal orifice.

At autopsy, the animal appeared well-nourished but small, weighing 450 gm. in contrast with the 700 gm. of completely castrated controls. The nipples were enlarged, measuring 1.25 cm. in height, and were covered with a cheesy, yellow crust (fig. 1). Both uterine horns and the cervix were enlarged, measuring 2.0 and 2.25 cm. in diameter, respectively. The entire uterus weighed approximately 12 gm.[3] Three gray nodules were on the right uterine horn, and a larger one in the angle formed by the junction of the horns (fig. 2). The nodules were 0.3–0.6 cm. in the largest diameter. A subserosal nodule, 1 cm. in diameter, compressed and partially obstructed the small intestine 5 cm. distal to the pylorus (fig. 3). There were no adrenal-gland abnormalities.

Microscopically, the uterine and intestinal nodules showed the characteristic structure of experimental, estrogen-induced, fibroid tumors, as described by Nelson, Lipschütz, and others (*1*, *2*) (figs. 2 and 3). Sections stained with phosphotungstic acid hematoxylin showed the nodules to be composed of interlacing bundles of spindle-shaped cells showing fibroglia. The blood vessels were not numerous and were of mature type. The largest nodule showed central hyalinization.

[1] Received for publication August 5, 1948.

[2] Present address, Department of Pathology, Washington University School of Medicine, St. Louis.

[3] The nipples of castrates, nonpregnant adults, and pregnant guinea pigs measure approximately 0.2, 0.4, and 1.0 cm. in height. The width of the uterine horns of castrated and nonpregnant adults measures approximately 0.2 and 0.6 cm. in diameter. The average weight of a nonpregnant adult's uterine horns and cervix is less than 1.0 gm.

FIGURE 1.—Genito-urinary tract and enlarged nipples. Fibroid nodules on right horn and at the junction angle of both horns. Right castration site larger than left.

Tissue at the sites from which each ovary had been removed was widely excised, fixed, blocked in paraffin, and serially sectioned. No ovarian tissue was demonstrable on the left. At the site of the right ovary there was a fragment of tissue measuring 2×3×2 mm. in the stained section. This fragment was completely encased in a nodule composed of fibrous tissue and fat (fig. 4, *A*). Degenerated (fig. 4, *B*) and apparently normal follicles (fig. 4, *C*) were identified in a number of sections. No "springreifen" (rupture-ready) follicles were present. No corpus luteal tissue was found.

DISCUSSION

The literature contains only one report of a spontaneous leiomyoma in a guinea pig (*4*). No fibroids of the uterus or intestines have been observed in family 13 guinea pigs.[4]

[4] Heston, W. E.: Personal communication.

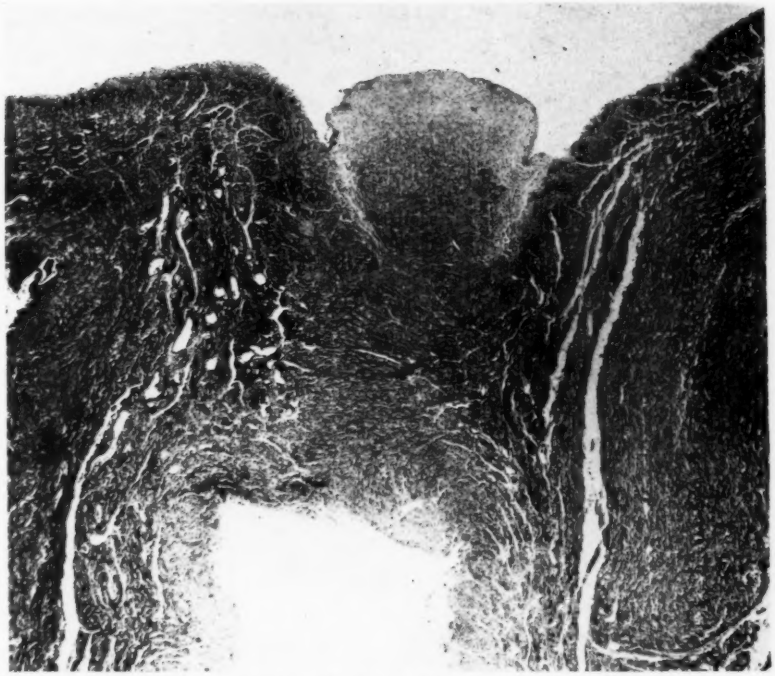

FIGURE 2.—Small fibroids at the junction of the uterine horns.

Schmidt described uterine fibroids in two guinea pigs examined 2 years following exposure to a localized, minimal, sterilizing dose of X-radiation (2,160 r) (*5*). She was able to detect excess female hormone in the urine of the X-radiated guinea pigs (*6*). The ovaries of these animals were of the interstitial-gland type. Ovulation did not occur, and no corpora lutea were formed.

On the evidence presented by Schmidt, it would appear that the excessive follicular hormonal excretion noted by her after X-radiation was causally related to the subsequent development of fibroids. Histologically, the mammary glands and the genital tract showed changes compatible with long-term estrogen effect.

FIGURE 3.—Subserosal nodule of the small intestine.

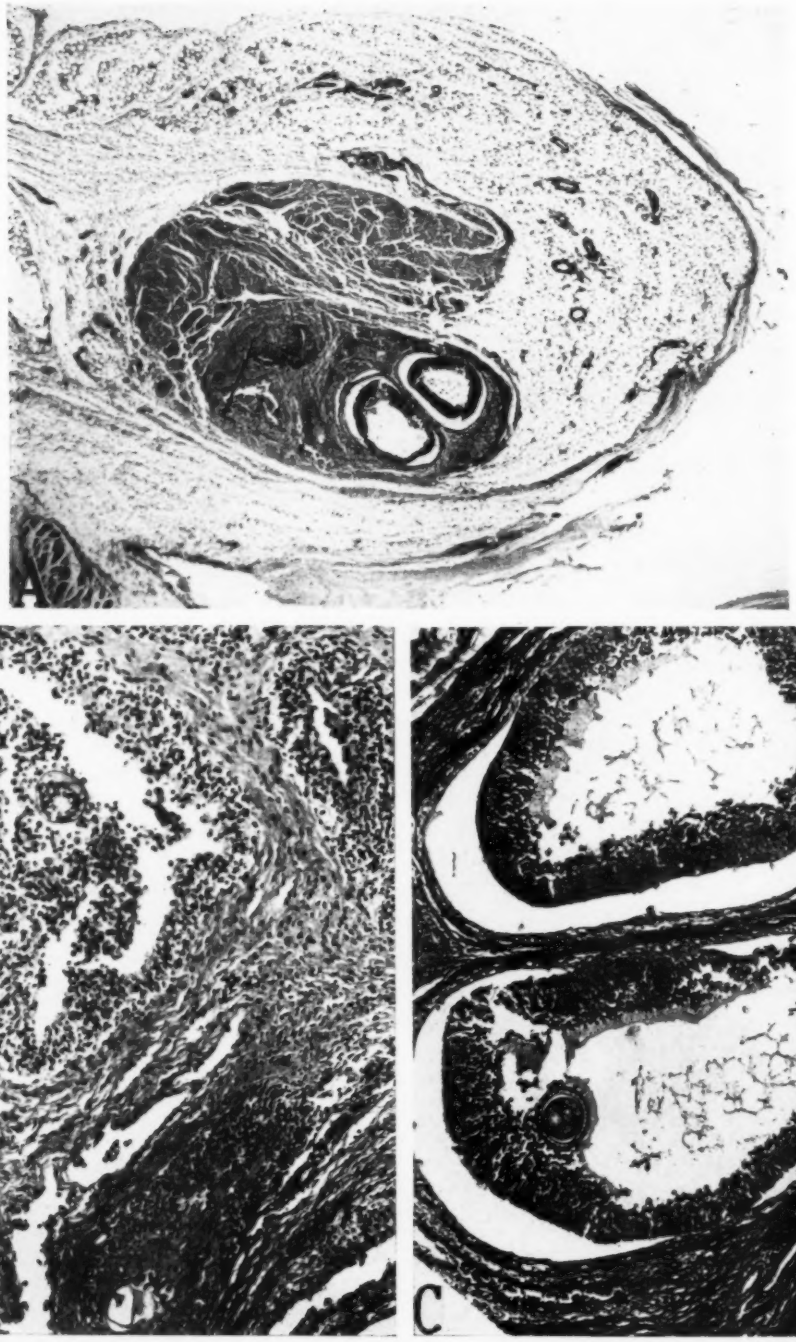

FIGURE 4.—*A*, Right ovarian fragment encased in fatty fibrous tissue. Two apparently normal follicles and three degenerated follicles are seen. Serial section revealed presence of ova or ova remnants in all. *B*, Enlargement of atretic follicle in *A*, with degenerated ovum. *C*, Enlargement of mature-type follicle in *A*, with well-formed ovum.

Manaro (7) reported two uterine adenofibromyomas developing in a guinea pig within 14 months following "extreme partial castration." He states that two follicles were in the ovarian fragment and that there was "thecal luteinization." It is entirely possible that luteal hormone, if produced at all, was insufficient to antagonize completely the effect of the follicular hormone. This animal developed an atypical uterine response not ordinarily found in animals experimentally stimulated with estrogen and not typical of animals partially castrated. The animal's vagina was found closed at death, the nipples were not noticeably enlarged, and the uterus weighed less than 2½ gm. While the development of uterine adenofibromyomas may have been related to partial castration, the possibility of a spontaneous origin could not be excluded.

In the present case, the suggestion that the fibroids were induced with endogenous estrogen unopposed by corpus luteum hormone is based upon the multiplicity of the tumors and their location in both the uterus and intestine, as is the case when tumors are experimentally induced with estrogenic preparations. That this animal was under the influence of excessive endogenous estrogen stimulation is suggested by the enlargement of the nipples and uterus, the open vagina, and the vaginal bleeding.

Factors which may have been significant in the development of fibroids in this animal include the fact that it was of an inbred strain (family 13), the partial castration before the first estrus, the encasement of the ovarian fragment in fat and fibrous tissue (with resultant possible prevention of follicular rupture), and the apparent failure to develop corpora lutea in the fragment.

SUMMARY AND CONCLUSIONS

A 6-month-old female guinea pig (family 13) developed multiple fibroids in the uterus and small intestine following partial castration. The single remaining ovarian fragment on the right was found to be encased in fat and fibrous tissue. It showed normal and degenerated follicles but no corpora lutea and no "springreifen" follicles. It is suggested that peri-ovarian adhesions may have prevented follicular rupture and that the hyperestrinism developing consequent to partial castration, unopposed by corpus luteum hormone, ultimately resulted in the formation of multiple fibroids.

REFERENCES

(1) Nelson, W. O.: Endometrial and myometrial changes, including fibromyomatous nodules, induced in the uterus of the guinea pig by prolonged administration of oestrogenic hormones. Anat. Rec. 68: 99–102 (1937).

(2) Lipschütz, A.: Induction and prevention of abdominal fibroids by steroid hormones, and their bearing on growth and development. Cold Spring Harbor Symposia on Quant. Biol. 10: 79 (1942).

(3) ———: Hyperplasie expérimentale de l'endomètre avec prolifération atypique de l'épithèle utérin apres des interventions ovariennes. Gynéc. et obst. 36: 408–426 (1937).

(4) Lipschutz, A.: Spontaneous fibromyoma in the female guinea pig. Arch. Path. 31: 702–705 (1941).

(5) Schmidt, I. G.: Changes in the genital tracts of guinea pigs associated with cystic and "interstitial gland" ovaries of long duration. Endocrinology 24: 69–81 (1939).

(6) Genther, I. T.: The oestrus producing principle in the urine of guinea pigs with X-radiated ovaries. Anat. Rec. Suppl. 60: 51 (1934).

(7) Manaro, J. M.: Adenofibromyomata in the uterus of a guinea pig after extreme partial castration. Endrocrinology 29: 619–621 (1941).

MASCULINIZING OVARIAN TUMOR OF ADRENAL TYPE [1]

By EDWARD J. MORTELL, M. D., *Saint Elizabeths Hospital, Washington, D. C.*[2]

INTRODUCTION

The so-called adrenallike tumor of the ovary presents a number of complex endocrine and pathologic problems. Recent reports have brought some clarification but also considerable controversy to this situation, particularly with regard to the pathologic aspects. In addition to masculinization, one may see various features of the Cushing syndrome, such as obesity, polycythemia, purplish striae, hypertension, hyperglycemia, etc. (*1*). The reason for the presence or absence of the latter is not yet apparent. Urinary hormone assays have also yielded perplexing results. In spite of intense masculinization, the measurable androgen excretion may be well within normal limits (*2*). In other cases, the 17-ketosteroid excretion is definitely increased (*1*).

Although there is fairly general agreement regarding the adrenal origin of these tumors, exceptions are not infrequent. In the case reported by Twombly (*3*), the histologic appearance was considered suggestive of ovarian rather than adrenal origin. Transitions from fibroblastic or mesenchymallike cells to fat-laden cells with the typical appearance of adrenal cortex cells led the author to suggest that this tumor might represent a "sort of histologic connecting link between the theca-cell tumor and the so-called 'adrenal cortical carcinoma of ovarian origin'." In another case, that of Curtis (*4*), gradual transition from polygonal adrenal type of cells to a stroma of spindle-shaped cells was noted. This was interpreted as indicating that adrenallike tumors of the ovary arise by metaplasia of stroma cells or other indifferent cells rather than from embryologically misplaced tissue in the ovary. Curtis rejected the idea that "luteinization" may account for this picture.

A feminizing testicular tumor described by Teilum (*5*) showed "morphological congruity" with the ovarian arrhenoblastoma series. The same tumor revealed gradual transition to clear-cut lipoid-cell areas, which resembled the ovarian tumors generally called luteoma or adrenal tumor. On this basis, he concluded that the latter type of ovarian tumor is to be regarded simply as a particularly lipoidal form of diffuse arrhenoblastoma.

According to Selye (*6, p. 437*), the origin of these tumors is uncertain, and the descriptive term "lipid cell tumor of the ovary" is most appropriate at the present time. Undoubtedly further study is necessary to complete our understanding of the functional activity and pathogenesis of these tumors.

CASE REPORT

PRESENT ILLNESS

The patient, a 46-year-old white married female, was first seen by the writer in November 1946. The initial symptoms began at the age of 40 in mid-1940 with the appearance of excessive facial hair. This started on the chin, spread to the upper lip, and eventually conformed to the usual male beard distribution. Heavy black coarse hair also appeared on the trunk and all extremities. Coincidentally the menstrual periods became greatly diminished in duration and amount of flow; there was no change in regularity until September 1941, at which time, without symptoms of any sort, the periods abruptly stopped. After this, the hirsutism increased markedly, and it became necessary to shave every other day. In addition, the hair on the top of the head fell out. No significant change in voice was noted, and there was but a 10-pound weight increase over a period of several years.

[1] Received for publication August 24, 1948.

[2] Acknowledgment is made to Dr. Emil Novak for the pathologic diagnosis; to Dr. Benton B. Westfall, National Cancer Institute, for the hormonal assays; and to Dr. Roy Hertz, National Cancer Institute, for many valuable suggestions.

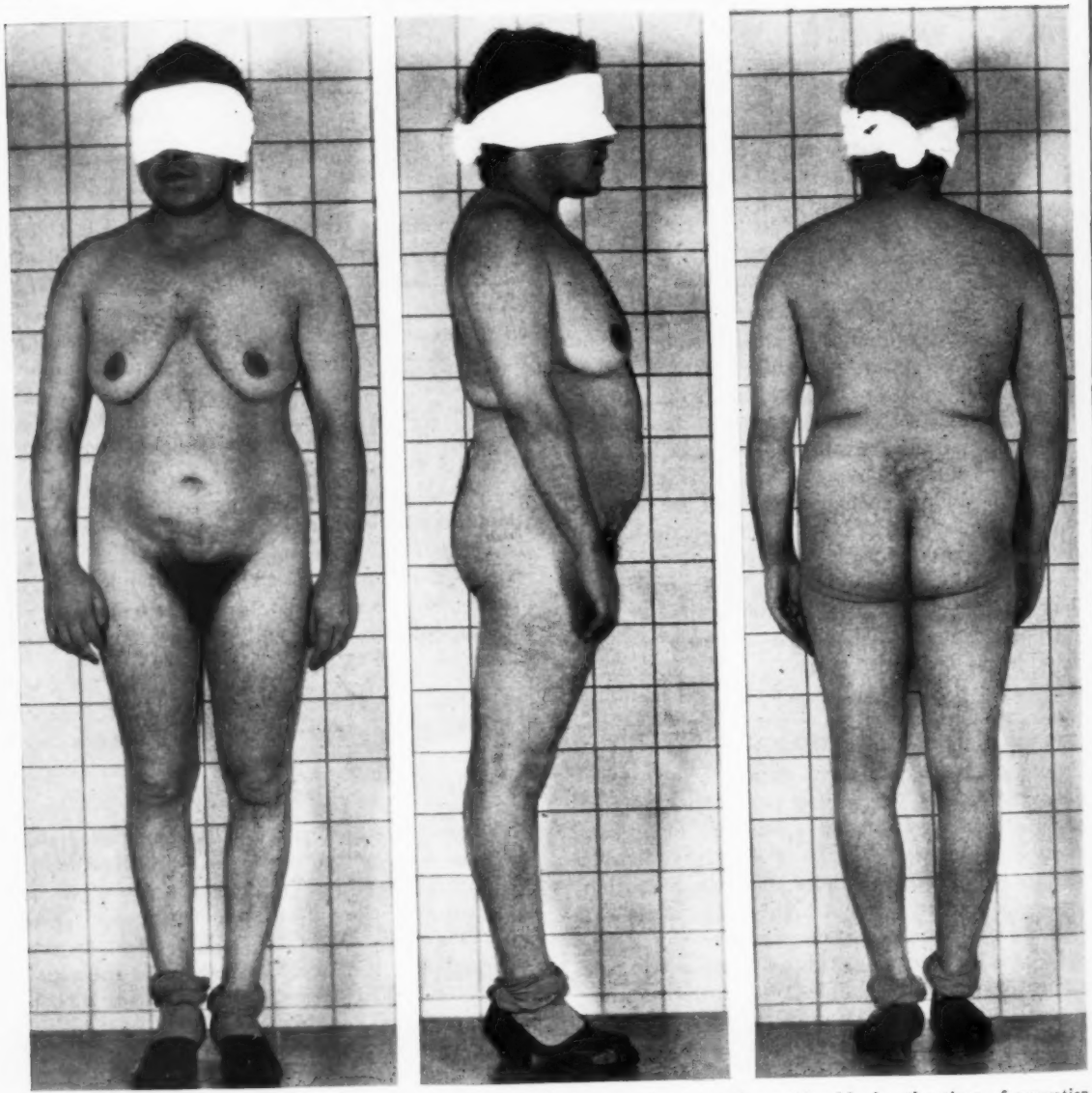

FIGURE 1.—Photographs taken on October 13, 1944. Hirsutism had increased considerably by the time of operation (March 7, 1947).

PAST MEDICAL AND PSYCHIATRIC HISTORY

Menses began at the age of 15, were irregular and prolonged during the first 2 or 3 years, then became regular with an interval of 35 to 40 days and moderately heavy flow for 6 to 7 days. The patient went through a normal pregnancy at 20, giving birth to a normal male child.

The patient had an exploratory laparotomy at age 23 because of an "acute abdomen." She was found to have pyosalpingitis, and a bilateral salpingectomy was performed. From the age of 33 to 36 years, the patient suffered from periodic nosebleeds. At 37, the patient had a cerebrovascular accident, of unknown etiology, which resulted in a right-sided hemiplegia. There were

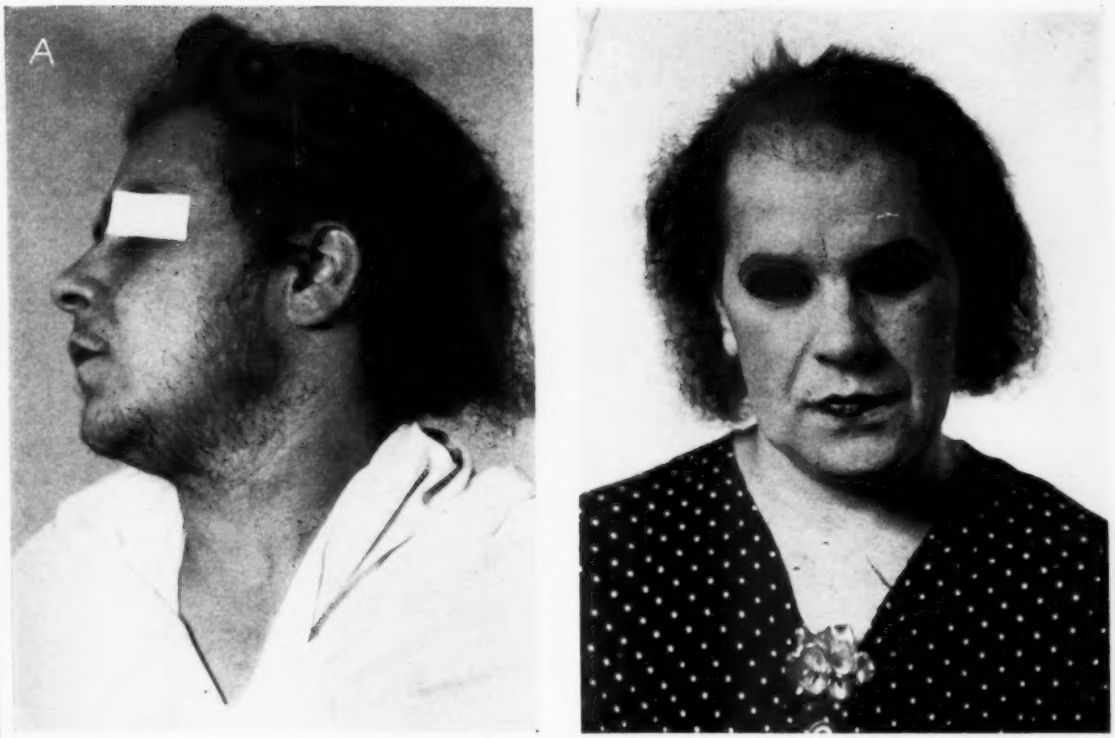

FIGURE 2.—*A*, Facial hirsutism; photograph taken October 13, 1944. *B*, Postoperative photograph taken November 30, 1948.

no records available of the blood pressure preceding or at the time of the vascular incident. Recovery was slow and incomplete, leaving her with a residual hemiparesis. Following this, a previously noted tendency to sexual promiscuity and alcoholic indulgence was strikingly increased. She lost all inhibition and ethical sense, lied indiscriminately, stole anything within reach, and was generally incorrigible. This behavior led to admission to St. Elizabeths Hospital in August 1944, at 44, where she has remained to the present time. The diagnosis of "psychosis associated with disturbance of cerebral circulation" was established. There was no indication of abnormal sexual inclinations while in the hospital. During short visits to her home, she made constant sexual demands on her husband.

FAMILY HISTORY

The immediate family history revealed several instances of hypertensive cardiovascular disease.

CLINICAL EXAMINATION

Examination in November 1946 showed profound masculinization (figs. 1, and 2, *A*). There was very marked facial and bodily hirsutism.[3] The area from the forehead to the occiput was virtually bald, with a ruff of thick, wiry, black hair remaining (fig. 3, *A*).[3] The facies resembled that of a male. There was no abnormality of complexion or pigmentation. The bodily musculature was prominent, and the contours were masculine in type. There was a slight degree of obesity, of the trunk in particular. The lungs and heart were negative. The blood pressure was 100/70. No abdominal masses or viscera were palpable, nor were purplish striae present. The escutcheon was masculine, and the clitoris was markedly enlarged. Pelvic examination under pentothal anesthesia, on March 4, 1947, revealed the uterus

[3] Since this paper was submitted for publication (Aug. 24, 1948), photographs were taken (Nov. 30, 1948) that show the changes that had taken place in the patient's appearance (fig. 2, *B*, and 3, *B*).

FIGURE 3.—*A*, Bald area of scalp; photograph taken February 14, 1947. *B*, Same area of scalp as *A*; photograph taken November 30, 1948.

to be somewhat enlarged. Both ovaries were slightly enlarged, but no tumor mass was noted. A dilatation and currettage were done on the same date. Neurological examination disclosed an old right-sided hemiparesis. Mental examination revealed evidence of an organic type of psychosis, with memory impairment, confabulation, grandiosity, paranoid trends, intellectual deterioration, and defective judgement.

LABORATORY EXAMINATIONS

The red blood cells numbered, 4,800,000, with 90 percent hemoglobin (November 14, 1946.) Total and differential leukocyte count was normal. Urinalysis, NPN, cholesterol, spinal fluid, and basal metabolic rate were normal. X-ray films of the skull, sella turcica, chest, and long bones were normal, as was an intravenous pyelogram. An oral glucose-tolerance test (November 12, 1946) gave the following results: fasting, 70 mg.; 45 minutes, 90 mg.; 75 minutes, 108 mg.; 135 minutes, 89 mg. All urines were negative for sugar. The urinary excretion of 17-ketosteroids in a 24-hour period (December 16, 1946) was 8 mg. The urinary gonadotropic hormone excretion in 24 hours (December 17, 1946) was greater than 20 and less than 40 mouse units.

OPERATION

On March 7, 1947, a bilateral oophorectomy and supravaginal hysterectomy were performed by Dr. W. A. Parker.

Both ovaries were somewhat larger than normal, and the right ovary was larger than the left. Section of the right ovary showed the smooth circular outline of a solid tumor, about 18 mm. in diameter, which was almost completely embedded in the ovarian stroma (fig. 4). It was pale yellow and softer than the surrounding ovarian parenchyma. The tumor had no capsule, but there was no sign of infiltrating growth. It consisted of fairly large, closely grouped cells

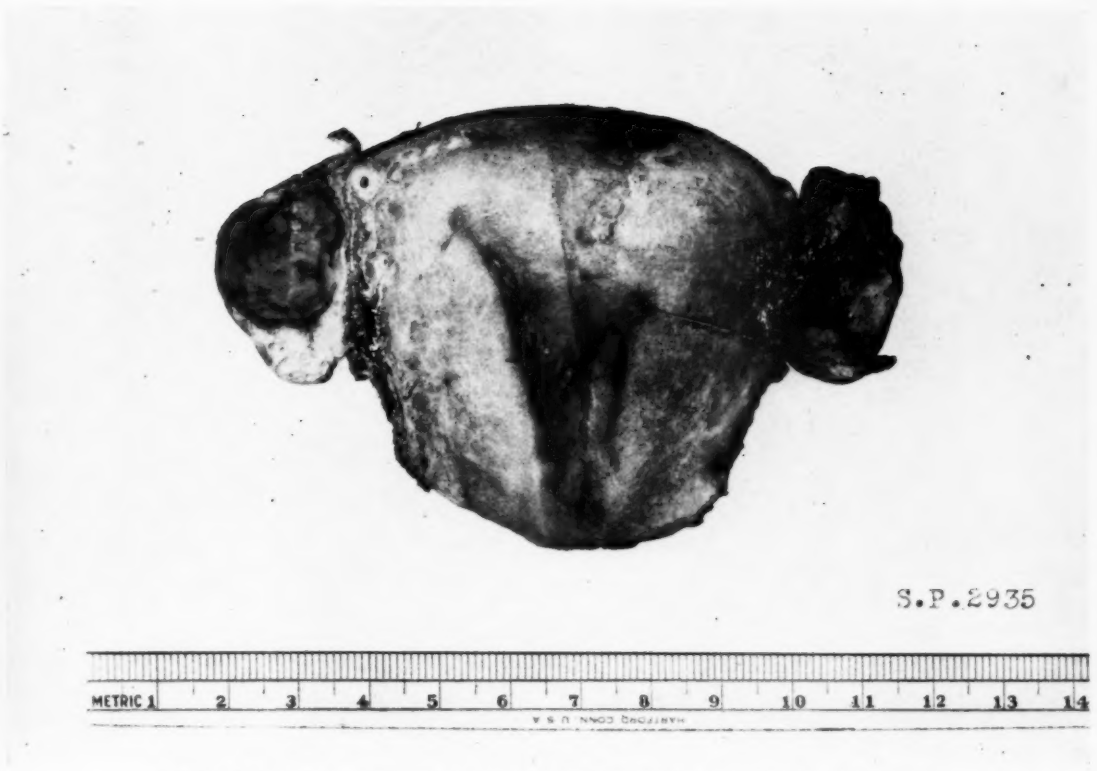

FIGURE 4.—Section of uterus and ovaries showing tumor embedded in right ovary.

without any recognizable architectural arrangement (fig. 5). The supporting tissue was very light. The nuclei tended to be round, rather chromatic, and had prominent nucleoli. The cell bodies were generally polygonal but occasionally somewhat fusiform. The cytoplasm was eosinophilic, pale, and granular. Mitoses were seen rarely. Sections stained with oil red II showed numerous small droplets of lipoid material in many of the cells.

Sections of the tumor were examined by Dr. Emil Novak, who made the diagnosis of adrenal tumor of the ovary.

Histologic examination of the left ovary revealed normal ovarian stroma. The uterus was slightly enlarged, showed evidence of recent curettage, but was otherwise not remarkable. The curettings, obtained 4 days preoperatively, revealed moderate atrophy of the endometrium.

POSTOPERATIVE COURSE

The immediate postoperative condition was uneventful except for the appearance of a fairly severe menopausal syndrome, which responded well to stilbestrol. Stilbestrol treatment was discontinued without recurrence of symptoms after 4 months. Between April 21 and May 8, 1947, the patient was given a course of deep X-ray therapy, totaling 3,200 r, in the lower quadrants.

Removal of the tumor resulted in a gradual but marked regression of the symptoms. Eighteen months after the operation the patient's condition was as follows: The facial hair was considerably diminished in extent and heaviness but still required shaving about once weekly. Though not so dense as normal, a good crop of hair was on the previously bald area of the scalp. Practically all the excessive hair on the trunk and extremities

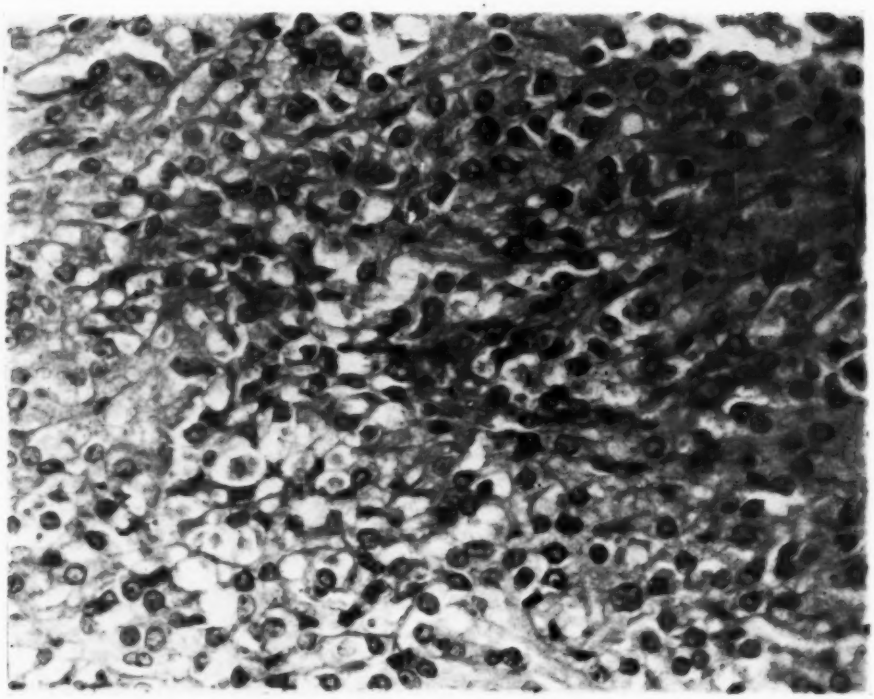

FIGURE 5.—Adrenal tumor of ovary, stained with hematoxylin and eosin.

had disappeared. The facies and bodily conformation were no longer masculine in appearance. The weight was stabilized at 127 pounds, about 15 pounds less than the preoperative level. The blood pressure was unchanged. Distribution of the pubic hair approached the usual feminine pattern. Marked involution of the clitoris had taken place; it was now normal in size and appearance.

There was no significant change in the patient's mental state. Her usual behavior patterns, including the strong sexual drive, were not perceptibly affected by removal of the tumor.

An oral glucose-tolerance test (July 22, 1947) showed a fasting blood sugar of 85.8 mg.; 30 minutes, 150 mg.; 60 minutes, 128 mg.; and 120 minutes, 115 mg. Corresponding urine specimens were negative for sugar. The 24-hour urinary excretion of 17-ketosteroids was 3.5 mg. on 1 occasion (November 29, 1947) and 2.4 mg. on another (December 11, 1947). The 24-hour urinary gonado-tropic hormone excretion was greater than 40 and less than 50 mouse units (December 11, 1947).

DISCUSSION

Except for the neurologic and psychiatric manifestations, the findings in this case are typical of adrenal tumor of the ovary. The question arises what relationship existed between the cerebrovascular accident and the tumor. It seems probable that the two conditions represent separate and distinct diseases, since the first indications of masculinization did not appear for more that 3 years after the cerebral apoplexy. The hypothesis that the cerebral lesion, in some occult fashion, might be responsible for the development of the tumor seems wholly untenable.

The normal preoperative level of 17-ketosteroid excretion was in strange contrast with the clinical appearance. Following the operation there was an apparent decrease in the 17-ketosteroid excretion, but the significance of this is not clear.

The present case illustrates the difficulty of establishing the origin of these tumors. Most of the cells strongly resemble those seen in the adrenal cortex, but areas of fusiform cells with rather poorly defined cell boundaries are also seen.

Interpretation of this latter feature provides the focus of much difference of opinion. In the absence of convincing evidence to the contrary, however, the presumption of adrenal origin seems quite reasonable.

The behavior of this patient is of interest. Following the cerebrovascular accident, her activity was characterized by the practically uninhibited operation of a small number of rigid behavior patterns. She became sexually promiscuous, overindulged in alcohol, and lost all moral restraint. Neither the presence nor the removal of the functioning tumor had any observable effect on her mental illness.

Of particular significance is the lack of effect on the patient's sexual activity. At no time was there any apparent alteration in her sexual patterns. While this reduction in reactivity may be attributed in part to the neurological defect, it is certainly also indicative of the relative importance of cerebral factors in human sexual behavior as contrasted with hormonal influences (*7*).

SUMMARY

A case of adrenal tumor of the ovary in a 46-year-old white female is described. The patient had generalized hirsutism, baldness, masculine contours, and enlargement of the clitoris. Preoperative urinary excretion of 17-ketosteroids was 8 mg. in 24 hours. Following removal of the tumor, there was marked regression in the evidences of masculinization.

REFERENCES

(*1*) Kepler, E. J., Dockerty, M. B., and Priestley, J. T.: Adrenal-like tumor associated with Cushing's syndrome (so-called masculino-blastoma, luteoma, hypernephroma, adrenal cortical carcinoma of ovary). Am. J. Obst. & Gynec. 47: 43–62 (1944).

(*2*) Douglass, M.: Masculinizing tumor of the ovary of the adrenal type. Am. J. Obst. & Gynec. 53: 190–198 (1947).

(*3*) Twombly, G. H.: Luteoma of the ovary. Am. J. Obst. & Gynec. 51: 832–841 (1946).

(*4*) Curtis, A. H.: The origin of adrenal-like tumor of the ovary. Am. J. Obst. & Gynec. 52: 115–122 (1946).

(*5*) Teilum, G.: Arrhenoblastoma—androblastoma. Homologous ovarian and testicular tumors. Acta path. et microbiol. scandinav. 23: 252–265 (1946).

(*6*) Selye, H.: Textbook of endocrinology. Acta Endocrinologica Université de Montréal, Montreal (1947).

(*7*) Beach, F. A.: Sexual behavior in mammals. Physiol. Rev. 27: 240–307 (1947).

SOME OBSERVATIONS ON THE NORMAL AND PATHOLOGIC ANATOMY OF THE KIDNEY OF THE MOUSE[1]

By THELMA B. DUNN, M. D., *National Cancer Institute, National Institutes of Health, Public Health Service, Federal Security Agency*

INTRODUCTION

Inbred strains of mice are considered indispensable for cancer research, and much of the progress toward understanding the inheritance of neoplastic diseases and the successful transplantation of tumors is directly attributable to the use of this valuable tool. Inbred mice supply a reproducible, homogeneous medium for many lines of biologic research, which might well be utilized by workers outside the field of cancer. Mice are comparatively inexpensive to purchase and to maintain, and large numbers of animals can be used in both experimental and control groups. The small size of the organs also makes it technically possible to do a comprehensive histologic study; for it is feasible to do serial sections on many organs, as the lungs and kidneys, and to take sections from all representative parts of such general systems as the blood vessels and hematopoietic tissues.

For these reasons, it is believed that mice would prove especially useful in studies of renal diseases. Unfortunately, the published reports regarding the neoplastic and nonneoplastic conditions in this species are widely scattered. Moreover, although much information has been gathered in laboratories such as the National Cancer Institute where thousands of mice are examined every year, observations on the kidney are usually incidental to the main purpose of the experiments, and hence a large part of the information on the kidney has remained unpublished. In this paper, facts relating to the kidney of the mouse gathered both from the literature and observations in the laboratory are discussed. Subjects for consideration are grouped under normal anatomy and physiology and pathologic anatomy.

[1] Received for publication August 31, 1948.

NORMAL ANATOMY AND PHYSIOLOGY

General Structure

The kidneys in the mouse are paired organs lying on either side of the vertebral column and behind the peritoneum. The right kidney is usually about 10 percent heavier than the left, and it is slightly higher in position. The adrenal on the right lies above and somewhat medial to the kidney and is so closely attached that it is often convenient to remove both organs together for microscopic section. The adrenal on the left is more widely separated from the kidney. The vessels of the left kidney are longer than those of the right, and the left renal vein passes over the aorta.

The general architecture of the mouse kidney closely resembles that of the rat. McFarlane (*1*) described the arrangement of tubules in the rat kidney and outlined four well-defined zones. Similar divisions are readily identified in the mouse (fig. 1). The following outline, modified from McFarlane, is helpful in indicating the section of the nephron which predominates in each zone. It is thus of assistance in identifying the segment affected by various toxic agents or abnormal deposits.

Zone	Predominant section of the tubule	Other sections of tubule
1 (outer zone of cortex).	Proximal convoluted tubule.	Distal convoluted tubule; broad limb of Henle; collecting tubule.
2 (inner zone of cortex).	Descending straight limb of proximal convoluted tubule.	Ascending broad limb of Henle; collecting tubule.
3 (outer zone of medulla).	Ascending broad limb of Henle.	Descending narrow limb of Henle; collecting tubule.
4 (inner zone of medulla).	Collecting tubule.....	Narrow limb of Henle.

The majority of the glomeruli lie in zone 1, and although this merges to some extent with zone 2,

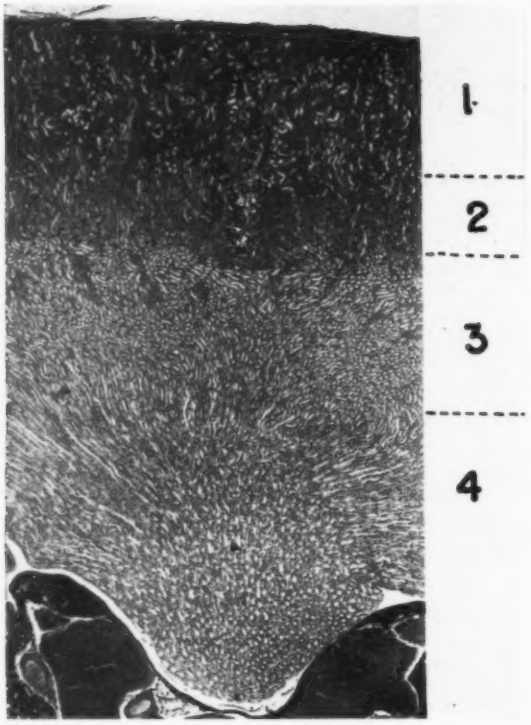

FIGURE 1.—Kidney showing segments of the nephron arranged in zones. 1, Outer zone of cortex; 2, inner zone of cortex; 3, outer zone of medulla; and 4, inner zone of medulla. Hematoxylin-eosin stain × 28.

if a section is cut so as to include both the papilla and the cortex, zone 2 can always be clearly defined since most of the tubules are cut longitudinally. Such a section passing through the papilla is usually to be preferred, since the condition of the papilla is especially informative in some types of renal disease in the mouse.

SIZE AND NUMBER OF THE GLOMERULI

Rytand (*2*), by use of an ingenious method for estimating the number and size of glomeruli in the mammalian kidney, studied animals ranging in size from the mouse to an elephant and determined that glomerular volume was closely related to kidney weight and to body weight. The mouse and the kangaroo rat were exceptions to the general rule, for although the kidney-body weight ratio was "normal," the glomerular volume in these 2 species was decreased per unit of kidney. Figures for the mouse based on the examination of 8 specimens were: body weight, 20 gm.; kidney weight, 0.123 gm.; glomerular radius, 36.7μ; number of glomeruli in 1 kidney, 12,430; and total glomerular volume of 1 kidney, 2.6 mm.^{3}

When these figures were compared with those for other mammals examined, the mouse had only one-half the total glomerular volume that was predicted from either kidney or body weight. Rytand suggested as an explanation for this discrepancy that the mouse excreted a concentrated urine and could live for a long time without water. (This is contrary to experience at the National Cancer Institute. Laboratory mice usually die if deprived of water for more than 48 hours.) Rytand also considered it possible that Heidenhain's claim that the tubules of the mouse secreted urea might be a reason why the mouse required a relatively small volume of glomerular tissue.

JUXTAGLOMERULAR APPARATUS

The first description of this controversial and elusive structure, the preglomerular apparatus, was made by Ruyter (*3*) in 1925. He was investigating mitochondria and used the mouse kidney in these studies. Ruyter called attention to granular cells located in the afferent glomerular artery. On further investigation, he found similar cells in the kidney of the rat, but he was unable to find them in the kidney of man, monkey, dog, cat, rabbit, and guinea pig. Oberling (*4*), in discussing these preglomerular cells, stated that the granulations in the human kidney are much more delicate and scattered and that it was easy to understand how Ruyter, accustomed to the bright aspect of these cells in the mouse, failed to find similar elements in material from man. Oberling further suggested that there are two types of granular cells, the mouse type and the human type, and that the cells in the various species resemble one or the other. The gratifying ease with which these granular cells can be demonstrated in the kidney of the mouse is in contrast with the difficulty of revealing them in man. They are especially easy to locate in sections fixed in Zenker-formol and treated by the periodic acid technique as described by McManus (*5*). By this method the staining quality of the granules in these special cells of the vessel wall is slightly different from that of any granules in tubular epithelial cells (fig. 2, *A* and *B*). Masson's trichrome stain is also satisfactory and shows a variation in the number

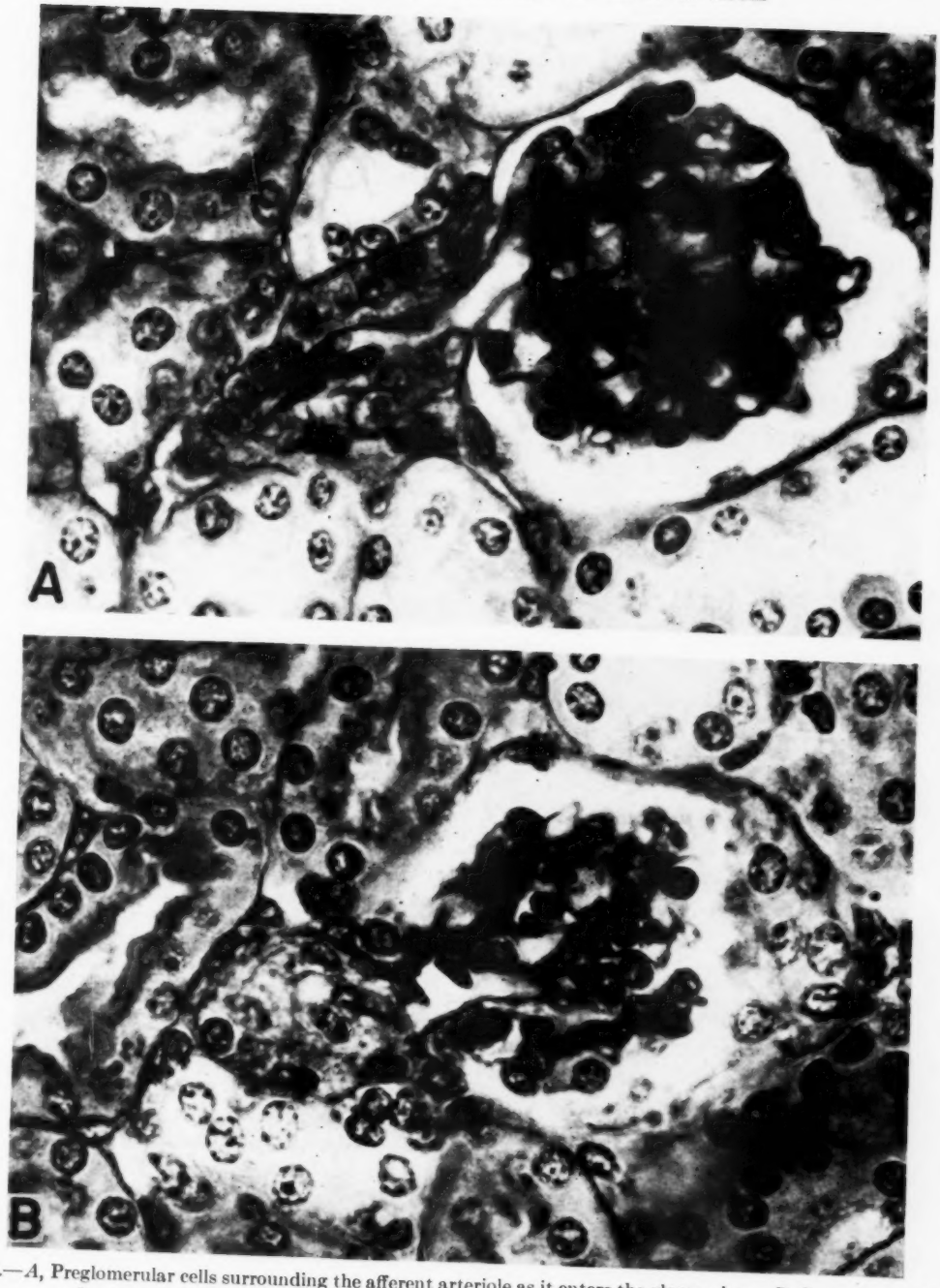

FIGURE 2.—*A*, Preglomerular cells surrounding the afferent arteriole as it enters the glomerulus. *B*, Granular preglomerular cells surrounding the lumen of the arteriole. Periodic acid technique. × 1100.

of granules and intensity of staining. The mouse, therefore, should be useful in investigations of the still unsettled problem of the function and pathologic alterations of this structure.

Sex Variation

Selye (*6*) stated that in many animal species the kidney of the male is larger than that of the female and that orchidectomy causes a decrease in renal size, while testoid administration to the castrated animal not only restores the volume of the kidney to normal but also may even cause considerable enlargement above normal. It thus appears that the kidney in many species may show a response to sex hormones. In addition to this difference in size related to sex, other readily evident sex differences are found in the mouse. It had been noted by several observers, among them Benda (*7*), that the parietal layer of Bowman's capsule in some glomeruli was lined by a cuboidal or columnar epithelium, but it remained for Crabtree (*8*) to demonstrate that these cuboidal-lined capsules were greatly increased in adult males in comparison with females and immature males (fig. 3, *A* and *B*). Crabtree (*9*) showed further that in castrated male mice the relative number of glomerular capsules lined by cuboidal epithelium remained small, but following treatment with testosterone the value returned to near that of normal males.

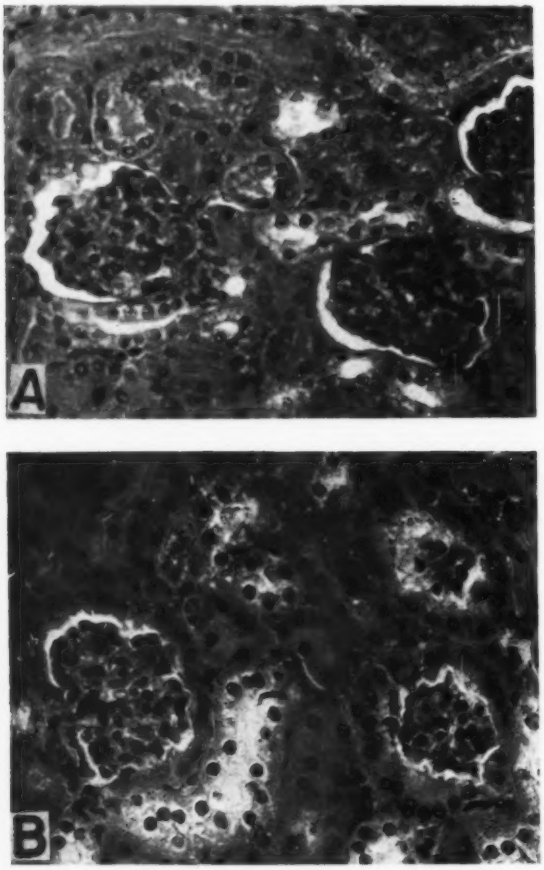

Figure 3.—Sex difference in kidney of mouse. *A*, Female: flattened epithelium lining parietal layer of Bowman's capsule; *B*, Male: cuboidal lining of parietal layer of Bowman's capsule. Hematoxylin-eosin stain. × 350.

This sex difference in the mouse is apparent in other ways besides morphology. Wicks (*10*) found in several inbred strains that persistent and marked proteinuria was present in males but not in females. Kochakian (*11*) showed that the kidneys of castrated male mice increased in size after the subcutaneous implantation of pellets containing various steroid hormones and that the alkaline phosphatase decreased both in total and per gram of tissue. In a later paper (*12*), he reported histochemical studies of kidneys of castrated male mice after stimulation with various androgens. With increasing dose levels, there was a progressive decrease in the enzyme as indicated by staining of the cells of the proximal convoluted tubules, and this proceeded from the proximal end toward the glomerulus, with a slight increase in concentration at the glomerular end. Kochakian did not report any studies on female mice. Emmel (*13*, *14*) also studied alkaline phosphatase activity, using the kidneys of albino mice. In one publication, the sex of the animals was not given; and in a second publication, only male animals were included. I noted a sex difference in distribution of the alkaline phosphatase in the mature mouse (*15*). Kidneys from several inbred strains of mice at varying ages were examined by the Gomori technique, and kidneys from a few rats, guinea pigs, and rabbits were also treated in this way, care being taken that the paired male and female kidneys were handled identically (table 1). A sex difference was found only in mice. In both sexes, there was an intense staining of the entire cell throughout a short segment of the proximal

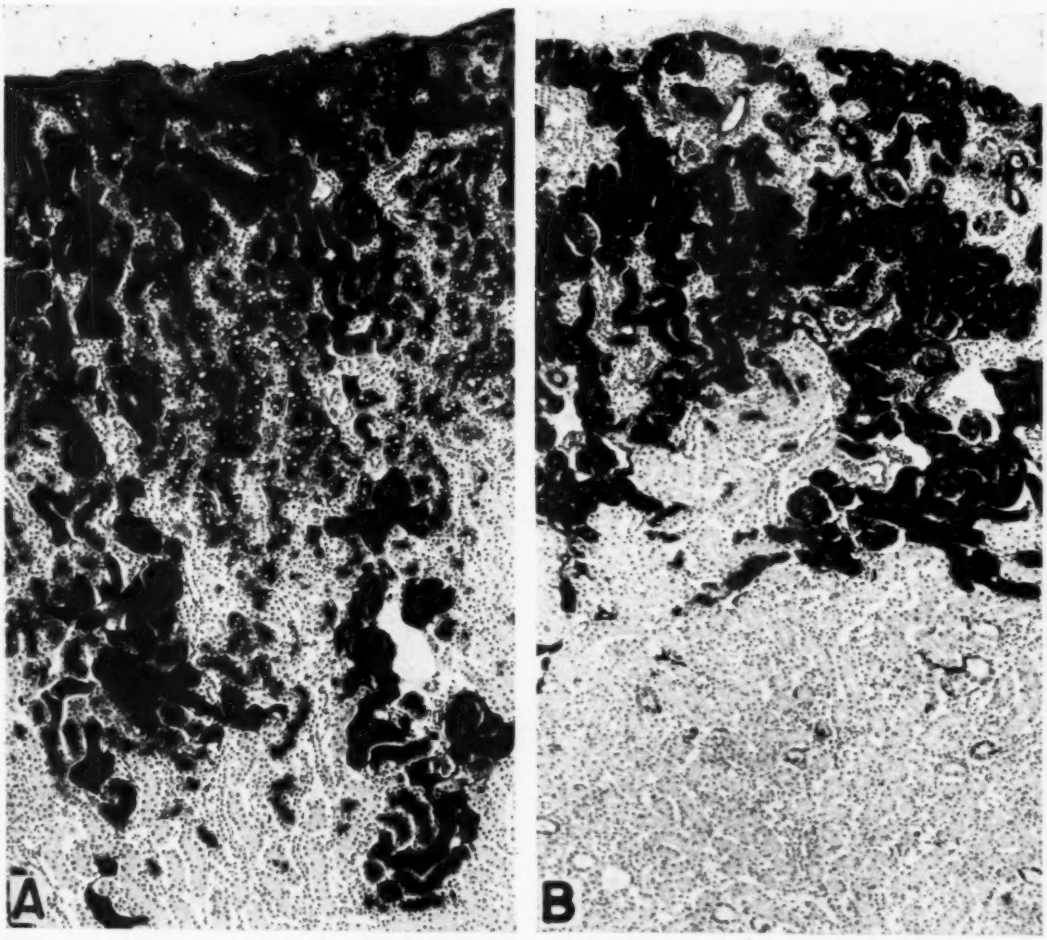

FIGURE 4.—Distribution of alkaline phosphatase in the kidney of the strain A mouse. *A*, male: staining affecting cells in proximal tubule in both zones of cortex, with staining of brush border only in more distal portion. *B*, Female: staining largely restricted to segment of proximal tubule in outer zone of cortex, with intense staining of entire cell. Alkaline phosphatase, Gomori method. × 90.

convoluted tubule for a short distance near the glomerulus (and the cuboidal lining of Bowman's capsule when this was present). In the male an additional segment showed an intense staining of the brush border only while the corresponding segment in the female was unstained (fig. 4, *A* and *B*). Less intensive degrees of staining might be found in the region of Henle's loop, but the staining of this segment of the nephron varied considerably with different strains of mice. It was thought to be most intense in strain dba females.

No investigation for possible changes in phosphatase distribution after alteration of the endocrine status or for possible minor differences in various inbred strains was made.

Kochakian (*16*) also reported chemical studies on the arginase activity of the tissues of the mouse after castration and treatment with various steroids. He stated that many steroids markedly increased and a few decreased the arginase content of the kidneys, although the enzyme content of the liver and intestine was unaffected.

TABLE 1.—*Alkaline phosphatase in male and female kidneys of mice, rats, guinea pigs, and rabbits*

Group	Age	Male and female kidney pairs	Strain	Result
Mice:			*Number*	
Mature	3-9 months	11	3 A 3 C3H 3 C 2 dba	Differences in sexes readily detected.
Newborn		5	1 A 1 C57 black 1 C3H 1 dba 1 C	No difference detected.
Young	1 month	4	2 C57 black 1 C3H 1 A	No difference detected in strains C57 black and A. Questionable difference in C3H.
	6 weeks		1 dba 1 C	No difference detected in strain C. A difference becoming apparent in dba.
Rats	Newborn to 9 months.	11	4 Marshall 4 Buffalo 3 Wistar	No sex difference at any age.
Guinea pigs	3 months	3		No difference detected.
Rabbits	5 months	1		Do.

PATHOLOGIC ANATOMY

CONGENITAL ANOMALIES

Congenital anomalies of the kidney have been infrequent in inbred strains of mice commonly used at the National Cancer Institute. A few instances were recorded of (1) congenital absence of one kidney, (2) variations from the normal in relative size of the two kidneys, (3) situs inversus viscerum in which the left kidney was higher in position than the right (a reversal of the usual situation), and (4) hydronephrosis. However, in certain groups of mice investigated in genetic studies at other laboratories, a high incidence of kidney anomalies was reported, usually in association with other congenital defects. Valuable data bearing on the mechanism of development of certain hereditary disturbances were acquired from these studies. Bagg (*17*, *18*) published a series of papers describing various abnormalities found in descendants of mice exposed to roentgen rays. It was concluded that the roentgen ray exposure of the ancestors was not directly causative. Of most interest, perhaps, were defects in the eyes and limbs, which Bonnevie (*19*) studied in the descendants and ascribed to the development of "myelencephalic blebs," extravasations from an excess of cerebrospinal fluid which moved through the subcutaneous tissues and came to rest in the orbital or limb-bud site. This fluid caused no permanent damage to the embryo, except at those sites where it accumulated in sufficient quantity to exert pressure on developing structures.

When hemorrhage from pressure and rupture of capillaries developed in these blebs, this apparently intensified the harmful effect, and a variety of anomalies resulted. It was Bonnevie's opinion that the kidney anomalies could not be explained as being due to the blebs or any similar formation, even though Bagg described the kidney defects as occurring in a stock homozygous for the gene for "myelencephalic blebs." Uncertainty, therefore, exists, whether the kidney abnormalities are due to the same gene. The commonest condition found affecting the urinary system was absence of one kidney and the ureter and renal vessels of the same side. The right and left sides were affected with nearly equal frequency. A slight difference in the size of the two kidneys, when compared with the normal, was the least serious condition encountered. Unilateral polycystic kidneys and hydronephrosis with distended ureters were observed infrequently. An explanation suggested for the development of hydronephrosis was obstruction of the ureter as it entered the bladder, but the mechanism by which polycystic kidneys developed was more difficult to conjecture. An interference with the embryological development and functional union of the component parts of the kidney was suggested by Bagg. Among the offspring of mice with single kidneys, complete absence of both kidneys was common. These mice without kidneys appeared normal at birth except that no urine was present in the bladder. In about 24 hours, however, they became sluggish, developed ascites, and died.

Brown (*20*) made a detailed study of the embryological development of these defective mice. Failure of the kidneys to develop was correlated with the failure of one or both ureters to make contact with the developing blastema of the kidneys, and it was the author's opinion that an associated aberrant vascular system retarded the normal developmental sequence and led to the kidney anomalies.

A kidney anomaly similar to that described by Bagg is found in Danforth's short-tail mice. A summary of the available information on this condition was given by Grüneberg (*21*). In

many instances, anomalies of the kidneys and ureters were found in the short-tailed mice. In the most extreme cases, both kidneys and ureters were completely missing; other short-tailed animals had apparently normal kidneys, although no histologic investigation had been reported. There was no direct correlation between tail length and the severity of the kidney anomaly. This anomaly differed from that reported by Bagg in the following details: kidneys of reduced size were more frequent, a normal ureter might be found in the absence of the kidney, and the left kidney was more frequently affected when the condition was hemilateral.

Sex Difference in Relation to Pathologic Lesions

The sex differences previously noted are probably significant in relation to certain pathologic processes. Eschenbrenner and Miller (*22*) found that female mice developed no necrosis of the convoluted tubules after doses of chloroform, which produced extensive necrosis in males and testosterone-treated, castrated males. I have occasionally found calcification developing in the kidneys of mice of the C3H strain kept as controls. The distribution of this calcific deposit showed a well-defined and consistent sex difference. In the male, the deposition was in the outer zone of the cortex, so that at autopsy the kidney surface appeared light yellow and granular. Microscopically, the calcium was seen in the glomeruli and proximal tubules near the capsule of the kidney, and a remarkable hypertrophy developed in a few uninvolved glomeruli which lay deep in the outer cortical zone. In the females, short segments of a few scattered tubules at the junction of the cortex and medulla were calcified (fig. *5*, *A* and *B*). Clinically, these mice appeared to be normally healthy and active, although at autopsy the bladder of the males was usually much distended with urine.

In addition to this idiopathic calcification in the kidneys of C3H mice, less definite forms of calcification are encountered in many strains of mice. The deposits may be found in epithelial cells in scattered segments of the tubules or in vessel walls. Although dietary deficiencies may have been present in some groups of mice, individual cases are found in which no cause for the calcium deposit has been determined.

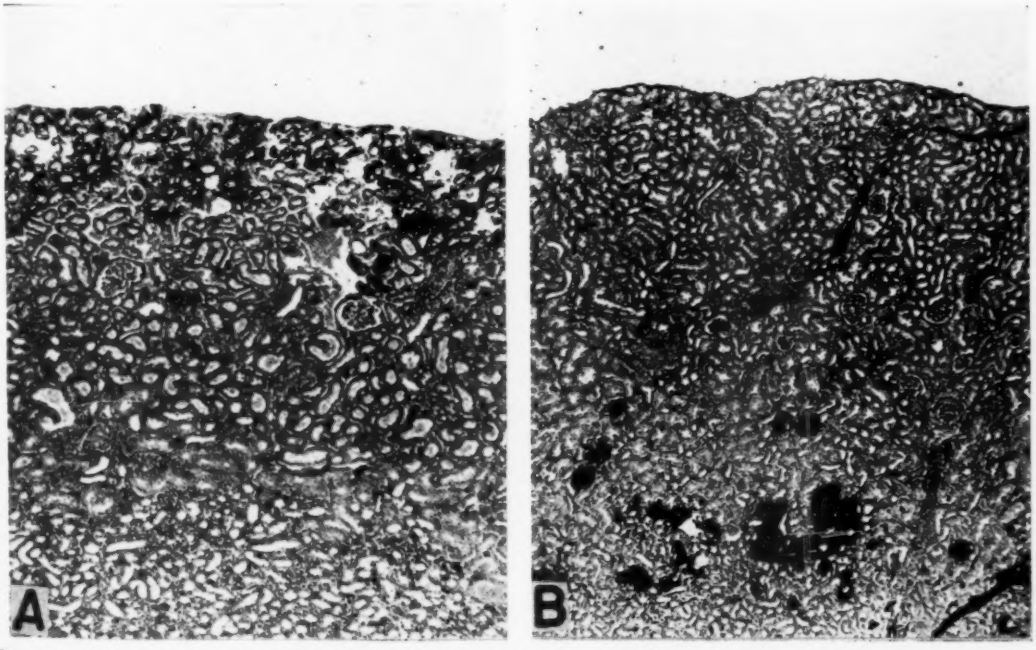

Figure 5.—Idiopathic deposition of calcium in kidneys of mice of strain C3H. *A*, Male: deposit in outer zone of cortex. *B*, Female: deposit in inner zone of cortex and outer zone of medulla. Hematoxylin-eosin stain. × 90.

Inflammatory Reaction, Urinary Obstructions, and Stone Formation

In cases of bacterial infection, the kidney frequently develops multiple abscesses and presents a picture of acute pyelonephritis, such as is seen in the human kidney. Stones in the pelvis are rare in untreated mice. Ascending infections are found where an obstruction occurs in the lower urinary tract, as not infrequently happens in old males with inflammation of the preputial glands. Burrows (*23*) described the development of hydronephrosis in female mice after the prolonged administration of estrogenic compounds. He suggested that a similar mechanism might be operating in the development of pyelitis in pregnant women, and that the condition in both species is due to disturbance of the neuromuscular apparatus and incomplete drainage from the kidney pelvis. In a later paper with Kennaway (*24*) he described the development of bladder distention and hydronephrosis in male and female mice following applications of estrin to the skin. An accumulation of keratinized material in the vagina, leading to urinary obstruction, was considered responsible in the female while in the male a similar condition developed from distension of the prostatic alveoli with keratin, and obstruction of the urethra. Hooker and Pfeiffer (*25*) noted a similar response in male mice of strain A when they were given large doses of estrogens in order to induce testicular tumors. The authors reported that many of the treated animals exhibited greatly distended bladders and an associated hydroureter and hydronephrosis which was occasionally of sufficient severity to prove fatal. Burns and Schenken (*26*) also reported that strain C3H mice treated with estrogen developed urinary stones in a third of 151 treated male mice, while 6.3 percent of untreated females developed stones in the bladder only. The stones in the treated animals were found mostly in the bladder, but occasionally they appeared in the urethra, ureters, and kidneys. The incidence which these authors reported in untreated mice is remarkably high, compared with our experience at the National Cancer Institute. Lacassagne (*27*) recorded hydronephrosis following injections of female sex hormone.

Perivascular round-cell infiltrations are frequently observed in the kidneys of old mice. A similar condition is usually found in other organs as well, and except for senility no other condition has been regularly found associated with this infiltration.

Parasitic Infestation

Laboratory mice are frequently infected by an organism, *Klossiella muris*, a sporozoan belonging to the order Coccidia, first described by Smith and Johnson (*28*). The organism develops and multiplies within the epithelial cells of the convoluted tubules, so that the affected cells become greatly enlarged and protrude into the lumen. A difference of opinion exists with regard to the pathogenicity of this organism. Smith and Johnson remarked that no so-called inflammatory reaction could be associated with various stages of the organism, although mechanical compression and obstruction led to cell destruction. Twort and Twort (*29*), on the other hand, considered *K. muris* as the causal agent in most cases of "nephritis." Infestation occurred spontaneously in 90 percent of their mice at 12 months of age, so controlled observations of noninfected mice were not possible. Our experience with infected and noninfected colonies of mice at the National Cancer Institute

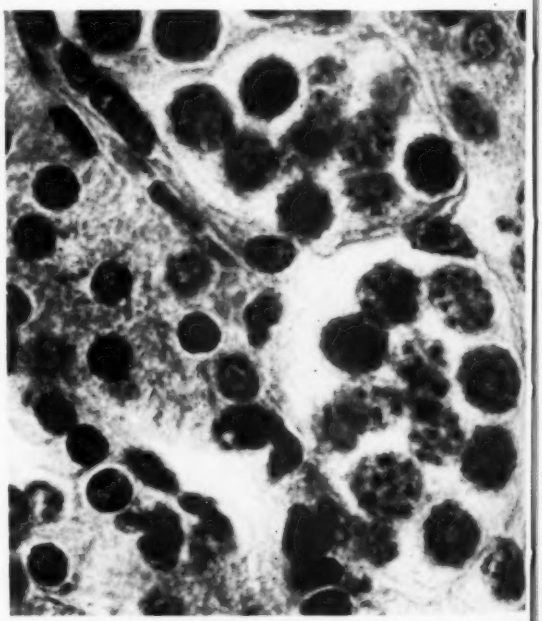

Figure 6.—*Klossiella muris* in tubular cells of kidney of mouse. Note absence of inflammatory reaction. Hematoxylin-eosin stain. × 1100.

makes us doubtful that these organisms cause any significant damage. Strain A mice in one colony at the National Cancer Institute are free of any infection with *K. muris*, while animals of another colony maintained as a separate line are often infected, yet no difference in longevity or general health has been detected in these two groups. Animals of strain dba kept in one animal room are frequently infected, yet these mice appear healthy and have a low incidence of renal disease. Kidneys having many parasites may show no evidence of inflammatory reaction (fig. 6). Others show areas of lymphocytic infiltration which cannot be directly ascribed to this infestation, since similar infiltrations may be found in uninfected kidneys.

Abnormal Deposits

HEMOSIDERIN

The mouse, like other laboratory animals, accumulates iron-positive pigment in the cells of the proximal convoluted tubules when the iron content of the blood rises above the glomerular threshold. This was demonstrated in the rabbit after hemolysis by Muir and Dunn (*30*) and in the dog after intravenous injection of hemoglobin by Newman and Whipple (*31*). Cappell (*32*) injected saccharated iron intravenously in the mouse. The initial deposit in the kidney was in isolated cells of the capillary walls of the glomeruli and intertubular tissue. When the injections were continued, granules of iron-positive pigment were prominent in the cells of the proximal convoluted tubules. These granules disappeared gradually when no further injections were given. I have found a great accumulation of such iron-positive granules in the kidneys of mice which had a hemolytic anemia resulting from the ingestion of toluidine blue. (Dunn, publication pending.) The granules were found not only in the proximal convoluted tubules but in the cuboidal epithelium lining Bowman's capsule (fig. 7).

This type of hemosiderosis which affects rather equally all the tubules presumably results from a filtration of iron-containing substances through the glomerulus. However, hemosiderosis affecting scattered groups of tubules is often found accompanying renal disease in mice. Cappell observed that in the kidneys of mice with "patchy chronic nephritis of spontaneous origin" the iron reaction appeared earlier and was more pronounced, which he presumed to be due to an increased permeability of the glomerular tufts. In the renal disease accompanying amyloidosis, iron-positive staining of the tubules in affected areas is usual, and in kidneys of strain A mice damaged by urethan, a positive prussion blue reaction in the tubules may be the earliest sign of injury.

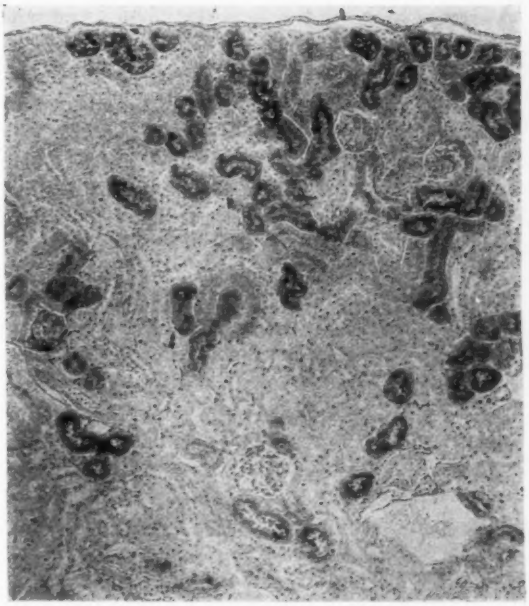

FIGURE 7.—Hemosiderosis in kidney of mouse; iron-positive granules in cells of proximal convoluted tubules. Prussian blue reaction. × 85.

AMYLOID INFILTRATION

A kidney disease of mice characterized by necrosis of the tip of the papilla, the formation of multiple cysts, and patchy atrophy of the tubular epithelium was described by Gorer (*33*) and by Kirschbaum (*34*). These authors suspected that some congenital hereditary factor was responsible, since the lesion occurred frequently in certain strains of mice, notably strain A. In a study by Dunn (*35*) in this laboratory, it was observed that the renal lesion was nearly always associated with amyloid deposition in other organs which developed spontaneously in a high percentage of strain A mice past 12 months of age. This form of amyloidosis had several points of similarity to the condition of primary or idiopathic amyloidosis in man, since no underlying inflammatory condition

was recognized, and a greater deposition was found in mesodermal tissues, especially the connective tissue of the gastrointestinal tract, the myocardium and the suprarenals, than in the liver, spleen, and lymph nodes. Amyloid deposition in the kidney papilla resulted in obstruction at this critical point, with consequent atrophy or dilatation of the tubules. The histologic features of this renal disease resembled chronic or healed pyelonephritis in the human being, where partial obstruction is also considered important in pathogenesis (fig. *8*, *A*).

It has been noted that mice of other strains, in which the incidence of spontaneous amyloidosis is low, will develop amyloid infiltration in the spleen and liver readily if chronic inflammatory conditions such as dermatitis or abscess develop, or from parenteral injections of a variety of substances, among them, sodium caseinate, as described by Smetana (*36*). In this secondary form of amyloidosis, the histologic changes in the kidney are often similar to those observed in the spontaneous disease of strain A. Heston (*37*), by means of crosses between strain A with a high incidence of spontaneous amyloidosis and strain L, in which this condition is not found, showed that the inheritance of the tendency to develop primary amyloidosis and the associated renal lesion is on a genetic basis and probably due to a single recessive gene.

These reports on renal lesions in mice are of interest and possible significance in relation to renal diseases in man. It has been reported that the American Negro develops hypertensive disease more frequently and at an earlier age than do individuals of other races in a similar environment. It has been further shown from autopsy material that this hypertension is often directly associated with organic renal disease, as reported by Taylor in Panama (*38*).

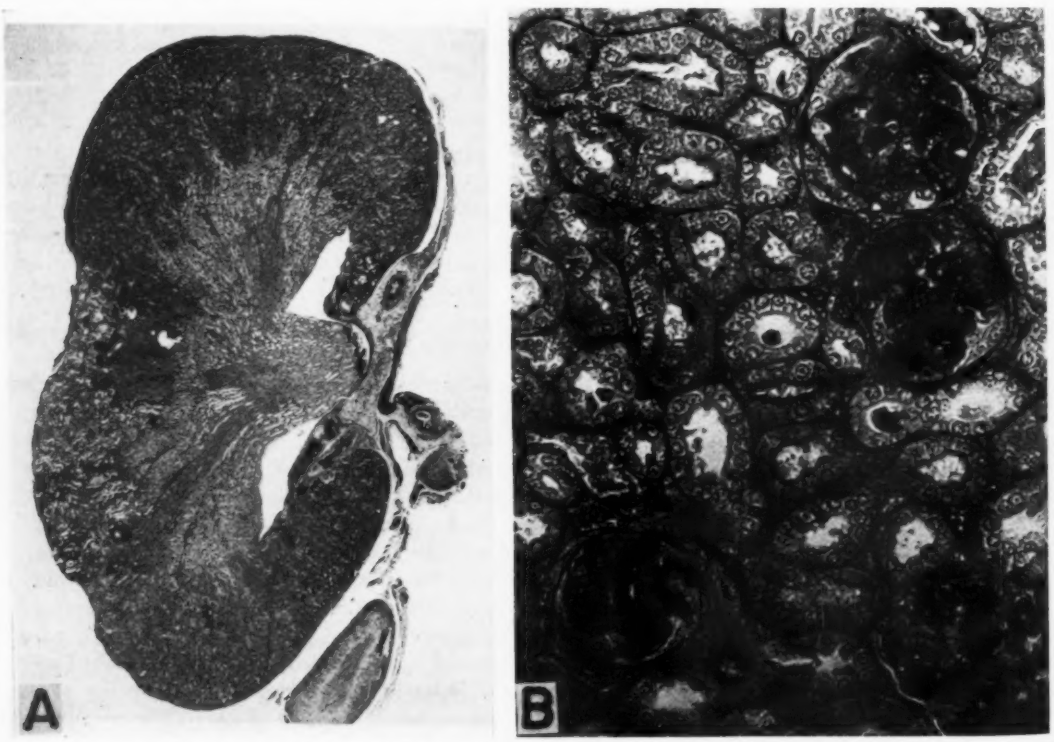

FIGURE 8.—Amyloidosis affecting kidney of mouse. *A*, Amyloid deposited in papilla causing obstruction and areas of atrophy of kidney tubules. Observe amyloid in adrenal. Hematoxylin-eosin stain. × 12. *B*, Amyloid deposited in glomerular loops. Observe that tubules appear nearly normal. Heidenhain-azan stain. × 350.

Dunn (*39*) reported a high incidence of a kidney lesion which fulfilled the histologic criteria of a chronic or healed pyelonephritis in Negro women dying with hypertension. Because of this racial incidence, an investigation for the possible existence of amyloid deposition in such cases in Negroes might be fruitful. Amyloid is easily overlooked in routine autopsies, and the kidney papillae, in which possible deposits will have serious consequences do not often receive a discriminating search for this substance.

Gorer described a condition in mice which he refers to as "hyaline disease." With hematoxylin-eosin staining, the glomeruli appear heavily infiltrated by a slightly eosinophilic, homogeneous material, while the tubules and papillae appear normal. I have seen a similar lesion occasionally, usually in very old mice of the C57 black strain, and I consider it another form of amyloid deposition affecting the glomeruli primarily (fig. *8*, *B*).

Besides these two conditions, one in which the main deposit is in the papilla, and the other affecting the glomeruli primarily, various combinations are found with amyloid deposition at these two sites and also between the tubules of the cortex. This multiple distribution is especially frequent if the amyloidosis is secondary.

Some hesitancy is proper in considering this homogeneous, hyaline infiltration as amyloid, since differential staining is frequently unsuccessful. A report by Turnbull (*40*), in which these deposits were carefully investigated, concluded that this substance can safely be called "mouse amyloid."

A point of interest is the appearance of mast cells in the kidneys in which amyloid deposits are present. Mast cells have not been seen in normal kidneys but are usually present in areas of tubular atrophy and fibrosis after amyloid obstruction.

Glomerular Lesions

SPONTANEOUS LESION IN STRAIN NH

Kirschbaum (*41*) described a spontaneous kidney disease in strain NH mice, which is said to resemble glomerulonephritis in man and is accompanied by clinical evidence of renal failure. This disease appears to be restricted to this strain of mice. We have not seen a similar condition in material examined at the National Cancer Institute.

LESION PRODUCED IN STRAIN A MICE BY URETHAN

An instance of the remarkable individuality which develops in inbred strains of mice is the induction of glomerular injury by urethan in strain A mice first reported by Dunn and Larsen (*42*). Kirschbaum and Bell (*43*) produced a similar condition in the same NH strain in which Kirschbaum described a spontaneous glomerular lesion. No other strain of mice examined at the National Cancer Institute (C, C3H, and I) or other laboratory animals (rat, guinea pig, and rabbit) in which the procedure has been tried have reacted in this way to urethan. This urethan lesion is notable in that the glomeruli are primarily affected (fig. 9), and the animal develops a generalized edema. Deposits of a hyaline substance accumulate in the glomerular tufts, adhesions between the visceral and parietal layer of Bowman's capsule are found which may form small cysts in Bowman's space. As the process continues, numerous hyaline casts are found in the tubules. No leukocytic reaction has been observed. A more detailed study of this lesion is now in progress at the National Cancer Institute, in connec-

FIGURE 9.—Glomerular lesion produced by urethan. Upper glomerulus shows adhesions and formation of small cysts between layers of Bowman's capsule. Lower glomerulus contains an amorphous hyaline substance. A few casts are seen in the tubules. Periodic acid technique. ×350.

tion with a study of urethan in the histogenesis of lung tumors.

Tumors

Primary neoplasms of the kidney are extraordinarily rare in the mouse. Tyzzer found 4 in a total of 83 tumors in 70 mice, and he described these in a series of 3 papers (*44*, *45*, *46*). All were of small size; 2 appeared to be intracystic growths; and 1 he classified as a hypernephroma because of its histologic similarity to the clear cell tumors commonly seen in man, which at that time were considered to be derived from adrenal cell rests in the kidney.

Haaland (*47*) described 2 adenocarcinomas of the kidney in a group of 333 tumors. One of these tumors was the size of a small walnut and replaced the kidney. The second, the size of a pea, was given a questioned diagnosis of hypernephroma. Slye, Holmes, and Wells (*48*) reported only five kidney tumors of epithelial origin in 33,000 autopsies. Three of these tumors were small, less than 5 mm. in diameter; they were encapsulated, and histologically the cells making up the tumor resembled renal epithelium. One of the five tumors was about the size of a normal kidney; histologically it did not appear to be of either kidney or adrenal-cell origin, and a diagnosis of possible mesothelioma was made. The remaining tumor was diagnosed as hypernephroma. These authors remarked that it was strange that they had found so few instances of epithelial neoplasms in the kidney of the mouse. Seven sarcomas of the kidney were diagnosed but no renal tumors of Wilms' type. Cloudman (*49*) reporting from the Jackson Memorial Laboratory at Bar Harbor, Maine, listed only 2 epithelial tumors of the kidney. One was diagnosed adenoma of renal tubules, and 1 a papillary cystadenocarcinoma.

From a review of these 13 published reports of epithelial tumors in the kidney of the mouse, certain similarities can be noted. All except 2 were small and apparently accidental findings. Three appeared to be intracystic growths, and all except 1 resembled cells of the kidney tubules or adrenal cortex. No successful transplantations were made, and only 2 of these tumors were thought to be malignant.

Observations at the National Cancer Institute are in accord with these reports from other laboratories. Epithelial tumors of the kidney have been rare. No figure has been compiled of the total number of mice examined, but autopsy reports of only eight primary epithelial tumors of the kidney are available. Two of these occurring in strain A mice were described by Lippincott, Edwards, Grady, and Stewart (*50*). Both were in old mice and were small. The other six tumors were also found in old mice of strain A or strain A hybrids, and were not associated with any experimental procedure. All were small and not identified as tumors until microscopic sections were examined, hence no attempt at transplantation had been made. Three of these six tumors were cystic and three were solid adenomatous growths (fig. 10, *A* and *B*). The cells of the solid tumors were arranged in cords. The cell nuclei were small and deeply stained, and the cytoplasm was eosinophilic and finely vacuolated. Mitotic figures were rare, and the tumor margins compressed but did not invade the normal kidney tissue (fig. 11). The cystic tumors were of interest, since they resemble tumors previously described by Tyzzer and Cloudman. This cyst formation shown by kidney tumors may be the explanation of small microscopic cysts lined by a single layer of epithelial cells which are occasionally found in the kidney (fig. 12). Such cysts may represent an early stage in the development of intracystic neoplasms, for they are unassociated with inflammatory processes, and no cause for them has been found.

Not only are spontaneous tumors of the kidney rare, but several attempts at induction of tumors derived from the epithelial cells of the kidney have been reported as unsuccessful. Ilfeld (*51*) embedded pellets of cholesterol and methylcholanthrene in the kidney in 51 mice of various inbred strains. Although 10 epidermoid carcinomas developed, there were no tumors resembling the adenomas found spontaneously in the mouse, the type which may be considered as a true or intrinsic tumor of the kidney and of specific renal cell origin. Esmarch, as quoted by Rask-Nielsen (*52*), injected methylcholanthrene, 10 mg., into 13 Bagg albino mice. Eleven developed spindle-cell sarcomas and one a squamous cell carcinoma. Stewart [2] in this laboratory inserted strings im-

[2] Stewart, H. L.: Personal communication.

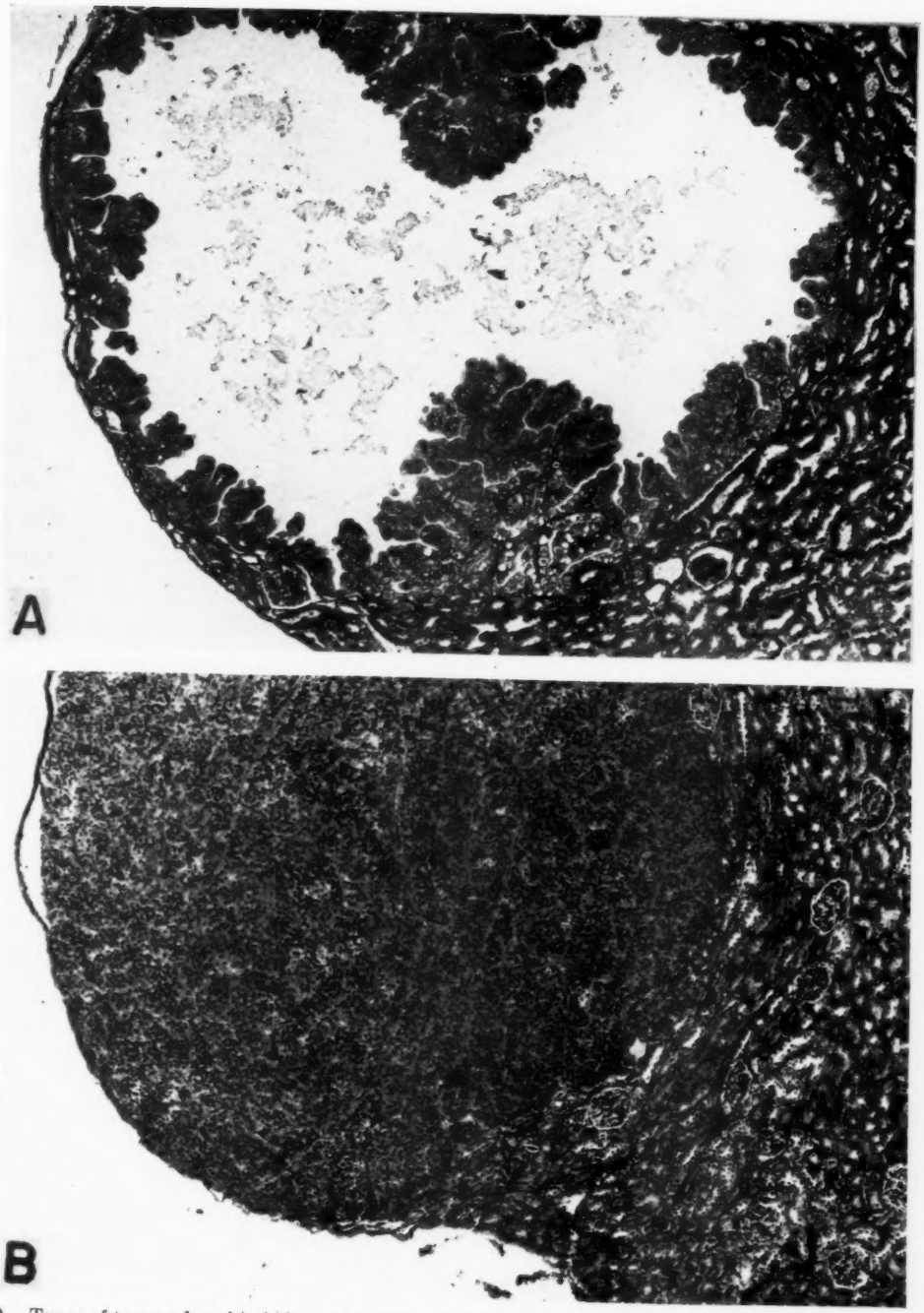

FIGURE 10.—Types of tumors found in kidney of mouse. *A*, Intracystic papillary growth; *B*, Solid adenomatous growth. Hematoxylin-eosin stain. × 85.

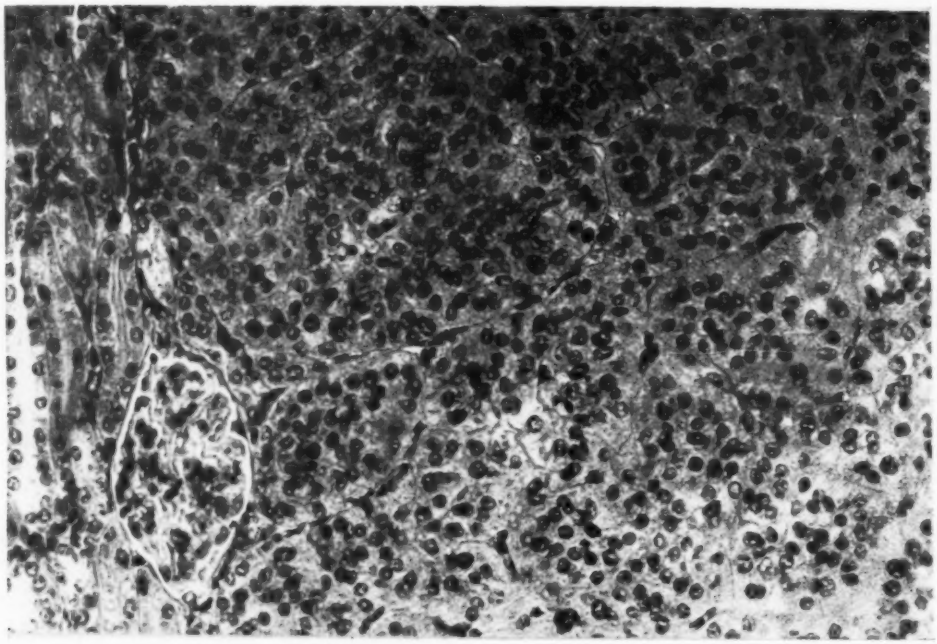

FIGURE 11.—High power view of adenomatous tumor of kidney shown in figure 10, *B*. Observe vacuolation of cells in lower right corner, and compression of glomerulus and kidney tubules. Hematoxylin-eosin stain. × 350.

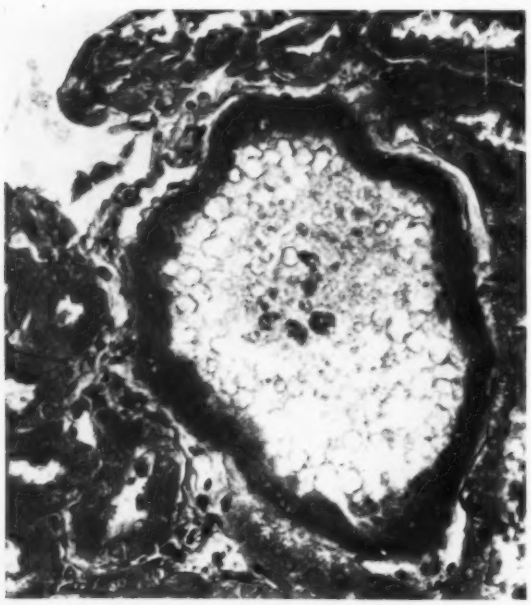

FIGURE 12.—Small cyst of kidney lined by cuboidal epithelium. A possible stage in the development of intracystic papillary tumors. Hematoxylin-eosin stain. × 350.

pregnated with methylcholanthrene, dibenzanthracene, or benzyprene into the kidney so that the carcinogen was in contact with cells of the kidney cortex. Twenty-two animals survived 5 to 15 months. Six sarcomas and three squamous-cell carcinomas developed, but no tumors which could be considered as derived from the renal epithelial cell, as is the Grawitz type tumor in man. Armstrong and Bonser (*53*) gave 2-acetyl-aminofluorene for a prolonged period to over 100 mice of 5 different strains. Tumors developed frequently in the bladder, liver, and female breast. One transitional cell carcinoma of the renal pelvis was found, but no renal tumors.

The rarity of spontaneous tumors in the kidney of the mouse and the failure to produce such tumors by carcinogens are perhaps as significant to the problem of cancer as is the susceptibility of other tissues. It is another illustration of the frequently reported observation that carcinogenic agents enhance a natural susceptibility, eliciting at an earlier age and in larger numbers those types of tumors most often found spontaneously. Where the spontaneous incidence of a tumor is low, the

artificial induction by carcinogenic agents is frequently unsuccessful.

Metastatic Neoplasms

Occasional metastases to the kidney result from the primary growth of sarcomas and carcinomas at distant sites, but except for leukemia, the kidney is a rare site of secondary growth. Wells, Slye, and Holmes (*5.4*) reported that of 2,865 mice bearing lung tumors which died spontaneously, 3.6 percent showed metastases outside the lungs, and 5 of these were to the kidney. In lymphatic leukemia, the kidney is a frequent site of infiltration, and some strains of transplanted leukemia show a special predilection for the kidney. I have seen two cases of mast-cell leukemia, in which accumulations of these cells were found in the kidney.

SUMMARY

From a review of the literature and unpublished observations made at the National Cancer Institute, the following information concerning the kidney of the mouse is presented:

The kidney of the mouse is similar to the kidney of the rat in general architecture and the arrangement of parts of the nephron into well-defined zones.

Granular cells of the preglomerular apparatus are easily demonstrated, particularly after treatment by the periodic-acid technique.

In comparison with the kidney of other mammals, the mouse kidney has a small amount of glomerular tissue in relation to kidney weight and body weight.

A sex difference is detectable in the kidney of the mouse. Morphologically, this consists in a higher ratio in the male of glomeruli lined by cuboidal epithelium. A difference in the distribution of alkaline phosphatase can also be demonstrated.

Congenital anomalies are infrequent. Absence of one or both kidneys, polycystic kidneys, and hydronephrosis are reported in association with other defects. Embryologic studies of the development of these anomalies are reported.

The sex of the animal affects the development of pathologic processes in the mouse. Examples are the relative resistance of females to chloroform poisoning and a difference in the location of calcium deposits in the kidney in strain C3H mice.

Infestation by *Klossiella muris* is frequent in some laboratories. This organism produces little if any inflammatory reaction or clinical manifestation of disease.

Iron deposition may be seen in the cells of the proximal convoluted tubules, when the glomerular threshold is exceeded by an iron compound in the blood, or when there is damage to the kidney glomerulus and a lowering of the normal threshold.

Renal lesions accompanying a generalized amyloidosis are frequently encountered in certain inbred strains. This lesion is similar in many histologic features to chronic pyelonephritis in man.

A lesion diagnosed as spontaneous glomerulonephritis is reported.

Renal lesions were produced in two inbred strains of mice treated with urethan.

Primary neoplasms of the kidney are extraordinarily rare in the mouse. No report on the successful induction of tumors reproducing the types which occur spontaneously has been found.

REFERENCES

(*1*) McFarlane, D.: Experimental phosphate nephritis in the rat. J. Path. & Bact. 52: 17–24 (1941).

(*2*) Rytand, D. A.: The number and size of mammalian glomeruli as related to kidney and to body weight, with methods for their enumeration and measurement. Am. J. Anat. 62: 507–520 (1938).

(*3*) Ruyter, J. H. C.: Uber einen merkwurdigen Abschnitt der Vasa afferentia in der Mauseniere. Ztschr. f. Zellforsch. u. mikros. Anat. 2: 242–248 (1925).

(*4*) Oberling, C.: Further studies on the preglomerular cellular apparatus. Am. J. Path. 20: 155–164 (1944).

(*5*) McManus, J. F. A.: Histological demonstration of mucin after periodic acid. Nature, London 158: 202 (1946).

(*6*) Selye, H.: Textbook of endocrinology. Acta Endocrinologica. Université de Montréal, Montréal (1947).

(7) BENDA, C.: Ein interessantes Structurverhaltnis der Mauseniere Anat. Anz. 2: 425 (1887).

(8) CRABTREE, C. E.: The structure of Bowman's capsule as an index of age and sex variation in normal mice. Anat. Rec. 79: 395–413 (1941).

(9) ———: Structure of Bowman's capsule in castrate and testosterone treated male mice as index of hormonal effects on renal cortex. Endocrinology 29: 197–203 (1941).

(10) WICKS, L. F.: Sex and proteinuria of mice. Proc. Soc. Exper. Biol. & Med. 48: 395–400 (1941).

(11) KOCHAKIAN, C. D.: The effect of various steroid hormones on the "alkaline" and "acid" phosphatases of the kidney of the mouse. Am. J. Physiol. 145: 118–122 (1945).

(12) ———: Histochemical study of alkaline phosphatase of the kidney of the castrated mouse after stimulation with various androgens. Am. J. Physiol. 152: 257–262 (1948).

(13) EMMEL, V. M.: The intracellular distribution of alkaline phosphatase activity following various methods of histologic fixation. Anat. Rec. 95: 159–175 (1946).

(14) ———: A cytochemical and quantitative study of the effects of potassium cyanide on alkaline phosphatase activity in the kidney and intestine. Anat. Rec. 96: 423–437 (1946).

(15) DUNN, T. B.: Sex difference in the alkaline phosphatase distribution in the kidney of the mouse. Am. J. Path. 24: 719–720 (1948).

(16) KOCHAKIAN, C. D.: The effect of castration and various steroids on the arginase activity of the tissues of the mouse. J. Biol. Chem. 155: 579–589 (1944).

(17) BAGG, H. J.: Hereditary abnormalities of the viscera. I. A morphological study with a special reference to abnormalities of the kidneys in the descendants of X-rayed mice. Am. J. Anat. 36: 275–311 (1925).

(18) ———: Hereditary congenital anomalies of the genito-urinary organs. Am. J. Surg. 7: 211–220 (1929).

(19) BONNEVIE, K.: Embryological analysis of gene manifestations in Little and Bagg's abnormal mouse tribe. J. Exper. Zool. 67: 443–520 (1934).

(20) BROWN, A. L.: An analysis of the developing metanephros in mouse embryos with abnormal kidneys. Am. J. Anat. 47: 117–171 (1931).

(21) GRÜNEBERG, H.: The genetics of the mouse. Cambridge Univ. Press (1943).

(22) ESCHENBRENNER, A. B., and MILLER, E.: Sex differences in kidney morphology and cholorform necrosis. Science 102: 302–303 (1945).

(23) BURROWS, H.: Pyelitis of pregnancy in the light of conditions found in mice after the prolonged administration of oestrogenic compounds. Proc. Roy. Soc. Med. 29: 404–406 (1936).

(24) BURROWS, H., and KENNAWAY, N. M.: On some effects produced by applying oestrin to the skin of mice. Am. J. Cancer 20: 48–57 (1934).

(25) HOOKER, C. W., and PFEIFFER, C. A.: The morphology and development of testicular tumors in mice of the A strain receiving estrogens. Cancer Research 2: 759–769 (1942).

(26) BURNS, E. L., and SCHENKEN, J. R.: Occurrence of urinary calculi in inbred strains (C3H) of mice treated with estrogen. Proc. Soc. Exper. Biol. & Med. 40: 497–498 (1939).

(27) LACASSAGNE, A.: Metaplasie epidermoide de la prostate provoquee, chez la souris, par des injections repetees de fortes doses de folliculine. Compt. rend. Soc. de biol. 113: 590–592 (1933).

(28) SMITH, T., and JOHNSON, H. P.: On a coccidium (Klossiella muris, gen. et. spec. nove.) parasitic in the renal epithelium of the mouse. J. Exper. Med. 6: 303–316 (1902).

(29) TWORT, J. M., and TWORT, C. C.: Diseases in relation to carcinogenic agents among 60,000 experimental mice. J. Path. & Bact. 35: 219–242 (1932).

(30) MUIR, R., and DUNN, J. S.: The retention of iron in the organs in hemolytic anemia. J. Path. & Bact. 19: 417–428 (1915).

(31) NEWMAN, W. V., and WHIPPLE, G. H.: Hemoglobin injections and conservation of pigment by kidney, liver, and spleen. The influence of diet and bleeding. J. Exper. Med. 55: 637'–652 (1932).

(32) CAPPELL, D. F.: The late effects of intravenous injection of colloidal iron. J. Path. & Bact. 33: 175–196 (1930).

(33) GORER, P. A.: Renal lesions found in pure lines of mice. J. Path. & Bact. 50: 25–30 (1940).

(34) KIRSCHBAUM, A.: Polycystic kidney disease in inbred mice. Anat. Rec. 88: 440 (1944). [Abstract of paper printed by Am. Assoc. of Anatomists (1944).]

(35) DUNN, T. B.: Relationship of amyloid infiltration and renal disease in mice. J. Nat. Cancer Inst. 5: 17–28 (1944).

(36) SMETANA, H.: Experimental study of amyloid formation. Bull. Johns Hopkins Hosp. 37: 383–391 (1925).

(37) HESTON, W. E., and DERINGER, M. K.: Hereditary renal disease and amyloidosis in mice. Arch. Path. 46: 49–58 (1948).

(38) TAYLOR, C. D.: The racial distribution of nephritis and hypertension in Panama. Am. J. Path. 21: 1031–1046 (1945).

(39) DUNN, T. B.: Chronic or healed pyelonephritis in negro women dying with hypertensive heart disease. South. M. J. 34: 593–597 (1941).

(40) TURNBULL, H. M.: The nature of the substance deposited in the spleen and liver of the mice in Dr. D. L. Parson's experiments. (Addendum to paper by Parson, D. L.: Tissue changes in experimental mice treated with pentose nucleotides.) J. Path. & Bact. 57: 18–20 (1945).

(41) KIRSCHBAUM, A.: A spontaneous glomerulonephritis in mice. Proc. Soc. Exper. Biol. & Med. 55: 280–281 (1944).

(42) DUNN, T. B. and LARSEN, C. D.: Hyalinization of glomeruli produced in strain A mice by the administration of urethan (ethyl carbamate). Fed. Proc. 5:220 (1946).

(43) KIRSCHBAUM, A., and BELL, E. T.: Induction of renal glomerular lesions by urethan in inbred mice susceptible to spontaneous glomerulonephritis. Proc. Soc. Exper. Biol. & Med. 64: 71–72 (1947).

(44) TYZZER, E. E.: The simultaneous occurrence of two non-related tumors in a mouse. J. A. M. A. 47: 1237–1241 (1906).

(45) ———: A series of twenty spontaneous tumors in mice with the accompanying pathological changes and the results of the inoculation of certain of these tumors into normal mice. J. M. Research 17: 115–197 (1907).

(46) ———: A series of spontaneous tumors in mice with observations on the influence of heredity on the frequency of their occurrence. J. M. Research 21: 479–518 (1909).

(47) HAALAND, M.: Spontaneous tumors in mice. 4th Scient. Rep. Imp. Cancer Research Fund, pp. 1–113 (1911).

(48) SLYE, M., HOLMES, H. F., and WELLS, H. G.: Primary spontaneous tumors in the kidney and adrenal of mice. Studies on the incidence and inheritability of spontaneous tumors in mice. Am. J. Cancer 6: 305–336 (1921).

(49) CLOUDMAN, A. M.: Spontaneous neoplasms in mice. *In* Biology of the Laboratory Mouse. Roscoe B. Jackson Memorial Laboratory. Blakiston Co. Philadelphia (1941).

(50) LIPPINCOTT, S. W., EDWARDS, J. E., GRADY, H. G., and STEWART, H. L.: A review of some spontaneous neoplasms in mice. J. Nat. Cancer Inst. 3: 199–209 (1942).

(51) ILFELD, F. W.: The experimental production of visceral tumors with hydrocarbons. Am. J. Cancer 26: 743–753 (1936).

(52) RASK-NIELSEN, R.: On the development of tumors in various tissues in mice, following direct application of a carcinogenic hydrocarbon. Acta path. et microbiol. scandinav. Suppl. 78: 9–144 (1948).

(53) ARMSTRONG, E. C., and BONSER, G. A.: The carcinogenic action of 2-acetyl-amino-fluorene on various strains of mice. J. Path. & Bact. 59: 19–27 (1947).

(54) WELLS, H. G., SLYE M., and HOLMES, H. F.: The occurrence and pathology of spontaneous carcinoma of the lung in mice. Cancer Research 1: 259–261 (1941).

819164—49——4

ALDOLASE IN THE SERUM AND TISSUES OF TUMOR-BEARING ANIMALS[1,2]

By JOHN A. SIBLEY and ALBERT L. LEHNINGER, *Department of Surgery, University of Chicago*

INTRODUCTION

In 1943 Warburg and Christian reported that five of the enzymes involved in glycolysis (aldolase (zymohexase),[3] triose phosphate isomerase, lactic dehydrogenase, and two of the transphosphorylases) were normally present in the blood serum of rats (*1*). They found that the levels of two of these enzymes, aldolase and triose isomerase, were increased above normal values in the serum of rats bearing the Jensen sarcoma. They presented data showing that the rise in serum aldolase paralleled the size of the tumor in relation to total body weight. The level of the enzyme in serum was found not to increase during pregnancy. After the intravenous injection of large amounts of crystalline aldolase into normal rats, the serum level rapidly declined to normal values implying that the normal level of aldolase in the serum is a resultant of a dynamic balance between rapid, massive liberation of the enzyme into the blood stream and rapid, massive removal. Since necrotic tumors showed no higher serum levels than non-necrotic tumors and since there was no arteriovenous difference in serum enzyme level noticed in the blood supply of the tumor, they concluded that the tumor itself was not the source of the increased level in the serum. Assay of various tissues revealed that muscle contained by far the highest content of aldolase, and Warburg and Christian suggested that the muscles are actually the source of the enzyme in serum.

In view of the fact that a high rate of aerobic glycolysis is a rather general biochemical characteristic of malignant cells, it is striking that one of the enzymes of the glycolytic mechanism should appear in large amounts in the serum of tumor-bearing rats. Although some enzymes normally present in serum are known to be elevated or depressed in tumor-bearing animals, the function of certain of these such as esterase, acid and alkaline phosphatases, etc., is not clearly understood in terms of cell physiology. However, the function of aldolase in cellular metabolism can probably be as accurately defined as the function of any known enzyme due to its high degree of substrate specificity and the extensive knowledge available concerning the role of glycolysis in carbohydrate metabolism.

Because of these considerations, it appeared to us that the findings of Warburg and Christian merited independent experimental examination and, if possible, extension. In this paper are presented the results of our study of the distribution of aldolase in normal and malignant tissues, in the serum of normal and tumor-bearing rats, and in human serum, and some of the factors governing the level of the enzyme in serum.

METHODS

Zymohexase (aldolase) was discovered in 1934 by Meyerhof and Lohmann (*2*) as an enzyme widely distributed in animal tissues which catalyzes the reversible cleavage of fructose-1,6-diphosphate (hexose diphosphate = HDP) into one mole of glyceraldehyde phosphate and one of dihydroxyacetone phosphate, the equilibrium between the two products being established by a second enzyme, triose phosphate isomerase. Aldolase activity was assayed by Meyerhof and Lohmann by determining the production of alkali-labile phosphorus, the phosphate of the triose phosphates being liberated by normal alkali at room temperature while that of hexose diphosphate is not. When used on tissue homogenates which contain considerable inorganic and esterified phosphate, this method is impractical on account of the necessity of running many blank determinations and also the possible effects of tissue phosphatases.

[1] Received for publication August 19, 1948.

[2] This investigation was supported by grants from the American Cancer Society recommended by the Committee on Growth, of the National Research Council, and Ben May, Mobile, Ala.

[3] Aldolase is the term preferred by American biochemists.

Warburg and Christian measured aldolase in a partial glycolytic system composed of substrate, test solution, crystalline triose phosphate dehydrogenase (which was free of aldolase), arsenate, and diphosphopyridine nucleotide (DPN). Cleavage of substrate caused appearance of glyceraldehyde phosphate which then reacted with DPN to produce the dihydro-coenzyme, which has a characteristic absorption at 340 mμ and which could therefore be determined spectrophotometrically. This highly refined method is of unquestioned reliability in assaying partially purified protein fractions such as the authors encountered in their purification of aldolase, but as shown by us (*3*) it is susceptible to large negative errors in crude tissue extracts due to interference by enzymes destroying DPN and the presence of certain DPN-linked hydrogen acceptors such as pyruvate, etc.

To circumvent these difficulties, a new method has been devised which is readily applicable to the rapid, accurate assay of the enzyme (*3*). This method is based on the colorimetric determination of the trioses formed by aldolase action through the production of a 2,4-dinitrophenylhydrazine derivative which yields a characteristic color in alkaline solution. The intensity of color formed is directly proportional to aldolase concentraction over a wide range, under the conditions adopted. In this paper, aldolase activity is expressed as the number of microliters of fructose diphosphate split in 1 hour at a temperature of 38° C. and a pH of 8.6 per stated weight of tissue or volume of serum. This unitage was adopted to facilitate comparison with the Q values widely used in measuring enzyme activity

$$(Q = \frac{\text{Microliters substrate decomposed (or product formed)}}{\text{Milligrams dry weight} \times \text{time in hours}}$$

where 1 micromole = 22.4 microliters). The tissue assays are expressed as microliters of HDP split per hour at 38° per gram of tissue (wet weight) and the serum values as microliters of HDP split per hour at 38° per milliliter. With the use of the assay method as described in a forthcoming publication (*3*) 0.05 to 0.10 ml. aliquots of rat serum and 0.5 to 1.0 ml. of human serum were found to lie within the optimum range of the method.

Animal experiments were performed on albino rats from a heterogeneous colony. The transplantable tumors used were sarcoma 39 and Walker carcinosarcoma 256. For measurement of serum levels, blood was obtained from the rats by cardiac puncture, care being taken to avoid hemolysis (the red cells contain a higher concentration of the enzyme per unit volume than does serum (*3*)) and to enter the heart directly on the first puncture (a significant amount of traumatized muscle material containing much aldolase may be obtained on repeated attempts at cardiac puncture). Human blood was drawn with care to prevent hemolysis and stored in the cold. Assays were done as soon as possible; however, the enzyme level fell only slightly over many days if the serum was kept cold. For tissue assay the animals were killed and bled, and the organs were rapidly removed and placed on ice. Samples were weighed, ground with an all-glass homogenizer in cold water, and diluted to an appropriate volume. Such dilute homogenates were found to be quite stable with respect to aldolase activity for many hours in the cold.

EXPERIMENTAL PROCEDURES AND RESULTS

Normal Level of Aldolase in Rat Serum

Confirming Warburg and Christian, we have found the enzyme to be present in the serum of normal rats. In a large series of normal rats, the average serum aldolase level was about 60 units per milliliter (60 μl. HDP split per hour at 38° C. per milliliter), values ranging from 40 to 90 units per milliliter. In any one rat the serum level was found to be remarkably constant over a period of weeks. There was no correlation with the size or sex of the animal. The aldolase levels determined by our method were somewhat higher than those noted by Warburg and Christian. This difference may be due to negative errors to which their method is prone (*3*).

Aldolase Levels in Serum of Tumor-Bearing Rats

Sarcoma 39 and Walker carcinosarcoma were implanted into adult rats, and the serum level was followed. As the tumors grew, the aldolase values rose from the normal level of 60 to 350 or more units per milliliter. The significant increases were not noted until the tumors were large. The

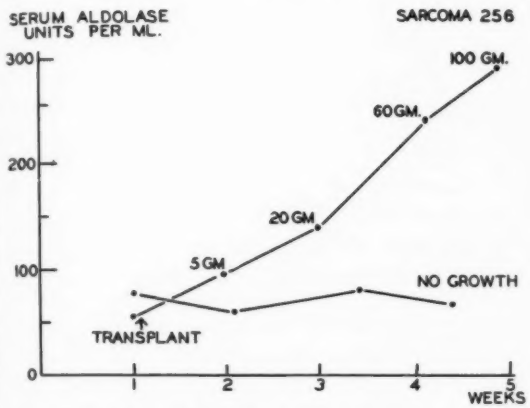

FIGURE 1.—Effect of tumor growth on serum aldolase.

sarcomas employed invariably showed necrosis, often massive, but the elevation of serum aldolase was roughly proportional to the amount of viable tumor tissue. Figure 1 shows a typical experiment, the serum aldolase levels during tumor growth being compared with the levels in a rat implanted with tumor at the same time but in which the tumor failed to grow. The approximated tumor weights are shown. In a series of some hundred rats bearing large tumors none failed to exhibit very high serum aldolase levels.

In order to determine whether the increase in serum aldolase was reversible, we implanted tumors, allowed them to grow until high serum levels resulted, and then completely excised the tumor surgically, a procedure which was possible even with massive tumors owing to their encapsulated nature. This treatment invariably resulted in a prompt fall of serum aldolase to normal levels, often within 24 hours. A typical experiment is shown in figure 2. If the sarcoma recurred because of incomplete removal, there was a subsequent rise in aldolase. An "autoexcision" sometimes occurred through massive sloughing of a large necrotic tumor, and in such cases there was a fall also. A sham operation on a tumor-bearing rat caused no decline in the serum enzyme. These findings, therefore, indicate a direct relationship of serum aldolase to the presence of viable tumor cells.

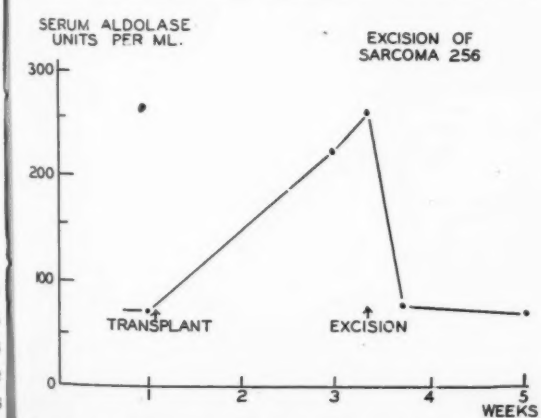

FIGURE 2.—Effect of excision of tumor on serum aldolase.

SPECIFICITY OF SERUM ALDOLASE RESPONSE

In rats bearing sarcoma 39 or Walker carcinosarcoma 256, cachexia was an invariable accompaniment of large tumor growth. That generalized wasting might be a factor in the elevation of aldolase was eliminated by following the serum level of fasting rats. Elevations did not occur although the animal might lose half its body weight. Rats bearing these tumors also became markedly anemic, which could conceivably be the cause of an elevation in serum aldolase, possibly from the destruction of red blood cells and liberation of the enzyme. However, the production of anemia by repeated bleeding or a hemolytic anemia resulting from a bartonella infection did not result in an increase in serum aldolase levels. Other types of infection did not alter the level nor did liver damage produced by administration of such drugs as carbon tetrachloride.

Since embryonic tissue and regenerating liver are known to have high rates of glycolysis, it was of interest to examine the effect of pregnancy and liver regeneration following partial hepatectomy on serum aldolase levels. In no stage of pregnancy was an increase of serum aldolase noted. Following partial hepatectomy (*4*), no increases were noted even during the period of most rapid liver regeneration. These conditions have been traditionally regarded as offering suitable controls for the specificity of biochemical changes due to the presence of malignancy.

EFFECT OF TUMOR-GROWTH INHIBITORS

The effect of a chemical agent known to injure malignant cells was studied. Ethyl carbamate has been shown by Huggins, Yü, and Jones (*5*) to retard the growth of sarcoma 39 in the rat. This

drug was given in doses of 80 mg. per 100 gm. body weight per day to rats bearing large, well-established tumors, either sarcoma 39 or Walker carcinosarcoma 256. Serum levels of enzyme were measured before and after the administration. Within 5 to 6 days after beginning of administration the typical high values dropped (fig. 3).

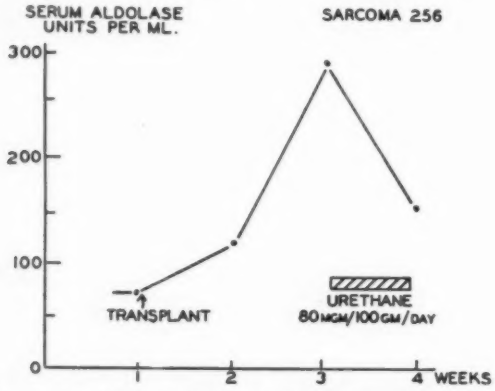

FIGURE 3.—Effect of urethan (ethyl carbamate) on serum aldolase of rat bearing large sarcoma 256.

Sodium amytal in doses which produced a degree of narcosis equal to that given by the above dosage of ethyl carbamate did not result in a fall of the serum level. Ethyl carbamate administered to normal rats caused no decline in the normal level of serum aldolase.

FATE OF INJECTED ZYMOHEXASE

The observation reported by Warburg that the intravenous injection of large amounts of crystalline aldolase resulted in only a temporary rise in serum level was confirmed. It was found that serum levels of over 400 units per milliliter were obtained 15 minutes after intravenous injection of approximately 5,000 units of enzyme yet were below 90 units per milliliter within 12 hours. The excess enzyme was not excreted in the urine in an active form.

COMPARISON OF TISSUES OF NORMAL AND TUMOR-BEARING RATS

A study of the aldolase content of rat tissues was made to determine the relative levels of tumor tissue as compared with other tissues and to determine if any difference existed between the tissues of the normal and tumor-bearing rat. Data are shown in table 1. Each value given represents the average of 10 to 16 determinations on the tissues of as many rats. Among the normal tissues, the highest concentration is found in skeletal muscle as might be expected because of the high glycolytic activity of muscle. The single value for muscle given by Warburg and Christian (*1*), if calculated on the same basis as the results given here, is higher than our average for muscle but within the normal range for this tissue. However, Warburg and Christian stated that liver and kidney contain very little aldolase, whereas our method indicates a substantial amount of aldolase in these tissues. We found (*3*) that crude extracts of rat kidney and liver when prepared by the method used by Warburg and Christian contain extremely potent factors causing disappearance of reduced DPN in their aldolase assay system, which occurs at rates comparable with the expected rate of reduction of DPN in their assay, assuming our value for these tissues is correct. It therefore appears that the low values reported by Warburg and Christian may be due to interference with their method of assay since the assay involves measurement of reduced DPN formed.

TABLE 1.—*Aldolase content of tissues of normal and tumor-bearing rats*

[Activity expressed as microliters HDP split per hour at 38° per gram wet weight of tissue [1]]

Tissue	Normal rats		Tumor-bearing rats	
	Mean	Range	Mean	Range
Muscle	74,000	52,400–105,000	78,500	72,000–105,000
Brain	15,800	11,100–19,000	18,500	13,000–22,000
Heart	15,600	12,000–19,000	19,800	16,000–23,000
Liver	12,100	8,500–14,700	7,600	4,720–9,680
Kidney	7,800	6,000–10,600	8,100	6,100–9,700
Spleen	4,800	3,100–6,400	6,200	3,400–8,100
Testis	2,900	2,500–3,400	3,500	3,000–3,800
Sarcoma 39			14,000	10,600–20,400
Walker carcinosarcoma 256			15,600	12,100–19,000

[1] These values are readily converted into Q values

$$\left(Q_{HDP}=\frac{\text{Cubic millimeters HDP split}}{\text{Milligrams dry weight}\times\text{hours}}\right)$$

by dividing by 200, assuming that 1 gm. wet weight equals 0.200 gm. dry weight.

Both sarcoma 39 and Walker carcinosarcoma 256 showed similar values of the order of magnitude of those for normal heart muscle. Warburg and Christian, on the basis of a comparison between the known glycolytic activity (anaerobic) of the Jensen sarcoma ($Q_{CO_2}^{N_2}$, up to 40 at 38° C.) and the aldolase content of Jensen sarcoma (which, if

maximally active, could yield a rate of $Q_{CO_2}^{N_2}$ 58), suggested that the aldolase content of the Jensen sarcoma could well be the limiting factor in anaerobic glycolysis of that tumor. We made similar calculations using our values for sarcoma 39 and Walker carcinosarcoma 256, which are somewhat higher than the value reported by Warburg and Christian for Jensen sarcoma. Assuming a maximal value for $Q_{CO_2}^{N_2}$ for slices of these tumors as about 40, our values for aldolase activity, expressed as $Q_{CO_2}^{N_2}$, are about 70. This value is sufficiently large to allow the statement that these tumors contain almost twice as much aldolase as is needed to account for the known rate of glycolysis in intact slices, provided that the enzyme is acting under optimum conditions in the tumor cells. It is of course unlikely that the enzyme in the intact tumor cell is actually functioning maximally, since there are probably great deviations in the intact cell from optimum pH conditions (pH 8.5) and optimum substrate concentration for aldolase. For instance, aldolase is only 40 percent as active at pH 7.0 as it is at its optimum pH of 8.5–9.0 (*3*). Although our figures for the tumors are higher than those of Warburg and Christian, we feel that these data might still be consistent with their suggestion that aldolase is the limiting factor in tumor glycolysis.

The only significant difference in the aldolase content of corresponding tissues from normal and cancer-bearing rats (table 1) was found in the case of the liver. Livers of cancer-bearing rats showed a significant decrease to somewhat more than half of the normal value. This finding is reminiscent of the decreases in liver catalase, *d*-amino acid oxidase, esterase, and arginase (summarized in (*7*)) in tumor-bearing animals.

Serum Aldolase in Human Cancer

Warburg and Christian stated they found no significant increase over normal values of serum aldolase in human beings with cancer. They pointed out that this might have been predicted since the increased levels seen in tumor-bearing rats were apparent only when the tumor weight exceeded 2–3 percent of the total body weight. In man, this corresponds to tumor weights of roughly 1.5 kg. for a just detectable increase. They concluded that the serum aldolase level was not of diagnostic usefulness in human cancer. Although our results are largely similar, we found that many patients with cancer have significantly elevated serum aldolase.

We found that the normal serum aldolase level in human beings is less than in rats, confirming Warburg and Christian, ranging between 3.5 and 8 units per milliliter with an average of 4.9 units per milliliter in a series of 123 samples from normal subjects and nonmalignant patients. Repeated determinations on the same subject were remarkably constant. No correlation could be made with age or sex. Pregnancy, anemia, polycythemia, or leukocytosis produced no deviation from normal levels.

The only definite elevations seen in the serum of patients without cancer were found in two cases of progressive muscular dystrophy (the only two studied), one case of obstructive jaundice, and one of gout. However, other cases of jaundice and gout clinically similar to the above showed normal levels (table 2).

Table 2.—*Aldolase content of human serum* [1]

Diagnosis	Number of cases	Range	Mean
Normal subjects	68	3.5–8.0	4.9
Pregnancy	14	3.4–8.4	5.0
Nonmalignant pathologies showing normal levels:			
Infectious diseases (urinary infections, tuberculosis, pneumonia, etc.)	20	3.2–8.2	5.1
Blood pathologies (anemias, polycythemia)	10	3.3–9.4	5.3
Miscellaneous pathologies (benign prostatic hypertrophy, bone fractures, liver cirrhosis, etc.)	11	3.1–9.4	5.1
	Cases showing elevation		*Levels found*
Nonmalignant cases showing elevation:			
Progressive muscle dystrophy	2	[2] (2)	20.8 14.3
Gout	1	(4)	12.6
Obstructive jaundice	1	(4)	13.8
Malignant cancers showing elevation:			
Carcinoma of breast	3	[2] (6)	11.8 36.0 12.0
Carcinoma of prostate	4	(42)	13.9 12.0 10.5 11.2
Carcinoma of pancreas	1	(1)	11.1
Carcinoma of stomach	2	(4)	27.5 12.5
Carcinoma of lung	1	(2)	11.8
Carcinoma of esophagus	1	(1)	10.9
Carcinomatosis (primary lesion not identified)	1	(4)	11.8
Chronic lymphatic leukemia	1	(3)	11.6
Hypernephroma	2	(7)	10.5 17.7
Acute myelogenous leukemia	1	(3)	26.6
Chondrosarcoma of bone	1	(2)	12.0
Carcinoma of rectum	1	(4)	14.7
Carcinoma of adrenal	1	(2)	14.0
Carcinoma of bladder	1	(2)	12.9
Malignant cancers showing normal levels: Tumors of testis (4); Hodgkins disease (6); carcinoma of cervix (2); fibrosarcoma (2); carcinoma of lip (1); colon (4); ovary (1); and thyroid (1).			

[1] Serum level given as microliters of HDP split per hour at 38° C. per 1.0 ml. of serum.

[2] Figures in parentheses indicate number of patients in each category tested. Those patients not showing elevation showed levels within or below the normal range.

The sera of 104 patients with proven malignant disease representing many types of cancer in various stages were studied. The average serum aldolase level of the cancer patients was 6.8 units per milliliter, or within the normal range of 3.0 to 8.0. However, included among the values contributing to this average were many cases whose levels were above the range of normal values, sometimes strikingly so. Also a few cancer cases showed extremely low levels, below the normal range. Although in any one normal subject the aldolase level remained remarkably constant from day to day, it was found that the aldolase levels of several cancer patients showed considerable fluctuation with time.

The reason for markedly elevated levels in some cases of cancer could not be determined; cases clinically similar to those exhibiting high levels usually showed normal values. Without greater understanding of the reason why certain cases show elevation, the levels of serum aldolase in the human are not of general diagnostic usefulness.

DISCUSSION

Experiments reported in this paper largely confirm the observations of Warburg and Christian that the serum aldolase activity in tumor-bearing rats is substantially increased over the normal level. In this investigation, sarcoma 39 and Walker carcinosarcoma 256 were studied whereas the German investigators used the Jensen sarcoma. In addition, it was established that surgical removal of large tumors causes a prompt decline of serum aldolase values to normal levels. Anemia, cachexia, infection, pregnancy, and active liver regeneration caused no changes in normal aldolase levels. The administration of ethyl carbamate, which is known to inhibit the early growth of these tumors, caused a decline of serum aldolase levels in rats with large, well-established tumors. These findings supplement those of Warburg and Christian and provide considerable evidence for the specificity of the response.

Experiments under way indicate that the level of serum aldolase may be a useful tool in assaying the effectiveness of potential chemotherapeutic agents in retarding the further growth of already well-established rat tumors. This situation parallels the usefulness of serum acid phosphatase as a guide in the diagnosis and therapy of metastatic carcinoma of the prostate in man (*6*).

Since intravenously injected enzyme rapidly disappears from the circulation, it is possible, as Warburg and Christian suggested, that the increased level of enzyme in the serum of tumor-bearing rats reflects a continuous and relatively massive discharge of enzyme into the circulation with concomitant rapid removal, establishing a dynamic balance.

Two possible sources of the excess enzyme may be postulated in this situation: (1) The excess enzyme may arise from the tumor itself. Warburg and Christian dismissed this possibility on the basis of their findings that tumors contain only enough enzyme to account for their known rates of glycolysis, that necrotic tumors are no more effective than nonnecrotic tumors in causing rise of serum aldolase, and that the venous return from a tumor contains no more enzyme than the general circulation; (2) the increased level may be due to a stimulation of enzyme release from some other organ by a systemic effect of the tumor. Warburg and Christian suggested that muscle tissue is a likely source because of its extremely high content of aldolase and their finding that other tissues, such as liver, contained very little. Our data, contrary to those of Warburg and Christian, demonstrate that other tissues, such as liver and kidney, also contain substantial amounts of the enzyme (*3*). In view of the wide distribution of the enzyme in rat tissues and especially in the liver, it now appears less warranted to single out muscle tissue as the most likely source. However, our finding that two cases of progressive muscular dystrophy showed very high serum levels indicates that a release of aldolase from muscle may well be possible. The liver might well be considered in this connection since our data show that the aldolase content of the liver of tumor-bearing rats is significantly lower than that of normal rat liver.

Although our data are consistent with those of Warburg and Christian on the possibility that aldolase may be the limiting enzyme of glycolysis in tumors, another interpretation may be placed on this finding. Greenstein (*7*) pointed out that the cancer cell may be functioning to the limit of its various catalytic systems whereas the normal cell usually contains a considerable reserve of

different enzymes. It is possible that the small reserve of the tumor aldolase, as calculated by Warburg and Christian and us, is not a specific characteristic of aldolase but may be true for other enzymes involved in glycolysis.

In view of the functional relationship of aldolase to the high and characteristic glycolysis of tumors, it is felt that further study of factors causing aldolase and other glycolytic enzymes to appear in the blood serum is called for.

SUMMARY

In confirmation of the work of Warburg and Christian, it was found that normal rat serum and human serum contain aldolase (zymohexase) by use of an independent analytical method. In rats bearing sarcoma 39 and Walker carcinosarcoma 256, the level of aldolase may increase to as high as seven times the normal value.

Cachexia, anemia, infection, pregnancy, and the presence of actively regenerating liver did not cause increased serum aldolase levels.

Surgical removal of the tumors caused a prompt decline of the serum aldolase to normal levels. Administration of ethyl carbamate, which is known to retard the growth of these tumors, also caused a decline of serum aldolase values.

Corresponding tissues of normal and tumor-bearing rats showed no large differences in aldolase content. The aldolase activity of the liver of tumor-bearing rats was significantly lower than that of normal livers.

Significant elevation of serum aldolase occurred in some 20 percent of 104 cases of human cancer tested. There was no obvious correlation with clinical findings.

REFERENCES

(1) Warburg, O., and Christian, W.: Gärungsfermente im Blutserum von Tumor-Ratten. Biochem. Ztschr. 314: 399 (1943).

(2) Meyerhof, O., and Lohmann, K.: Über die enzymatische Gleichgewichtsreaktion zwischen Hexosediphosphorsäure und Dioxyacetonphosphorsäure. Biochem. Ztschr. 271: 89 (1934).

(3) Sibley, J. A., and Lehninger, A. L.: Determination of aldolase in animal tissues. J. Biol. Chem. (In press).

(4) Higgins, G. M., and Anderson, R. M.: Experimental pathology of liver; restoration of liver of white rat following partial surgical removal. Arch. Path. 12: 186–202 (1931).

(5) Huggins, C., Yü, S. T., and Jones, R.: Inhibitory effects of ethyl carbamate on prostatic cancer. Science 106: 147–148 (1947).

(6) Huggins, C., and Hodges, C. V.: Studies on prostatic cancer. I. Effect of castration, of estrogen and of androgen injection on serum phosphatases in metastatic carcinoma of the prostate. Cancer Research 1: 293–297 (1941).

(7) Greenstein, J. P.: Biochemistry of cancer. Academic Press (1947).

CYTOLOGICAL STUDIES ON THE NATURE OF THE CYTOPLASMIC PARTICULATES IN THE CLOUDMAN S91 MOUSE MELANOMA, THE DERIVED ALGIRE S91A PARTIALLY AMELANOTIC MELANOMA, AND THE HARDING-PASSEY MOUSE MELANOMA [1] [2]

By M. W. Woods, H. G. duBuy, Dean Burk, and Marie L. Hesselbach, *National Cancer Institute* and *Laboratory of Physical Biology, National Institutes of Health, Public Health Service, Federal Security Agency*

INTRODUCTION

Theories concerning the potential role of abnormal self-duplicating mitochondria in determining certain types of animal neoplasms have been proposed in various forms in the literature (*1–6*). Most of the factual information available concerning the hereditary nature and potential pathogenicity of mitochondria has been obtained from studies in plants, where mitochondria have long been demonstrated to have the ability to differentiate into plastids (*7*). The self-perpetuating nature of plant mitochondria has been established from studies involving mutant or "tagged" plastids (*4–15*). These studies have shown that the hereditary components of the mitochondria, the "chondriogenes," [3] can, in mutant states, induce pathologic conditions that are highly similar to various syndromes produced by infectious viruses (*14–16*). In both mitochondrial and viral diseases, morphology, growth, and metabolism may be similarly and characteristically affected (*15–18*). Nuclear genes may, of course, also influence the development of the syndromes induced by abnormal mitochondria or viruses.

The data obtained with plants point to a number of corresponding experimental approaches that might be made with animal neoplasms. The transplantable Cloudman S91 mouse melanoma, and the derived Algire S91A partially amelanotic melanoma, would appear to be particularly desirable material for such a study, since the particulates of these tumors, like the plastids of plants, are differentially "color-tagged." The Harding-Passey mouse melanoma (*20*) furnishes material of a somewhat different type. The present paper reports cytological data from a study of these three tumors. The recent symposium on the biology of melanomas furnishes an excellent background review (*21*). Pertinent data on the growth and pathology of the Cloudman S91 and S91A tumors have been given by Algire (*22*). Harding and Passey have reported certain cytological characteristics of their tumor (*20*), while recently Grand and Cameron (*23*) have described the cell types in the same tumor as seen in tissue culture. We have been concerned here chiefly with the cytoplasmic particulates visible in cells isolated from teased cancer tissue.

A preliminary report of the present paper and the accompanying one (*24*) has already been presented (*25*).

MATERIALS AND METHODS

In this study, the Cloudman S91 melanoma was maintained chiefly by transplantation in dba mice and to a lesser extent in strain C mice. The Algire S91A partially amelanotic derivative of this tumor was also maintained in both strains of mice. The Harding-Passey tumor, however, was carried in C mice only.[4] In this and the accompanying paper (*24*) the tumors employed for critical study were actively growing and readily transplantable.

Implants were generally made intramuscularly, although occasionally subcutaneous implants were employed. Material for cytological study was obtained by killing the animals by neck dislocation, immediately followed by removal of the tumor tissue. After trials with various media it was found that details of the cytoplasmic particulates

[1] Received for publication, May 18, 1948.

[2] Mrs. Clara Fischer Smith rendered valuable aid in the conduct of these studies.

[3] While Imai (*19*) proposed the term "plastogene" to denote the hereditary mechanism of the plastid, the term "chrondriogene" (*5*) is considered preferable as it can logically be extended to cover the hereditary systems of mitochondria of both plant and animal origin.

[4] Initial tumor material was kindly furnished by Dr. Glenn H. Algire and Miss Frances Y. Legallais, who have also provided many helpful suggestions.

of the tumor cells could be best observed in fresh tissue recently placed in a saline composed of 0.013 molar NaCl and 0.120 molar KCl. In most cases 0.073 to 0.29 molar sucrose (2.5 to 10 gm. per 100 ml. solution) was added. Cells of the S91 and S91A tumors were also examined in 0.876 molar sucrose (30 gm. per 100 ml. solution) made up with either physiological saline or with distilled water both with and without adjustment of the pH to 7.0. Repeated attempts to stain the cytoplasmic particulates of cells with Janus green B immersed in 0.876 molar sucrose solutions were unsuccessful, probably due to the low oxygen tension of such media. Material was also fixed in a solution containing 10 ml. of freshly distilled formalin (40 percent formaldehyde solution distilled over sodium carbonate) to 90 ml. of distilled water. Such material was useful for determination of gross morphological features but not for detailed microscopic examination.

Temporary mounts of teased tumor tissue were found to be much more satisfactory than sectioned material because it was possible to remove whole cells from the tumor mass, thus facilitating observation of the total cytoplasm of a given cell.

Material was examined either unstained or following application of saline solutions (0.145M NaCl or a mixture of 0.013M NaCl and 0.12M KCl) of Janus green B (0.0005 to 0.005 percent) or of neutral red (0.005 percent), both at pH 7.2, with and without 5 to 10 percent sucrose. In some instances animals were injected intraperitoneally with 0.5 ml. of 1 percent trypan blue, 24 to 48 hours prior to killing, in order to more readily differentiate the phagocytic cells. Cytological observations reported here are based on studies of 20 or more tumors of each strain. Microscopy was carried out with the ordinary light microscope, employing a 2-mm. 90×apochromatic oil immersion objective of N. A. 1.30 used in conjunction with 15×compensating oculars and an achromatic oil immersion condenser of N. A. 1.30, and with the phase contrast microscope.

RESULTS

S91 Melanoma

TUMOR GROWTH

When initially received the S91 melanoma was in its nineteenth serial passage in dba mice and the S91A amelanotic melanoma in its twenty-first passage in C mice. In this study both tumors grew well in strain dba, which is their strain of origin, and less well in strain C.

Tumors 15–50 days old were studied, varying in size from 3 to 10 mm. in diameter. Most tumors required at least 20 days to attain 1 cm. diameter.

VARIATIONS IN MELANIN CONTENT

As described by Algire (*22*), the melanin content of the S91 tumor varies considerably (fig. 1, *A* and *B*). Transplants from the darkest areas produced the darkest tumors, whereas transplants from light-colored areas yielded tumors with irregular melanin content. While we made no attempt to obtain a fully amelanotic tumor by sub-transfer from light-colored areas of the S91 tumor, Algire showed that this can be done. Although large S91A tumors (3–5 gm.) were obtained which appeared macroscopically free of melanin, on microscopic examination it was not uncommon to find variable amounts of melanin in portions of some of them.

MICROSCOPIC APPEARANCE

The tumor cells proper, making up the bulk of the actively growing tumor, were variably elongated and occurred in masses, as described by Algire (*22*). It was possible to cause the tumor mass to flatten out so that individual cells could be examined in an isolated condition. In saline preparations without added sucrose, the elongated cells generally assumed an approximately spherical shape when freed from the tumor mass (fig. 1, *B*). Mitotic figures were frequently encountered in such cells although no attempt was made to follow cell divisions. The tumor cells of the S91 melanoma were characterized by a low adhesiveness as judged by the ease with which the cells became separated under the pressure of the cover slip, or by teasing.

Phagocytic cells containing varying numbers of melanin granules, both free and clumped, were scattered throughout the active tumor mass. These could be identified by their large and often irregular intracellular bodies. These bodies often stained heavily with neutral red and sometimes contained clumps of melanin granules. The phagocytic cells also contained varying numbers of blue-stained particulates when the tumor-bearing animals had been previously injected with

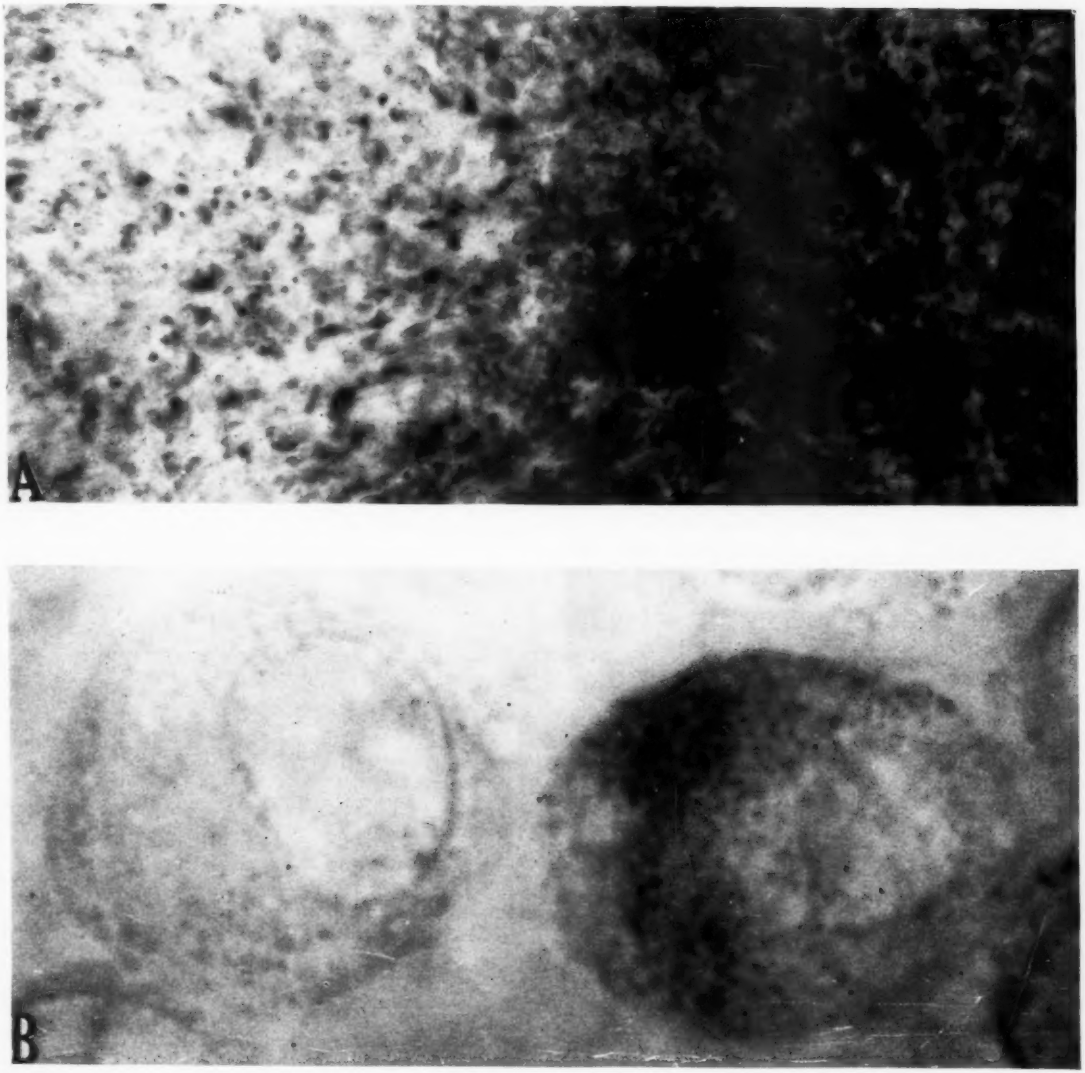

FIGURE 1.—S91 melanoma. *A* (upper), Portion of tumor showing melanotic (dark) and amelanotic (light) areas. × 294. *B* (lower), Tumor cell containing predominantly melanized granules (right) and tumor cell containing colorless granules only (left). The cells have been pushed out of the tumor mass and have rounded up in the mounting medium consisting of a 0.013M NaCl–0.120M KCl solution. Enlarged to × 3977 from an initial magnification of × 1220.

trypan blue. Phagocytic cells that contained relatively small amounts of trypan blue-stained or other coarse granular matter, often contained rod-shaped or filamentous mitochondria. In the more common phagocytes, containing large amounts of coarse granular material (colored blue in trypan blue-injected animals), filamentous mitochondria were not seen.

The melanin content varied greatly in the tumor cells depending upon the region from which the cells were taken. This variation in melanin content was due not only to variations in the number of melanin granules per cell but also to great differences in the intensity of color in the individual granules. These two phenomena did not necessarily coincide. Most of the melanin

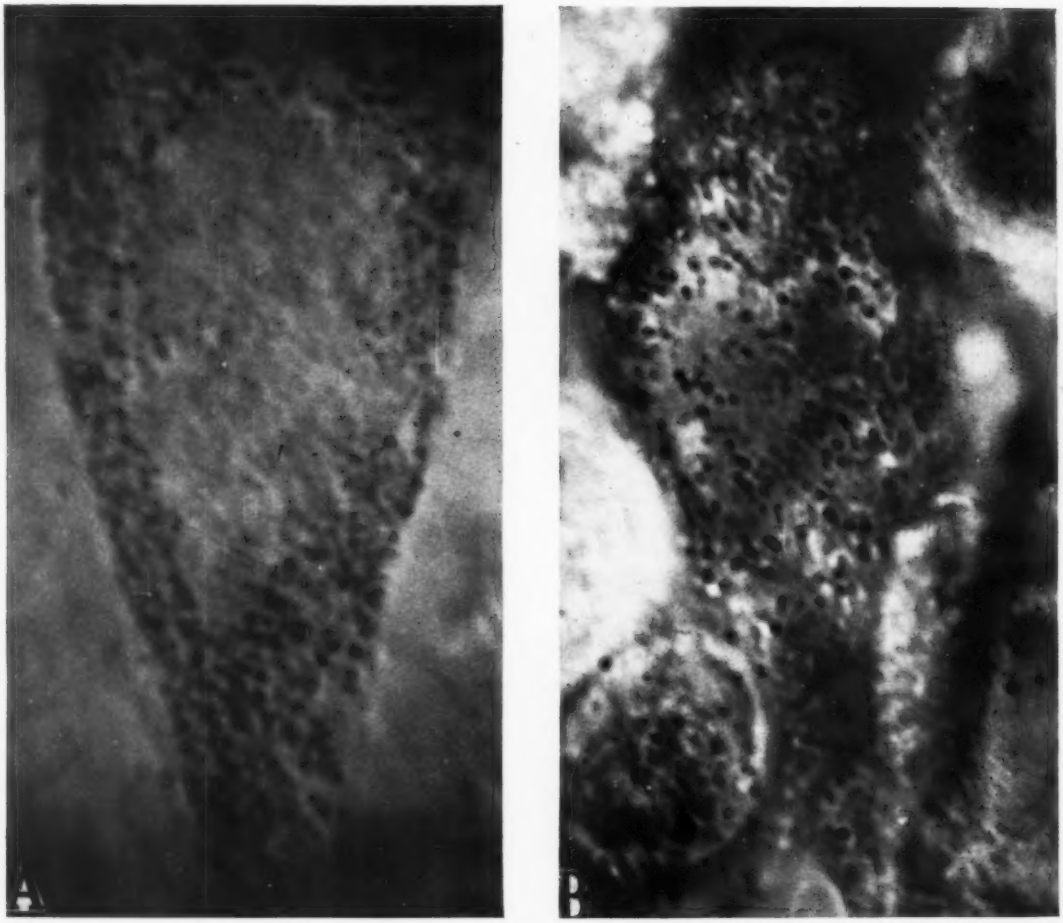

FIGURE 2.—S91 melanoma. Two tumor cells in which only melanized granules could be observed. Outlines of the nucleus can be seen in the cell at the left with overlying melanized granules out of focus. Both cells mounted in saline with 5 percent sucrose. Cell at left unstained, cell at right has melanin granules stained with 0.005 percent neutral red. Enlarged to approximately ×4900 from an initial magnification of ×1220.

granules ranged in size from about 0.3μ to 1.0μ in diameter, as determined photomicrographically and by means of a calibrated ocular micrometer. There appeared to be no uniform relationship between size and melanin content of the granules. While there was considerable difference in the size of the granules between different tumor cells, within any one tumor cell the granules were predominantly of about the same size.

Studies on S91 tumors from dba mice showed that there were three types of cells with respect to the distribution of melanized and colorless granules in the cytoplasm, i. e., (1) cells with melanized granules and apparently no visible colorless granules (fig. 2), (2) cells with both melanized and colorless granules (fig. 1, *B*; fig. 3), and (3) cells with colorless granules only (fig. 1, *B*; fig. 4). While the melanized granules showed all gradations of melanin content, within any one cell the granules were quite uniform in this respect. The first type of cell was most numerous in the dark-colored portions of the S91 tumor but was found to some extent scattered in the lighter colored areas (fig. 1, *A*). The other two types of cells were most frequently encountered in the lighter colored portions of the tumors.

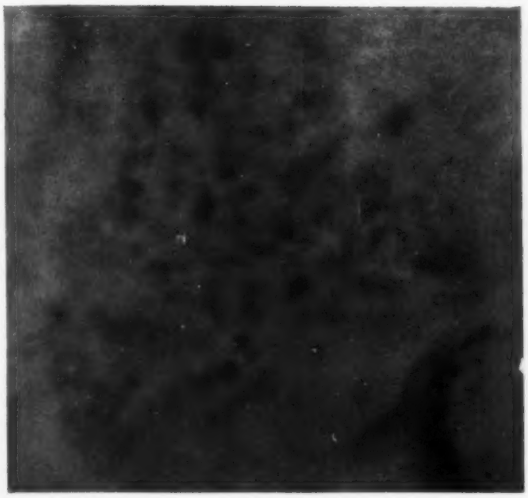

FIGURE 3.—S91 melanoma showing part of a tumor cell which contained both melanized granules (appear black) and colorless granules (appear gray). The cell was mounted in 0.013M NaCl–0.120M KCl solution with 5 percent sucrose and supravitally stained with neutral red (colored melanized granules) and Janus green B (colored amelanotic granules). Photo on process panchromatic film using Wratten green (B) filter. Enlarged to × 5978 from an initial magnification of × 1220.

Studies of lung metastases, mounted in 0.876M sucrose and examined with both light and phase microscopy, showed that the tumor cells were apparently of type 1, with small, strongly melanized granules.

Filamentous mitochondria were not observed in the three types of tumor cells in the S91 melanoma. In cells mounted in 0.876M sucrose in distilled water (30 gm. per 100 ml. of solution) the cytoplasm sometimes developed a striated appearance. Frequently the cytoplasmic granules were arranged in rows or beadlike strings.

When tissue was mounted in a 0.005 percent solution of neutral red in saline plus 0.146M sucrose, pH 7.2, even those melanin granules with a slight degree of melanization stained a pronounced red. The colorless granules under such conditions were not stained. If, following the neutral red stain, a relatively strong solution of Janus green B (0.005 percent) was applied, staining of the colorless granules could be obtained without blue coloration of the nucleus or red-stained granules (fig. 3). Because of the concentrations of Janus green B employed, this staining may not always have been supravital; however, it is important to note that nuclear staining did not take place in the cells in which observations were made.

The affinity of melanin granules for neutral red, at any stage of melanization, is so pronounced, that any Janus green B stain, subsequently applied is no longer effective. This technique, which is

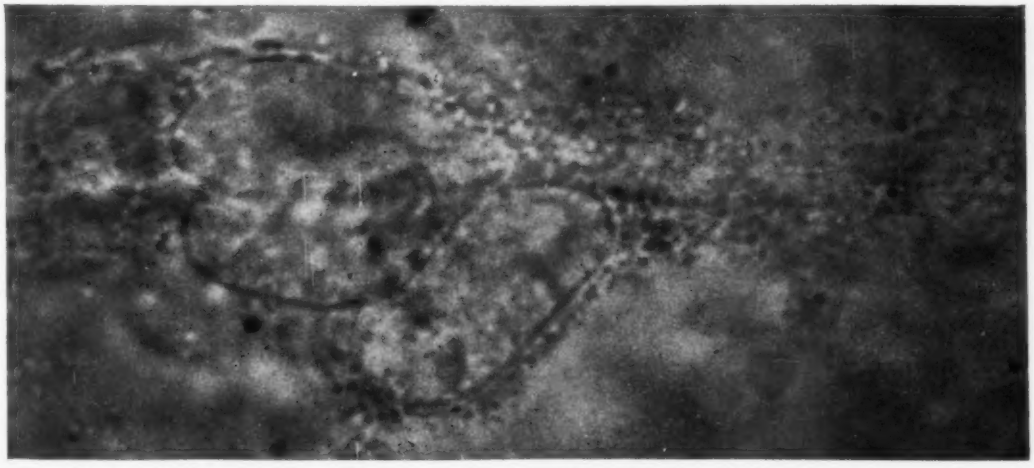

FIGURE 4.—S91A partially amelanotic melanoma. Group of amelanotic tumor cells in which small, granular, colorless particulates can be seen in the cytoplasm. Mounted in 0.013M–0.120M KCl solution plus 2.5 percent sucrose. Light stepped down to enhance contrast. Enlarged to × 2806 from an initial magnification of × 1220.

somewhat similar to one employed by Smith (*26*) in studying melanin granule development in avian retina, makes possible a ready differentiation of colorless granules even when they are greatly outnumbered by melanized granules.

Staining with 0.0005 to 0.0025 percent Janus green B, without prior neutral red staining often, though not always, resulted in blue coloration of both colorless granules and melanin granules. Melanized granules became greenish black (fig. 5), due to the addition of the blue color to the natural brown color of the granules. This staining gave every indication of being vital, since it took place in the absence of nuclear staining and only in freshly prepared material maintained under sufficiently aerobic conditions. Dependence of staining on an adequate oxygen supply was evidenced by the fact that destained granules could be recolored either by flowing aerated dye solution under the cover slip or merely by removal and replacement of the latter. Prolonged application of the stain often resulted in a visible accumulation of the rose derivative of Janus green B in the cell. Such behavior towards Janus green B is of course identical with that displayed in many other tissues by particulates generally classified as mitochondria (*7*).

FIGURE 5.—S91 melanoma. Tumor cell in which only melanized granules could be observed. The granules have all been colored greenish-black by the addition of Janus green B to the natural brown of the melanin granules. The nucleus, which was unstained, lies out of focus under the clear area in the central portion of the photomicrograph. Cell mounted in 0.013M NaCl—0.120M KCl solution. Enlarged to × 5734 from an initial magnification of × 1220.

S91A Partially Amelanotic Melanoma

In general the same cell types occurred in the Algire partially amelanotic melanoma as were found in the amelanotic portions of the tumor from which it was originally derived. There was a tendency for the cells to be more adherent in the amelanotic tumor than in the S91 melanotic melanoma. The cytoplasm of the amelanotic tumor cells contained colorless granules (fig. 4) of sizes (0.3μ to 1.0μ in diameter) similar to those observed in cells of the S91 tumor. These stained reversibly with Janus green B (0.0005 to 0.005 percent) in the absence of nuclear staining as in the parent tumor (fig. 6). The colorless granules were the only cellular structures which showed any visible coloration by the dye under such conditions. They did not stain with 0.005 percent neutral red under any conditions. While precise counts of the number of granules per cell were not made, on the whole the S91A cells contained fewer granules than the melanized S91 cells. As in the case of the S91 tumor, filamentous mitochondria were not found apart from those in occasional phagocytic cells. In 0.876M sucrose solutions the S91A cells behaved like the amelanotic cells of the S91 tumor.

Certain S91A tumors contained melanotic areas which ranged in size from microscopic spots of several cells to regions a centimeter in diameter. Such melanotic areas included cells in which only melanized granules could be observed. These granules, which were often of a very light shade of brown, stained with 0.005 percent neutral red as in the parent melanotic tumor. They also stained with Janus green B, if this dye was applied alone. Phagocytes containing clumps of melanin granules were frequently observed in melanotic areas occurring in S91A tumors.

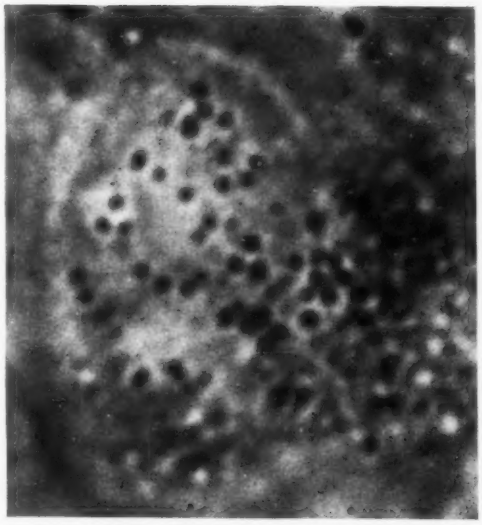

FIGURE 6.—S91A partially amelanotic melanoma, showing part of an amelanotic tumor cell mounted in 0.013M NaCl-0.120M KCl solution plus 5 percent sucrose and stained with Janus green B. The dark blue particulates decolorized about 5 minutes after the photomicrograph was taken, the nucleus remaining uncolored throughout. Enlarged to × 5368 from an initial magnification of × 1220.

In certain slow-growing or necrotic S91A or S91 tumors or in cases in which the host tissue surrounding the tumor showed considerable inflammation, large numbers of intercellular fibers were observed. The associated cell bodies, which resembled fibrocytes, contained long filamentous mitochondria. In such tumors, cells with exclusively granular mitochondria could still be found. Such abnormal tumors were not used in the investigations reported here.

HARDING-PASSEY MELANOMA

TUMOR GROWTH

The tumors were grown in strain C mice. After 60–90 days' growth, they attained weights of 10 gm. or more and were firm, virtually nonnecrotic, and grossly black.

Tumors 14–90 days old were studied, varying in size from 3 to 30 mm. in diameter.

CYTOLOGY OF THE HARDING-PASSEY MELANOMA

The tumors were composed chiefly of two cell types, melanoblasts and a macrophage system, the latter comprising 50–80 percent of the total tumor mass. The melanin granules throughout the tumor mass were approximately spherical, varying in size from 0.3μ to 1.3μ.

THE MELANOBLASTS

The melanoblasts were very fragile in physiological saline solutions (0.85 percent), but the addition of approximately 0.3M sucrose or fixation in 10 percent formalin made it possible to tease them out of the tumor mass in more or less intact form. Five-thousandths percent Janus green B stained the melanin granules of melanoblasts mounted in sucrose-saline solution before the nuclei showed any staining. However, as in the S91 melanoma, if the melanin granules were first stained with 0.005 percent neutral red, they did not become stained with 0.005 percent Janus green B subsequently applied.

In marked contrast with the relatively undifferentiated tumor cells of the Cloudman S91 melanoma, the melanoblasts of the Harding-Passey tumor were differentiated into two distinct parts: (1) A spindle-shaped nucleated portion (perikaryon) in which both melanized and frequently nonmelanized granules occurred (figs. 7, *B* and 8); and (2) elongated, often branched dendrites with cytoplasm filled with melanin granules (fig. 7, *A*). In the dendritic portion, no colorless granules could be detected, although various grades of melanization could be observed in different melanoblasts. The melanin granules varied considerably in size (approximately 0.3μ to 1.3μ) between the dendrites of various melanoblasts. However, within any one dendritic area the granules were quite uniform in size. In the nucleated area of the cell, the granules varied in color from dark brown to colorless and varied in size from 0.3μ to 0.8μ (fig. 8). Both melanized and nonmelanized granules could be stained with 0.005 percent Janus green B. If, however, the preparation was first treated with 0.005 percent neutral red and then stained with Janus green B, the colorless granules, which did not stain with the first dye, were colored blue whereas the melanized granules were red. Staining with a mixture of the two dyes produced a similar result. The neutral red staining was irreversible whether applied after the Janus green B or simultaneously with it.

The number of colorless granules in the cytoplasm of the nucleated area of the melanoblast

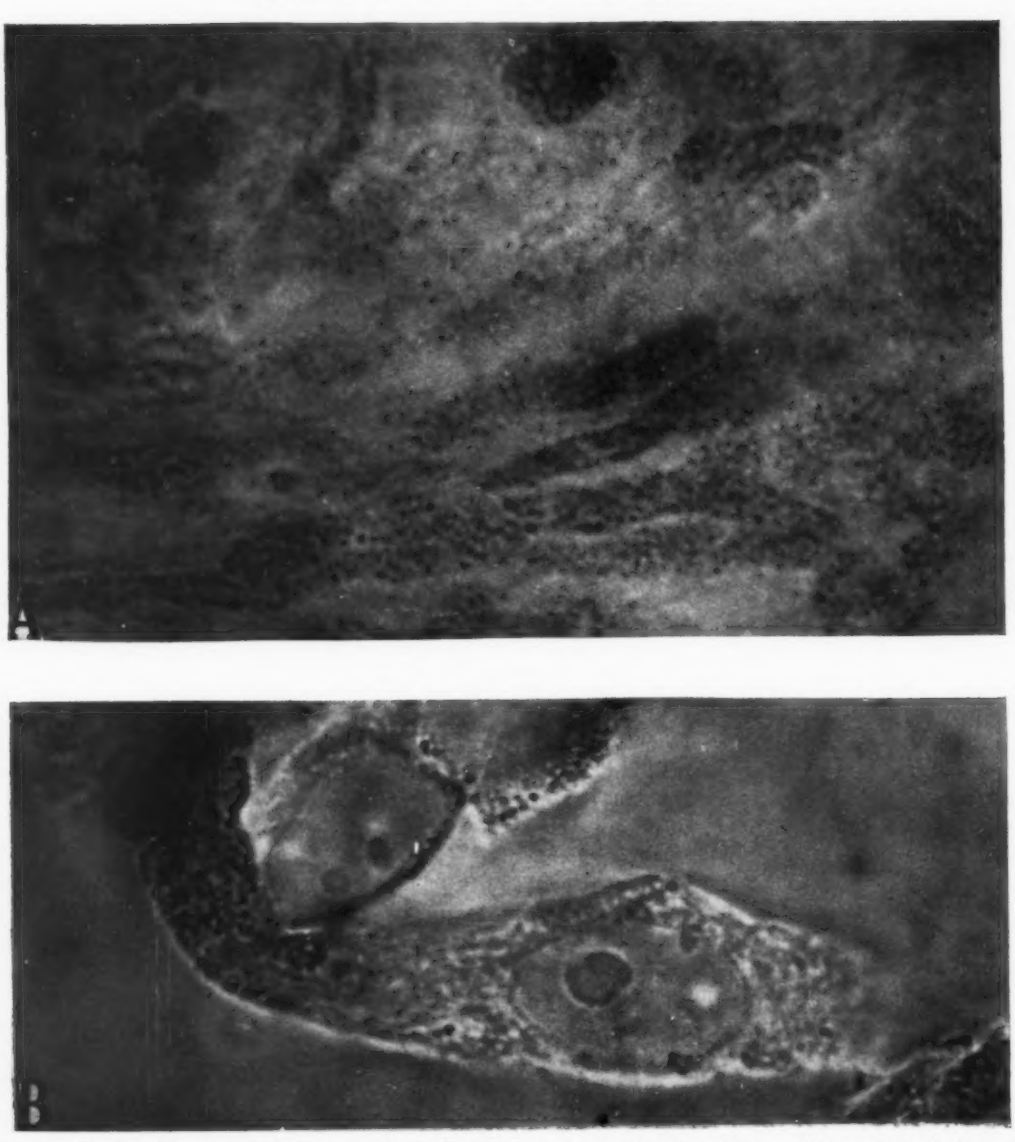

FIGURE 7.—Harding-Passey melanoma. *A* (top), Dendritic portions of melanoblasts. Note spherical classmatosed fragments. *B* (bottom), Nucleated portion of melanoblast and adjacent melanin-filled dendritic area at left. Both *A* and *B* fixed in 10 percent neutral formalin. Enlarged to × 2660 from an initial magnification of × 1220.

was low in relation to the number of melanized granules in this area and always extremely low in relation to the total number of melanized granules in the entire cell. In the nucleated areas of some melanoblasts from old tumors, colorless granules could not be found. This description of Harding-Passey melanoblasts is similar to the description of human epidermal melanoblasts as given by Masson (*27*).

Occasionally approximately spherical structures composed of melanin granules embedded in a colorless matrix (figs. 7, *A* and 9) were found free in the tissue mass. While the size of the granules contained in these bodies varied considerably.

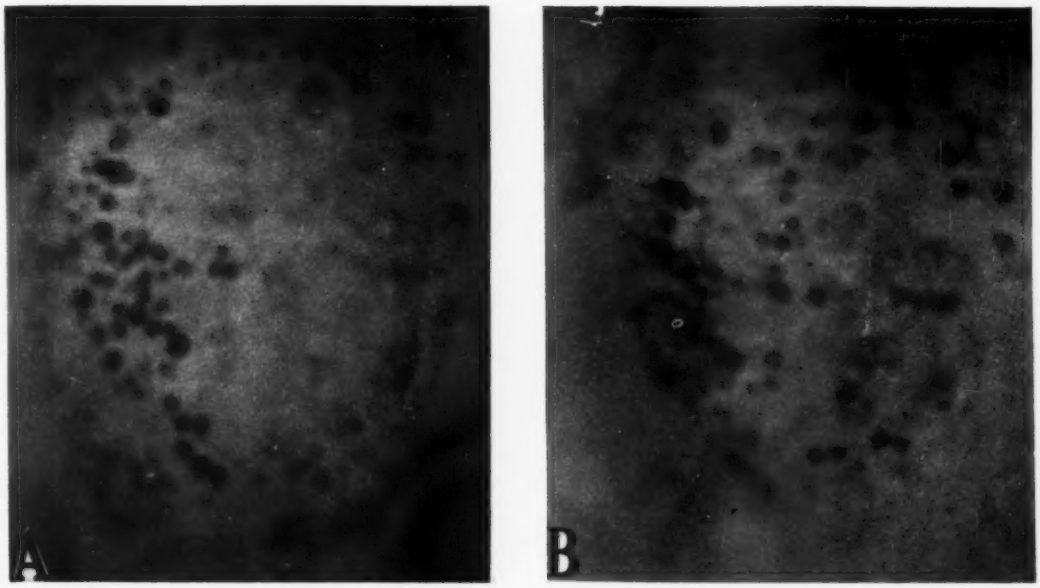

FIGURE 8.—Harding-Passey melanoma. *A* (left), Nucleated portion of melanoblast mounted in 0.013M NaCl–0.120M KCl solution plus 5 percent sucrose and stained with neutral red and Janus green B. All but a few granules were melanized and stained red. *B*, Another focal level of the same area. Photomicrograph taken on process panchromatic film with Wratten green (B) filter. Enlarged to × 5856 from an initial magnification of × 1220.

there was relatively little variation within any one body. These compound structures probably correspond to portions of the melanoblast dendrites separated off by clasmatosis, as observed in tissue culture by Grand and Cameron (*23*) and Grand (*28*).

THE MACROPHAGES

Macrophages (figs. 9 and 10), making up approximately 50 to 80 percent of the total tumor mass, were filled with brown inclusions of two types. The predominant type was a compound spherical structure containing pigment granules embedded in a colorless matrix (fig. 9), presumably the compound structure just referred to. In any one inclusion, the melanin granules were relatively uniform in size, but there was considerable variation in granule size among different bodies in a given cell (fig. 9). The differences between the size of the granules in the compound bodies found in a single macrophage can be explained on the basis that clasmatosed fragments of both young and old cells, containing either small or large granules, may be taken up by individual macrophages. There was also wide variation in the size of individual compound bodies and in the number of granules contained in them. A variable number of single granules was also often present in the macrophages.

The second type of inclusion, somewhat smaller, showed no evident internal differentiation but was clearly and uniformly stained by neutral red.

A few rare cells, believed to be immature phagocytes, were found to contain colorless filamentous structures that amounted to an estimated 1 to 2 percent of the total number of inclusions in the cell. In suspensions of particulates obtained by macerating tumor tissue in 30 percent sucrose, colorless filamentous structures were clearly visible in the phase microscope. In all instances, however, they represented only a negligible part of the total number of particulates. Such preparations showed, in conformity with the observations on intact cells, that the colorless granules were strongly outnumbered by those showing some degree of melanization. The accompanying paper (*24*) describes the centrifugal separation of these colorless elements from the melanized granules.

Janus green B in a concentration of 0.005 percent stained single melanin granules, as well as

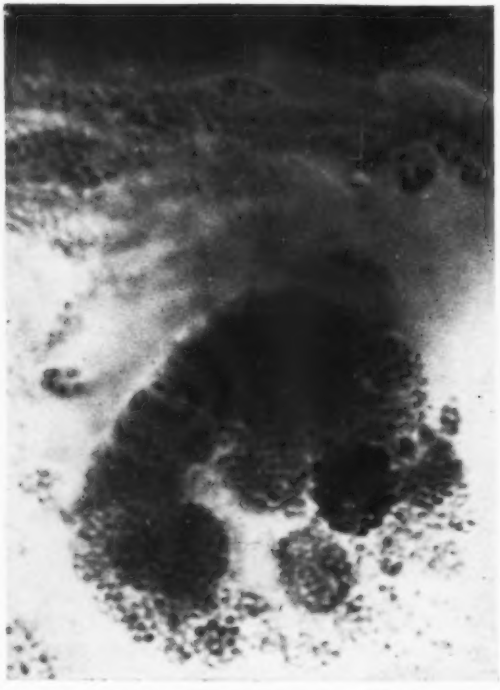

FIGURE 9.—Harding-Passey melanoma. Single macrophage containing compound granular bodies (clasmatosed fragments of melanoblast dendrites) in which the contained melanin granules differ in size. Portions of two dendrites and a spherical, clasmatosed fragment can be seen in the upper part of the photomicrograph. Fixed in 10 percent neutral formalin. Enlarged to × 2684 from an initial magnification of × 1220.

those in the compound bodies, without staining the nucleus. On the other hand, nonmelanized particulates could not be observed in the macrophages with this staining technique. Neutral red in the same concentration stained the granules in the compound bodies in addition to the amorphous structures and the single granules; additional staining with 0.005 percent Janus green B did not reveal the presence of blue-staining particulates. The nuclei of the macrophages were almost obscured by the masses of cytoplasmic inclusions (fig. 10) but could be readily differentiated in killed cells by staining with 0.05 percent trypan blue. In tumors borne by animals that had been injected intraperitoneally with trypan blue 24 to 48 hours previous to examination, only a very few of the pigment-loaded macrophages contained the dye. The dye in such cases was always confined to the more amorphous bodies (type 2) and was never found in the compound multigranular structures (type 1).

DISCUSSION

As previously stated, there appeared to be an inverse relationship between the number of melanin granules and the number of colorless granules in the cells of the Harding-Passey and the S91 melanoma. In both types, tumor cells were found in which colorless granules could not be detected, but only granules of various degrees of melanization. While there were wide differences between cells with respect to the amount of melanization of the granules, the granules within any one S91 cell or in any one dendrite of a Harding-Passey cell were of relatively uniform color. An exception was the nucleated area of the Harding-Passey melanoblast, in which granules in varying stages of melanization could be found.

Smith (*29*) described similar intracellular uniformity in the pigmented epithelium cells of the retina of the embryo chick's eye in plasma culture:

> Even though the cells were so different in appearances and showed such marked variation in the size and shape of the granules, one was impressed with the fact that the granules, in any particular cell under observation, were always about the same size, shape and color, and were evenly distributed throughout the cytoplasm.

These observations of Smith are comparable, of course, only with the dendritic portion, not with the nucleated portion of the Harding-Passey tumor melanoblast.

The S91A partially amelanotic melanoma contained predominantly cells with only colorless granules of the same appearance as the colorless ones in the parent S91 melanoma. These colorless granules, as well as those of the S91 and Harding-Passey melanomas, stained reversibly with Janus green B. Neither in the cells of the S91A amelanotic melanoma nor in cells of the Harding-Passey or S91 melanoma could rod-shaped mitochondria be detected, although special efforts were made to detect such rod-shaped bodies, including the use of 30 percent sucrose solutions. From the results, it can be concluded that the cytoplasm of these actively growing melanomas and the partially amelanotic melanomas was virtually free of rod-shaped mitochondrial elements. With the exception of the variably melanized particles, the colorless granules

FIGURE 10.—Harding-Passey melanoma. Group of four macrophages. The nuclei appear as light-colored areas partly obscured by inclusions. Both compound and nongranular inclusions are present in the cells. Fixed in 10 percent neutral formalin. Enlarged to × 2684 from an initial magnification of × 1220.

were the only structures in the cell which stained reversibly with Janus green B and thus behaved in a manner characteristic for mitochondria in other tissues.

In many lightly melanized cells of the S91A partially amelanotic melanoma, the only granules that could be observed in the cytoplasm were indistinguishable, except for their melanin content, from those in the completely amelanotic cells of the same tumor. As in the case of the granules of completely amelanotic cells, these were the only cytoplasmic structures which stained with Janus green B. The granules in the nucleated relatively amelanotic portion of the Harding-Passey melanoblast stained like the amelanotic and melanotic granules of the S91 tumors.

While Smith (*26*) showed that the melanin granules in cells of the chick retina stain with neutral red but not with Janus green B when these stains are used in mixture, it is important to note that in the present study these stains were applied separately as well as in combination. The results show that even very lightly melanized granules in the mouse melanomas have a high affinity for neutral red and if once stained with this dye will not become colored by Janus green B. However, if Janus green B is applied alone, the melanized granules will take up the stain. This staining of the melanin granules takes place in the absence of nuclear staining and is dependent upon an adequate oxygen supply.

The S91 and the Harding-Passey melanomas differed in that individual cells of the S91 melanoma contained colorless granules simultaneously with granules of relatively uniform melanin content, whereas in the nucleated portion of the Harding-Passey melanoblasts colorless granules often occurred along with granules in various stages of melanization. Furthermore, completely amelanotic cells or multicellular areas were found in the S91 tumors, a condition not observed in any of the approximately 40 Harding-Passey tumors examined by us. In this connection, it should be noted that Harding and Passey (*20*) did observe amelanotic areas in their cultures of the tumor discovered by them and succeeded in de-

riving amelanotic melanomas from these. While Algire (*22*) showed that on repeated sub-culture the amelanotic areas of the S91 tumor yield strongly amelanotic tumors, none of the Harding-Passey transplants maintained in our cultures has shown any tendency to become amelanotic.

The results of the present study suggest that the S91 melanoma cells may carry two types of granules, i. e., one, incapable or nearly incapable of melanization, in the same cell with a type having the ability to become strongly melanized. In some areas, these two types of granules became separated, forming completely melanotic or completely amelanotic cells. The presence in the same tumor of completely melanotic and completely amelanotic cells (fig. 1) suggests the possibility of cytoplasmic segregation similar to that observed in plant cells (*14*). Whether the occasional melanotic cells found in the amelanotic melanoma represent a true reversion to the original tumor type or are an indication that an alternative pathway for limited melanin formation under special conditions remains open for the amelanotic cells cannot be answered at present. Further studies on this problem are in progress.

In contrast, the observations on the Harding-Passey melanoma indicate that in this tumor all the granules are capable of melanization, the process of melanization occurring progressively in the nucleated portion of the cell. Masson (*27, p. 24*) described "premelanin granulation" as taking place in the nucleated portion (perikaryon) of the human epidermal melanoblast.

The occurrence of cytoplasmic particulates (mitochondria), which possess varying inherent powers of pigment elaboration and which may be cytoplasmically segregated in successive cell divisions, is well known in plants (*9, 10, 11, 14, 15*). The present data do not establish the existence of such hereditary particulates in animal cells, but the observations in the S91 melanomas are consistent with such a view.

The study of Mason, et al. (*30*) which provided an electron-microscopic comparison of various forms assumed by melanin granules taken from tumor and nontumor sources does not give information as to granule origin. In the latter connection, Kopac (*31*) suggested that "the aggregation of submicroscopic particles to form the microscopically visible granules (the pigment granules) may be similar to those processes, though not well understood, that form mitochondria." However, it should be borne in mind that data from plant cells show that mitochondria possess definite and specific properties of heredity, i. e., can be considered self-duplicating organelles of the cytoplasm. Data at present available do not warrant the conclusion that the melanin granules of the cell are built up by a process of aggregation of smaller granules.

It is realized that the ultimate nature of the cytoplasmic granules in the mouse melanomas cannot be elucidated solely on the basis of morphological structure or staining reactions. The second paper of this series presents the results of studies on certain metabolic and chemical properties of the amelanotic and melanotic granules of the three mouse melanomas reported here.

SUMMARY

The Cloudman S91 melanoma has been observed to contain tumor cells of three types with respect to cytoplasmic granules visible by light and phase microscopy: (1) Cells with melanized granules only; (2) cells with colorless granules only; and (3) cells with all proportions of melanized and colorless granules. The derived S91A Algire partially amelanotic melanoma contained predominantly cells possessing only colorless granules of the same type as those in the amelanotic cells of the parent melanoma. The various types of granules described were the only cytoplasmic structures in the tumor cells that stained with Janus green B under conditions not resulting in nuclear staining.

The tumor cells proper of the Harding-Passey mouse melanoma were branched melanoblasts, in which either colorless granules or granules in all stages of melanization, could be found in the nucleated portion (perikaryon). The elongated dendrites of the cells contained only granules of uniform melanization. Completely amelanotic tumor cells were not observed in the Harding-Passey tumor.

In contrast with Janus green B, which stained both melanized and nonmelanized granules of the S91 and Harding-Passey tumors, neutral red stained the first type of granule only. If the melanin granules were first stained with neutral red, they did not become colored by Janus green B.

REFERENCES

(1) GRAFFI, A.: Zellulare Speicherung cancerogener Kohlenwasserstoffe. Ztschr. f. Krebsforsch. 49: 477–495 (1939).

(2) ———: Einige Betrachtungen zur Ätiologie der Geschwülste speziell zur Natur des wirksamen Agens der zellfrei übertragbaren Hühnertumoren. Ztschr. f. Krebsforsch. 49: 501–551 (1940).

(3) CLAUDE, A.: Distribution of nucleic acids in the cell and the morphological constitution of cytoplasm. Biol. Symp. 10: 111–129 (1943).

(4) duBUY, H. G., and WOODS, M. W.: Evidence for the evolution of phytopathogenic viruses from mitochondria and their derivatives. II. Chemical evidence. Phytopathology 33: 766–777 (1943).

(5) duBUY, H. G., and WOODS, M. W.: A possible common mitochondrial origin of the variegational and virus diseases in plants and cancers in animals. *In* Am. Assoc. Advancement Sc. Research Conf. on Cancer, pp. 162–169. Lancaster Press (1945).

(6) WOODS, M. W., and duBUY, H. G.: Cytoplasmic diseases and cancer. Science 102: 591–593 (1945).

(7) GUILLIERMOND, A.: The cytoplasm of the plant cell. *In* A New Series of Plant Science Books, v. 6, p. 247, Chronica Botanica Co., Waltham, Mass. (1941).

(8) CORRENS, C.: Vererbungsversuche mit blass (gelb) grünen und buntblättrigen Sippen bei Mirabilis jalapa, Urtica pilulifera, und Lunaria annua. Ztschr. f. Ind. Abst. u. Vererb. 1: 291–329 (1909).

(9) YASUI, K.: Studies on the maternal inheritance of plastid characters in Hosta japonica Asch. et Graeb. Albomarginata Mak and its derivatives. Cytologia 1: 192–215 (1930).

(10) IMAI, Y.: Recurrent auto- and exomutation of plastids resulting in tricolored variegation of Hordeum vulgare. Genetics 21: 752–757 (1936).

(11) ———: Chlorophyll variegations due to mutable genes and plastids. Ztschr. f. Ind. Abst. u. Vererb. 71: 61–83 (1936).

(12) KNUDSON, L.: Permanent changes of chloroplasts induced by X-rays in the gametophyte of Polypodium aureum. Bot. Gaz. 101: 721–758 (1940).

(13) RHOADES, M. M.: Genic induction of an inherited cytoplasmic difference. Proc. Nat. Acad. Sc. 29: 327–329 (1943).

(14) WOODS, M. W., and duBUY, H. G.: Evidence for the evolution of phytopathogenic viruses from the mitochondria and their derivatives. I. Cytological and genetical evidence. Phytopathology 33: 637–655 (1943).

(15) WOODS, M. W., WOODS, A. F., and duBUY, H. G.: Comparative action of viruses and mutant chondriogenes on plant cells. Phytopathology 37: 442 (1947).

(16) WOODS, M. W., and duBUY, H. G.: The effect of tobacco-mosaic virus on cellular respiration. Phytopathology 32: 288–302 (1942).

(17) WOODS, M. W., and duBUY, H. G.: Synthesis of tobacco-mosaic virus protein in relation to leaf chromoprotein and cell metabolism. Phytopathology 31: 978–990 (1941).

(18) WOODS, M. W., and duBUY, H. G.: Oxidizing enzymes in variegated leaves and in isolated normal and mutant plastids. Am. J. Bot. 33 (10): 12a (Abstract) (1946).

(19) IMAI, Y.: The behavior of the plastid as a hereditary unit: The theory of the plastogene. Cytologia, Fujii Jubil. Vol. pp. 934–947 (1937).

(20) HARDING, H. E., and PASSEY, R. D.: A transplantable melanoma of the mouse. J. Path. & Bact. 33: 417–427 (1930).

(21) The Biology of Melanomas. Spec. Publ. of New York Acad. Sc. v. 4, pp. 1–466, New York (1948).

(22) ALGIRE, G. H.: Growth and pathology of melanoma S91 in mice of strains dba, A and C. J. Nat. Cancer Inst. 5: 151–160 (1944).

(23) GRAND, C. G., and CAMERON, G.: Tissue culture studies of pigmented melanomas: fish, mouse, and human. *In* The Biology of Melanomas, v. 4, pp. 171–175. Spec. Publ. New York Acad. Sc. (1948).

(24) duBUY, H. G., WOODS, M. W., BURK, D., and LACKEY, M. D.: Enzymatic activities of isolated amelanotic and melanotic granules of mouse melanomas and a suggested relationship to mitochondria. J. Nat. Cancer Inst. 9: 325–336 (1949).

(25) WOODS, M. W., duBUY, H. G., BURK, D., HESSELBACH, M. and LACKEY, M. D.: Mitochondria and associated subcellular particulates in mouse melanomas. (Abstract) Cancer Research (in press) (1948).

(26) SMITH, D. T.: The pigmented epithelium of the embryo chick's eye studied in vivo and in vitro with special reference to the origin and development of melanin pigment. Bull. Johns Hopkins Hosp. 31: 239–246 (1920).

(27) MASSON, P.: Pigment cells in man. *In* The Biology of Melanomas, v. 4, pp. 15–51. Spec. Publ. New York Acad. Sc. (1948).

(28) GRAND, C. G.: Neoplasm studies. IV. Clasmatosis in the melanoblast. Am. J. Cancer 33: 394–400 (1938).

(29) SMITH, D. T.: Evidence showing the existence of two distinct types of pigment cells capable of giving rise to melanotic tumors. Bull. Johns Hopkins Hosp. 36: 185–198 (1925).

(30) MASON, H. S., KAHLER, H., MacCARDLE, R. C. and DALTON, A. J.: Chemistry of Melanin. IV. Electron micrography of natural melanins. Proc. Soc. Exper. Biol. & Med. 66: 421–431 (1947).

(31) KOPAC, M. J.: Some cytochemical aspects of pigmented cells. *In* The Biology of Melanomas, v. 4, pp. 423–432. Spec. Publ. New York Acad. Sc. (1948).

ENZYMATIC ACTIVITIES OF ISOLATED AMELANOTIC AND MELANOTIC GRANULES OF MOUSE MELANOMAS AND A SUGGESTED RELATIONSHIP TO MITOCHONDRIA[1] [2]

By H. G. DUBUY, M. W. WOODS, DEAN BURK, and MARY D. LACKEY, *Laboratory of Physical Biology* and *National Cancer Institute, National Institutes of Health, Public Health Service, Federal Security Agency.*

INTRODUCTION

This paper reports studies on enzyme activities of the melanized and nonmelanized cytoplasmic granules of three types of mouse melanomas, with the use of Warburg manometric techniques, in an attempt to elucidate further their role in the living cell. Some steps toward chemical characterization are also reported. Separation techniques were employed which had proved suitable for the isolation of mitochondrial elements in enzymically active states. A preliminary report on such enzymatic findings has already been presented (*1*).

LITERATURE REVIEW

A previous paper (*2*) reported cytologic evidence that the Cloudman S91 mouse melanoma possesses two types of cytoplasmic granules; one that is capable of pronounced melanization, and one that is either incapable of such melanization or is at least limited in its capacity to become pigmented. The derived Algire S91A partially amelanotic melanoma possessed the latter type of granules. On the other hand, in the Harding-Passey melanoma all the granules apparently had the capacity to become strongly melanized. The cytoplasmic granules in both the pigmented and nonpigmented condition had certain cytologic properties which are characteristic of granular types of mitochondria in other tissues, e. g., size, shape, and reversible staining with Janus green B in the absence of nuclear staining by this dye. These amelanotic derivatives could be analogous to the plant variegations which are caused by mutated (morphologically "tagged") mitochondrial derivatives. These melanomas might therefore be comparable with plant tissues, in which the presence of mutant mitochondria determines abnormalities in pigmentation and metabolism (*3*, *4*, *5*).

A further study of this material offered the opportunity to determine whether the enzymatic activities reported by Greenstein and Algire (*6*), Hogeboom and Adams (*7*), and Burk et al. (*8*) were especially connected with the cytoplasmic granules. Furthermore it was of interest to determine whether certain enzyme systems characteristic of mitochondria in other tissues (*9*, *10*) also occurred on the melanized and nonmelanized granules of the mouse melanomas.

The significance of the mitochondrial system and its derivatives in cellular metabolism has long been recognized, especially in the realm of plants. Horning and Petrie (*11*) demonstrated the intense morphological changes in this system during seed germination. The recognition of plastids as mitochondrial derivatives (Guilliermond (*12*)) led to the establishment of their role in carbohydrate, fat, and protein metabolism, and especially in photosynthesis. The significance of mitochondria in animal-cell physiology was indicated by the work of Bensley and Hoerr (*13*), Graffi and Junkmann (*9*), Lazarow (*14*), Claude (*15*), Hogeboom, Schneider, and Pallade (*10*), Lehninger (*16*), and others.

Methods for successful purification of mitochondria and plastids are based mainly on the consideration that osmotically active aggregates of a coacervate nature have to be dealt with. Thus certain concentrations of salts, with or without the addition of sugars (Warburg and Lüttgens (*17*), Hoerr (*18*), Granick (*19*), duBuy and Woods (*20*), French and Rabideau (*21*)) or other substances, are required for proper conservation and are followed by filtration and selective centrifugation methods. Recently Hogeboom et al. (*10*) and Lehninger (*16*) applied modification of the earlier

[1] Received for publication May 18, 1948.

[2] Mrs. Clara Fischer Smith aided in the conduct of these studies.

819164—49——5

sucrose extraction techniques to the separation of animal mitochondria in enzymatically active states.

MATERIALS AND METHODS

The S91 melanoma and the S91A partially amelanotic melanoma were carried by serial transplantation in dba mice. The S91A tumor was in addition carried by C mice, and the Harding-Passey melanoma exclusively in this strain. Techniques of transfer were as previously described (*2*).

The animals were killed by neck dislocation followed by immediate removal of the tumor tissue. The latter was at once placed in ice-chilled 0.85 percent sodium chloride solution until weighing. Extraction and separation procedures were carried out in a cold room at about 3° C. In some of the experiments purified sea sand, previously washed in order to remove the finest grains, was added in approximately equal proportion by weight. An equal amount of 0.85 percent sodium chloride, or sucrose-saline (2.5 to 5 percent sucrose, and in a few cases 30 percent sucrose without saline) was then added, and the mixture ground 10 to 15 minutes in an ice-chilled glass mortar. Additional saline or sucrose-saline was then added to give a total amount of solution not to exceed three times the original weight of wet tissue, and the mixture filtered through a Buchner funnel containing a layer of pyrex glass wool. In a number of experiments the tissue was ground without sand, but filtration procedures were not changed. In homogenates of this type, the pH was approximately 7.0 after filtering.

Following filtration, separation of the particulates was accomplished essentially by Hoerr's techniques (*18*). This involved a 20-minute centrifugation at about 400 r. p. m. in an angle centrifuge (about 26 g) followed by 3-5 runs of 1 minute at higher speed (about 3,400 r. p. m. or 1,700 g). The number of short runs was determined by the degree of purification of the granules, as noted each time by microscopic examination. A long run of 20 to 40 minutes at the same high speed was then made to sediment the microscopically visible granules. In certain experiments, final fractionations involved separation at speeds either lower or higher than 3,400 r. p. m. These are specifically referred to. Granules used in chemical tests for nucleoprotein constituents were always subjected to at least two further suspensions and recentrifugations in physiological saline without phosphate. A number of experiments was performed at centrifugal forces up to 19,000 g, using a Servall angle head centrifuge.

The material for the metabolic experiments was suspended in a buffered 0.85 percent sodium chloride solution (100 mg. K_2HPO_4 per liter saline, brought to pH 6.9 with saturated KH_2PO_4).

TABLE 1.—*Oxidative enzyme activities* [1] *of particulate fractions of various mouse melanomas*

Melanoma	Addition [2]							
	None (endogenous)	PPDA cytochrome C [3] (cytochrome oxidase)	Succinate cytochrome C [4]	Succinate	PPDA [5]	Tyrosine	Dopa	Dry weight (mg./ml.) [6]
Algire S91A amelanotic melanoma:								
Average	0.3	41.6	27.3	13.2	17.1	(−)2.5	1.2	1.3
Range	(−)3.3–4.2	26.3–68.5	12.3–39.5	4.4–18.9	14.4–20.1	1.0–(−)4.6	0–2.8	0.83–2.14
Determinations, number	4	6	8	8	6	4	8	4
Cloudman S91 melanotic melanoma:								
Average	3.2	53.6	40.0	17.0	24.2	1.3	16.2	2.06
Range	2.8–3.6	31.8–81.5	7.8–70.2	11.6–28.2	12.3–45.5	1.1–1.9	10.8–23.8	1.58–2.9
Determinations, number	4	8	6	6	8	4	8	3
Harding-Passey melanotic melanoma:								
Granules:								
Average	1.6	15.1	11.1	3.9	7.4	15.1	27.3	3.6
Range	.3–3.6	11.1–17.9	4.7–17.7	.9–5.7	3.7–10.0	1.5–26.8	24.5–32.2	2.45–4.2
Determinations, number	8	6	14	14	6	8	8	6
Compound bodies:								
Average	.5	7.5	7.4	0	4.4	.6	25.7	1.7
Range	(−).9–1.9	6.7–8.4	6.4–8.4	----------	4.3–4.5	0–1.2	14.7–36.7	1.38–4.7
Determinations, number	2	2	4	4	2	4	2	3

[1] Expressed as Q_{O_2}, or cubic millimeters O_2 consumed/milligrams dry weight/hour.
[2] PPDA, 0.02M; cytochrome C, 10^{-3}M; succinate, 0.02M; L-tyrosine, 0.02M; L-dopa, 0.01M (D,L-dopa, 0.02M, in 1 experiment).
[3] Yields a relative measure of cytochrome oxidase activity.
[4] Yields a relative measure of succinic oxidase activity.
[5] Yields a relative measure of cytochrome C content.
[6] The number of dry-weight determinations is equal to the number of individual granule preparations reported on, whereas the number of determinations includes replicate assays.

The following relative enzyme activities were determined: (1) Cytochrome oxidase (paraphenylenediamine (PPDA) with and without cytochrome C added); (2) succinic oxidase (succinate with and without cytochrome C added); (3) cytochrome C (PPDA added); (4) tyrosinase (L-tyrosine added); and (5) dopa oxidase (3,4-dihydroxyphenylalanine (both L- and D, L-forms of dopa added)). Some preliminary experiments were conducted with cyanide to determine the effect of these inhibitors on some of the enzyme systems measured.

The Q_{O_2} values (cubic millimeters O_2 consumed/milligrams dry weight/hour) reported in table 1 were obtained in Warburg vessels where the vessel constants were of the order of 0.5, and with particulate dry weights per vessel of the order of 2 mg. (1–4 mg.). The Q_{O_2} values were therefore numerically about equal to the observed millimeter-pressure change per vessel per hour. The Q_{O_2} values were corrected for autoxidation of substrate blanks (no particulates present), both with and without added cytochrome C, but not for endogenous activity (no substrate). The endogenous activity was virtually insignificant in terms of the experimental error involved.

RESULTS

Oxidative enzyme activities (Q_{O_2} values) of particulate fractions of the mouse melanomas under study are reported in table 1; time courses of oxidation and photomicrographs of types of particulates employed are given in figures 1–7.

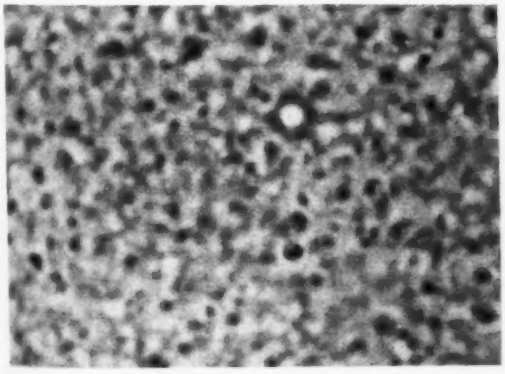

FIGURE 1.—S91A amelanotic melanoma. Suspension of centrifugally isolated amelanotic granules stained with 0.05-percent Janus green B. The diffuse gray background is composed of granules not in focus. A small fat globule can be seen as a brightly illuminated sphere in the upper right of center. Enlarged to × 3660 from an initial magnification of × 1220.

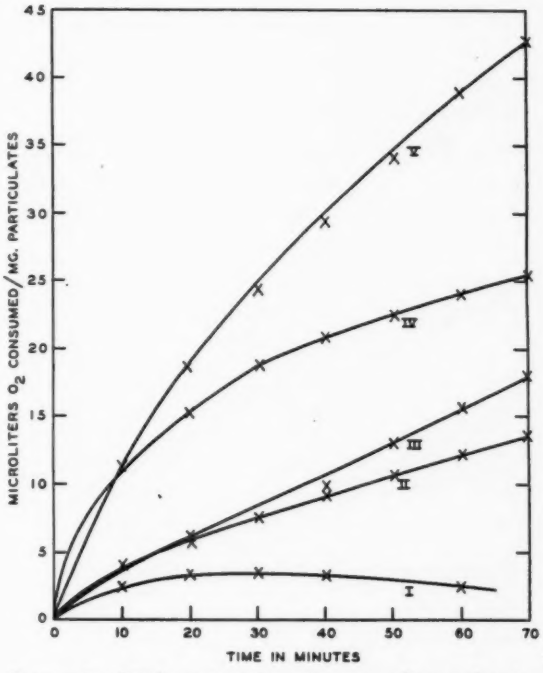

FIGURE 2.—S91A amelanotic melanoma. Curves showing time courses for rates of reaction of centrifugally isolated amelanotic granule preparations with various substrates. Curves are based on averages of experiments for which complete data during 60 to 70 minutes were available. I, no additions; II, 0.02M succinate; III, 0.02M PPDA; IV, 0.02M succinate plus 10^{-5}M cytochrome C; V, 0.02M PPDA plus 10^{-5}M cytochrome C.

ALGIRE S91A AMELANOTIC MELANOMA GRANULES

Purified centrifugal fractions of amelanotic particulates were prepared in 0.85 percent NaCl at pH 6.9. Table 1 presents the results obtained with such suspensions. A photomicrograph of a representative purified preparation is given in figure 1.

Figure 2 illustrates the time course for the oxidative activities involved. In comparison with the results of figure 4, it can be seen that the rates of reaction of the enzymes presented are very similar to those of the S91 melanoma particulates. However, no curves are presented for tyrosine or dopa, since no experimentally significant gas exchanges occurred upon addition of these substrates

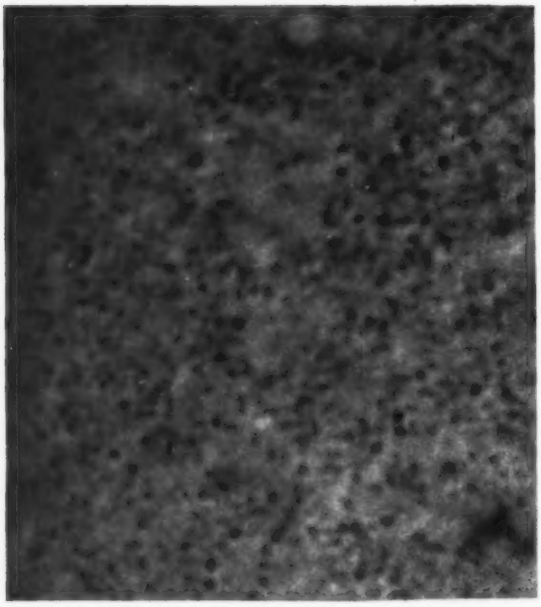

FIGURE 3.—S91 melanoma. Suspension of centrifugally isolated melanized granules unstained. The diffuse gray background is composed of granules not in focus. Enlarged to × 3660 from an initial magnification of × 1220.

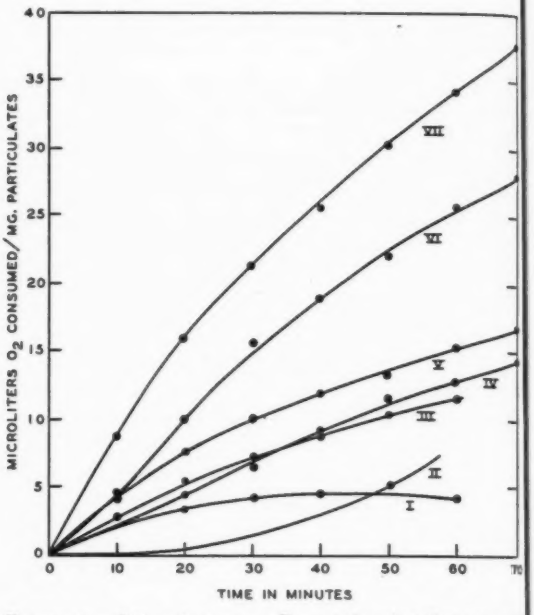

FIGURE 4.—S91 melanoma. Curves showing time courses for rates of reaction of centrifugally isolated melanized granule preparations with various substrates. Curves are based on average of experiments for which complete data during 50 to 70 minutes were available. I, no additions; II, 0.02M L-tyrosine; III, 0.02M succinate; IV, 0.01M L-dopa; V, 0.02M PPDA; VI, 0.02M succinate plus 10^{-5}M cytochrome C; VII, 0.02M PPDA plus 10^{-5}M cytochrome C.

under any conditions studied. In view of the derivation of the S91A partially amelanotic melanoma from the S91 melanoma, the absence of dopa-oxidase activity is significant.

CLOUDMAN S91 MELANOMA GRANULES

The tissue of the S91 melanoma always contained some cells with a variable number of colorless granules. In dissecting the tumors, predominantly amelanotic areas were avoided. A total separation of the amelanotic granules present was not attempted, but microscopic examination showed that the final suspensions were composed mainly of melanized granules. Oxidative enzyme activities obtained with such suspensions are recorded in table 1. The suspensions were again prepared in saline at pH 6.9, and a representative preparation is illustrated in figure 3.

The appreciable oxygen uptake in the presence of either PPDA or succinate, without added cytochrome C, indicates the presence of a considerable endogenous concentration of the latter substance in the particulates.

The time course of the oxidative activities is represented in figure 4. The rates of reaction remained relatively constant for the various substrates, with the exception of tyrosine. The highest rate was obtained with PPDA and cytochrome C. The oxidation of tyrosine was not appreciable (Q_{O_2} of 1.3, uncorrected for the endogenous average Q_{O_2} of 1.3 also), whereas the oxidation of D,L- or L-dopa was relatively pronounced. The enzyme activities encountered were of the same order of magnitude as those obtained with the S91A granules, except for the presence of dopa oxidase. With tyrosine, no detectable darkening of the medium was obtained with granules of either tumor, whereas S91 granules gave marked darkening with dopa.

HARDING-PASSEY MELANOMA GRANULES

In table 1 are summarized results obtained with purified Harding-Passey granules (fig. 5).

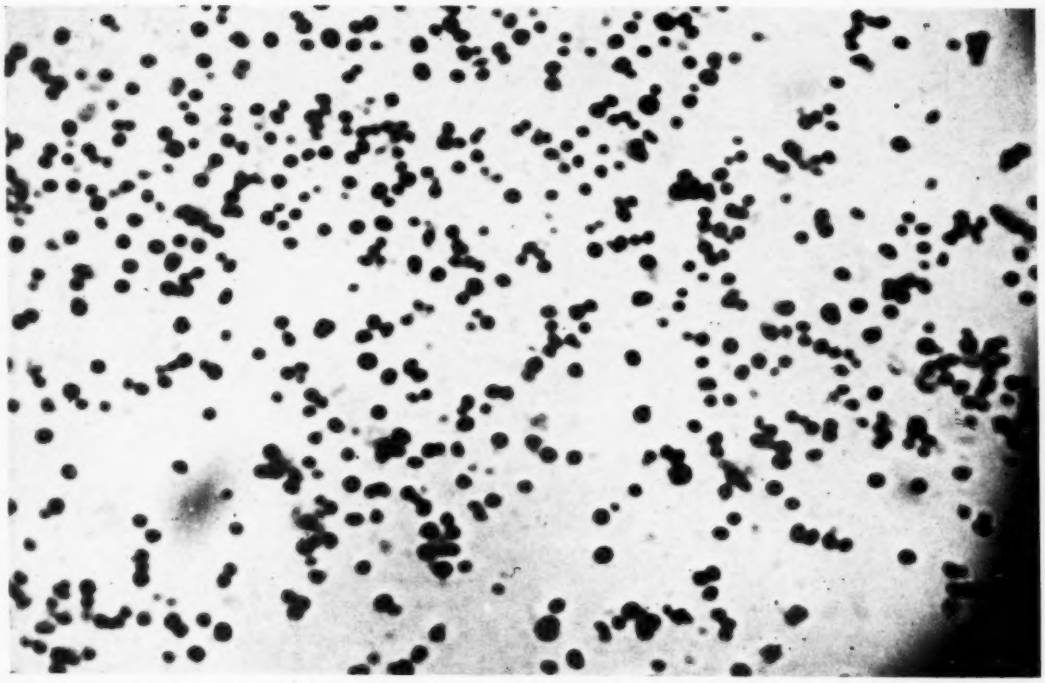

FIGURE 5.—Harding-Passey melanoma. Smear of centrifugally isolated melanized granules stained with neutral red and photographed on process panchromatic film using a Wratten green (B) filter. Note range in size and pigmentation. Completely colorless granules were not observed in this preparation. Enlarged to × 3660 from an initial magnification of ×1220.

Added to the table are results obtained with compound bodies (fig. 6), the probable origin of which is discussed in the preceding paper (*2*).

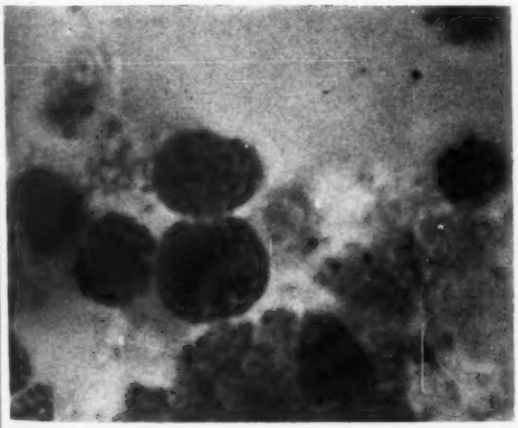

FIGURE 6.—Harding-Passey melanoma. Centrifugally isolated compound bodies. Note difference in size of the melanin granules in different bodies. Enlarged to X 3660 from an initial magnification of × 1220.

The difference between fragments with respect to the size of the contained granules, as shown in figure 6, are also discussed in the preceding paper. These compound bodies appear to be made up of melanized granules surrounded by a portion of the cell membrane and associated cytoplasm of the clasmatosed melanoblast dendrite. Most of them are in the macrophages. Such a history might be expected to have some effect on the enzyme activities of these granules.

Whereas the enzyme activities of the purified Harding-Passey melanized granules did not differ qualitatively from those of purified S91 melanized particulates (with the exception of definite action on tyrosine), the Q_{o_2} values averaged somewhat lower in the former, except with dopa and tyrosine. There was considerable variation between experiments, particularly in the values for succinic oxidase and cytochrome oxidase, probably due in part to tumor age differences. Some preparations oxidized tyrosine readily (Q_{o_2} values 23.2 to 26.8) while others did so very slowly (Q_{o_2} of 1.5 to 8.7).

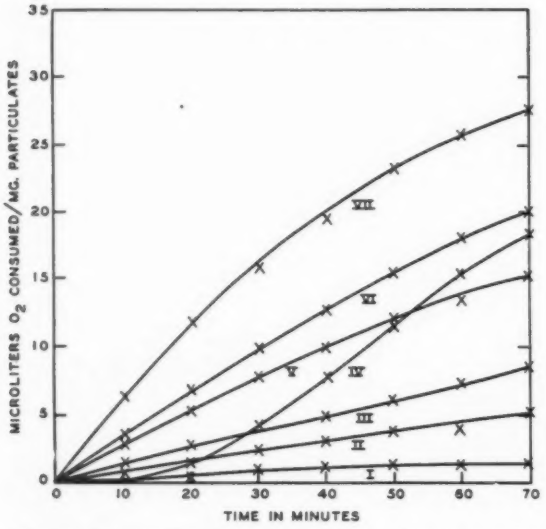

FIGURE 7.—Harding-Passey melanoma. Curves showing time courses for rates of reaction of centrifugally isolated melanized granule preparations with various substrates. Curves are based on averages of experiments for which complete data during 70 minutes were available. I, no additions; II, 0.02M succinate; III, 0.02M PPDA; IV, 0.02M tyrosine; V, 0.02M succinate plus 10^{-5}M cytochrome C; VI, 0.02M PPDA plus 10^{-5}M cytochrome C; VII, 0.01M L-dopa.

The oxidation of dopa was much more uniform (Q_{o_2} of 24.5 to 32.2). However, the relative activities of the enzymes of the Harding-Passey melanoma in separate runs were of the same order of magnitude. This was also the case with the enzyme activities of the S91 and S91A particulates.

In the Harding-Passey tumor, it was possible to obtain, by selective centrifugation, a pellet comprised exclusively of melanized granules. Such preparations displayed no essential enzymatic difference from preparations slightly contaminated with colorless granules.

Figure 7 presents graphically the data obtained with the Harding-Passey particulates, as a time course average of experiments available for the period of time covered. In comparison with figures 2 and 4, it can be seen that the cytochrome system activity of the Harding-Passey tumor particles is lower per milligram dry weight than that of the other two tumors. This might be due to the fact that the melanin content of the Harding-Passey particulates is higher than that of the others, thus increasing the relative dry weight in relation to enzyme activity.

An outstanding characteristic is the high dopa-oxidase activity. This is in keeping with the high melanin content of the Harding-Passey granules. The curve for tyrosinase shows the typical initial lag phase.

To determine the influence of cyanide on the oxidation of PPDA (0.02M), with and without added cytochrome C (10^{-5}M), a few experiments were conducted with Harding-Passey melanin granules. KCN was added to the alkali in the center well of the Warburg vessel and to the buffer in which the particulates were suspended in such manner as to give a final concentration in the latter of approximately 10^{-3}M cyanide. Appropriate controls were run. In two experiments the Q_{o_2} values for PPDA without added cytochrome C or cyanide were 3.1 and 4.4. Addition of cytochrome C raised these to 15.8 and 20.0, respectively. On the other hand, in the presence of 10^{-3}M cyanide, the values were 2.1 and 3.1 with added cytochrome C and 0.8 and 1.4 without added cytochrome C. It is obvious that cyanide largely eliminated the stimulating effect of cytochrome C.

DISTRIBUTION OF ENZYMATIC ACTIVITIES

In order to demonstrate that the main activity of the enzymes studied was associated with the fraction which contained the granules, a number of experiments were performed in which the activity of the homogenate, after filtering through glass wool, was compared with the activities of a resuspended pellet obtained by submission to low centrifugal force (26 to 75 g; fraction 1), a resuspended pellet obtained by submission of the remaining supernatant of the first centrifugation to high centrifugal force (1,900 g; fraction 2), and the remaining supernatant (fraction 3). It was found that a force of 1,900 g active for 20–30 minutes was required to throw down most of the microscopically visible granules. This was due to the fact that the content of tissue colloids in the suspension fluid was deliberately maintained at a high level (1 part tissue by weight to not over 3 parts physiologic saline). Following resuspension in physiologic saline the particles sedimented much more readily.

The results are expressed in Q_{O_2} values for homogenate and fractions (table 2) as well as in gas uptake of a certain amount of homogenate as compared with the total gas uptake of the three fractions obtained from the same amount of homogenate (table 3). In comparing the Q_{O_2} values of table 1 with those of table 2, it should be kept in mind that in order to allow a comparison between homogenate activity and the sum total activity of its constituent elements the respective pellets could not be washed, as a certain amount of the enzymes or cofactors might be washed off, following further treatment. Furthermore, for the same reason, the separation of the various subcellular elements was not brought to absolute completion. However, fraction 1, in the case of the S91 and S91A melanomas contained many granules, nuclei, some cell fragments, and cytoplasmic aggregates, and some fat globules; fraction 2 contained mainly granules, but very few nuclei and fat globules; and fraction 3, generally a few small mitochondria and fat globules and the fluid phase. The bulk of the fat globules was found on the surface of the last fraction. Most of it adhered to the walls of the centrifuge tubes when the fraction was removed. This fat was discarded. In the case of the Harding-Passey melanoma, fraction 1 contained also the large majority of the compound bodies which derived from the phagocytes.

TABLE 2.—*Q_{O_2} values (expressed as cubic millimeters O_2 consumed/milligrams dry weight/hour) of filtered tissue homogenates of three types of melanomas as compared with the Q_{O_2} values of the homogenates separated into three fractions: Fraction 1, many granules plus some other cell material; fraction 2, mainly granules; and fraction 3, mainly supernatant fluid* [1]

Melanoma	Homogenate	Fraction 1	Fraction 2	Supernatant
Algire S91A:				
PPDA 0.02M	3.5	7.4	3.3	Gas produced.
PPDA 0.02M, cytochrome C 10^{-5}M.	10.7	19.7	21.4	1.5
Cytochrome C 10^{-5}M	1.1	.7	.3	.8
Succinate 0.02M	4.1	5.5	4.0	.2
Succinate, cytochrome C 10^{-5}M	8.6	22.5	13.1	.8
Dry weight, milligrams/milliliter.	23.90	13.54	10.90	10.46
Cloudman S91:				
PPDA 0.02M, cytochrome C 10^{-5}M.	8.2	21.4	38.4	1.2
Cytochrome C 10^{-5}M	.8	.3	Gas produced.	.6
D, L-dopa 0.01M	2.3	4.4	3.3	.9
Endogenous	.5	Gas produced.	Gas produced.	.2
Dry weight, milligrams/milliliter.	37.6	15.0	7.94	27.0
Harding-Passey:				
PPDA 0.02M	3.3	4.4	8.4	1.7
PPDA 0.02M, cytochrome C 10^{-5}M.	5.0	7.6	11.2	1.6
Cytochrome C 10^{-5}M	.6	1.0	.9	.5
D, L-dopa 0.005M	7.2	23.6	27.3	12.4
Endogenous	.6	.7	1.1	.1
Dry weight, milligrams/milliliter.	32.28	9.50	16.6	24.4

[1] 0.5 ml. of each suspension was used per vessel. The remainder of the 1 ml. total liquid volume per vessel was made up with the appropriate amounts of substrate and buffer solutions. All values based on the first 30 minutes of gas uptake and represent the average of duplicate determinations.

TABLE 3.—*Total oxygen uptake in cubic millimeters of the homogenate of three types of melanomas as compared with the total gas uptake of three fractions obtained for the same amount of homogenate* [1]

Melanoma	Homogenate	Fraction 1	Fraction 2	Fraction 3	Fractions 1, 2, 3
Algire S91A:					
PPDA 0.02M	1,137	498	218	60	776
PPDA 0.02M-cytochrome C 10^{-5}M.	3,461	1,337	1,402	190	2,929
Cytochrome C 10^{-5}M	346	48	19	101	168
Succinate 0.02M	1,318	375	263	29	667
Succinate-cytochrome C 10^{-5}M	2,770	1,526	857	101	2,484
Total dry weight—mg	322.7	67.7	65.4	125.5	258.6
Cloudman S91:					
PPDA 0.02M-cytochrome C 10^{-5}M.	4,647	3,216	3,044	372	6,632
Cytochrome C 10^{-5}M	441	48	24	21	93
D, L-dopa 0.01M	1,335	658	264	288	1,210
Endogenous	252	86	30	84	200
Total dry weight—mg	564.0	150.0	79.4	307.8	537.2
Harding-Passey:					
PPDA 0.02M	2,645	42	1,899	920	2,861
PPDA 0.02M-cytochrome C 10^{-5}M	4,040	722	2,554	876	4,152
Cytochrome C 10^{-5}M	445	94	211	286	591
D, L-dopa 0.005M	5,845	2,238	6,201	6,675	15,114
Endogenous	465	68	244	68	380
Total dry weight—mg	807.0	95.0	227.4	536.8	859.2

[1] All values based on duplicate determinations.

It was deemed superfluous to determine the activity of the ground tissue before filtering through glass wool, because this fraction would have contained nothing more than the homogenate, except varying amounts of whole cells and small pieces of tissue. The value of the activity of such a complex would be doubtful, since the activity could not with any degree of certainty be ascribed to any particular sub-cellular elements.

Table 2 presents the oxygen uptake per hour per milligram dry weight of homogenate or fraction, calculated for the first half hour of gas exchange following tipping. The main enzyme activity is located in the granular fraction. The supernatant fraction showed appreciable gas uptake only when dopa was given as substrate. Apparently dopa oxidase is either loosely bound to the particulates and can be easily removed, or a small portion of it is always present in the supernatant. The first alternative seems more accept-

able on the basis of our experience, that the greater the precautions in preparing the particulates, the greater the percentage of activity found in the particulate fraction.

The Q_{O_2} values of the particulate fractions 1 and 2 were invariably higher than those of the original homogenate indicating that a considerable quantity of enzymatically inactive material was removed during centrifugal purification. It should be mentioned here that the enzyme activities for the fractions may not always be the highest that can be obtained, since on limited dilution (1 : 10) of the homogenate or the particulate fractions, some further increases in Q_{O_2} values were found when the concentration of material was high (15–20 mg. dry weight) per vessel. However, this does not detract from the main fact that the greatest enzyme activity is to be found in the particulate fractions and not in the supernatant.

For further comparison of the fractions, data are given in table 3 in which the total gas uptake during the first 30 minutes after tipping was calculated for a given amount of homogenate and for the three fractions obtained from the same amount of homogenate. By summating the separate values for fractions 1, 2, and 3 and comparing this total gas uptake with that of a corresponding amount of homogenate, it can be seen that there is a reasonable agreement between the two sets of values.

This agreement further supports the interpretation given before, that the increase of Q_{O_2} values of the three fractions over that of the homogenate, as presented in table 2, was mainly due to removal of enzymatically inactive material from the fractions 1 and 2, and not to the removal of an inhibitor. The dilution effected by the preparation of the fractions would otherwise have yielded values for total gas uptake appreciably greater for the summated fractions than for the homogenate. An exception occurred in the case of the dopa runs of the Harding-Passey fractions, where the total gas uptake is about two and a half times the total gas uptake of the original unfractionated homogenate. This exceptional behavior may be related to the more complex character of the Harding-Passey homogenates, but its nature remains to be determined.

Microscopic examinations of the various melanized particulate fractions showed that the contaminating colorless particulates were numerically insignificant. However, to make certain that the major part of the enzymatic activities measured occurred on the melanin granules, several experiments were performed in which virtually complete separation of the melanin granules and colorless particulates was achieved. In one experiment the centrifugal separations were carried out in 0.85 percent NaCl-5 percent sucrose, and in another experiment 30 percent sucrose was employed as the starting solution. Both experiments resulted in the isolation of melanized granule fractions in which no colorless particulates could be observed. These fractions possessed very significant activities for the oxidation of dopa, or of succinate in the presence of added cytochrome C. The second experiment is described in detail. In this case, a single large (14-ml. volume) Harding-Passey tumor was cut into small pieces and immediately placed in 5 volumes of iced 30-percent sucrose solution (30 gm. sucrose per 100 ml. of solution). After soaking for approximately 1 hour, the tissue was removed and homogenized by grinding in a mortar with fresh 30-percent sucrose solution and filtered in the usual manner. The filtered homogenate upon centrifugal fractionation yielded successive sediments under the following conditions: (1) 4,200 g for 20 minutes, (2) 4,200 g for 20 minutes, and (3) 19,000 g for 20 minutes. A fourth fraction was obtained by diluting the supernatant remaining from fraction 3 with distilled water to give a final sucrose concentration of 5 percent, and then centrifuging at 19,000 g for 20 minutes. All pellets were resuspended in 5 percent sucrose. Microscopic examinations of the suspensions, using phase and ordinary microscopy, showed that fraction 1 contained masses of melanin-containing compound bodies (from phagocytes), large free melanin granules, and nuclei. Colorless granules of the type often occurring in the perikaryon of the melanoblast were not observed. Fraction 2 contained melanized granules only and an occasional compound body. Fraction 3 contained almost exclusively melanized granules, although these were small and often of a lighter shade of brown than in the preceding fractions. Only trace contaminations with colorless filaments or granules were present in fraction 3. Fraction 4, which was sedimented in 5 percent sucrose, was composed largely of colorless granules with a few

of the smallest melanin granules and an occasional filamentous particulate. These colorless granules corresponded to those often observed in the intact perikaryons of tumor cells. The Q_{O_2} values in the presence of 0.02M succinate and 10^{-5}M cytochrome C were 5.5 for the homogenate, 4.0 for fraction 1, 6.0 for fraction 2, 5.6 for fraction 3, 10.9 for fraction 4, and gas production for the supernatant. With dopa (0.01M) the corresponding values were 13.3, 12.4, 10.1, 9.5, 21.3, and 2.0, respectively.

The gas exchange for fraction 4, calculated on the basis of the amount of this fraction derived from 1 ml. of the original homogenate, gave per hour a total gas uptake of 6.8 microliters. This value calculated for all the melanized fractions obtained from 1 ml. of the original homogenate was 108 microliters. These results show that most of the succinoxidase activity was contained in the melanized granule fractions. The comparparable values for dopa were 6.5 for fraction 4 and 243.4 for the fractions containing the melanized particulates. With dopa also the supernatant was active, yielding 82.4 microliters per hour on a comparable basis.

Chemical Characterization of Particulates

The work of many investigators has shown that ribose type nucleoprotein is a regular constituent of mitochondria and plastids (*15*, *20*). Therefore, preliminary chemical studies, following in general a previously described procedure (*20*), were undertaken to determine whether the melanized granules of the Cloudman S91 melanoma contained nucleoprotein. The same tests were run on the colorless granules of the S91A amelanotic melanoma for comparison.

Centrifugally purified, washed (physiologic saline) granules from both types of tumors were subjected to hydrolysis in 0.1N sodium hydroxide for 18 hours at 0° C. The pH was then adjusted to 7.6 and the mixture centrifuged at 2,000 r. p. m. (600 g) until the supernatant was clear. This supernatant was pale brown in the case of the S91 melanoma preparation and uncolored in the amelanotic melanoma S91A. Such supernatants when diluted 10 times with 0.85 percent sodium chloride displayed strong absorption curves [3] in the ultraviolet as determined with a Beckman spectrophotometer, and corresponding to curves for nucleic acid, with maximum absorption at approximately 2580 Å. The orcin-HCl ferric chloride reagent (*22*) gave a strongly positive reaction for pentose. Tests for organic phosphorus were run by incinerating micro-portions of the dried supernatants with calcium hydroxide, acidifying on a spot plate with nitric acid followed by addition of ammonium molybdate, benzidine and sodium acetate (*23*, *p. 173*). Tests for phosphorus were strongly positive. Ribose nucleic acid from a commercial source was used as a comparative material in all tests. On the basis of spectrophotometric comparisons (absorption of ultraviolet light at 2580 Å) of a known concentration of ribose nucleic acid, and the material obtained by alkaline hydrolysis of the washed S91 melanin granules, the latter apparently contained approximately 20 percent nucleic acid, calculated on a total-dry-weight basis. This value, however, may be too high because of possible absorption at 2580 Å by components other than nucleic acid.

The preparation of melanized granules used in these tests were determined by direct microscopic examination to be practically free of colorless granules. No phosphates were used in any of the solutions employed in isolation or preparation of the granules.

DISCUSSION

A number of factors must be considered if the morphological integrity of particulates is to be preserved. Bensley (*24*, *p. 32*) noted that—

> Mitochondria and submicroscopic particulates are stable in 0.85 percent NaCl solutions, but swell and lose substance if the electrolyte content is much reduced. They dissolve in water on the alkaline and on the acid side of their pH stability range. The latter has not been determined with accuracy but is known to be dependent also on electrolyte concentration. We have not been able to find that the stability is much influenced by the substitution of NaCl for the normal inorganic constituents of the cell water, but the enzymatic activities apparently are.

With respect to the preservation of enzymatic activities, our results and those of Graffi and Junkmann (*9*) show that these need not be lost in saline suspensions.

It is obvious that enzyme activities might be lost or constituent components leached out of the granules, or both, without gross changes in their form or color. In unpublished studies with plant

[3] Dr. Silvio Fiala and Mrs. Lois Barnhart Macri made the determinations of the ultraviolet-absorption spectra.

819164—49——6

plastids, we found that at a constant pH of 6.9 the total concentration of phosphate is critical in determining whether catechol oxidase remains attached to the plastid structure or is lost to the supernatant. When such loss occurred, it could also be shown spectrophotometrically that the plastid structure was partially broken down because chlorophyll absorption bands appeared in the supernatant. This chloroplast disintegration, although sufficient to result in loss of all detectable catechol oxidase from the particulate structure, was not enough to cause gross microscopic changes. It is well known that phenol oxidases, unlike, e. g., cytochrome oxidase, can be liberated with relative ease from cell structures. This fact does not warrant the assumption that the original presence of such enzymes on cytoplasmic particulates is without biological significance.

In this connection, it is significant to note that, as might be expected upon particulate concentration, the Q_{O_2} values reported here for the enzyme activities of the granules are in general greater than the values reported in studies performed with slices of melanoma tissue (Burk et al. (*8*)) and melanoma tissue homogenates (Greenstein and Algire (*6*); Hogeboom and Adams (*7*)). Graffii and Junkmann (*9*) and Hogeboom et al. (*10*) reported that practically all the succinic oxidase activity of the cell was localized in the mitochondrial fraction.

While the colorless granules present in the S91 preparations undoubtedly contributed to the enzyme activity measured, the numbers present could not on the basis of microscopic estimates account for more than about 10 percent of the total activity. On the other hand, the presence of such colorless granules could be expected, on a dry weight basis, to lower slightly the Q_{O_2} values for dopa oxidation. In the case of the Harding-Passey tumor, fractions composed exclusively of melanized granules were obtained. These possessed high enzyme activities. In the preceding paper data are reported on the staining of the granules with Janus green B, on the manner of distribution of the granules in various stages of melanization, and on the probable occurrence of nucleoprotein of the ribose type in the granules. These data and those reported in the present paper show that the melanized granules possess all the distinctive characteristics usually attributed to mitochondria: appropriate size (from 0.2μ to 1.0μ), reversible staining with Janus green B, chemical components similar to those of mitochondria, and characteristic enzyme systems (cytochrome oxidase, succinic oxidase). At least three possibilities suggest themselves. The first is that a virus-like entity, or a new type of granule of exogenous origin, occurs in the melanomas, and that this entity takes over the mitochondrial functions of the cell. One might hypothesize also that a new granular type of cellular element, of endogenous origin, appears which replaces all, or all but a few, of the normal complement of mitochondria. In this case, the enzymic activities demonstrated were due either to the combined activity of the new granules and the normal mitochondria, to the new type of granule only, or to a few remaining normal mitochondria. The latter would, to account for the activities actually measured, have to have their activity increased at least a thousand fold. A third possibility is that the granules constitute altered normal mitochondria, which have acquired the property of melanization either prior to, due to, or following the development of malignancy and have lost or largely lost this property in the case of the amelanotic derivative of the S91 melanoma.

Since mitochondrial derivatives and mitochondrial mutations have been demonstrated to exist in plants, this third alternative is offered as the most satisfactory interpretation of the available data.

Against the first alternative stand the facts that the granules in question attain sizes (1μ) considerably in excess of known animal viruses and display enzyme activities to an extent not demonstrated for viruses. Similar considerations weigh against the second possibility. It seems improbable that a few remaining normal mitochondria could have increased their activity to account for the gas exchanges measured (table 2 and p. 333). It also seems improbable that a new type of granule has arisen possessing all the properties mentioned.

This leaves as most probable the third alternative, that the granules are derived from the mitochondria of the cell. Such a derivation would account fully for the properties of the granules studied thus far. It would particularly apply to the granules of the S91A melanoma. In most

of the tumor cells of this melanoma, only colorless granules could be detected. These granules stained reversibly with Janus green B and showed all the above-mentioned properties but did not carry dopa oxidase. The only remaining alternative would be that these cells constituted a unique case, demonstrating the existence of mammalian cells not possessing mitochondria.

SUMMARY

Centrifugally isolated preparations of the granules of the Algire S91A, Cloudman S91, and the Harding-Passey mouse melanomas possessed the following enzyme activities, cytochrome oxidase, succinic dehydrogenase, and cytochrome C. The granules of the amelanotic S91A melanoma did not possess tyrosine or dopa-oxidase activities which were displayed by the melanized granules of the Harding-Passey melanoma. The granules of the S91 melanoma possessed dopa-oxidase activity but no appreciable tyrosinase activity under the conditions employed.

Cyanide largely eliminated the stimulating effect of cytochrome C on the oxidation of paraphenylenediamine as determined with the Harding-Passey granules. The data here reported are consistent with the view that the cytoplasmic granules in the melanomas studied represent a modified form of mitochondria.

REFERENCES

(1) Woods, M. W., duBuy, H. G., Burk, D., Hesselbach, M. L., and Lackey, M. D.: Studies of mitochondria and associated sub-cellular particulates in mouse melanomas. (Abstract) Cancer Research 8: (In press) (1948).

(2) Woods, M. W., duBuy, H. G., Burk, D., and Hesselbach, M. L.: Cytological studies on cytoplasmic particulates of the Cloudman S91 mouse melanoma, the derived Algire S91A partially amelanotic melanoma, and the Harding-Passey mouse melanoma. J. Nat. Cancer Inst. 9: 311–323 (1949).

(3) Woods, M. W., and duBuy, H. G.: Evidence for the evolution of phytopathogenic viruses from mitochondria and their derivatives. I. Cytological and genetic evidence. Phytopathology 33: 637–655 (1943).

(4) Woods, M. W., and duBuy, H. G.: Oxidizing enzymes in variegated leaves and in isolated normal and mutant plastids. Am. J. Bot. 33 (10): 12a (1946).

(5) Woods, M. W., Woods, A. F., and duBuy, H. G.: Comparative action of viruses and mutant chondriogenes on plant cells. Phytopathology 37: 442 (1947).

(6) Greenstein, J. P., and Algire, G. H.: Comparative oxidase activity of melanotic and amelanotic melanomas. J. Nat. Cancer Inst. 5: 35–38 (1944).

(7) Hogeboom, G. H., and Adams, M. H.: Mammalian tyrosinase and dopa oxidase. J. Biol. Chem. 145: 273–279 (1942).

(8) Burk, D., Algire, G. H., Hesselbach, M. L., Fischer, C. E., and Legallais, F. Y.: Characterization of tissue metabolism of transplanted mouse melanomas by high oxidative response to paraphenylenediamine. J. Nat. Cancer Inst. 7: 425–429 (1947).

(9) Graffi, A., and Junkmann, K.: Beitrag zum chemischen Aufbau normaler und maligner Zellen. Klin. Wchnschr. 24: 78–81 (1946).

(10) Hogeboom, G. H., Schneider, W. C., and Pallade, G.: Cytochemical studies of mammalian tissues. I. Isolation of intact mitochondria from rat liver; some biochemical properties of mitochondria and submicroscopic particulate material. J. Biol. Chem. 172: 619–636 (1948).

(11) Horning, E. S., and Petrie, A. H. K.: The enzymatic function of mitochondria in the germination of cereals. Proc. Roy. Soc., London, s. B, 102: 188–206 (1927).

(12) Guilliermond, A.: The cytoplasm of the plant cell. *In* A New Series of Plant Science Books, v. 6. Chronica Botanica Co., Waltham, Mass. (1941).

(13) Bensley, R. R., and Hoerr, N. L.: Studies on cell structure by the freezing-drying method. V. The chemical basis of the organization of the cell. Anat. Rec. 60: 251–266 (1934).

(14) Lazarow, A.: The chemical structure of cytoplasm as investigated in professor Bensley's laboratory during the past ten years. *In* Frontiers of Cytochemistry, Hoerr, N. L., editor, Biological Symposia, v. 10, pp. 9–26. Jacques Cattell Press, Lancaster, Pa. (1943).

(*15*) CLAUDE, A.: Distribution of nucleic acids in the cell and the morphological constitution of cytoplasm. Biol. Symposia 10: 111–129 (1943).

(*16*) LEHNINGER, A. L.: Quantitative study of products of fatty acid oxidation in liver suspensions. J. Biol. Chem. 164: 291–306 (1946).

(*17*) WARBURG, O., and LÜTTGENS, W.: Weitere Experimente zur Kohlensäureassimilation. Naturwissenschaften 32: 161 (1944).

(*18*) HOERR, N. L.: Methods of isolation of morphoiogical constitutents of the liver cell. *In* Frontiers of Cytochemistry, Hoerr, N. L., editor, Biological Symposia, v. 10, pp. 185–232. Jacques Cattell Press, Lancaster, Pa. (1943).

(*19*) GRANICK, S.: Quantitative isolation of chloroplasts from higher plants. Am. J. Bot. 25: 558–560 (1938).

(*20*) duBUY, H. G., and WOODS, M. W.: Evidence for the evolution of phytopathogenic viruses from mitochondria and their derivatives. II. Chemical evidence. Phytopathology 33: 766–777 (1943).

(*21*) FRENCH, C. S., and RABIDEAU, G. S.: The quantum yield of oxygen production by chloroplasts suspended in solutions containing ferric oxalate. J. Gen. Physiol. 28: 329–342 (1945).

(*22*) LE PAGE, G. A., and UMBREIT, W. W.: Methods for the analysis of phosphorylated intermediates. *In* Manometric Techniques and Related Methods for the Study of Tissue Metabolism, by Umbreit, W. W., Burris, R. H., and Stauffer, J. F., ch. 15. Burgess Publishing Co., Minneapolis (1945).

(*23*) FEIGL, F.: Laboratory manual of spot tests. Academic Press Inc., New York (1943).

(*24*) BENSLEY, R. R.: Chemical structure of cytoplasm. *In* Frontiers in Cytochemistry (Biological Symposia X). pp. 323–334. Jacques Cattell Press, Lancaster, Pa. (1943).

PHYSICOCHEMICAL STUDIES OF REVERSIBLE AND IRREVERSIBLE COMPLEXES OF COBALT, HISTIDINE, AND MOLECULAR OXYGEN [1]

By JOHN Z. HEARON,[2] and DEAN BURK, *National Cancer Institute, National Institutes of Health, Public Health Service, Federal Security Agency*, and ARTHUR L. SCHADE, *Overly Biochemical Research Foundation, New York*

CONTENTS

	Page
Introduction	337
Formation of cobaltodihistidine and related compounds	339
Intermediate species	343
Amino acids other than histidine	347
Co-ordination of histidine with metals other than cobalt	348
The reversible oxygen reaction: the formation of oxy-bis(cobaltodihistidine)	349
Irreversible oxygen reactions of cobaltodihistidine	354
Rearrangement without oxygen uptake	358
Production of carbon dioxide and hydroxyl ion	359
Oxygen interactions with cobalt and histidine derivatives	360
Oxygen interactions with cobalt and various amino acids and ammonia	363
Oxygen interactions with other metal-histidine complexes	364
Combinations with carbon monoxide and cyanide	366
Optical properties	367
Magnetic properties	370
Summary	370
References	372
Appendix I	373
Appendix II	374
Appendix III	376

INTRODUCTION

The trace metals have attracted much attention regarding their possible role in cellular metabolism. Of these metals, cobalt has appeared in numerous biochemical phenomena and has been investigated from many points of view. The prominence assumed by cobalt is due in good measure to its long-established importance as an essential element for cattle and sheep and to its pronounced effect upon hematopoiesis in the production of polycythemia or in the alleviation of spontaneous or induced anemias in both benign and malignant diseases.[3] More specific phases of the study of cobalt include, for example, the activation of arginase (*1*), carboxylase (*2*), choline esterase (*3*), and phosphoglucomutase (*4*, *5*); repression of erythrocyte respiration (*6*), and the striking protection (in vitro) of brain respiration against high oxygen pressure (*7*), as well as similar protection against convulsion (in vivo) caused by high oxygen pressure (*8*).

In general it is true that these various over-all effects have not yet been interpreted mechanistically in terms of specific properties of the cobalt ion. Although in the realm of metallo-organic chemistry, the individual reactions of Co^{++} that have been studied are almost innumerable, few of these reactions have been of sufficient physiologic importance to interest the biochemist or to implement his interpretations of the biological effects of this element.

Whereas it might be said that cobalt appears most often in the role of an essential element or

[1] Received for publication August 12, 1947.

[2] Senior Research Fellow, National Cancer Institute, Public Health Service, now at Department of Physiology, University of Chicago. Valuable aid was provided in this investigation by Marie L. Hesselbach, Hilton Levy, Lois Barnhart Macri, Robert W. Reinhart, and Clara Fischer Smith.

[3] Since this paper was submitted for publication, the following publications have shown that crystalline vitamin B_{12} possesses activity with respect to pernicious and other anemias, and the "animal protein factor," contains cobalt in its molecular composition, and is the only vitamin yet known to contain this or any other metal:

(1) RICKES, E. L., BRINK, N. G., KONIUSZY, F. R., WOOD, T. R., and FOLKERS, K.: Crystalline vitamin B_{12}. Science 107: 396-397 (1948).

(2) SHORB, M. S.: Activity of vitamin B_{12} for the growth of *Lactobacillus lactis*. Science 107: 397-398 (1948).

(3) WEST, R.: Activity of vitamin B_{12} in Addisonian pernicious anemia. Science 107: 398 (1948).

(4) SMITH, E. L.: Purification of anti-pernicious anaemia factors from liver. Nature, London 161: 638-639 (1948).

(5) ———: Presence of cobalt in the anti-pernicious anaemia factor. Nature, London 162: 144-145 (1948).

(6) RICKES, E. L., BRINK, N. G., KONIUSZY, F. R., WOOD, T. R., and FOLKERS, K.: Vitamin B_{12}, a cobalt complex. Science 108: 134 (1948).

(7) OTT, W. H., RICKES, E. L., and WOOD, T. R.: Activity of crystalline vitamin B_{12} for chick growth. J. Biol. Chem. 174: 1047 (1948).

an activator, our biologic studies, detailed elsewhere, have dealt predominately with the properties of cobalt as an inhibitor, comparable with some antibiotics. The chemical work reported here was originally prompted by observations on the bacteriostatic action of Co^{++} and its ability to inhibit tissue respiration. The presence of Co^{++} in concentrations of 1–100 p. p. m. exerted a bacteriostatic effect upon various microorganisms (*9*). All bacterial species tested were sensitive to Co^{++} (*9, 10*). Its reversible bacteriostatic action contrasted sharply with the bacteriocidal action of many heavy metals. The inhibition of bacterial growth due to Co^{++} was readily reversed by the addition of histidine. This reversal of cobalt inhibition by histidine is specific in the sense that other naturally occurring amino acids, with the possible exception of cysteine, did not exhibit this effect to any marked extent (*9*). Bacterial respiration was also inhibited by Co^{++}, at somewhat higher concentrations than those required for 100-percent growth inhibition (*9, 10*). Of particular interest is the fact that cobalt appeared to inhibit respiration of growing bacteria. The respiration rate per unit weight of dry-matter growth was usually higher in growing cells than that in resting cells; Co^{++} reduced the respiration of the growing cell to the level of the resting cell (*10*). This fact indicates that Co^{++} inhibits components of oxidative metabolism concerned with cell division and growth. It is of significant interest that the effect of an agent having these properties may be controlled and reversed simply and completely by the naturally occurring amino acid histidine.

The results of these studies and their obvious inferences suggested the study of the effect of Co^{++} on animal-tissue respiration. It was found that mouse-tissue respiration was inhibited by Co^{++} at concentrations of 5–100 p. p. m. The respiration of various tissues differed in sensitivity to Co^{++}, embryo and tumor tissue being particularly sensitive (*11*). The effect of Co^{++} upon tissue respiration was not reversed by histidine (*10, 12*). The inhibition was highly progressive with time, but the time course of progression could be halted by the addition of histidine; also the inhibition could be prevented by the addition of histidine at an early stage or at the time of initial addition of Co^{++} (*12*). Apparently the combination of Co^{++} with the tissue components involved is irreversible in contrast with the bacterial components, or the rate of elimination of cobalt by histidine is slower.

The foregoing results made desirable the emphasis and study of at least three important biologic observations: (1) The fact that the effect of cobalt may be reversed under appropriate conditions; (2) the fact that the reversibility may be accomplished in particular by the naturally occurring amino acid histidine; and (3) the fact that cobalt often operated by inhibiting growth respiration in contradistinction to endogenous or resting respiration. Further chemical studies led to results indicating that cobalt combines with histidine to form a reversible co-ordination complex, and that in contrast with most amino acids such combination can readily be effected at concentrations and pH ranges that are physiologically applicable. Certain characteristics of this reaction and properties of the complex thereby formed were previously reported (*12–15, 17*).

Early in the chemical work the rather unusual observation was made that the histidine-cobalt complex combines reversibly with molecular oxygen. This relatively uncomplicated system shows many striking similarities to the hemoglobin-oxyhemoglobin system and is even more similar to the hemocyanin-oxyhemocyanin system. The characteristics of the oxygenation reaction and the electronic structure of the oxygenated complex were briefly outlined previously (*13–16*) and are considered in some detail in this and a previous paper (*17*).

The results of a thorough study of the chemical reactions in the cobalt-histidine system and in the cobalt-histidine-O_2 system would be of importance for two widely different reasons: (1) Cobalt is potentially a unique and useful tool in the study of growth and growth-respiration relations. The value of adequate knowledge of the combination of cobalt and histidine, by which the inhibition may be reversed at will, and of the availability of the constants of the systems involved is obvious. (2) The theoretical implications of a structurally simple oxygen carrier which embodies many features of the natural oxygen carriers are equally obvious.

In response to these two incentives, we have carried out such a chemical study. As must al-

ways be the case when a new subject is engaged, the results are not uniformly complete. Certain points were not exhaustively investigated because of time limitations, others by choice. However, salient features of the system are adequately delineated. Results obtained in physicochemical studies of the complexes of cobalt, histidine, and molecular oxygen and of related complexes are reported.

FORMATION OF COBALTODIHISTIDINE AND RELATED COMPOUNDS

The addition of Co^{++} to a solution of histidine at pH 7–7.5 produces a marked fall in pH. At concentrations of the order of 0.01 M histidine and 0.005 M Co^{++}, or greater, two moles of base per mole of Co^{++} are required to return the solution to the original pH. This fact indicates that the reaction between cobalt and histidine under these conditions results in the formation of two H^+ per mole of Co^{++}; further, since at pH ~7.5 histidine is predominately in that form that carries only one acid group, viz, $—NH_3^+$, these findings require that two histidine molecules combine with one cobaltous ion. This stoichiometry is also borne out by various curves that follow, and by the fact that if to a given amount of ~0.1 M histidine in solution Co^{++} is added in increments and the system titrated back to the original pH after each addition, then, when the molar ratio of added Co^{++} to histidine attains 1:2, further addition of Co^{++} does not result in the release of titratable H^+.

In the presence of Co^{++}, the titration curve of histidine is displaced in a manner such that the $—NH_3^+$ group is titrated over a pH range appreciably lower than the normal pK of this group. The displacement is somewhat greater in the presence of oxygen. These points are shown in figure 1.

Except to state that the study of the restricted reaction between cobalt and histidine must be conducted in the essential absence of oxygen, we defer the oxygen interaction to a succeeding section. Figure 1 shows that the titration curve of histidine is the usual one exhibiting flattened regions corresponding to the titration of the imino $\left(\overset{+}{=}NH—\right)$ and amino ($—NH_3^+$) groups. In the presence of Co^{++}, the two flat regions are

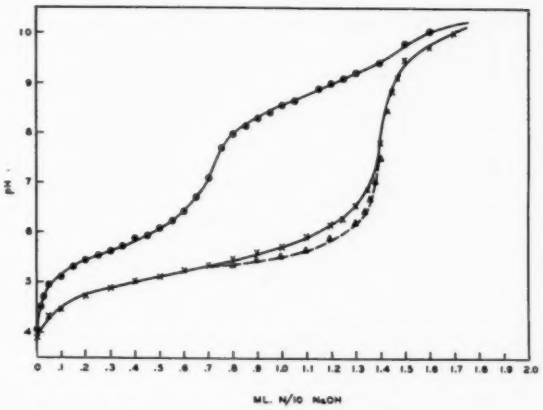

FIGURE 1.—Titration of histidine in the presence of cobalt.

● 72 μM of histidine hydrochloride under N_2;
✕ 72 μM of histidine hydrochloride plus 36 μM Co^{++} as $CoCl_2$ under N_2;
▲ As above, but under O_2.
T=25° C.: initial volume, 5.5 ml.

no longer separated by the sharp inflection but merge insensibly into a single flat region which terminates in a sharp rise corresponding, on the abscissa, to the total available histidine. The results represent those of an acid titrated in the presence of a solute which combines preferentially with the anion thereby increasing the observed acid strength. The sharp rise in the cobalt-histidine curve corresponds therefore to the completion of the formation of the cobalt-histidine complex. Figure 2 clearly demonstrates the stoichiometry of the reaction. This set of curves illustrates the results obtained when 0.5 mM of histidine is titrated in the presence of 0, 0.0625, 0.125, and 0.250 mM of Co^{++}, respectively. In curve 1, the first end point is at the completion of the imino group titration; in curves 2–4, the end points occur when the total imino protons plus two moles of amino protons per mole of cobalt have been titrated, the remaining or excess amino protons in curves 2–3 being titrated in the region of the normal pK. In view of these results, it is regarded as established that the final complex formed under these conditions of completion, consists of one cobaltous ion per two histidine anions. This complex is therefore referred to hereinafter as cobaltodihistidine.

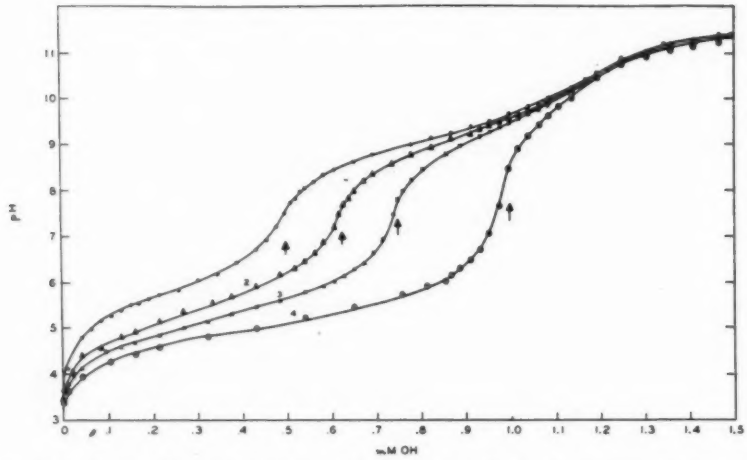

FIGURE 2.—Titration of histidine in the presence of varying amounts of Co^{++}. The arrows indicate theoretical end points or inflections. Curve 1, no cobalt; curve 2, 62.5μM Co^{++}; curve 3, 125μ M Co^{++}; and curve 4, 250μ M Co^{++}. In all titrations, 500μ M of histidine hydrochloride; *T*, 25° C.; initial volume, 10 ml.; all titrations under N_2.

While it is perfectly clear that the end product, as deduced above, is cobaltodihistidine, the complete analysis of the curves in the present instance is somewhat complicated by the fact that the coordinating base is capable of bearing two ionizable protons of widely different pK values. Attempts were made first to analyze the curves over the pH range where the dissociation of the $-NH_3^+$ group was negligible, on the basis of the following equilibria:

$$\phi H_2^+ \rightleftharpoons \phi H + H^+, \; K_{imino} = K_i = \frac{[\phi H]\,[H^+]}{[\phi H_2^+]} \qquad (1)$$

$$2\phi H + Co^{++} \rightleftharpoons \phi_2 Co + 2H^+, \; K_2 = \frac{[\phi_2 Co]\,[H^+]^2}{[\phi H]^2\,[Co^{++}]} \qquad (2)$$

where ϕ^- is the histidine anion, 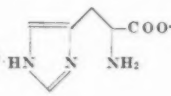 ;

ϕ_2Co is 2 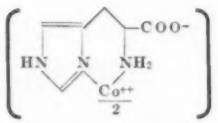 , i. e., cobaltodihistidine; and reaction 2 is actually the net sum of reactions 2a and 2b:

$$2\phi H \rightleftharpoons 2\phi^- + 2H^+, \; K_{amino} = K_a = \frac{[\phi^-]\,[H^+]}{[\phi H]} \qquad (2a)$$

$$2\phi^- + Co^{++} \rightleftharpoons \phi_2 Co, \; K_{\phi-} = \frac{[\phi_2 Co]}{[\phi^-]^2\,[Co^{++}]} \qquad (2b)$$

It was assumed in the analysis that cobalt occurred only as Co^{++} and ϕ_2Co. However, equilibrium constants for the formation of ϕ_2Co calculated on this basis were unsatisfactory and showed a steady decrease with increasing pH. Therefore one or more additional reactions giving rise to one or more additional species must occur, and the foregoing equilibria are not adequate to describe the system. Furthermore, when in the analysis of complete curves it becomes necessary to include an intermediate species, the number of variables must exceed the number of relations between them by one. It is imperative, in order to solve the problem at all, to employ some approximation procedure, or to isolate in a restricted region of pH and concentration a single reaction, and then when the equilibrium constant has been determined, to employ this expression as the additional required relation.

The equilibrium relation of particular interest was that for reaction 2, i. e., the formation of cobaltodihistidine from histidine as the latter exists under essentially physiologic conditions, pH ~7.5. It seemed desirable, therefore, to proceed directly to conditions under which ϕH_2^+ and ϕ^- were negligible and the predominant reaction was that giving rise to cobaltodihistidine.

It is easily shown that the desired pH is the isoelectric point, where ϕH_2^+ and ϕ^- are a minimum, and amount to about 2 percent of the total histi-

dine. The value of K_2, the equilibrium constant for reaction 2, was determined by adding to a solution of histidine, previously adjusted to the isoelectric pH at the given temperature, a given amount of Co^{++} and titrating back to the original pH. The total concentration of cobalt and histidine, the equilibrium pH, and the amount of added base, constituted the necessary data. All titrations were carried out using a Beckman glass electrode pH meter. The solutions were kept substantially oxygen-free during the titration by passing tank N_2 through the flasks, and were maintained at a constant temperature in a thermostated water bath. Since the reaction is essentially complete at pH $\sim$7.5, total histidine ca. 1×10^{-2} M, and equivalent cobalt, the concentrations of these two latter reactants were decreased so that the reaction was only 60–80 percent complete, and, in addition, large volumes were employed in order that titration be sufficiently large for accuracy. The total volume was of the order of 200 ml. initially; corrections were always applied for the volume of added base. The total concentration of histidine was of the order of 10^{-4} M and the total Co^{++} approximately one-half this value. Different commercial preparations of these reactants were employed without difference in result. Determinations were carried out from 19° to 40° C. The value of the isoelectric pH was calculated at each temperature from the relation $pH_I=\frac{1}{2}(pK_{amino}+pK_{imino})=\frac{1}{2}(pK_a+pK_i)$ where, using $\Delta H_{imino}=6.9$ k cal mol^{-1} and $\Delta H_{amino}=9.4$ k cal mol^{-1} (*18*), the pK's are given by

$$pK_a=6.93\left(\frac{298}{T}-1\right)+9.17$$

$$pK_i=5.06\left(\frac{298}{T}-1\right)+6.00$$

The value of K_2 was calculated from the expression

$$K_2=\frac{[H^+]^2[t/2]}{[c-t]^2[b-t/2]}$$

where t is the titration value in mol.l^{-1} of added base, and c and b are the molar concentrations of total histidine and cobalt, respectively. The foregoing expression is not exact and involves the neglect of certain terms. The use of this expression may be argued directly by assuming that 2 moles of added base are required to form 1 mole of complex, i. e., $t/2=[\phi_2Co]$ and that the material balance is given by

$$b=[Co^{++}]+[\phi_2Co]$$

$$c=[\phi H]+2[\phi_2Co].$$

The validity of these assumptions under the conditions employed and the quantitative importance of operating in the region of the isoelectric pH are shown explicitly in appendix I. The constant K_2 thus obtained is a "hybrid" quantity (*19–20*) in that $[H^+]$ is in terms of activity and the remaining factors are in terms of concentration; the accuracy of the data, however, by no means warrants the exclusive consideration of activities.

Tables 1 and 2 give the values of K_2 determined as above. It was somewhat difficult, with the set-up employed, to obtain reliable values at temperatures less than 15° C. because of the marked increase in the affinity of the complex for O_2 at low temperatures. (See table 11.) It is evident that the attached uncertainty (average error) is rather large in the determinations. Of this, the following may be said: It can be shown (appendix II) that for the reaction in question, when $c\sim2b$, the minimum error in K_2 is obtained when the reaction is 37 percent complete. When operating in the neighborhood of the isoelectric pH, very dilute solutions are required to fulfill this condition. With the arrangement here described, N/50–N/100 NaOH gives reliable magnitudes of t, but the response of so dilute a system to added increments of base is fairly sluggish; more dilute solutions are undesirable on this basis, and hence the best balance of all factors has been struck. It can also be shown (appendix II) that when the reaction is 70 percent complete, as was usually the case here, the propagated error in K_2 is about 1.5 times the minimum possible error. For approximately a 1-percent

TABLE 1.—*Values of K_2 from 15° to 40° C.*

T (° C.)	($K_2\pm\epsilon^1$) $\times 10^7$		Number of determinations
15	0.78	±0.11	5
19	.88	±.03	4
25	2.00	±.34	7
31	3.10	±.38	7
35	5.50	±.90	5
38	7.50	±.67	5
40	8.20	±.85	5

[1] ϵ = Average error of the mean ($=\Sigma$ dev/n $(n-1)^{1/2}$).

error in t the propagated error in K_2 is about 28 percent. The mean of the average error of a single determination for all determinations here is 26 percent.

TABLE 2.—*Examples of determinations of K_2 at 25° and 40° C.*

T (° C.)	pH	b (mol. l^{-1} $\times 10^3$)	c (mol.l^{-1} $\times 10^3$)	t (mol.l^{-1} $\times 10^3$)	K_2 ($\times 10^7$)	K_2 average ($\times 10^7$)
40	7.30	0.243	0.485	0.371	6.30	8.20±0.85
40	7.30	.173	.243	.197	13.00	
40	7.29	.243	.485	.373	7.00	
40	7.29	.123	.246	.162	7.20	
40	7.30	.123	.246	.164	7.50	
25	7.59	.469	.938	.789	1.60	2.00± .34
25	7.61	.566	.925	.833	1.90	
25	7.61	.455	.757	.681	3.10	
25	7.60	.318	.636	.509	1.60	
25	7.61	.469	.938	.770	1.00	
25	7.58	.354	.707	.606	4.00	
25	7.59	.470	.939	.752	.76	

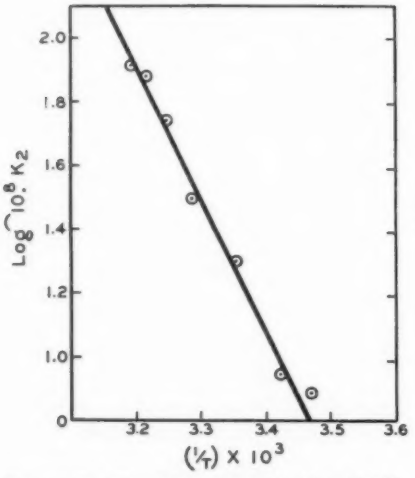

FIGURE 3.—Graphical determination of ΔH_2.

Figure 3 shows the plot of $\log_{10} K_2 \cdot 10^8$ vs. $1/T$, from which ΔH_2 has been determined. From K_2, ΔH_2, and the knowledge of pK_{amino}, and ΔH_{amino}, the equilibrium constant and ΔH of the reaction 2b may be determined, since $K_2 = K_{\phi^-} \cdot K^2_{amino}$.

Table 3 gives the thermodynamic quantities for both reactions 2 and 2b.

The calculated ΔH for reaction 2b is 0.3 k cal mol^{-1}, which is zero within experimental error. In considering this value, it should be borne in mind that, strictly, the reactions should be written in terms of solvated ions,

$$2\phi H_{(aq)} + 2H_2O \rightleftharpoons 2\phi^-_{(aq)} + 2H_3O^+ \qquad (2a')$$

$$2\phi^-_{(aq)} + Co^{++}(H_2O)_p \rightleftharpoons \phi_2Co(H_2O)_{p-q} + qH_2O \qquad (2b')$$

$$2\phi H_{(aq)} + Co^{++}(H_2O)_p \rightleftharpoons \phi_2Co(H_2O)_{p-q} + (q-2)H_2O + 2H_3O^+ \qquad (2')$$

and that the state of solvation of the complex is not known. Probably $q=4$, i. e., $4H_2O$ are expelled when the four N:Co^{++} bonds are formed.

TABLE 3.—*Thermodynamic quantities in the formation of cobaltodihistidine at 25° C.*

Reaction	K [1]	ΔH [2] (k cal mol^{-1})	$\Delta F°$ (k cal mol^{-1})	$\Delta S°$ (e. u. mol^{-1})
(2) $2\phi H + Co^{++}$	$K_2 = 1.9 \times 10^{-7}$	+19.1	+9.1	+34
(2b) $2\phi^- + Co^{++}$	$K_{\phi^-} = 4.2 \times 10^{11}$	±.0	−15.0	+30

[1] K_2 taken from figure 3. $K^2_a = 10^{-15.34}$ $mol.^2 l^{-2}$.
[2] $\Delta H_a = +9.4$ k cal mol^{-1} (*18*).

From the chemical point of view, the reaction of importance is the chelation of the histidine anion with Co^{++}, reaction 2b. In practice, however, and in biologic studies in particular, it is the over-all reaction 2 that must be considered. It is of some interest to inquire into the practical implications of the value of K_2 in terms of the extent of reaction 2. In our experience, the most frequent requirement has been to specify at a fixed pH, usually in the range 7–7.5, the concentration of free cobalt for a given total concentration of cobalt and varying ratios of histidine to cobalt. It is convenient to define χ as the equivalent ratio of histidine to cobalt: $\chi = c/2b$. If z is the molar concentration of cobaltodihistidine and β the fraction of the total cobalt bound as complex, then $z = \beta b$. The expression for K_2 is

$$K_2 = \frac{[H^+]^2 z}{[c-2z]^2[b-z]}$$

Upon the introduction of c from the definition of χ and z in terms of β, one obtains, after solution for χ,

$$\chi = A\left[\frac{\beta}{1-\beta}\right]^{\frac{1}{2}} + \beta,$$

where $A = \dfrac{[H^+]}{2b\sqrt{K_2}}$.

From a plot of β vs. χ the value of β for a given χ may be determined; for a desired β the required χ may be computed directly. Figure 4 gives the extent of combination of cobalt with histidine as

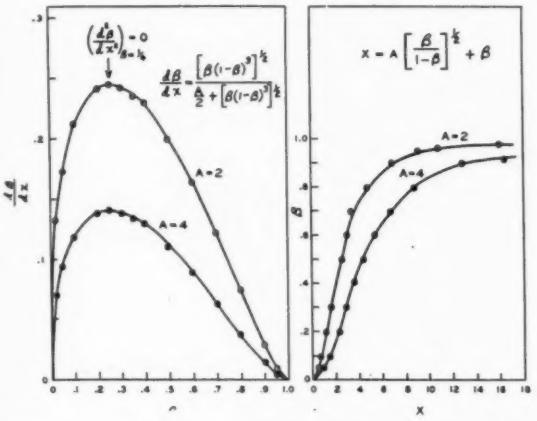

FIGURE 4.—Fractional completion of reaction 2 as a function of χ.

a function of χ at various levels of total cobalt; the inflection occurs when $\beta=\frac{1}{4}$, i. e., where $d\beta/d\chi$ is a maximum.

INTERMEDIATE SPECIES

To return to the analysis of the titration curves, we may begin by outlining the possible intermediate species that seem most likely to occur. One possibility is that the formation of cobaltodihistidine takes place through the association of one Co^{++} and two histidine anions in two consecutive steps:

$$\phi^- + Co^{++} \rightleftharpoons \phi Co^+ \quad (3)$$
$$\phi^- + \phi Co^+ \rightleftharpoons \phi_2 Co. \quad (4)$$

The intermediate complex would then be the species ϕCo^+, cobaltohistidine, consisting of one Co^{++} and one histidine anion and bearing a formal net charge of one. A second possibility follows from the fact that the histidine molecule contains two basic groups. When Co^{++} is bound in the form of cobaltodihistidine, the protons, originally present on the charged amino and imino groups, have both been expelled. The possibility thus exists that the two protons on each histidine molecule have been lost consecutively; that is, that the first step involves the formation of a complex, from one Co^{++} and two ϕH_2^+, with the concomittant expulsion of two H^+. The intermediate complex would in this case contain two ionizable H^+ in its make-up. The reaction would be

$$2\phi H_2^+ + Co^{++} \rightleftharpoons (\phi H)_2 Co^{++} + 2H^+ \quad (5)$$
$$(\phi H)_2 Co^{++} \rightleftharpoons \phi_2 Co + 2H^+. \quad (6)$$

We must also entertain the further possibility that the first step in the foregoing reaction also consists of two consecutive steps.

Since the intermediate complex seemed to occur predominately at lower pH values, it was desirable to work at such values and to include in the analysis rather high concentrations of reactants in order that appreciable complex formation would occur at the lower pH values. That Co^{++} is appreciably bound at fairly low pH values is readily demonstrated by curves obtained in the presence of excess Co^{++}. A set of curves obtained by titrating a given amount of histidine in the presence of increasing amounts of Co^{++} is shown in figure 5. It is evident from the figure that at any given addition of base the pH is lower the higher the cobalt concentration. It is possible to practically complete the total titration at pH$<$5.2 in curves 3–7. A similar family of curves may, of

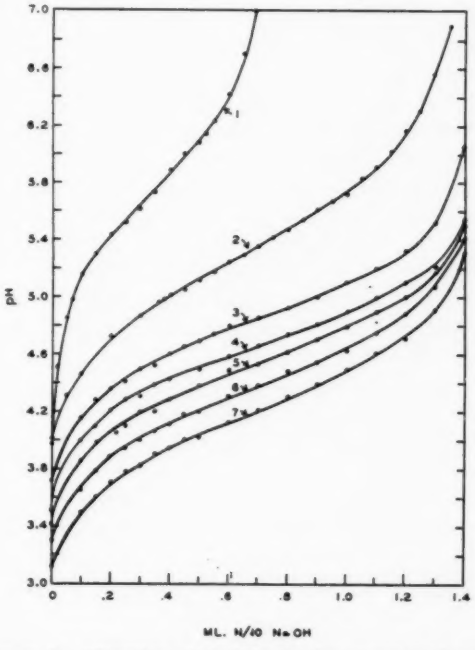

FIGURE 5.—Titration of histidine in the presence of excess Co^{++}. Curve 1, No Co^{++}, initial volume, 5.5 ml.; curve 2, 36 μM Co^{++}, initial volume, 5.5 ml.; curve 3, 180 μM Co^{++}, initial volume, 6.0 ml.; curve 4, 360 μM Co^{++}, initial volume, 6.0 ml.; curve 5, 720 μM Co^{++}, initial volume, 6.0 ml.; curve 6, 1440 μM Co^{++}, initial volume, 6.0 ml.; and curve 7, 2880 μM Co^{++}, initial volume, 6.0 ml. In all cases, 72 μM histidine hydrochloride. T°=25° C. All titrations under N_2 gas.

course, be obtained by employing increasing excess of histidine at a fixed level of cobalt. In this case the total available acid is being increased. In the present case (fig. 5), instead of increasing the number of acid groups by increasing the amount of histidine, we have increased the effective strength of a fixed number of acid groups.

In order to test the first of the above-mentioned possibilities in regard to the nature of the intermediate species, the reaction system was considered to be:

$$\left.\begin{aligned} \phi H_2^+ &\rightleftharpoons \phi H + H^+, \quad K_i = \frac{[H^+][\phi H]}{[\phi H_2^+]} \\ \phi H &\rightleftharpoons \phi^- + H^+, \quad K_a = \frac{[H^+][\phi^-]}{[\phi H]} \end{aligned}\right\} \overline{K} = K_i K_a$$

$$\left.\begin{aligned} \phi^- + Co^{++} &\rightleftharpoons \phi Co^+, \quad K_3 = \frac{[\phi Co^+]}{[\phi^-][Co^{++}]} \\ \phi^- + \phi Co^+ &\rightleftharpoons \phi_2 Co, \quad K_4 = \frac{[\phi_2 Co]}{[\phi Co^+][\phi^-]} \end{aligned}\right\} \begin{aligned} K_{\phi^-} &= K_3 K_4 \\ &= K_2 K_a^2 \end{aligned}$$

In order to compute $[\phi^-]$, $[\phi Co^+]$, and $[Co^{++}]$, and hence K_3, we must eliminate or compute the concentration of every species of cobalt and histidine. Since the pH value, the total concentration of cobalt and histidine, and the titration value are known, the required concentration terms may be computed from six relations among the species involved. The details of this procedure are given in appendix III. Suffice it to state here that:

$$[\phi^-] = \frac{2c - t + \frac{K_w}{[H^+]} - [H^+]}{\frac{2[H^+]^2}{\overline{K}} + \frac{[H^+]}{K_a}} \qquad (A)$$

$$[Co^{++}] = \frac{(c-b) - [\phi^-]\left\{\frac{[H^+]^2}{\overline{K}} + \frac{[H^+]}{K_a} + 1\right\}}{K_{\phi^-}[\phi^-]^2 - 1} \qquad (B)$$

$$[\phi Co^+] = b - [Co^{++}]\{1 + K_{\phi^-}[\phi^-]^2\} \qquad (C)$$

where K_w is the ion product of water, $K_w = [OH^-][H^+]$. The analysis has been applied to values taken from the curves in figure 5. The details and resulting value of K_3 are shown in table 4 for data taken from curves 2 and 3 of figure 5. The decrease in the values of b and c are due to corrections made for dilution as base is added. It is readily seen that the values of K_3 are fairly constant over the range of pH and $[\phi^-]$ covered. In the experimental set-up for curves 2 and 3, the ratio of histidine to cobalt was 2 and 0.4, respectively. The results of other experiments in which this ratio was raised to 4 and 0.8 are shown in tables 5 and 6. The latter experiments are not presented here graphically. The titration data were plotted (pH vs. milliliters N/10 NaOH), smooth curves were drawn, and the pH and corresponding value of b, c, and t were taken from the two curves. These data are presented in tables 5 and 6. The value of K_2 is satisfactorily constant. The data in tables 4–6 show that, although the agreement within a set is excellent, there is nevertheless a difference between each set which may be significant. Thus, it is interesting to note that the magnitude of K_3 bears no evident relation to total cobalt, total histidine, total molarity, or ionic strength but has a practically linear relation to the ratio of histidine to cobalt. This point is clearly shown in table 7. The reason for this trend, which seems real enough, is not known. The mean of all the K_3 determinations is 1.98 ± 0.07 l.mol^{-1} at 25° C. From K_3 and K_{ϕ^-} we may compute K_4. The value of all the constants of the system may then be given at 25° C. as follows:

$K_3 = 1.98 \times 10^7$ l.mol^{-1} $\qquad K_2 = 2.00 \times 10^{-7}$

$K_4 = 2.12 \times 10^4$ l.mol^{-1} $\qquad K_i = 1.00 \times 10^{-6}$ mol.l^{-1}

$K_{\phi^-} = 4.11 \times 10^{11}$ l^2.mol^{-2} $\qquad K_a = 6.75 \times 10^{-10}$ mol.l^{-1}.

The values of ΔH_2 and ΔH_{ϕ^-} have been given. No studies have been made of the temperature coefficients of K_3 and K_4. From the fact that $\Delta H_{\phi^-} = \Delta H_3 + \Delta H_4$ was zero, it may be expected that values of ΔH_3 and ΔH_4 would be equal and opposite. The ratio $K_3/K_4 \sim 10^3$, which considerably exceeds any minimum ratio which would result from statistical effects alone.[4]

[4] If four positions in Co^{++} are filled by two pairs of (bonded) groups then $K_3/K_4 = 6/1$ when all pairs of positions are possible and equally likely. This corresponds to filling four tetrahedral co-ordinate positions. If certain pairs are restricted, such as the diagonally opposite pairs in a planar configuration which are not available to a bidentate molecule, then $K_3/K_4 = 4/1$. Six (octahedral) positions, filled by two sets of three (bonded) groups lead to $K_3/K_4 = 8/1$. If only two pairs of six available (octahedral) positions are filled by two pairs of (bonded) groups, $K_3/K_4 = \frac{12}{5}/\frac{1}{2}$. Note that these statements apply only when the groups involved are bonded together as in a polydentate molecule.

TABLE 4.—*Calculation of K_3 from titration data*

DATA FROM CURVE 2, FIG. 5

$f\times10^3$ (mol. l^{-1})	pH	$b\times10^3$ (mol. l^{-1})	$c\times10^3$ (mol. l^{-1})	$[\phi^-]$ (mol.l^{-1})	$[Co^{++}]\times10^3$ (mol.l^{-1})	$[\phi Co^+]\times10^3$ (mol.l^{-1})	K_3 l.mol^{-1}
1.79	4.45	6.44	12.9	5.90×10^{-9}	5.70	0.74	2.20×10^7
3.51	4.73	6.32	12.6	2.00×10^{-8}	5.35	.97	.91
5.17	4.87	6.21	12.4	3.3×10^{-8}	4.11	2.10	1.55
6.78	5.02	6.11	12.2	5.82×10^{-8}	3.21	2.90	1.55
8.34	5.15	6.00	12.0	$.924\times10^{-7}$	2.36	3.64	1.66
9.84	5.25	5.90	11.8	1.27×10^{-7}	1.55	4.35	2.22
11.29	5.35	5.82	11.6	1.70×10^{-7}	.69	5.13	4.36

DATA FROM CURVE 3, FIG. 5

.827	4.00	29.8	11.9	7.22×10^{-10}	29.4	0.409	1.89×10^4
1.64	4.15	29.6	11.8	1.37×10^{-9}	28.8	.800	2.02
3.23	4.35	29.0	11.6	3.13×10^{-9}	27.4	1.60	1.17
4.76	4.49	28.6	11.4	5.36×10^{-9}	26.4	2.25	1.59
6.25	4.61	28.2	11.2	8.34×10^{-9}	25.3	2.94	1.40
7.70	4.71	28.7	11.1	1.17×10^{-8}	24.0	3.71	1.32
9.10	4.79	27.3	10.9	1.48×10^{-8}	23.0	4.30	1.26
10.5	4.86	26.9	10.7	1.75×10^{-8}	21.8	5.06	1.32
11.8	4.92	26.4	10.6	1.98×10^{-8}	20.7	5.75	1.42
13.1	5.00	26.1	10.4	2.34×10^{-8}	19.8	6.35	1.37
14.3	5.09	25.7	10.3	2.83×10^{-8}	18.7	6.96	1.31
15.5	5.20	25.4	10.1	3.48×10^{-8}	17.8	7.60	1.23
16.7	5.33	25.0	10.0	4.45×10^{-8}	16.8	8.19	1.09
17.8	5.51	24.7	9.86	5.46×10^{-8}	15.9	8.77	1.01

T°=25°C. $K_1=10^{-6}$, $K_2=10^{-9.17}$, $K_\phi{}^-=4.2\times10^{-11}$
$K_w=10^{-14}$, $\overline{K}=10^{-13.17}$

TABLE 5.—*Calculation of K_3 from titration data* [1]

N/10 NaOH (in milliliters)	$f\times10^3$ mol.l^{-1}	pH	$b\times10^3$ mol.l^{-1}	$c\times10^3$ mol.l^{-1}	$[\phi^-]\times10^9$ mol.l^{-1}	$[Co^{++}]\times10^3$ mol.l^{-1}	$[\phi Co^+]\times10^3$ mol.l^{-1}	K_3 l.mol^{-1}
0.1	1.64	4.30	5.90	23.6	5.68	5.25	.65	2.17×10^7
0.2	3.22	4.50	5.80	23.2	13.5	4.60	1.20	2.00
0.3	4.76	4.62	5.71	22.9	22.5	4.16	1.55	1.66
0.4	6.25	4.72	5.62	22.5	31.8	2.32	3.30	4.74
0.5	7.70	4.84	5.54	22.2	53.1	2.59	2.95	2.14
0.6	9.10	4.91	5.45	21.8	71.4	2.05	3.40	2.32
0.7	10.5	5.00	5.36	21.5	98.0	1.05	4.31	4.20
0.8	11.8	5.10	5.29	21.2	148	.84	4.45	3.58

[1] T°=25° C. Other data as in Table 4. 144μM=Histidine and 36μM Co^{++}. Initial volume, 6.00 ml.

TABLE 6.—*Calculation of K_3 from titration data*

N/10 NaOH (in milliliters)	$f\times10^3$ mol.l^{-1}	pH	$b\times10^3$ mol.l^{-1}	$c\times10^3$ mol.l^{-1}	$[\phi^-]\times10^9$ mol.l^{-1}	$[Co^{++}]\times10^3$ mol.l^{-1}	$[\phi Co^+]\times10^3$ mol.l^{-1}	K_3 l.mol^{-1}
0.1	1.41	4.00	25.4	20.3	1.23	24.9	0.5	1.63×10^7
0.2	2.78	4.17	25.0	20.0	2.55	23.7	1.3	2.15
0.3	4.11	4.30	24.6	19.7	4.26	22.2	2.4	2.51
0.4	5.40	4.39	24.3	19.5	6.32	21.8	2.5	1.82
0.5	6.68	4.47	24.0	19.2	8.59	20.9	3.1	1.73
0.7	9.09	4.59	23.4	18.7	13.2	19.1	4.29	1.70
0.9	11.4	4.69	22.8	18.2	18.4	17.3	5.50	1.74
1.20	14.7	4.82	22.0	17.6	27.4	15.0	6.98	1.70
1.40	16.7	4.91	21.4	17.1	35.2	13.4	8.00	1.70
1.60	18.6	5.00	20.9	16.8	45.0	12.0	8.91	1.65
1.80	20.5	5.10	20.4	16.5	58.6	10.6	9.84	1.58

T°=35° C. Other data as in table 4. 144μM histidine HCl and 180μM Co^{++}. Initial volume, 7.00 ml.

TABLE 7.—*Mean value of K_3 in relation to the ratio histidine: Co^{++}*

K_3 mean value	Ratio histidine/Co^{++}	Total histidine in system (μM)	Total Co^{++} in system (μM)	Total molarity (histidine+Co^{++})$\times10^3$	Mean from data in—
1.44	0.4	72	180	4.17	Curve 3, figure 5.
1.69	.8	144	180	4.57	Table 6.
2.06	2.0	72	36	1.93	Curve 2, figure 5.
2.75	4.0	144	36	2.95	Table 5.

One feature of the relations employed here, which imposes certain limitations on the calculation of K_3 in this manner, must be clearly pointed out: in solving for $[Co^{++}]$ it was necessary to divide by $K_\phi{}^-[\phi^-]^2-1$. Thus we exclude the condition $K_\phi{}^-[\phi^-]^2=1$, for which equation B fails to define $[Co^{++}]$. It may readily be shown that the numerator in equation B is equivalent to $[\phi_2Co]-[Co^{++}]$ and the denominator equivalent to $\frac{[\phi_2Co]}{[Co^{++}]}-1$. The numerator and denominator must change signs at the same time, and $[Co^{++}]$ must remain positive under all conditions; at the point where both numerator and denominator pass through zero, $[Co^{++}]$ is indeterminate. (See appendix III.) It is clear that mathematically no difficulty is involved. Practically, however, there is a difficulty. When an excess of Co^{++} is used, i. e., $b>c$, the indeterminate point is *not* reached; that is, $[\phi_2Co]$ can never exceed $[Co^{++}]$. Under all other conditions this indeterminate point must be encountered. In the neighborhood of this point the value of $[Co^{++}]$ becomes extremely unreliable, for the quantity is then given by the difference between nearly equal numbers. In fact it is found on occasion that negative values for $[Co^{++}]$ may seemingly be obtained over a short pH range. At the end of this range the values, though again positive, are highly uncertain. In curve 2 (fig. 5) for example, the last value stated was the last reliable value for $[Co^{++}]$ and K_3. At the next point, .12 pH units higher, $[Co^{++}]$ was 0.04×10^{-3}, and this value was uncertain by nearly 200 percent. For tables 4 to 6, the values given are those computed up to this region of uncertainty. However, in curve 3 (fig. 5) and table 6, this difficulty was not encountered at all and in table 5 only two points have been omitted.

In spite of the limitations imposed by equation B, the latter does suggest an independent method of determining K_ϕ^- from these data, for, when the numerator becomes zero, $K_\phi^- = 1/[\phi^-]_0^2$, where $[\phi^-]_0$ is the concentration of ϕ^- at this point. Actually the data as obtained here allow only order of magnitudes to be computed. The numerator became negative when $[\phi^-]_0$ was $\sim 0.4\times10^{-6}$ to 1.8×10^{-6} mol.$^{-1}$, giving K_ϕ^- the values $\sim 6\times10^{12}$ and $.3\times10^{12}$ as extremes. The mean of the above $[\phi]_0$ values, 1.6×10^{-6}, is very close to the value, 1.55×10^{-6}, required to give K_ϕ^- the value (4.2×10^{11}) previously determined. Data carefully obtained with this point in mind should yield good values of K_ϕ^- in a manner somewhat more simple than the direct determination described previously.

In view of the foregoing results, it does not seem likely that the accumulation of complexes other than ϕCo^+ and ϕ_2Co occurs to a significant extent. Other possibilities must, however, be examined and ruled out if possible. The second of the above-mentioned possibilities, the consecutive loss of two protons, is one which obviously would not need to be considered in the case of compounds containing only one basic group. Still it must be borne in mind that amino acids containing only an amino and a carboxyl group form complexes with Co^{++} (and other metals), presumably by coordination through these two groups. If a similar situation obtained in the case of histidine, it seems distinctly possible that, after coordination with Co^{++} had been effected through the $-NH_2$ and $-COO^-$ groups, the imino groups might still bear acidic protons.

In the interest of historical completeness, it may be stated that the possibility described in equations 5 and 6 was examined before the possibility of equations 3 and 4, and that suggestive, apparently credible results were provisionally obtained. These results are briefly summarized. If reactions 5 and 6 took place, evidence of the occurrence of $(\phi H)_2 Co^{++}$ should be obtainable best at a low pH and preferably with high cobalt concentrations to insure considerable complex formation at such a pH. Equilibrium constants computed for reaction 5 from the expression

$$K_5 = \frac{[H^+]^2[t/2]}{[c-t]^2[b-t/2]},$$

where b, c, etc., are defined as before, showed a consistent rise with pH; for example:

pH	3.8	4.0	4.2	4.4	
$K_5\times10^7$	----	11.4	15	18	curve 3, figure 5
	12	13	16	34	curve 4, figure 5
	14	16	20.5	148	curve 5, figure 5

This is not totally unexpected, since as the pH increases reaction 6 comes into play. The values of K_5 were calculated and then extrapolated back to $t=0$. The value so obtained was 9×10^{-7}. From K_5, K_2 and K_i the equilibrium constant of reaction 6 may be obtained:

$$K_6 = \frac{K_2}{K_5}K_i^2 = 22\times10^{-14}.$$

This gives the interesting result that the ionization constant for one H^+ from $(\phi H)_2CO^{++}$ is $\sim \sqrt{K_6} \sim 10^{-6}$, which is the order of magnitude of K_i, as it would be expected if the value of K_i were not greatly changed in the complex. It appears, however, that the degree of constancy which was observed in K_5 may be explained on the basis of reaction 3. Over the pH range covered in the determination of K_5 the expression

$$\frac{[H^+]^2[t/2]}{[c-t/2]^2[b-t]}$$

is seen to differ from the approximate expression for $K_3\cdot\overline{K}$ by a factor, viz, $\sim(c-t)$, which remained practically constant over the range involved. $K_3\overline{K}$ is the equilibrium constant for the reaction

$$\phi H_2^+ + Co^{++} \rightleftharpoons \phi Co^+ + 2H^+.$$

It should follow that $K_5(c-t) \sim K_3\overline{K}$. The value of $K_3\overline{K}$ is 1.2×10^{-8} while $K_5(c-t)$ is 1.1×10^{-8} when $(c-t)$ is taken as $\sim c$ from curve 3, figure 5. It is clear, therefore, that an equilibrium expression involving $[H^+]^2$ should give approximately a constant value provided the term $(c-t)$ raised to the second power, does not vary greatly. It is also possible to explain, on this basis, why the values of K_5 increased with pH, and more rapidly at higher Co^{++} concentrations; for to reach a given pH the required value of t becomes greater as b is increased. Thus $c-t$ undergoes the greatest change when b is greatest.

The accuracy with which K_3 and the corresponding reaction 3 describe the sequence of events at low pH values leaves little room for other possibilities. The occurrence of stepwise association in the formation of chelate compounds, as

portrayed in reactions 3 and 4 appears to be rather common. For example, Keefer (*21*) has shown this to be the case for Cu^{++} with alanine or glycine, and Calvin and Wilson (*22*) have demonstrated the stepwise association of Cu^{++} with a large variety of β-diketones and ortho-hydroxy aryl aldehydes. It might be assumed a priori that the stability of ϕCo^{+} would exceed that of $(\phi H)_2Co^{++}$ on the basis that, if a given number of co-ordination positions in Co^{++} are to be filled, that complex in which the co-ordinating groups are bonded together is most stable (*22*).

It may be concluded, therefore, that the set of constants given on p. 344 completely defines the system under all conditions investigated. As a result of these findings, it is logical to assume that the complexes ϕCo^{+} and ϕ_2Co arise from the histidine anion, ϕ^{-}, and that histidine occurs in no cobalt complex until both imino and amino protons have been lost.

AMINO ACIDS OTHER THAN HISTADINE

The interest here in the reaction of other amino acids [5] with Co^{++} is limited to two aspects. In general the other naturally occurring amino acids, with the possible exception of cysteine, are less effective than histidine in overcoming biologic Co^{++} inhibitions. After it was ascertained that this biologic effect of histidine was due to complex formations with Co^{++}, studies were made to determine whether the difference between histidine and other amino acids was reflected in the comparative affinities of histidine and other amino acids for Co^{++}. Secondly, it was of eventual interest to contrast the other Co^{++}-amino acid complexes with cobaltodihistidine in regard to their ability to carry oxygen.

It is not unexpected that most amino acids should form some type of complex with Co^{++}, as well as with other transition metals. The literature is replete with studies of examples of such complexes.

It was found that under comparable conditions of pH and concentration, the extent of combination of Co^{++} with histidine considerably exceeds that with other amino acids except cysteine. The magnitude of the shift in the titration curve in the presence of Co^{++} may be used as an index of the extent of complex formation. This shift, expressed in terms of added NaOH, is essentially the result which would be obtained directly by the addition of Co^{++} to the amino acid solution and back titration to the original pH; for if Co^{++} is added at any point on the amino acid curve, the pH falls to the corresponding value on the Co^{++}-amino acid curve, and the distance on the abscissa, which must be traveled along the cobalt amino acid curve, gives the additional NaOH necessary to restore the initial conditions. Figure 6 shows the shift so obtained, expressed in percent of the maximum possible shift, plotted as a function of pH, for several amino acids. It is evident that at pH 6–7, where the combination of histidine and Co^{++} is nearly complete, the other acids show ~50-percent combination or less.

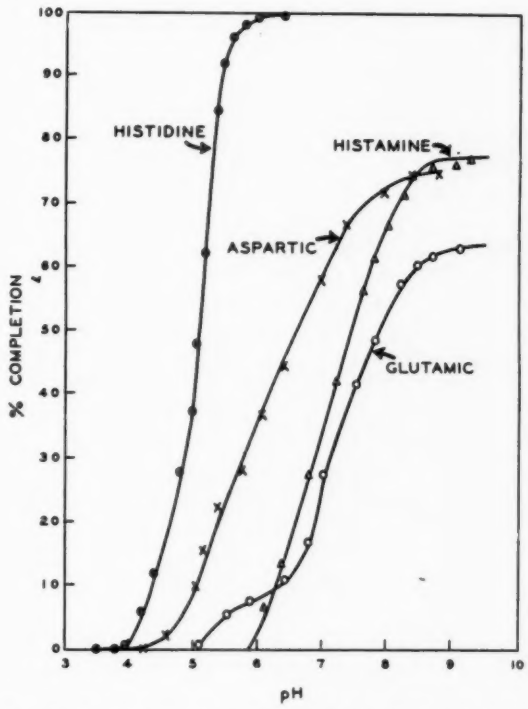

FIGURE 6.—Extent of combination of cobalt and amino acids; 100 percent based on 2:1 ratio, amino acid 0.01M, cobalt 0.005M.

Since at a sufficiently high pH the combination of cobalt and any amino acid may be made appreciable, the situation may be restated by asserting that Co^{++} is able to compete with H^{+}, for co-ordination with $-\ddot{N}H_2$, most successfully in the

[5] Histidine derivatives are discussed in a subsequent section of the paper.

case of histidine (except for cysteine, which contains the reactive —SH group). The shift in the titration curve may then be regarded as the extent to which protons on $—NH_3^+$ have been replaced by Co^{++}. Table 8 gives some results obtained by the direct method of back titration. Cysteine is an exception to the foregoing generalization. Cysteine, unlike histidine, combines in a 3:1 ratio with Co^{++}. The occurrence of this complex at pH 7–8 was early reported by Michaelis on the basis of oxidation-reduction reactions (*23*). We have observed that the affinity of cysteine for Co^{++} is manyfold that of histidine for Co^{++}. A stoichiometric quantity of cysteine will combine completely with Co^{++} (yielding $3H^+$ per Co^{++}) even in the presence of a tenfold excess of histidine.

TABLE 8.—*Combination of Co^{++} with α-amino acids at 25° C.*

Amino acid	Percent combination	pH
Proline	2.5	6.1
Tryptophane	6.3	6.0
Glutamine	9	6.0
Glycine	9	6.0
Glutamic acid	10	6.0
Alanine	10	6.0
Arginine	10.5	7.5
Alanine	11	6.5
Lysine	<15	<7.30
Glycine	24	6.5
Proline	34	7.54
Lysine	38	10.0
Aspartic acid	39	6.0
Histidine	97	6.0
Cysteine	99	6.0

0.005 M. Co^{++}, 0.01 M. amino acid (except 0.036 M. arginine, 0.018 M. Co^{++}, which represents the maximum obtainable combination under these conditions since at pH~8.0 $Co(OH)_2$ begins to precipitate out).

As regards the affinity of the various amino acids for cobalt and the stability of the chelate compounds formed, it may be stated that, in the absence of other factors, the basicity [6] of the coordinating groups is the determining factor, i. e., the tendency of the amino N to coordinate with H^+ parallels its tendency to coordinate with Co^{++}. This point, as well as the importance of resonance effects, has been pointed out by Calvin and Wilson (*22*). Since the basicity of the amino groups of most of the amino acids falls into a rather narrow range, it may be concluded that the coordination properties of histidine are greatly influenced by the presence of the imidazole ring N. This factor, and the resonance possibilities in the histidine molecule, not present in other amino acids, are fully discussed in a previous paper (*17*).

[6] An illustration of the effect produced in the equilibrium constant by the operation of this factor is found in the section on histidine derivatives.

COORDINATION OF HISTIDINE WITH METALS OTHER THAN COBALT

A study of the coordination of histidine with metals other than cobalt was undertaken largely in order to compare these complexes with cobaltodihistidine in regard to O_2 carrying ability. The metals studied were Fe^{++}, Cu^{++}, Ni^{++}, Mn^{++}, Fe^{+++}, and Cu^+. The occurrence of complex formations, as well as the ratio of histidine to metal in each complex, was established from titration data in a manner analogous to that described for Co^{++}. Figures 7 and 8 give the titration results. The curves for Cu^{++} and Ni^{++} (fig. 7) are similar to that for Co^{++}. In both cases, the displacement of the curve is appreciable at considerably lower pH values than for Co^{++} at the same concentration. The titration data indicate that the ratio is 2:1 for histidine: metal. The cupric complex was a deep blue

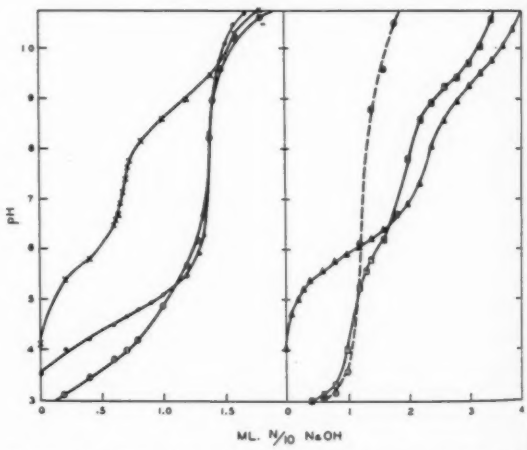

FIGURE 7.—Titration of histidine in the presence of various metals.

- 72 M histidine·HCl. Initial volume, 3.5 ml.
- 72 M histidine·HCl plus 36 μM Ni^{++}. Initial volume, 3.5 ml.
- 72 M histidine·HCl plus 36 μM Cu^{++}. Initial volume, 3.5 ml.
- 160 M histidine·HCl plus 40 μM Fe^{++}. Initial volume, 6.5 ml.
- 80 M histidine·HCl plus 40 μM Fe^{+++}. Initial volume, 6.5 ml.
- 40 μM Fe^{+++}. Initial volume, 6.5 ml.

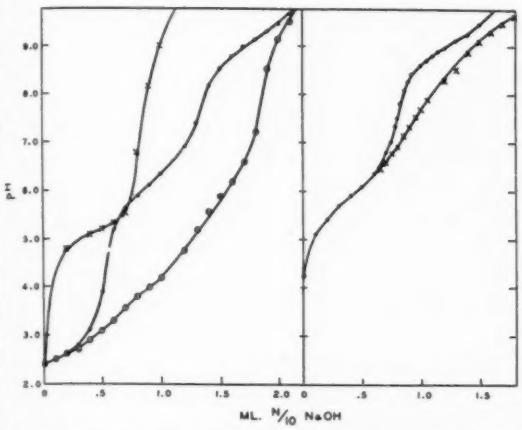

FIGURE 8.—Titration of histidine in the presence of Cu^+ and Mn^{++}. Right hand figure, 80 μM histidine·HCl ± 40 μM Mn^{++}.

Left hand figure, 40 μM Cu^+ plus 50 μM HCl
●—● 80μM histidine·HCl plus 50 μM HCl
◉—◉ 80 μM histidine·HCl plus 50 μM HCl plus 40 μM Cu^+.
All initial volumes 7 ml.

resembling remarkably the $Cu(NH_3)_4^{++}$ ion. The Ni^{++} complex was also blue taking on about the same color as an equivalent concentration of $CuSO_4$.

Fe^{++} ion also combines in a 1:2 ratio with histidine. Here it is necessary to employ a substantial excess of histidine ($\geqq 2\chi$) in order that the metal not be precipitated out as the hydroxide at high pH values; stated otherwise, histidine in too low concentration cannot compete successfully with OH^- for Fe^{++}. In the case of Fe^{+++}, this situation became so prominent that it was not possible to demonstrate titrimetrically the formation of a Fe^{+++}-histidine complex. This fact is shown in figure 7. The results are clarified when a solution containing Fe^{+++} and histidine is titrated with OH^-, the resulting curve consists of "titration" of free Fe^{+++} to $Fe(OH)_3$, followed immediately by a normal histidine curve. This point is referred to again in discussing the oxygen reaction of the Fe^{++}-histidine complex. Suitable solutions of Cu_2Cl_2 could be obtained only by making the mixture quite acid initially. The Cu^+-histidine curve thus embodies the additional feature introduced by the presence of HCl (one mole of HCl per mole of Cu^+). Otherwise the results are straightforward and lead to the conclusion that here, too, a 2:1 histidine: Cu^+ complex is formed.

With Mn^{++}, the extent of combination with histidine at the concentrations employed was small (fig. 8), the affinity of histidine for Mn^{++} being such that precipitation of the hydroxide occurs at higher pH values. Because of the poor coordination in the cases of Fe^{+++} and Mn^{++}, no further work was done with these metals. The oxygen interactions of the remaining complexes are discussed in a succeeding section.

THE REVERSIBLE OXYGEN REACTION: THE FORMATION OF OXY-BIS(COBALTODIHISTIDINE)

As previously mentioned, the titration curves of histidine in the presence of cobalt may be appreciably shifted by the presence of oxygen. The presence of oxygen also induces a marked color change in the solution. An anaerobic solution, if sufficiently dilute, is practically colorless; if more concentrated, slightly pink; but when oxygenated, it becomes deep amber. The color change may be reversed by flushing the solution with N_2 or H_2, and the cycle repeated essentially indefinitely. Further, if the system, histidine+Co^{++}, poised in an atmosphere of N_2 at a pH such that the cobalt is incompletely bound, is oxygenated, the pH falls. This fall in pH is reversible with oxygen pressure and may be completely abolished by returning the system to an atmosphere of N_2, and this cycle may be repeated many times. These changes, an example of which is shown in table 9, illustrate qualitatively the equilibrium nature of the oxygen reaction and offer a fairly sensitive and convenient method for ascertaining oxygen interaction in similar systems. The pH shifts described may be interpreted qualitatively on the basis of the following equilibria:

$$2\phi H + Co^{++} \rightleftharpoons \phi_2Co + 2H^+ \qquad (2)$$

$$n\phi_2Co + mO_2 \rightleftharpoons (\phi_2Co)_n(O_2)_m. \qquad (7)$$

These equilibria indicate that the complex, cobaltodihistidine, combines reversibly with molecular oxygen. The effect of oxygen pressure is to force the equilibria to the right and is thus reflected as an increase in H^+ concentration. It may be readily demonstrated manometrically that ϕ_2Co takes up oxygen reversibly. Quanti-

tatively, the change in pH is very difficult of analysis, and the problem is best approached by studying the reactions separately.

TABLE 9.—*pH of the equilibrium system cobalt-histidine as a function of oxygen pressure*

Gas phase	pH	Remark
N_2	5.50	Colorless.
10 percent O_2	5.42	Amber.
Air	5.40	Do.
45 percent O_2	5.36	Deep amber.
70 percent O_2	5.32	Do.
100 percent O_2	5.30	Do.
Air	5.40	Amber.
N_2	5.50	Colorless.

360 μM histidine, 180 μM Co^{++}, 2.95 ml. N/10 NaOH; volume, 10 ml.

The oxygen reaction may be studied by forming ϕ_2Co in a closed system and observing the oxygen uptake at a given pressure of oxygen. This is conveniently carried out in the Warburg apparatus by mixing $CoCl_2$ and histidine at such concentrations and pH that ϕ_2Co is completely formed. The total cobalt is then in the forms ϕ_2Co and $(\phi_2Co)_n(O_2)_m$, and the resultant equilibrium is determined by the oxygen reaction alone. Experiments of this type have been carried out at oxygen pressures of 5–100 percent, temperatures of 14°–15° C., and concentrations of cobaltodihistidine of $1\text{–}2\times10^{-2}$ mol.l^{-1}. The reaction volume (fluid volume) was about 1.0 ml. and thus contained 10–20 μM of total Co^{++} and somewhat more than twice this amount of histidine. This set-up, in the usual apparatus, gave pressure changes of 40–150 mm. of manometer fluid, which were easily handled and accurately assessed. The histidine, neutralized to a predetermined pH such that upon mixing with Co^{++} the desired pH was obtained, was placed on the floor of reaction vessel and the $CoCl_2$ in one side arm. The vessels were equilibrated with the appropriate gas phase and shaken in a constant-temperature bath. The components were mixed and the time course of the reaction followed until equilibrium was attained. The final oxygen consumption, the total concentration of cobaltodihistidine, and the partial pressure of O_2 comprise the necessary equilibrium data.

Especially at the higher temperatures (38° and 45° C.) there was considerable irreversible oxygen uptake within an hour. Although this reaction is relatively slow with respect to the rate at which the reversible equilibrium is attained, it is often necessary to correct for such irreversible reaction. In view of the fact that reaction 2 (the formation of ϕ_2Co) may be reversed by lowering the pH, the entire system may be readily and completely reversed by tipping strong acid into the system. By this means, it is possible to recover the reversible oxygen quantitatively (or to determine at any time the extent of any irreversible O_2 reaction). This procedure was carried out in the present experiments by tipping 0.4 ml. of 1.2N HCl, into the reaction vessel. Because of the fall in pH upon mixing the cobalt and histidine and the great drop in pH upon acidification with HCl, KOH and filter paper were included in the central insets of all reaction vessels to eliminate the effect of any evolution of CO_2 inadvertently present in the solution of alkaline histidine.

Table 10 gives results obtained in four sets of experiments. The data are presented on the basis of the following considerations: The equilibrium expression for reaction 7 is

$$K_{P_{O_2}}=\frac{[\phi_2Co]_n[O_2]_m}{[\phi_2Co]^n[P_{O_2}]^m}$$

where P_{O_2} is the partial pressure of O_2 at equilibrium; m and n are coefficients to be determined by the experiment. The experimental data are satisfactorily reproduced only by the relation obtained when the values $n=2$, $m=1$ are assigned. If a is the total (or initial) concentration of ϕ_2Co and x is the concentration of the oxygenated complex at equilibrium, then

$$a=[\phi_2Co]+2[(\phi_2Co)_2O_2],$$

and on the basis of the above coefficients

$$K_{P_{O_2}}=\frac{x}{(a-2x)^2}\frac{1}{P_{O_2}}$$

whence

$$K_{P_{O_2}}^{\frac{1}{2}}(a-2x)=(x/P_{O_2})^{\frac{1}{2}}.$$

Therefore a plot of $(x/P_{O_2})^{\frac{1}{2}}$ vs. x should yield a straight line of slope $-2K_{P_{O_2}}^{\frac{1}{2}}$ and x intercept $a/2$. Thus, obedience to the proposed equation will be indicated by the linearity of the plot and a reasonable value for the x intercept. Evidently the $K_{P_{O_2}}$ obtained in this manner includes the constant of the reaction $O_2(g)\rightleftharpoons O_2(aq)$ usually expressed by

$$\alpha = \frac{\left[\frac{\text{milliliters } O_2 \text{ at STP}}{\text{milliliters fluid}}\right]}{P_{O_2}(\text{atm.})}.$$

In order to obtain a constant, which we shall call K_{O_2}, in terms of concentration, and to eliminate from the over-all effect of temperature the effect of temperature on α, the solubility term is introduced into the equilibrium expression to give

$$K_{O_2} = \frac{x}{(a-2x)^2} \frac{1}{P_{O_2}\alpha'} \text{ where } \alpha' = \alpha/22.4.$$

TABLE 10.—*Oxygen uptakes of cobaltodihistidine as a function of* P_{O_2} *and temperature*

T (° C.) [1]	Percent O_2 (water vapor-free basis)	P_{O_2} atm.	v μl.	$(v/P_{O_2})^{\frac{1}{2}} f_1$	$x = v \cdot f_2$ mol. $l^{-1} \times 10^2$	v irreversible μl.
14	100	0.974	206	2.46	0.920	.....
	21	.195	205	5.46	.915	.....
	10	.0876	198	8.00	.885	.....
	4.6	.0217	189	15.70	.845	.....
26	100	.963	136	1.84	.405	.....
	33	.314	113	2.96	.337	.....
	21	.198	115	3.74	.343	.....
	7	.0629	92	5.92	.274	.....
38	100	.929	95	1.75	.283	.....
	33	.304	68	2.58	.203	.....
	21	.193	57	2.97	.170	.....
	7	.0607	39	4.36	.116	.....
45	100	.899	113	2.49	.505	22
	21	.187	57	3.88	.254	17
	10	.0886	34	4.35	.152	24
	4.6	.0385	25	5.65	.067	15

[1] At 14° C., $\alpha = 0.035$; $f_1 = 0.169$; $f_2 = 4.46 \times 10^{-5}$; $f_3 = 0.985$; $v_f = 1.0$ ml.
At 26° C., $\alpha = 0.028$; $f_1 = 0.155$; $f_2 = 2.98 \times 10^{-5}$; $f_3 = 0.970$; $v_f = 1.5$ ml.
At 38° C., $\alpha = 0.024$; $f_1 = 0.173$; $f_2 = 2.98 \times 10^{-5}$; $f_3 = 0.935$; $v_f = 1.5$ ml.
At 45° C., $\alpha = 0.022$; $f_1 = 0.222$; $f_2 = 4.46 \times 10^{-5}$; $f_3 = 0.905$; $v_f = 1.0$ ml.
At 14° and 45°, total $Co^{++} = 1.8 \times 10^{-2}$ mol. l^{-1}; $\chi = 2.5$; pH = 7.75; $\beta > 0.9995$; at 26° and 38°, total $Co^{++} = 1.2 \times 10^{-2}$ mol. l^{-1}; $\chi = 1.5$; pH = 6.3; $\beta \geq 0.993$–0.997.

The original data have been converted by the use of factors. The ratio $(v/P_{O_2})^{\frac{1}{2}}$, where v = the observed oxygen uptake in μl. at S. T. P., and P_{O_2} = the equilibrium pressure of oxygen in atmosphere, is converted to the dimensionless ratio $\frac{\text{mol. } l^{-1}}{\text{mol. } l^{-1}}$ by the factor $f_1 = \left\{\frac{10^{-6}}{\alpha \cdot v_f}\right\}^{\frac{1}{2}}$, where v_f is the reaction volume in liters. The dimensions of f_1 are $\text{atm}^{\frac{1}{2}} \mu l.^{-\frac{1}{2}}$. The uptake v is converted to mol. l^{-1} of oxygenated complex by the factor $f_2 = \frac{10^{-6}}{22.4 v_f}$. The dimensions of f_2 are mol. $\mu l.^{-1} l^{-1}$. The percent oxygen in the gas phase is converted to the initial partial pressure, $P^{\circ}_{O_2}$, in atmosphere, by $f_3 = \frac{P_{\text{total}} - P_{H_2O}}{100(760)}$ where P_{total} is the total (atmospheric) pressure, and P_{H_2O} is the vapor pressure of H_2O, both in millimeters Hg. The

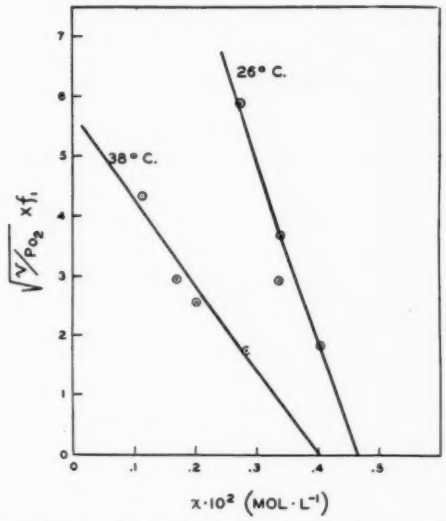

FIGURE 9.—Graphical determination of K_{O_2} at 38° and 26° C.

equilibrium pressure is then $P^{\circ}_{O_2} - h.10^{-4}$, where h = the change in the manometer reading in millimeters of manometer fluid and 1 atmosphere = 10^4 mm. manometer fluid. In practice, the h correction is small and may be entirely eliminated by the proper choice of total concentration and reaction vessel size. In table 10 are given the experimental and derived quantities and the values of α, f_1, f_2, f_3, and v_f.

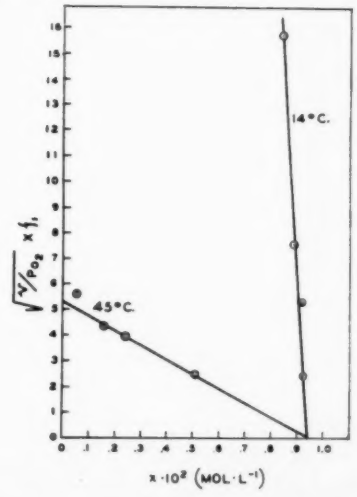

FIGURE 10.—Graphical determination of K_{O_2} at 14° and 45° C.

Figures 9 and 10 show the graphs from which the values of K_{O_2} have been determined. In figure 9, the 38° and 26° lines have intercepts giving a the values 0.81 and 0.93×10^{-2} mol.l^{-1}, respectively. The theoretical value in these cases is 1.2×10^{-2} mol. l^{-1}. In figure 10 the 45° and 14° lines have intercepts giving a the value 1.88×10^{-2} mol.l^{-1}. The theoretical value here is 1.80 mol.l^{-1}. These fits are regarded as satisfactory. Equations, based upon other assumptions (as to values of m and n), plotted in a manner designed to give a linear graph, show distinct curvature and yield entirely unreasonable values of a, deviating from theoretical values of a by orders of magnitude. It is therefore concluded that two moles of cobaltodihistidine combine with one of O_2 and that if other intermediate oxygenated complexes occur their concentration at equilibrium is negligible for they do not accumulate to an extent sufficient to invalidate the equilibrium expression shown above. We therefore refer to the reversibly oxygenated complex as oxy-bis(cobaltodihistidine), and the over-all equilibrium may be recapitulated in chart 1 below (cf. (*17*)).

A practical use that might be made of oxy-bis-(cobaltodihistidine) in manometry would be to employ it as an O_2 buffer, just as $HCO_3^- - CO_3^=$ mixtures are used as CO_2 buffers. With the bicarbonate mixtures the pressure of CO_2 is fixed, and hence the only pressure changes can be restricted to O_2 changes. Similarly, with oxy-bis-(cobaltodihistidine) (in a side arm) it would be possible to keep the pressure of O_2 sufficiently fixed and constant, so that pressure changes could be limited to those due to evolution or absorption of CO_2. This would be useful, not only in glycolysis and respiration studies, but especially in photosynthesis where it may be desired to focus attention exclusively upon the CO_2 exchange.

The slopes of the four lines in figures 9 and 10 give the values of K_{O_2} from $(\text{slope}/2)^2 = K_{O_2}$. The values so obtained, along with the values of $K_{P_{O_2}}$ are tabulated in table 11. From the temperature coefficient of K_{O_2} the heat of oxygenation may be determined. Figure 11 shows the plot of $\log_{10} K_{O_2}$ *vs.* $\frac{1}{T}$ from which ΔH_{O_2} has been estimated. At 25° C. the thermodynamic quantities of the oxygen reaction are: $\Delta H_{O_2} = -38.2$ k cal./mol.; $\Delta F° = -9.1$ k cal./mol.; $\Delta S° = -97.6$ e. u./mol. Had the solubility constant for O_2 been incorporated into the equilibrium constant, $\Delta H_{25°C.}$

TABLE 11.—*Equilibrium constant of the reversible oxygen reaction (7) as a function of temperature*

T (° C.)	K_{O_2} (l^2 mol^{-2})	$K_{P_{O_2}}$ (l. mol^{-1} atm^{-1})
14	4.86×10^{7}	$7.61\times10^{}$
26	2.30×10^{8}	$2.88\times10^{}$
38	4.76×10^{5}	$5.10\times10^{}$
45	7.60×10^{8}	74.6

CHART 1.

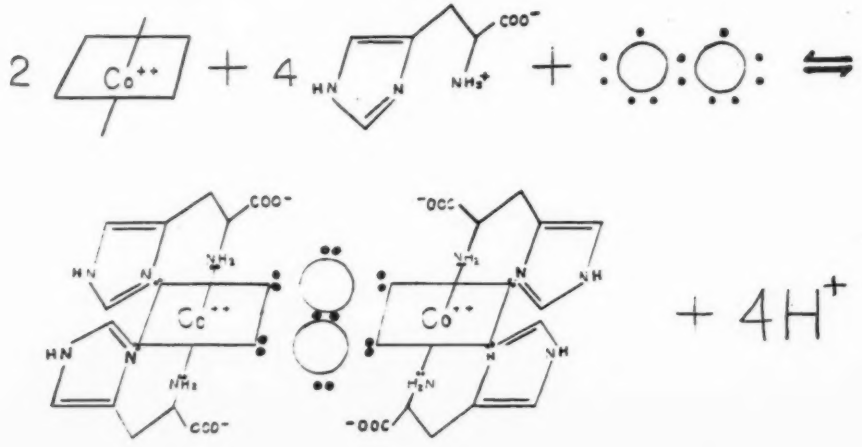

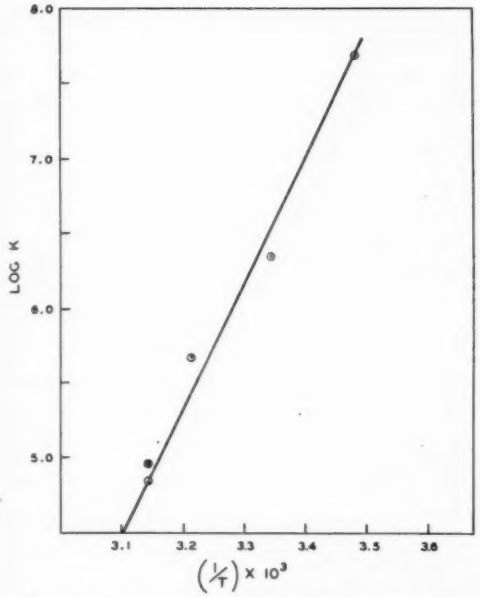

FIGURE 11.—Graphical determination of ΔH_{O_2}.

would be increased by about 3 k cal. mol^{-1} ($\log \alpha$ is not a linear function of 1/T, and this difference will vary with temperature), $\Delta F°$ would be about 4 k cal. mol^{-1} more positive, and $\Delta S°$ about 24 e. u. mol^{-1} more negative.[7]

It is now of some interest to give the explicit relation between x and P_{O_2} and to examine the extent of the oxygenation process as a function of P_{O_2}, temperature, and concentration. The relation

$$K_{O_2}=\frac{x}{(a-2x)^2}\cdot\frac{1}{P_{O_2}\alpha'}$$ upon rearrangement

becomes $$x^2-\left(a+\frac{1}{4K_{O_2}\alpha' P_{O_2}}\right)x+a^2/4=0$$

which yields as a solution [8] for x

$$x=\frac{1}{2}\left(a+\frac{K'}{P_{O_2}}-\sqrt{\left(a+\frac{K'}{P_{O_2}}\right)^2-a^2}\right)$$

where $K'=\frac{1}{4K_{O_2}\alpha'}$. If we define r as the fractional oxygenation then $r=\frac{2x}{a}$. Introducing this definition into the foregoing expression, by multiplying by $2/a$, gives:

$$r=\left(1+\frac{K'}{aP_{O_2}}\right)-\sqrt{\left(1+\frac{K'}{P_{O_2}}\right)^2-1}$$

Figure 12 shows a set of curves constructed from this final equation at equally spaced temperatures from 12.5°–50° C. The curves at 37.5° have been computed for $a=0.01$, 0.02, and 0.04 mol.l^{-1}, all others for $a=0.02$ mol.l^{-1}. The curves bear a remarkable resemblance to a set of rectangular hyperbolas, but it is at once evident from the expression for r that the r vs. P_{O_2} curve may be obtained by the composition of ordinates of the hyperbola

$$y_1=1+\frac{K'}{aP_{O_2}}$$

and the function

$$y_2=-\sqrt{\left(1+\frac{K'}{aP_{O_2}}\right)^2-1}.$$

The curves are characterized by a region of rather steep slope at low P_{O_2} values and an asymptotic approach to $r=1$ at high P_{O_2} as x approaches $a/2$. The slope is given at any r by

$$\frac{dr}{dP_{O_2}}=2K_{O_2}\alpha' a\,\frac{(1-r)^3}{1+r},$$

and the initial slope is, therefore, proportional to K_{O_2}; the initial slope is likewise proportional to a as is shown in the three 37.5° C. curves. At a given temperature, for a fixed r, the required P_{O_2} is determined by a. That the required P_{O_2} is in fact inversely proportional to a is readily deduced from the original expression for K_{O_2}; for example the "half-saturation pressure" is given by

[7] It is interesting to examine the value of ΔH more closely. The most plausible electronic formulation of oxy-bis(cobaltodihistidine) (as has been discussed (17)) demands that each of the two unpaired electrons in the O_2 molecule form a covalent bond with an unpaired electron on the cobalt ion. This necessarily involves changing the O_2 molecule from the normal electronic state : $\ddot{O}:\ddot{O}:$ to the $\cdot\ddot{O}:\ddot{O}\cdot$ form. The heat of dissociation of the O_2 molecule is 118 k cal. and the heat of formation of the O—O bond −35 k cal. (24). Thus the change $O_2 \longrightarrow$ —O—O— involves a heat change of 83 k cal. Now the net ΔH of the oxygenation reaction must be $\Delta H_{O_2}=83+\Delta H_{bonds}$, where ΔH_{bonds} is the heat of formation of the cobalt-oxygen bonds formed. Therefore $\Delta H_{bonds}=121$ k cal., and if only two $Co^{++}-O_2$ bonds are formed, the ΔH per bond is about 61 k cal. (If two covalent and two coordinate bonds are formed, each pair will have this ΔH) (Cf. (17).) This does not take into account the possibility that other bonds, cobalt-H_2O or cobalt-carboxyl, may have to be broken in the process.

[8] It is easily shown that the solution with the plus sign is physically inadmissable.

$$(P_{O_2})_{r=a/4} = \frac{1}{K_{O_2}\alpha' a}.$$

This obviously means that the required P_{O_2} for half-saturation may be reduced tenfold if a is raised tenfold, etc. This feature, along with the dependency of the slope of the r vs. P_{O_2} curve upon a, distinguishes the curves from an oxygenation function which is described by the hyperbola and may be regarded physically as a direct consequence of the fact that two moles of cobaltodihistidine are required to carry one O_2 molecule. The half-saturation pressures at the four temperatures, 12.5°, 25.0°, 37.5°, and 50° C. are: 3.8×10^{-4}, 9.6×10^{-3}, 0.15 and 1.69 atmospheres. These values are for $a = 0.02$ mol.l^{-1}; from the a dependency of the half-saturation pressure the value at any a is readily obtained. For comparison the oxygen tension of venous and arterial blood are indicated in figure 12. It is seen that, at $a = 0.02$ mol.l^{-1} and 37.5°, oxy-bis(cobaltodihistidine) operates between 47 and 31 percent saturation, over the arterial-venous pressure range, whereas oxyhemoglobin operates between 95 and 60 percent saturation, and oxymyoglobin between 98 and 94 percent (*25, pp. 127–136*), respectively.

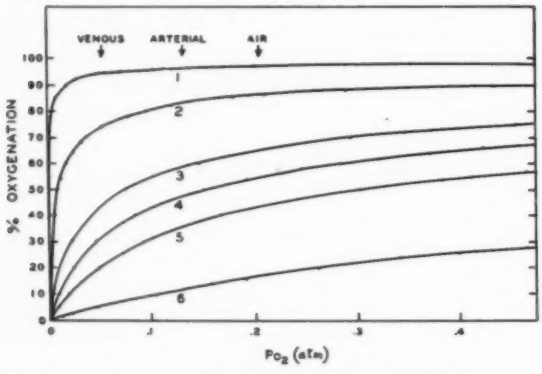

FIGURE 12.—Oxygenation curves of cobaltodihistidine: Curve 1, 12.5° C., $a = 0.02$ mol.l^{-1}; curve 2, 25.0° C., 0.02; curve 3, 37.5° C., 0.04; curve 4, 37.5° C., 0.02; curve 5, 37.5° C., 0.01; and curve 6, 50.0° C., 0.02.

IRREVERSIBLE OXYGEN REACTIONS OF COBALTODIHISTIDINE

As already mentioned, a relatively slow irreversible uptake of oxygen takes place following the rapid reversible uptake. No thoroughly detailed knowledge is available as yet regarding the nature of the irreversible reaction or the structure and composition of any compounds formed. The problems involved may be pointed up and the general character of the reaction delineated by discussing results obtained so far. The complete irreversible reaction is an almost undecipherable series of events that may be shown to involve under varying experimental conditions several recognizable phases, including (1) eventual absorption of a second molecule of O_2 by oxy-bis(cobaltodihistidine), without production of OH^-; (2) an initial irreversible rearrangement of oxy-bis(cobaltodihistidine) without notable additional O_2 uptake; and (3) under certain conditions, especially with excess amino acid base (high pH or high histidine/Co^{++} concentration ratios), production of some CO_2 and OH^-.

It is certain that cobaltodihistidine may be dissociated by acid and that the reversible oxy-bis(cobaltodihistidine) may be disrupted by acid with the complete evolution of O_2 and the discharge of amber color. When the irreversible reaction sets in, the recovery of O_2 by acidification is not complete nor is the color discharged; the solution gradually loses its amber color to become deep pink as the irreversible reaction proceeds. It will be seen later that the final irreversible

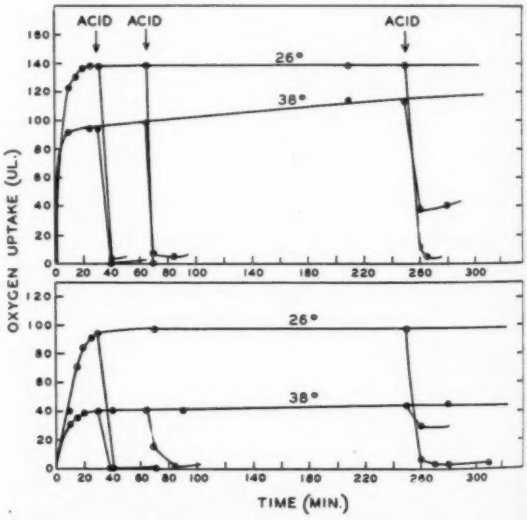

FIGURE 13.—Recovery of reversible oxygen by acidification. Upper graph, 100 percent O_2; lower graph, 7 percent O_2. Data from experiment reported in table 10.

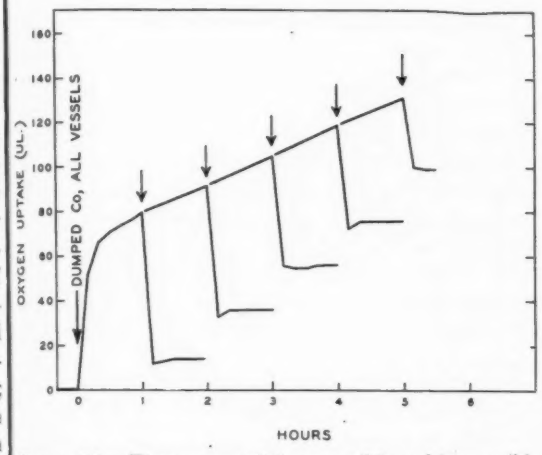

FIGURE 14.—Time course of the reversible and irreversible oxygen uptake of cobaltodihistidine. Data in table 13.

complex gives a typical absorption spectrum, unlike that of either of the reversible complexes.

Figures 13 and 14 illustrate graphically the recovery of O_2 by acidification. Recovery is complete when upon acidificaton the previous uptake falls back to zero. Irreversible uptake is measured by any net uptake after acidification. It may be seen from figures 13 and 14 that the total O_2 uptake rate curve eventually breaks sharply, as might be expected in an approach to an equilibrium; however, the rate usually does not become zero but may go into a virtually linear phase that may be maintained for hours and the slope of which increases markedly with temperature and is apparently a function of oxygen pressure also.

The final irreversible oxygen uptake commonly corresponds closely to one mole of O_2 per atom of Co^{++}, as may be instanced in table 12. The rate of attainment of final uptake depends in part upon oxygen pressure. The 21- and 100-percent oxygen experiments are fairly close to the ratio $O_2/Co^{++}=1.0$; the 10- and 4.6-percent runs would require roughly another 50 hours to reach completion at the rate shown. The theoretical uptake for $O_2/Co^{++}=1.0$ is 404 μl. in the experiments shown in table 12. (In a few other experiments the uptake has appeared to attain 1.1 to 1.2, slightly exceeding 1.0, in a manner that we believe, without absolute certainty, however, is beyond experimental error and indicative of some additional secondary reactions.) The O_2 equivalence for the oxidation of cobaltous ion to cobaltic ion by the reaction

$$2Co^{++}+\frac{1}{2}O_2+2H^+=2Co^{+++}+H_2O \qquad (8)$$

would be 101 μl., which is far less than the usual observed O_2 consumption in table 12 and, therefore, does not quantitatively account for it. If the reversible oxygen complex were oxidized to the cobaltic form and this form were irreversible, viz

$$2\phi_2Co+O_2\rightleftharpoons(\phi_2Co)_2O_2 \qquad (9)$$

$$(\phi_2Co)_2O_2+\frac{1}{2}O_2+2H^+\text{——}(\phi_2Co)_2{}^{++}O_2+H_2O \qquad (10)$$

where ϕ_2Co^+ would be cobal*ti*dihistidine, the theoretical uptake would be 303 μl. and the ratio O_2/Co^{++} would be 0.75, not 1.0.

TABLE 12.—*Irreversible oxygen consumption at 45° C.*

O_2 (percent)	Oxygen uptake μl.	Time in hours	Rate at time μl. hr.$^{-1}$	O_2/Co^{++}
4.6	288	19	<1	0.72
10	335	19	~1	.83
21	352	18	~1	.87
100	395	18	0	.98

18μM. Co^{++}, 90 μM histidine, volume 1.0 ml.
O_2 equivalent for $O_2/Co^{++}=1$, 404 μl.
($T°=45$) pH=7.75–7.80 (initial); 7.70–7.90 (final).

Both of the foregoing reactions involving the possible formation of Co^{+++} demand the formation of one mole of OH^- per mole of Co^{++} oxidized to Co^{+++}. The formation of this amount of free hydroxyl should be readily detectable. The pH of the vessels in the experiments recorded in table 12 was 7.75–7.80 initially. The pH during and at the termination of the reaction fell in the range 7.70–7.90; the variation had no relation to the amount of oxidation which had occurred. The oxidation of 18 μM of cobalt from Co^{++} to Co^{+++} is equivalent to 0.18 ml. of N/10 NaOH. The minimum change for this amount of base in the system as set up would be about 1.0 pH units, giving a pH of 8.7 in the most unfavorable case. The conclusion that no Co^{+++} was formed, based on lack of pH change alone, must be qualified by the admission of the possibility that the production of OH^- was exactly balanced by some concurrent reaction, or that the cobaltic complex coordinates with OH^- to give an unionized com-

plex. However, the oxygen uptakes, in conjunction with the failure to detect the required production of OH^- (table 15), seem to warrant the assertion that no Co^{+++} is formed in the irreversible reaction; moreover, it is shown subsequently that this assertion is supported by magnetic data.

If it be granted that the irreversible oxygen reaction does or need not entail the formation of Co^{+++}, the next question concerns a more detailed interpretation of the given oxygen-uptake data in terms of reaction mechanism. One possibility, among others, which naturally suggests itself is that one mole of oxy-bis(cobaltodihistidine) reacts, with or without preliminary irreversible rearrangement or other intermediate steps, with one mole of O_2 to form an irreversible complex of the formula $(\phi_2Co)_2(O_2)_2$. This suggestion is prompted by the observed final ratio of O_2/Co^{++} of unity and by the fact that the irreversible oxygen increases at a faster rate than does the total or "additional" oxygen consumed after the break in the rate curves of figures 13 and 14. If the reactions

$$2\phi_2Co + 2O_2 \rightleftharpoons (\phi_2Co)_2O_2 + O_2 \rightarrow Irr.,$$

where Irr. is the final irreversible complex, occur, and the reversible equilibrium is rapidly attained, the rate of oxygen uptake during the linear phase should be essentially that of the second step. On this basis, each mole of O_2 consumed in the second step should cause the irreversibility of a total of two moles, i. e., one O_2 taken up in the second step would be irreversible and would render irreversible the O_2 originally present in the complex. It should then be found that the rate of increase of irreversible oxygen approaches twice that of the additional uptake in the linear phase. This is at least approximately the case, and regardless of the basis it is a significant point that the two rates should compare in this way. For example, at 38° C. and 100 percent O_2 (fig. 13), the reversible uptake is 95 μl., when the irreversible is negligible; when the total uptake has increased 20 μl. the irreversible is 39 μl. (240 minutes), and so on. This point is shown most clearly in figure 14, in which the rate of the linear phase is 12.6 μl. hour^{-1} and the best line through the irreversible points has a slope of 22.5 μl. hour^{-1}, giving a ratio of 1.8. Actually the observed ratio should be somewhat less than 2.0, since when the irreversible conversion has not been too great, the depletion of $(\phi_2Co)_2O_2$ by this means is followed by partial replacement from ϕ_2Co and O_2. This replacement involves the uptake of reversible oxygen, and the total uptake, being increased by this amount, is slightly greater than one half the irreversible. As the available ϕ_2Co becomes depleted, the extent of this replacement tends to fall off in accordance with dependency of r upon a discussed in the previous section. This line of reasoning also serves to explain the fact that the amount of $(\phi_2Co)_2O_2$ becomes negligible before all the cobalt is in the irreversible form. This means that when the total concentration of ϕ_2Co is small, the value of r is such that only negligible amounts of $(\phi_2Co)_2O_2$ are maintained at equilibrium.

While these general findings are in agreement with the idea that $(\phi_2Co)_2O_2$ may become irreversibly oxidized by one O_2, the discussion may be made more precise as follows. Let us assume that one mole of irreversible oxygen "removes" one mole of Co^{++} from the system and on this basis compute the amount of $(\phi_2Co)_2O_2$ remaining after any amount of irreversible uptake has occurred; from this the recoverable O_2 may then be computed and compared to the observed values.

The complete system is:

$$2\phi H + Co^{++} \rightleftharpoons \phi_2Co + 2H^+ \qquad K_2 = 7.3\times10^{-7} \quad (2)$$

$$2\phi_2Co + O_2 \rightleftharpoons (\phi_2Co)_2O_2 \qquad K_{O_2} = 3.1\times10^{-5} \text{ l.}^2 \text{ mol.}^{-2} \quad (9)$$

$$(\phi_2Co)_2O_2 + O_2 \rightarrow Irr. \quad (11)$$

If one mole of irreversible oxygen represents one mole of irreversibly bound Co^{++}, as demanded by this postulate, the remaining cobalt is given by $b = b_o - v_t/22.4v_t\times10^6$ where v_t is the irreversible uptake in microliters; b_o the initial total cobalt in mol.l^{-1}, and the other terms are defined as before. Here we are considering, as has been implied in the last paragraph, that the total cobalt available to the first two reversible reactions is given by b. When the first of the foregoing reactions is complete, the total concentration of ϕ_2Co is b, and the concentration of $(\phi_2Co)_2O_2$ is obtained from K_{O_2}. As Co^{++} is effectively removed from the system, there is a redistribution of Co^{++} among free Co^{++}, ϕ_2Co and $(\phi_2Co)_2O_2$ within the con-

ditions of constraint imposed by K_2, K_{O_2}, and the material balance

$$b=[Co^{++}]+[\phi_2Co]+2[(\phi_2Co)_2O_2]$$

$$c=[\phi H]+2[\phi_2Co]+4[(\phi_2Co)_2O_2].$$

In the present case $\chi=1$; thus $c=2b$ and $[\phi H]=2[Co^{++}]$ and we have

$$b=[Co^{++}]+[\phi_2Co]+2[(\phi_2Co)_2O_2]$$

$$K_2=\frac{[H^+]^2[\phi_2Co]}{4[Co]^3}$$

$$K_{O_2}=\frac{[(\phi_2Co)_2O_2]}{[\phi_2Co]^2P_{O_2}\alpha'}$$

from which

$$b=A[\phi_2Co]^{1/3}+[\phi_2Co]+B[\phi_2Co]^2$$

$$A=\frac{10^{-2/3pH}}{(4K_2)^{1/3}},\ B=2K_{O_2}\alpha'P_{O_2}.$$

This relation gives $[\phi_2Co]$ when both reversible reactions are simultaneously in equilibrium. The solution for $[\phi_2Co]$ allows the computation of $[(\phi_2Co)_2O_2]$ from K_{O_2}.[9]

The results are shown in table 13, from which it is evident that the agreement, which is quite good, as it should be, when the irreversible uptake is zero or negligible, becomes progressively poorer. The lack of agreement becomes so great in the later stages that one might reasonably doubt whether one mole of Co^{++} is removed by one mole of irreversible O_2. In order to ascertain how badly the postulate has failed and to attempt to determine the actual ratio of cobalt "removed" to irreversible O_2, we shall reverse the logic used. Taking the observed quantity of recoverable oxygen, we compute, at any time, the concentration of $(\phi_2Co)_2O_2$ in solution and from this quantity the concentrations of Co^{++} and ϕ_2Co. The proper summation of these terms then gives the total reversible cobalt at that time. By comparing the amount of cobalt removed to the uptake of reversible oxygen, we arrive at the ratio, $\Delta b/\Delta I$, moles of Co^{++} removed from a reversible state per mole of irreversible oxygen. For the purpose of this calculation the cobalt balance is expressed in terms of $[(\phi_2Co)_2O_2]$ alone, viz,

$$b=2[(\phi_2Co)_2O_2]+N[(\phi_2Co)_2O_2]^{1/2}+B[(\phi_2Co)_2]O_2^{1/6}$$

$$N=(1/K_{O_2}\alpha'P_{O_2})^{1/2} \qquad B=\frac{10^{-2/3pH}}{(4K_2)^{1/3}}$$

$[(\phi_2Co)_2O_2]=v_r/22.4v_l\times10^6$, v_r=reversible O_2 in μl.

TABLE 13.—*Comparison of computed and observed quantities of recoverable oxygen*

Time (in hours)	Total O_2 μl	Irreversible O_2 μl	b. 10^3 mol. l^{-1}	P_{O_2} atm	$[\phi_2Co]$ .10^3 mol. l^{-1}	$[(\phi_2Co)_2O_2]$ .10^3 mol. l^{-1}	Reversible O_2	
							Calculated μl	Observed μl
0	0	0	7.2	0.196	6.95	0	0	0
0.5	71	0	7.20	.191	5.70	1.25	70	71
1.0	80	14	7.00	.190	5.56	1.17	66	66
2.0	92	36	6.60	.189	5.23	1.09	60	56
3.0	105	56	6.20	.188	4.94	.975	54	49
4.0	119	76	5.79	.187	4.65	.865	48	43
5.0	131	100	5.39	.186	4.28	.740	41	31

$P_{O_2}=0.196-\frac{v_r}{1.4}\times10^{-4}$ 18μM Co^{++} 36μM histidine Volume=2.5 ml. pH=7.0

It is perhaps superfluous to make explicit the assumption involved here: the foregoing relation is equivalent to the assertion that if $[(\phi_2Co)_2O_2]$ is the concentration of oxy-bis(cobaltodihistidine) found at equilibrium, then there must exist also the equilibrium concentrations of Co^{++} and ϕ_2Co demanded by K_2 and K_{O_2}, and the sum of these species must represent the total (reversible) cobalt. It is clearly necessary that the assumptions be made that the irreversible reaction is sufficiently slow, that the reversible reactions are at all times at equilibrium (ample justification for which appears from a cursory glance at fig. 14), and that no other reversible intermediates accumulate.

The results are shown in table 14. The first value of b, when the irreversible uptake is zero, should correspond to the total initial cobalt placed in the system which was 7.20×10^{-3} mol.l^{-1}. The computed value is in excellent agreement. The mean value of $\Delta b/\Delta I$ is 1.46 ± 0.07. It thus seems necessary to conclude that 3/2 moles of Co^{++} are removed per mole of irreversible O_2. It is to be emphasized that this finding is not incompatible

[9] We shall not stress the mode of solution for $[\phi_2Co]$ by successive approximations but point out that the calculation of β from

$$x=\frac{[H^+]}{2b\sqrt{K_2}}\left[\frac{\beta}{1-\beta}\right]^{\frac{1}{2}}+\beta,$$

and setting $a=\beta\cdot b$ in the equation

$$r=\left(1+\frac{K'}{aP_{O_2}}\right)-\sqrt{\left(1+\frac{K'}{aP_{O_2}}\right)^2-1},$$

gives $[(\phi_2Co)_2O_2]\sim r\cdot b\cdot\beta\cdot\frac{1}{2}$ as an excellent approximation which is sufficiently accurate; in fact, when β approaches 1.0 sufficiently closely, the result is exact.

with, and indeed has no immediate bearing upon the fact that the finally attained ratio is $Co^{++}/O_2 = 1.0$. Immediately a molecule of cobalt, in any form whatsoever, is irreversibly bound, it is effectively removed from the system and no longer contributes to the material balance as set up. If several species of intermediate complexes occurred, let us say

$$4\phi H + 2Co^{++} \leftrightharpoons 2\phi_2Co(+4H^+); + O_2 \leftrightharpoons (\phi_2Co)_2O_2 \xrightarrow{\text{rearrangement}} (\phi_2Co)_2O_2\ Irr?) \xrightarrow{1/3\ O_2} (Irr.)_1 \xrightarrow{2/3\ O_2} (Irr.)_2 \longrightarrow (Irr.)_n (\text{i.e.}, (\phi_2Co)_2(O_2)_2), \quad (12)$$

then, as soon as a molecule of cobalt enters the first irreversible state it is lost to the preceding equilibria, and its loss is reflected in the cobalt balance even though additional O_2 may be required to achieve one or all of the steps from this state to the final state $(\phi_2Co)_2(O_2)_2$. It must be pointed out that to state that 3/2 Co^{++} are removed by one mole of irreversible O_2 is to assume tacitly that the irreversible uptake is that associated with the removal of Co^{++} to the first irreversible state, i. e., that the O_2 uptake entailed in $(Irr)_1 \rightarrow (Irr)_n$ is negligibly slow relative to that involved in the transition to $(Irr)_1$. This assumption seems to be justified since at 5 hours the Co^{++} has been removed to the extent of 36 percent, and the irreversible uptake is 25 percent of its predicted final value. Were the uptake due to $(Irr)_1 \rightarrow (Irr)_n$ absolutely negligible the ratios of these percents would be 0.67. The actual ratio is 0.69.

TABLE 14.—*Calculation of disappearance of reversible* Co^{++}[1]

Time (in hours)	Irreversible uptake (μl)	Reversible uptake (μl)	$[(\phi_2Co)_2O_2]$ (mol.l^{-1} $\times 10^5$)	$[\phi_2Co]$ (mol.l^{-1} $\times 10^5$)	$[Co^{++}]$ (mol.l^{-1} $\times 10^5$)	$b \times 10^5$ (mol.l^{-1})	$\Delta b/\Delta I$
0.5	0	71	1.28	4.48	0.742	[2] 7.25	.....
1	14	66	1.18	4.33	.239	6.93	1.28
2	36	56	1.00	3.99	.232	6.23	1.58
3	56	49	.876	3.75	.228	5.73	1.52
4	76	43	.768	3.52	.224	5.28	1.45
5	100	31	.554	3.19	.216	4.65	1.46

[1] Data from figure 14 and table 13. Values of P_{O_2} are identical with these of table 13.

[2] Theoretical value when irreversible uptake is zero is 7.20×10^{-5} mol.l^{-1}.

Finally it should be noted that these data do not allow a unique choice as to whether oxy-bis(cobaltodihistidine) is directly oxidized or whether it is the unoxygenated form, ϕ_2Co, which is irreversibly oxidized. It may be argued, quite logically, that ϕ_2Co is irreversibly oxidized and that, due to the replacement of ϕ_2Co from $(\phi_2Co)_2O_2$, some O_2 is evolved which tends to offset the uptake. This would account also for the fact that the irreversible oxygen increases at a faster rate than does the total uptake. If such were the case, then, during the phase of the reaction covered by the data being discussed, the reaction would be written as

$$\phi_2Co + 2/3\ O_2 \longrightarrow (Irr)_1 \overset{1/3\ O_2}{\longrightarrow - - - \longrightarrow} (Irr)_n. \quad (12')$$

Additional rate studies, of a different type, are required, as is evident from the foregoing analysis, in order for a choice to be made. It may be recalled that in the case of hemoglobin it is apparently the reduced (unoxygenated) form that is irreversibly oxidized to methemoglobin (*26*, *27*). This is readily seen to be deficient as an analogy, however, for we feel that it has been clearly shown that no valence change in cobalt is involved, and so we do not press the analogy further.

Rearrangement Without Oxygen Uptake

None of the foregoing considerations preclude the mechanistic possibility that $(\phi_2Co)_2O_2$ rearranges as suggested in equation 12 to some irreversible form not involving additional uptake of O_2, transiently or otherwise. An observable rearrangement phase is clearly demonstrated in figure 13 by the curve for 38° C. and 7 percent O_2, where between 65 and 250 minutes the irreversible O_2 uptake has increased markedly, whereas the total O_2 uptake has increased negligibly and the reversible uptake (as the difference) has decreased correspondingly. Tables 15 and 16 also show large increases in irreversible O_2 uptake compared to simultaneous small or negligible increases in total O_2 uptakes. Furthermore, in table 15 the total O_2 uptake has not attained a ratio of O_2/Co^{++} of unity but only approaches 0.5 (17/36 μM), (allowing for the fact that only 36 of the 72 μM of Co^{++} can react stoichiometrically with the 72 μM histidine available), yet virtually all of this O_2 has become irreversible with an uptake corresponding only to the compound $(\phi_2Co)_2O_2$ rather than the compound $(\phi_2Co)_2(O_2)_2$. The conditions invariably giving this result are not yet fully understood, but a condition of "excess" Co^{++} (or deficient histidine, $\chi < 1$) is apparently favorable. The same condition also ap-

pears to supress formation of CO_2 and OH^-, which in table 15 has not occurred within experimental error. In the experiments of tables 12 and 13, already discussed, OH^- formation was likewise not observed, and χ was not greater than unity.

TABLE 15.—*Nonformation of hydroxyl ion and carbon dioxide during consumption of oxygen gas by cobaltodihistidine and excess cobalt at 25° C. in manometric vessels* [1]

Reaction measured	Time in hours				
	0	⅙	1	12⅚	29
O_2 consumed, micromoles:					
Total	0	13.0	13.8	15.3	17.7
Reversible	0	12.2	10.0	1.6	.6
Irreversible	0	.8	3.8	13.7	17.0
Percent reversible	0	94	73	11	3
Final pH [2]	8.20			8.30	8.35
OH^- produced, micromoles [3]	0			<1	<1
CO_2 produced, micromoles [3]	0	0	0	<.5	<.5
OH^- produced/irreversible O_2	0			<.07	<.06
CO_2 produced/irreversible O_2	0	0	0	<.03	<.30

[1] 1.5 ml. 0.054 M (72 μM=28.8 millimolal final concentration in reaction mixture) histidine monohydrochloride (preneutralized to pH 9.6) in main compartments of Warburg vessel; 1.0 ml. 0.072 M (72 μM=28.8 millimolal final concentration in reaction mixture) cobalt chloride in left side arms (tipped at zero time); 0.40 ml. 1.16 N HCl and 0.1 ml. bromphenol blue in right side arms (tipped at times indicated to obtain first the irreversible O_2 values); fluted filter papers and 0.30 ml. saturated $Ba(OH)_2$ in wells into which acidified reaction mixtures eventually shaken for complete acidification; gas phase, O_2.

[2] Determined with Beckman pH meter after respective indicated times after tipping cobalt into histidine in replicate Warburg vessels in which acid in right side arm was not tipped into reaction mixture. Initial pH=8.20 and back titrations at subsequent times brought to this value for determination of any hydroxyl ion produced.

[3] 7.4 μM CO_2 blank in reagent control vessels at $t=0$, subtracted from values reported for $t \geqq 0$.

TABLE 16.—*Formation of hydroxyl ion and carbon dioxide during consumption of oxygen gas by cobaltodihistidine and excess histidine base (pH∼9.0) at 25° C. in manometric vessels* [1]

Reaction measured	Time in hours					
	0	⅙	1	2½	8⅓	20
O_2 consumed, micromoles						
Total	0	15.7	16.2	17.0	20.0	27.0
Reversible	0	15.4	12.2	8.3	2.0	0
Irreversible	0	.3	4.0	8.7	18.0	27.0
Percent reversible	0	98	73	49	10	0
Final pH [2]	8.94	8.94	8.99	9.03	9.12	9.31
OH^- produced, micromoles [2]	0	0	.5	3.2	11.1	15.5
CO_2 produced, micromoles [3]	0	0	0	1.6	4.1	7.2
OH^- produced/irreversible O_2	0	0	.14	.37	.62	.58
CO_2 produced/irreversible O_2	0	0	0	.18	.23	.27

[1] 2 ml. 0.072 M (144 μM=57.6 millimolal final concentration in reaction mixture) histidine monohydrochloride (preneutralized to pH 9.8) in main compartments of Warburg vessel; 0.5 ml. 0.072 M (36 μM=14.4 millimolal final concentration in reaction mixture) cobalt chloride in left side arms (tipped at zero time); 0.40 ml. 1.16 N HCl and 0.1 ml. bromphenolblue in right side arms (tipped at times indicated to obtain first the irreversible O_2 and then by complete mixing of all liquids in the vessel the total CO_2 values); fluted filter papers and 0.30 ml. saturated $Ba(OH)_2$ in wells into which acidified reaction mixtures eventually shaken for complete acidification; gas phase, O_2.

[2] Determine with Beckman pH meter after respective indicated times after tipping cobalt into histidine in replicate Warburg vessels in which acid in right side arm was not tipped into reaction mixture. Initial pH=8.94 and back titrations at subsequent times brought to this value for determination of any hydroxyl ion produced.

[3] 9.8 μM CO_2 blank in reagent control vessels at t=0, subtracted from values reported for t≧0.

It may be added that under anaerobic conditions cobaltodihistidine is converted very rapidly (within a few minutes at 25° C.) by strong H_2O_2 (e. g., 0.03 ml. super-oxal per ml. of reaction mixture) to an irreversible complex similar to or identical with that obtained with O_2. An appreciable amount of reversible complex, presumably oxy-bis(cobaltodihistidine) is also formed, probably via O_2 released by catalytic decomposition of H_2O_2.

Production of Carbon Dioxide and Hydroxyl Ion

Under conditions of excess histidine base ($\chi > 1$ and pH 8.0 to 8.5 or greater) as in table 16, CO_2 and OH— production may be observed, although a ratio of OH^- produced/irreversible O_2 uptake as great as unity has never yet been observed, as would be required if the OH^- production were to be ascribed to the oxidation of Co^{++} to Co^{+++}. The nature of the reactions producing CO_2 and OH- remain to be established definitely, but it would appear probable that partial decarboxylation of histidine to produce the corresponding amine is involved ($-CHNH_2COO^- + HOH \rightarrow -CH_2NH_2 + HCO_3^-$). This would result in a group of greater base strength (higher pK) and hence a noticeable increase in pH and a production of OH^-. The difference in pK between histidine and histamine would of course account for considerably less than one equivalent of OH^-. Part of the OH^- observed would also be due to transfer of CO_2 from the reaction mixture into the $Ba(OH)_2$ in the well ($HCO_3^- \rightarrow CO_2 + OH^-$). The OH^- formation would thus exceed the CO_2 production, in harmony with the results of table 16. Other experiments similar to those in table 16 (with $\chi > 1$) indicate an eventual O_2 uptake/Co^{++} of unity, even though the ratio in table 16 is only 0.75 by 20 hours. It is interesting to note that Co^{++}-histidine-O_2 system can under certain conditions simulate respiration, yielding a respiratory quotient (R.Q.=CO_2 produced/O_2 consumed) of as high as 0.27 in table 16 and up to 0.5 in other experiments not detailed here. With other amino acids than histidine values approximating unity have been obtained. Organic oxidation and decarboxylation is perhaps not surprising in view of the fact that oxy-bis(cobaltodihistidine) may be regarded as an organic peroxide (R-O-O-R) and oxidizing agent.

OXYGEN INTERACTIONS WITH COBALT AND HISTIDINE DERIVATIVES

In view of the fact that cobaltodihistidine exhibits the unusual property of combining reversibly with oxygen, it was of some interest to study the cobalt complexes of various histidine derivatives from this point of view. The following compounds were studied: histamine, 3-methyl histidine, 1-methyl histidine, 3-benzyl histidine, dibenzyl histidine, and the peptides, anserine, carnosine, L-alanyl-L-histidine, and α-L-aspartyl-D-histidine. With the exception of histamine, rather limited amounts of these compounds were available, and extensive studies of a highly definitive nature were not carried out. It was demonstrated, however, that in every case the compound combines with Co^{++} and that the resulting complex is capable of carrying oxygen reversibly, although in certain cases (most notably carnosine) the irreversible reaction sets in exceedingly rapidly even at room temperature. While the data are neither sufficiently extensive nor accurate to warrant strict comparison and interpretations, some interesting features may be pointed out.

Table 17 gives the results obtained in the manometric experiments. The design of these experiments was similar to those described in the case of cobaltodihistidine as regards mixing of components, equilibration, and determination of reversible O_2 by acidification. It may be seen that O_2 is taken up fairly rapidly and that over the time of the observation the O_2 is essentially completely reversible by the acid method, except in the case of the peptides. The amount of O_2 taken up varies greatly, and a better comparison is afforded by calculation of the equilibrium constant in each case. In order to insure an appreciable oxygen uptake in all cases, the runs were made in pure O_2 (except histamine). In certain cases, this was obviously necessary (dibenzyl- and 1-methyl-histidine); however, in other instances the system was near saturation with respect to O_2, and the computed constants from one P_{O_2} cannot be highly accurate. Further, while there is no reason in the case of the methyl histidines and the benzyl histidines to assume that the stoichiometry of the oxygen reaction is different from that of histidine (calculations were made on the basis of 2 chelate: O_2), this is

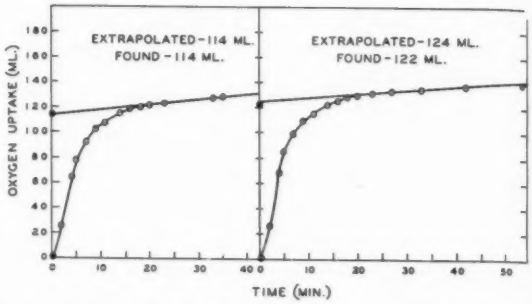

FIGURE 15.—The time course of the oxygen uptake of cobalt-anserine. Experimental set-up in table 17.

not necessarily the case with the peptides. In these compounds, additional groups, amino, carboxyl, or both, capable of coordinating with Co^{++}, are present, and chelates entirely different from cobaltodihistidine may be formed. It is possible that three or five coordinated chelates are formed which combine in a 1:1 ratio with O_2.

It is also necessary in calculating the K_{O_2} to make some assumptions regarding the irreversible reaction. The irreversible reaction in the case of the three peptides shown here is apparently quite different from that in histidine. The time curve of the reaction is shown for anserine in figure 15. As in the case of histidine, the rate curve breaks sharply into a linear phase but the rate does not become zero, i. e., no true equilibrium is attained. In contrast with the histidine data presented, the irreversible O_2 corresponds closely to the additional uptake in the linear phase, that is, the total uptake and irreversible O_2 increased at the same rate. If the linear phase is extrapolated back to $t=0$, the extrapolated value agrees well with that found by acidification. A tentative mechanism accounting for this would be that the irreversible O_2 is added to or oxidizes the molecule at a position which does not interfere (greatly) with the reversibility of the oxygenation:

$$2X+O_2 \rightleftharpoons X_2O_2 \xrightarrow{O_2} X'_2O_2 \rightleftharpoons 2X'+O_2$$

where

X=the original chelate, and X′=the altered chelate;

thus X and X′ would be indistinguishable on an

equilibrium basis and the K_{O_2} would be given by

$$K_{O_2}=\frac{X_r}{(a-2X_r)^2P_{O_2}}, \text{ since } X_2O_2=X_r,\ X=a-2X_r.$$

In this particular case, the total and reversible uptakes did not differ greatly. The irreversible reaction with aspartyl- and alanyl-histidine requires a different interpretation. Here the rate curves break sharply at ~15 min., and the rate becomes zero. At subsequent times, the recoverable O_2 has dropped markedly although the total uptake has remained constant. It is difficult to think that an irreversible reaction could remove the reversibly oxygenated complex without the shift in the reversible equilibrium being reflected as further oxygen uptake, except upon the basis of rearrangement as noted with histidine in instances (table 15). The value of the equilibrium constant in these two cases has been calculated on the assumption that the equilibrium concentration of unoxygenated chelate is given by the initial minus the irreversible oxygen minus twice the reversible. While this assumption regarding the irreversible reaction may not be correct, widely different assumptions fail to change the order of magnitude of the calculated constant.

The values of K_{O_2} calculated on the basis indicated are collected in table 18. It is evident that the presence of a methyl group in the 3-position of the histidine molecule (a substitution which changes the general properties of histidine little if any) is of little consequence in the O_2 reaction; while the presence of a methyl in the 1-position markedly interferes with oxygenation. This is perhaps understandable on the basis of steric considerations since two chelates must be placed in fairly close apposition to carry one O_2. It then does not become surprising that the K_{O_2} for 3-benzyl histidine approximates that for histidine. Comparison of the mono- and dibenzyl-histidine clearly shows that the effect of a large substituent on the amino nitrogen is to decrease the K_{O_2} value rather markedly.

One theoretical point of interest in the peptides is that, because of the presence of additional groups, they are capable of forming upon chelation with cobalt a system consisting of at least two (possibly three in the case of aspartyl histidine) rings which are bonded together. In this one respect, at least, these chelates should approach more closely the naturally occurring polydentate compounds. The stabilizing effect of the bonding together of co-ordinating groups in chelate compounds was stressed by Calvin and Wilson (*22*). It was logical to hope that this factor of stability, and even a different stoichiometry, would lead to more desirable carrier properties and a closer approach to biological reality. It is evident

TABLE 17.—*The oxygen uptake of various histidine derivatives*

Derivative	[Co++] (mol.l$^{-1}\times10^3$)	[Derivative] (mol.l$^{-1}\times10^3$)	pH	Gas phase	O_2 uptake	Recoverable O_2	
						Percent	Time
							Minutes
Dibenzyl-histidine	7.5	15	7.5–7.7	O_2	67	100	20
	7.5	30	7.5–7.7	O_2	49	100	40
3-Benzyl-histidine	7.5	15	7.6	O_2	159	100	40
	7.5	30	7.6	O_2	154	100	40
1-Methyl-histidine	7.5	15	7.90	O_2	19	100	24
	7.5	30	7.90	O_2	25	100	44
	7.5	60	7.90	O_2	19	100	60
3-Methyl-histidine	7.5	30	7.80	O_2	129	100	16
	7.5	60	7.80	O_2	150	99	45
Aspartyl-histidine	9.4	37.5	7.85	O_2	148	48	24
	9.4	37.5	7.85	O_2	153	26	44
Alanyl-histidine	7.5	30	8.0	O_2	152	41	44
	7.5	30	8.0	O_2	142	29	60
Anserine	7.5	30	7.5–8.0	O_2	126	91	35
	7.5	30	7.5–8.0	O_2	139	87	55
	3.0	30	8.2	Air	63.6	100	13
	3.0	30	8.2	Air	64.0	101	46
	3.0	30	8.2	Air	64.4	100	60
	3.0	30	8.2	Air	62.9	100	20
Histamine	3.0	30	8.2	O_2	69.0	100	13
	3.0	30	8.2	O_2	69.0	100	46
	3.0	30	8.2	O_2	69.4	100	60
							Hours
	3.0	30	8.2	O_2	68.0	100	21

T=23° C., $\alpha'=1.29\times10^{-3}$ mol.l^{-1} atm.$^{-1}$, P_{O_2} (oxygen) =0.975 atm., P_{O_2} (air) =0.195 atm., β (histamine) =0.95–0.98. Each vessel except histamine contained 15 μM Co++; histamine vessels 7.5 μM.

TABLE 18.—*Values for K_{O_2} at 23° C. for cobalt complexes of histidine, and histidine derivatives*

Compound	K_{O_2} (l^2 mol^{-2})	Ratio to K_{O_2} for histidine
Histamine	4.7×10^7	7.8
3-Benzylhistidine [1]	12.0×10^6	2.0
Histidine	6.0×10^6	1.0
3-Methylhistidine [2]	2.5×10^6	.42
Aspartylhistidine [3]	1.2×10^6	.2
Alanylhistidine [1]	1.2×10^6	.2
Anserine [2]	4.2×10^5	7.0×10^{-2}
Dibenzylhistidine [1]	4.5×10^4	7.5×10^{-3}
1-Methylhistidine [2]	8.7×10^3	1.6×10^{-3}

[1 2 3] Kindly supplied by Prof. D. Wright Wilson, Prof. Vincent du Vigneaud, and Dr. J. P. Greenstein, respectively.

from the data presented here that whatever increase in stability might have been gained is offset by the occurrence of the more rapid irreversible oxygen reaction. It seems, from this point of view, to be of little interest to study this type of compound (peptides) further.

The comparison between histidine and histamine is of particular interest and will be made in somewhat greater detail. In the first section of this paper (and in a previous paper (*17*)) the structure of cobaltodihistidine has been indicated to be that wherein four coordination positions of Co^{++} are filled by four nitrogens of two histidine anions. Whether or not the carboxyl groups participate in the bonding has not been stressed. Since ordinary monocarboxylic α-amino acids presumably form complexes by co-ordination through the carboxyl and amino groups, it is possible that a similar situation obtains in the case of histidine, i. e., that six co-ordination positions are occupied by two amino nitrogens, two imino nitrogens, and two carboxyls. In view of the fact that cobaltodihistidine reacts with oxygen and in view of the manner in which this occurs, it is clear that coordination positions are open in the cobalt atom or at least can be made available. In the following discussion it is shown that the carboxyl group is essential neither for chelation with Co^{++} nor for the oxygen-carrying ability of the chelate compound formed. All the properties of histidine, in these respects, are exhibited by histamine, although the presence of the carboxyl group has, quantitatively, a rather marked effect. The effect of the presence of the carboxyl operates in opposite directions in the two reactions discussed, viz, increases chelation with Co^{++} and decreases oxygenation of the resulting complex.

It is grossly evident from titration data (fig. 6, cf. figs. 1 and 2) that the tendency for histidine to combine with cobalt is distinctly greater than that of histamine. Estimates from these data give K_2 (histamine)$=3.6\times10^{-12}$ at 25° C. It will be recalled that K_2 (histidine)$=1.9\times10^{-7}$ at 25° C.

The difference in the tendencies (Δ F°) for the two complexes to form is at once evident from this and amounts to 6.5 k cal mol^{-1}. Since there is a substantial difference in the values of $pK_{(amino)}$ for histidine and histamine, a closer approach to the true difference in stability of the two complexes is gained by eliminating this factor. If the values of $pK_{(amino)}$ for histidine and histamine are taken as 9.17 and 9.86,[10] respectively, the values of $K\phi^-$ are calculated $K\phi^-$ (histidine)$=4.11\times10^{11}$ and $K\phi^-$ (histamine)$=1.89\times10^8$ at 25°. These values give, as a measure of difference in stability, $\Delta F°$ (stability)$=-\Delta F°$ (histidine)$-(-\Delta F°$ (histamine))$=4.12$ k cal mol^{-1}. (This is readily seen to be equivalent to diminishing the over-all 6.5 k cal mol^{-1} by RTln $10^{2|\Delta pK|}$ where Δ pK is the difference in the $pK_{(amino)}$ values.) This difference in stability may be directly attributed to the presence of the carboxyl group since the two $pK_{(imino)}$ values for histidine and histamine are practically identical (*28*); it is not expected that the presence of the carboxyl group would influence the properties of the imidazole ring to any appreciable extent.

The value of K_{O_2} for cobaltodihistamine has been estimated from oxygen uptakes at oxygen pressures of $\sim$0.2 atmosphere and $\sim$1.0 atmosphere. The value taken from the graph in figure 16 is 5×10^7 $l.^2$ mol^{-2} at 23° C. The value for cobaltodihistidine at 23° is 6×10^6 $l.^2$ mol^{-2}. The ratio of these constants corresponds to a $\Delta F°$ (stability) of 1,220 cal mol^{-1}. This is almost identical with the change in stability (1,250 cal mol^{-1}) of oxy-bis-(cobaltodihistidine) produced by raising the temperature from 25° to 37.5°. The effect of this difference is most strikingly brought out by comparing the r vs. P_{O_2} functions. It has been seen that the half-saturation pressure is given by

$$(P_{O_2})_{r=a/4}=\frac{1}{K_{O_2}a\alpha'}.$$

[10] This value was calculated from the data of Levy (*28*) as follows: Levy gives $pK_{(amino)}=9.7$ at 30° C. The Δ H of ionization of NH_4^+, $CH_3NH_3^+$ and $C_2H_5NH_3^+$ all fall, at 25°, in the range $+13.0\pm0.3$ k cal mol^{-1} (*18*); with the assumption that $\Delta H_{(amino)}$ of ionization of 2-imidazole ethylamine also falls in this range, the value of $pK_{(amino)}$ is computed to be 9.86 at 25°.

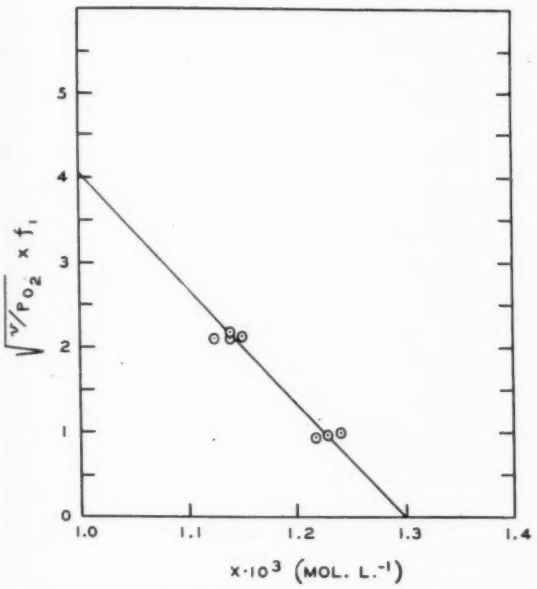

FIGURE 16.—The graphical determination of K_{O_2} for cobaltodihistamine.

For two complexes, the half saturation pressures are related by

$$\frac{(P_{O_2})'_{x=a/4}}{(P_{O_2})_{x=a/4}} = \frac{K_{O_2}}{K'_{O_2}}.$$

Thus for one-half saturation, the P_{O_2} for the histidine system must be about eight times that for the histamine system.

The effect of the carboxyl group in the two reactions here discussed may be interpreted as follows: The enhanced stability of cobaltodihistidine as compared with the corresponding histamine complex may be due to the electrostatic interaction between the $-COO^-$ groups and Co^{++}. It is not possible to state whether the carboxyl group participates in the same manner as the N atoms since all the bonds are essentially ionic (*17*). The enhanced stability of the oxygenated form of the histamine complex is possibly due to the steric effect of the two COO^- groups. Since two chelates carry one O_2 molecule, it is necessary, as previously mentioned, that two chelate molecules be brought in fairly close apposition in the formation of the oxygenated complex. Similar studies with esters of histidine wherein the carboxyl group is present but electrically neutral, and with histidine amide, in which resonance in the carboxyl group [11] is also greatly depressed, would be of great interest in this connection. We have not yet carried out such studies.

Lastly, the rather limited number of experiments with histamine indicate that the irreversible oxygen reaction is exceedingly slow in this case. For example, at the end of 20–25 hours at ~25° C., 100 percent of the oxygen uptake was recoverable from the histamine complex, whereas with histidine, under comparable conditions, about 70 percent of the total uptake was reversible at 17 hours. This observation may later be of some value in determining the nature of the irreversible reaction.

OXYGEN INTERACTIONS WITH COBALT AND VARIOUS AMINO ACIDS AND AMMONIA

Histidine and certain of its derivatives are by no means the only amino compounds that react with Co^{++} and O_2 gas under physiological conditions to yield reversibly oxygenated, yellow-brown compounds. Table 19 lists miscellaneously a number of α-amino acids and ammonium hydroxide, all of which give yellow-brown, reversibly oxygenated complexes that are also transformed spontaneously into pink irreversible forms, as in the case of histidine, but usually much faster. Irreversible O_2 consumption, without intermediate reversible oxygenation, has been observed with methionine, cysteine, aspartate, and α-alanine, and no O_2 consumption at all with β-alanine, under conditions tested.[12] At 45° C. histamine shows some irreversible oxidation, although in the previous section none was observed at 25°.

It is especially interesting that ammonium hydroxide, containing no carbon atoms, likewise gives reversible oxygenation and irreversible oxidation products, with the same series of color changes, as do the amino acids, with the proviso

[11] Spectroscopic studies by Gordy and Stanford (*29*) suggest that in esters it is the $\diagdown C{=}O \diagup$ group which coordinates in the formation of hydrogen bonds.

[12] Other compounds, including these four, glycyl-glycine, glutamine, ornithine, and putrescin, have been reported upon more recently by the following: S. Fiala: Oxygenace a oxygenaceni modely. Biologicke Listy 28: 201–208 (1947); D. Burk, S. Fiala, J. Hearon, M. Hesselbach, H. Levy, and A. L. Schade: Reversible oxygenation, irreversible oxidation, and decarboxylation of cobalt-amino acid complexes with oxygen gas. Fed. Proc. 7: 342 (1948); and D. Burk, J. Hearon, S. Fiala, A. L. Schade, and H. Levy: Cobaltodihistidine and related compounds and their significance in oxygenation of metalloproteins. 113th meeting, Am. Chem. Soc., Chicago, 1948, pp. 340–350.

TABLE 19.—*Reversible and irreversible combinations of oxygen gas with cobaltous ion and various α or β amino acids or ammonia in manometric vessels* [1]

Reaction measured		Amino acids or NH_4OH																
		Histidine	Histamine	Lysine	Arginine	Serine	Glutamic	Trypto-phane		Proline		Asparagine	Glycine	Methio-nine	β-Alanine	NH_4OH		
Micromoles		108	180	288	216	216	216	216	216	216	216	144	288	72	72	2,000	2,500	1,500	1,500
Co^{++} (micromoles)		36	9	72	72	72	72	72	72	72	72	36	72	36	36	36	18	36	18
Volume (milliliters)		2.0	1.0	5.0	4.0	4.0	4.0	4.0	4.0	4.0	4.0	2.5	5.0	1.5	1.5	1.4	1.0	1.3	1.3
Initial pH		9.7	8.0	8.9	8.5	9.1	8.6	9.8	8.4	9.0	7.0	9.0	8.5	8.0	8.0	*ca.* 14	*ca.* 14	*ca.* 14	*ca.* 14
Temperature (°C.)		25	45	25	25	25	25	25	25	25	25	30	25	28	28	25	25	0.2	° 0.2
O_2 Consumed, micromoles	*Minutes*																		
Total	8–10	15.6	.....	9.9	11.2	9.1	.....	4.8	.....	.....	.....	.....	.....	.....	.....	17.6	.....	.....	4.0
	21–24	.....	4.0	.....	.....	12.5	3.8	.....	4.8	1.8	.....	.....	.....	.....	.....	.....	.....	.....	.....
	35–40	.....	.....	.....	.....	.....	.....	.....	.....	.....	.....	.....	.....	6.6	0	.....	10.3	.....	.....
	60–70	16.5	4.0	19.7	.....	.....	4.4	10.3	5.2	.....	0	3.0	1.3	9.0	0	.....	.....	.....	4.2
	125	.....	.....	.....	.....	.....	.....	.....	.....	.....	.....	.....	.....	7.4	0	.....	.....	.....	.....
	500	.....	.....	.....	.....	.....	.....	.....	.....	.....	.....	.....	.....	.....	.....	.....	.....	9.1	5.2
	600	.....	4.3	.....	.....	.....	.....	.....	.....	.....	.....	.....	.....	.....	.....	.....	.....	.....	.....
Reversible	8–10	15.1	.....	5.5	5.4	3.7	.....	1.7	.....	.....	.....	.....	.....	.....	.....	17.2	.....	.....	3.2
	21–24	.....	3.6	.....	.....	2.4	2.9	.....	2.0	1.3	.....	.....	.....	.....	.....	.....	.....	.....	.....
	35–40	.....	.....	.....	.....	.....	.....	.....	.....	.....	.....	.....	.....	0	0	.....	8.8	.....	.....
	60–70	13.5	3.0	4.3	.....	.....	1.8	2.5	1.3	.....	.....	.6	.3	0	0	.....	.....	.....	3.3
	125	.....	.....	.....	.....	.....	.....	.....	.....	.....	.....	.....	.....	0	0	.....	.....	.....	.....
	500	.....	.....	.....	.....	.....	.....	.....	.....	.....	.....	.....	.....	.....	.....	.....	.....	4.0	1.0
	600	.....	.4	.....	.....	.....	.....	.....	.....	.....	.....	.....	.....	.....	.....	.....	.....	.....	.....
Irreversible	8–10	.4	.....	4.4	5.8	5.4	.....	3.1	.....	.....	.....	.....	.....	.....	.....	.4	.....	.....	.8
	21–24	.....	.4	.....	.....	10.1	.9	.....	2.8	.5	.....	.....	.....	.....	.....	.....	1.5	.....	.....
	35–40	.....	.....	.....	.....	.....	.....	.....	.....	.....	.....	.....	.....	6.6	0	.....	.....	.....	.....
	60–70	3.0	1.0	15.4	.....	.....	2.6	7.8	3.9	.....	0	2.4	1.0	9.0	0	.....	.....	.....	.9
	125	.....	.....	.....	.....	.....	.....	.....	.....	.....	.....	.....	.....	7.4	0	.....	.....	.....	.....
	500	.....	.....	.....	.....	.....	.....	.....	.....	.....	.....	.....	.....	.....	.....	.....	.....	5.1	4.2
	600	.....	3.9	.....	.....	.....	.....	.....	.....	.....	.....	.....	.....	.....	.....	.....	.....	.....	.....
Percent reversible	8–10	97	.....	56	48	40	.....	35	.....	.....	.....	.....	.....	.....	.....	98	.....	.....	80
	21–24	.....	90	.....	.....	19	77	.....	42	72	.....	.....	.....	.....	.....	.....	.....	.....	.....
	35–40	.....	.....	.....	.....	.....	.....	.....	.....	.....	.....	.....	.....	0	0	.....	86	.....	.....
	60–70	82	75	21	.....	.....	40	24	24	.....	0	18	24	0	0	.....	.....	.....	79
	125	.....	.....	.....	.....	.....	.....	.....	.....	.....	.....	.....	.....	0	0	.....	.....	.....	.....
	500	.....	.....	.....	.....	.....	.....	.....	.....	.....	.....	.....	.....	.....	.....	.....	.....	44	20
	600	.....	9	.....	.....	.....	.....	.....	.....	.....	.....	.....	.....	.....	.....	.....	.....	.....	.....

[1] All amino acids in gas phase of tank oxygen, NH_4OH in gas phase of air. Fraction of reversible oxygen remaining determined from gas evolution upon tipping at indicated time values of excess HCl from side arm into reaction mixtures. KOH in wells absorbs any incidental CO_2 evolved. 1 $\mu MO_2 = 22.4$ mm.[3]

that the concentration and pH be high enough.[13] The oxygenation phenomenon was not observed with ammonium hydroxide, or NH_3 at alkaline pH's below 10, when the concentrations were of the order of only 0.01 to 0.1M, and under the conditions employed as in the case of the amino acids reported in table 19.

[13] The early work of Werner and his colleagues at the turn of the century, demonstrating the existence of reversibly oxygenated "oxy-cobaltiac," has recently been reviewed by L. Michaelis (Molecular oxygen as a ligand in metal porphyrins and other metal-complex compounds. Fed. Proc. 7: 509–514 (1948); Molecular oxygen as a ligand in metal complex compounds. 113th meeting, Am. Chem. Soc., Chicago, 1948, pp. 32C–33C; and Another case of reversible oxygenation. Arch. Biochem. 17: 201–203 (1948)), who has also described the reversible yellow-brown back to pink color changes obtained upon alternately passing O_2 and N_2 through Co^{++}—ammonium hydroxide solutions, followed by eventual formation of irreversible dark pink products; measurements of actual O_2 uptake and release during these changes were not reported.

OXYGEN INTERACTIONS WITH OTHER METAL-HISTIDINE COMPLEXES

The histidine complexes of Cu^{++}, Ni^{++}, Cu^{+}, and Fe^{++} were studied with respect to their ability to perform as oxygen carriers.

The Cu^{++} and Ni^{++} complexes, in experiments carried out under the conditions already described for cobaltodihistidine, as well as at much higher concentrations, showed no oxygen uptake. The presence of oxygen produced no shift in the titration curves of histidine in the presence of Cu^{++} or Ni^{++}. We conclude, therefore, that the Cu^{++} and Ni^{++} complexes of histidine do not react with molecular oxygen, irreversibly or reversibly. This statement with respect to cupric ion complexes seems to be a rather general truth (*22*).

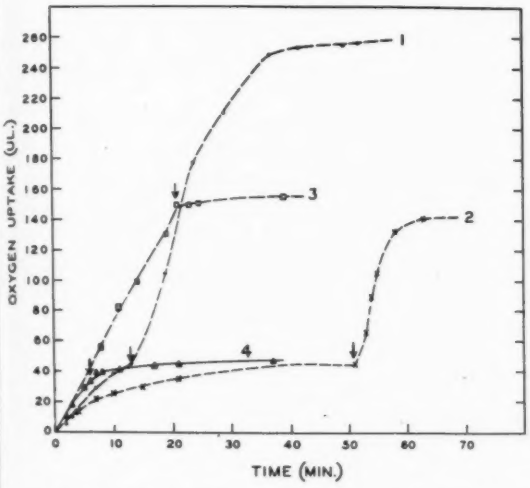

FIGURE 17.—Oxygen uptake of the histidine complexes of Fe^{++} and Cu^{+}. Curves 1 and 2, 80 μM histidine plus 40 and 20 μM Cu^{+}, respectively, pH=7.7, volume=1.5 ml. Curves 3 and 4, 240 μM histidine plus 40 μM Fe^{++}, volume=1.5 ml.; pH=6 in curve 3, pH=7.5 in curve 4.

The Cu^{+} complex of histidine, at a pH of about 7.0, took up oxygen rapidly. When the system was acidified, as in the cobaltodihistidine experiments, with the object of demonstrating reversible oxygen uptake, the rate was actually greatly increased, and the reaction complete a short time thereafter. This is shown in figure 17. The vessels which received strong HCl at a fairly early stage took up a total amount of oxygen roughly corresponding to the reaction, $H^{+}+Cu^{+}+\frac{1}{4}O_2=Cu^{++}+\frac{1}{2}H_2O$, but the observed value was invariably somewhat higher than $\frac{1}{4}O_2$. For example, in figure 17, curve 1, 11.5 μM of O_2 was utilized whereas 10μM correspond to the above reaction; in curve 2, in which the system was acidified about 40 minutes later, 6.3 μM of oxygen was utilized; the theoretical value was 5.0 μM. As illustrated by these two experiments, the discrepancy between the foregoing reaction and the actual finding seems to be greatest when oxidation has proceeded longest before acidification. When allowed to proceed, without acidification, for 3 to 4 hours, the oxygen uptake went as high as 21 μM of O_2 for 40 μM of Cu^{+}, or more than twice the oxygen equivalence for the formation of Cu^{++}. The oxidation continued at a low rate almost indefinitely. The pH of the system, Cu^{+}+histidine, rose upon oxygenation. This is consistent with the formation of Cu^{++} according to the reaction but opposite in direction to that expected if oxygenation of the complex had occurred. The rapid, accelerated oxidation in the presence of strong HCl is best explained as the oxidation of Cu^{+} to Cu^{++}, facilitated by complex formation with Cl^{-} (probably the formation of $CuCl_2^{-}$(*30*)). That the reaction at pH 7.0 is not simply the formation of Cu^{++} is indicated by the oxygen uptakes and by the visible changes occurring in the solution; the solution becomes dark-colored, resembling charred organic matter. The formation of the Cu^{++} complex alone should be indicated by the appearance of the typical, deep, clear blue. It seems most likely that the oxidation of histidine is being catalyzed by Cu^{+}; however, no further studies have been made. In any event the reaction is not a reversible oxygenation and in no way resembles the oxygenation reaction of cobaltodihistidine.

The Fe^{++} complex took up oxygen at a rate similar in magnitude to that of cobaltodihistidine. The uptake was not reversible; acidification stopped the reaction at once (fig. 17), but no oxygen could be recovered. If the reaction were allowed to proceed to completion, in 2 to 3 hours, 30 to 50 percent more oxygen was utilized than corresponds to the reaction

$$H^{+}+Fe^{++}+\tfrac{1}{4}O_2=Fe^{+++}+\tfrac{1}{2}H_2O.$$

On the glass electrode rather large pH shifts could be produced by oxygenating the system. The pH fell as in the case of cobaltodihistidine, but these changes were not reversible even at 0° C. Prolonged oxygenation led to some precipitation. So far as oxygen utilization is concerned, the Fe^{++} complex of histidine would seem to be another of the many examples (*31*) of autoxidizable Fe^{++} complexes. It has been shown that histidine cannot compete with OH^{-} for Fe^{+++}. It was expected that when Fe^{+++} was formed, the hydroxide would precipitate. The shift in pH upon oxygenation was at least in the same direction as in the case of cobaltodihistidine, but unsuccessful attempts were made manometrically and on the electrode to demonstrate a reversible phase by employing low temperatures and short reaction

times. It seems probable, however, that the production of H^+ when the Fe^{++}+histidine system is oxygenated may be explained by the reactions:

$$H^+ + Fe^{++} + \tfrac{1}{4}O_2 = Fe^{+++} + \tfrac{1}{2}H_2O$$
$$Fe^{+++} + 3OH^- = Fe(OH)_3 \text{ (ppt.)},$$

which give a net removal of $2OH^-$ per Fe^{+++} formed.

In summary, then, of the metals studied here those (Cu^+, Fe^{++}) whose histidine complexes showed any reaction with oxygen did so in an irreversible manner; the remaining ones (Cu^{++}, Ni^{++}) showed no oxygen reaction at all.

COMBINATIONS WITH CARBON MONOXIDE AND CYANIDE

The number of oxygen-carrying compounds is limited, and the classes of such compounds is of course still more limited. Of the best studied naturally occurring carriers, the situation regarding combination with carbon monoxide and cyanide may be said to be as follows: Reduced hemoglobin, which carries oxygen, has, as is well known, a rather high affinity for carbon monoxide, with which it combines reversibly and in the same proportion as with oxygen. Reduced hemoglobin does not combine with cyanide. On the other hand, methemoglobin combines with cyanide but with neither carbon monoxide nor oxygen. In hemocyanin the valence state of the copper atom is by no means clear (compare (*32*) with (*33*)); however, it is definitely established that this respiratory pigment does not combine with carbon monoxide but does combine with cyanide (*34*).[14]

It was of some interest to determine how the oxygen-carrying, and structurally rather simple cobaltodihistidine compared with the natural and more complicated carriers as regards carbon monoxide and cyanide interaction. A direct method for ascertaining, qualitatively, carbon monoxide interaction has already been mentioned though not specifically with reference to carbon monoxide; namely, the shift in pH of the equilibrium system histidine, cobalt, cobaltodihistidine. If carbon monoxide combines with cobaltodihistidine, reversibly or otherwise, this should be indicated by a shift in pH similar to that produced by oxygen. Were the combination reversible, the pH could be returned to the initial value by flushing the system with N_2. Conversely, if carbon monoxide does not combine with cobaltodihistidine, a shift in pH already established by oxygen should be reversed by carbon monoxide and no shift should be observed upon changing from carbon monoxide to N_2 and vice versa. These experiments were carried out.

Carbon monoxide was prepared by the action of warm (40°–50° C.) H_2SO_4 upon concentrated formic acid (90 percent). The gas was led through a flask of concentrated NaOH, then alkaline pyrogallol, and collected over water. A solution of histidine and cobalt was titrated with NaOH to the desired pH, under tank N_2, on the glass electrode. The gas inlet was shifted, as required, from carbon monoxide to 100 percent oxygen or N_2. The results are given in table 20. These data indicate that cobaltodihistidine does not combine with carbon monoxide and that carbon monoxide functions as an inert gas, such as N_2, in reversing the oxygenation of cobaltodihistidine. Manometric experiments were carried out which support this conclusion in all details. Reaction vessels were set up in the manner described previously for determining oxygen uptake. The vessels were first flushed with N_2 purified with pyrogallol, and the N_2 displaced completely with 100 percent carbon monoxide. Alkaline pyrogallol was placed in the center cups to remove traces of oxygen in the carbon monoxide. The vessels were equilibrated on the bath, and after the slight uptake due to the removal of traces of oxygen by the pyrogallol, the cobalt was tipped from the side arm into the histidine. No uptake was observed. These experiments were conducted at 24° C. at a total concentration of cobaltodihistidine of 2.4×10^{-2} mol.l^{-1}. When it was certain ($\sim$ 2 hrs.) that no uptake was forthcoming, the vessels were opened to the atmosphere and equilibrated with air. The typical amber color of oxy-bis(cobaltodihistidine) was almost immediately produced. The release of O_2 by acidification checked well with the theoretical figure. This last step was carried out for the following reason: An alkaline solution of $CoCl_2$ will take up carbon monoxide; although at the pH which $CoCl_2$ normally assumes in distilled H_2O ($\sim$ 4.5), no reaction occurs. However, in order to control this point, i. e., to ascer-

[14] If the methemocyanin is indeed the cupric form of the pigment, it would seem (*32*) that methemocyanin also combines with oxygen and in the same proportion as does hemocyanin.

tain that during the flushing of the reaction vessels with carbon monoxide the $CoCl_2$ in the side arm was not depleted and hence the failure to observe any carbon monoxide uptake, the vessels were exposed to air and the normal oxygenation was observed. The final conclusion that cobaltodihistidine did not combine with carbon monoxide is thus firmly established. Some discussion of this result is given elsewhere (*17*). It would be of great interest to have the results of carbon monoxide studies on the vast number of cobalt compounds not in aqueous solution studied by Calvin, Bailes, and Wilmarth (*35*), especially the class (their type II) which combines reversibly with oxygen in a ratio of one cobalt to one O_2.

TABLE 20.—*Effect of carbon monoxide on the pH of the cobalt-histidine system*

Gas phase	pH	Remarks
N_2	5.28	Colorless.
CO	5.28	Do.
N_2	5.28	Do.
Air	5.20	Amber.
100 percent O_2	5.11	Deep amber.
CO	5.28	Colorless.
N_2	5.28	Do.

144 μ M histidine, 36 μ M Co^{++}, vol. = 7.0 ml.

Study of possible cyanide interaction by methods involving pH shifts in the system is precluded by the difficulties introduced by the basicity of the CN^- ion. The problem was therefore approached in the following manner. If CN^-, in excess, be introduced into the equilibrium system "cobaltodihistidine, O_2, oxy-bis(cobaltodihistidine)" the ensuing possibilities are that CN^- competes with O_2 for cobaltodihistidine, that CN^- competes with histidine for Co^{++}, or that no interaction occurs. Both of the first two possibilities would be expected to entail the evolution of O_2 from the bound form, followed or accompanied (perhaps in the first case, surely in the second) by a subsequent, irreversible uptake of oxygen. The irreversible uptake in both cases would result from the fact that the cobalt atom would be in a co-ordination state such that autoxidation to the cobaltic form is easily accomplished.[15] Experiments designed on this reasoning were carried out. A solution of cobaltodihistidine thoroughly equilibrated with air was placed in the main room of the Warburg vessels and excess KCN in the side arm. In order to minimize the difficulties consequent upon the volatility of HCN, the required amount of solid KCN was weighed directly into the side arm. The vessels were equilibrated on the bath, and the KCN was rinsed into the solution by tipping. Controls were also run, in which strong HCl was tipped into oxygenated cobaltodihistidine, and KCN into $CoCl_2$ equivalent to the cobaltodihistidine in the other vessels. The results are shown in table 21.

The results of experiments 1 and 2 give the total recoverable (reversible) oxygen [16] and the oxygen uptake of Co^{++} in the presence of excess CN^-, respectively. The uptakes in experiment 3 are readily seen to be the difference between the output of the total releasable oxygen and the uptake of the $Co(CN)_6^{----}$ complex. These experiments support the conclusion that CN^- causes O_2 to be released from oxy-bis(cobaltodihistidine) by combining with Co^{++} to form a complex that is then irreversibly oxidized.

TABLE 21.—*Cyanide interaction with oxy-bis(cobaltodihistidine)*

Experiment No.	Co^{++}-histidine [1]	Co^{++} [2]	KCN [3]	HCl [4]	Oxygen uptake
	Milliliters	*Milliliters*	*Milligrams*	*Milliliters*	*Microliters*
1	1.5			0.4	+121
2		1.5	150		+150
3	1.5		150		+31

[1] 0.0118 M Cobaltodihistidine, pH = 8.0, equilibrated with air.
[2] 0.0118 M $CoCl_2$.
[3] 150 mg. solid KCN = 2.3×10^{-3} moles; tipped from side arm.
[4] 1.2 N HCl; tipped from side arm. T = 31° C. All results average of 3 runs.
Final pH in 2 and 3 was 11±.

OPTICAL PROPERTIES

The absorption spectra of cobaltodihistidine, oxy-bis(cobaltodihistidine), and the final irreversible complex have been obtained. The curves were obtained by means of a Beckman spectrophotometer. Solutions of cobaltodihistidine were prepared at pH values and concentrations such that the formation of the complex was essentially complete, and the concentrations of free Co^{++} and histidine were negligible. Some difficulty was encountered in preparing the solutions oxygen-free; the method finally used was to mix the components in an evacuated tube, and, a tube being

[15] Octahedrally coordinated cobaltous complexes are well-known (*24*) to be easily oxidized to the cobaltic state. One of the complexes in question, $Co(CN)_6^{----}$, is a good example. The cobaltous-histidine-cyanide complex would be such an example only if the complex were covalent.

[16] These experiments were conducted at 31° C. immediately after the oxygenation of the cobaltodihistidine. It is not anticipated therefore that any irreversible uptake had occurred.

chosen which would be received by the cuvette holder, to take the readings directly on the solution in the tube. Traces of O_2 produce a color change easily detected even visually; since the curves were reproducible, it is believed that the curve presented represents the spectrum of a pure solution of cobaltodihistidine.

Solutions containing appreciable concentrations of oxy-bis(cobaltodihistidine) are extremely dense optically. Suitable curves were obtained by equilibrating a solution of known concentrations of cobaltodihistidine with a low partial pressure of O_2. The fractional oxygenation may be computed from the equilibrium expression and the concentration of oxy-bis(cobaltodihistidine) and cobaltodihistidine calculated. From the absorption coefficient of cobaltodihistidine and the observed optical density at any wavelength, the absorption curve of the oxygenated complex may be calculated. The curve in figure 18 was obtained in this manner.

Three milliliters of 0.01333 M histidine and one milliliter of 0.02 M $CoCl_2$ were placed in separate compartments of a Thunberg tube, and the system was thoroughly evacuated. The outlet was closed, and the components were mixed. The histidine was previously neutralized so that the final pH after mixing was 7.9–8.0. The resulting solution was 0.005M with respect to cobaltodihistidine. The evacuated tube was placed in the cuvette holder and the absorption curve run against a water blank in an identical tube.

This solution was equilibrated in the same tube with commercial tank H_2 estimated to contain 0.25 percent O_2. At the observed temperature, 25° C., the fractional oxygenation was computed to be 0.105. From this value and the total concentration of cobaltodihistidine the concentration of oxy-bis(cobaltodihistidine) was calculated to be 0.261×10^{-3} mol.l^{-1}, the concentration of cobaltodihistidine 4.48×10^{-3} mol.l^{-1}. The diameter of the Thunberg tube was 1.28 cm. In calculating the data to a path length of 1.00 cm., the diameter of the tube was taken as the path length in the Thunberg tube. This introduces no error in the corrected curve of oxy-bis(cobaltodihistidine), but the absolute value of the extinction coefficients may be in error by approximately 7 percent. A solution of the irreversible complex was prepared by mixing equal volumes of preneutralized 0.4M histidine and 0.2 M $CoCl_2$ and shaking the solution for about 24 hours, in air at 40° C. The final solution, 0.1 M with respect to Co^{++}, was diluted to contain 0.005 M Co^{++} before taking the absorption spectrum. The final pH was 7.85.

The curve shown for Co^{++} was obtained on a 0.02 M solution of $CoCl_2$, and the results were computed to 0.005 M Co^{++} for comparison.

Figure 18 shows the spectral curves of Co^{++}, cobaltodihistidine, oxy-bis(cobaltodihistidine) and the irreversible complex. The cobalt curve shows a maximum at 510 mμ. Upon the formation of cobaltodihistidine the maximum is shifted to 486 mμ and enhanced about fourfold. Upon oxygenation, the absorption is greatly increased, especially at all wavelengths shorter than about 625 mμ; the oxygenated complex exhibits a rather broad maximum at 385 mμ. In the irreversible complex, the maximum is returned to the region of 490 mμ. In all cases, steadily increasing general absorption was observed at wavelengths shorter than shown here. The comparative absorptions are made clear by the extinction coefficients given in table 22.

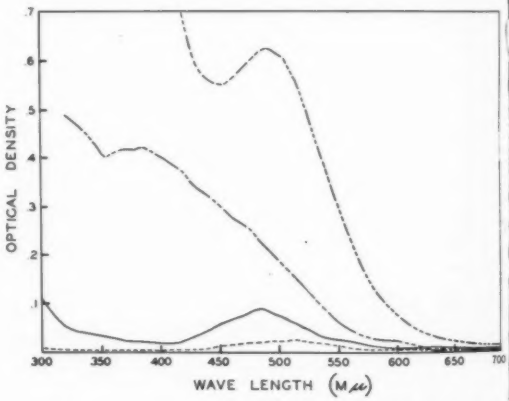

FIGURE 18.—The absorption spectra of Co^{++}, cobaltodihistidine, oxy-bis(cobaltodihistidine) and the irreversible complex. T=25° C.
– – – – $CoCl_2$ 0.005 M., l=1.00 cm.
——— Cobaltodihistidine 0.005M. l=1.00 cm. pH=7.9.
— · — · oxy-bis(cobaltodihistidine) 0.261 x 10^{-3} M. l=1.00 cm. pH=7.9.
— · · — · · Irreversible complex 0.005 M (cobalt). l=1.00 cm. pH~8.

TABLE 22.—*Molar extinction coefficients of cobalt compounds*

Compound	Maximum wavelength mμ	Coefficient l.mol^{-1} cm.$^{-1}$
$Co^{++}(Cl^-)_2$	510	5.1
Cobaltodihistidine	486	18.4
Oxy-bis(cobaltodihistidine)	385	1,620
Irreversible complex	490	[1] 125

[1] Based on moles of total cobalt, since the number of atoms of Co per mole of complex is not known definitely.

Even though, as is indicated in the next section, the cobalt is bonded ionically in cobaltodihistidine and covalently in the irreversible complex, the absorption maxima practically coincide. In certain instances (*36*), it was possible to correlate spectra and covalently bonded structures.

Suitable determinations were made of the optical rotation of cobaltodihistidine. The greater absorption of light in the case of the other complexes precludes accurate determinations in those cases.

A solution of 0.01M cobaltodihistidine was prepared anaerobically, as previously described, by mixing 9 ml. of 0.0266M histidine and 3 ml. of 0.04M $CoCl_2$. The solution was transferred under purified N_2 by means of a purified N_2-swept syringe to the rotation tube. Rotations were also obtained on L-histidine prepared by dissolving 2.00 gm. of histidine-hydrochloride monohydrate in H_2O, neutralizing to pH=8.0, and diluting to 50 ml. The final solution contained 2.95 gm./100 ml. of histidine (.02M).

Rotations were obtained, a Schmidt and Haensch double quartz-wedge polarimeter being used. In the initial experiment, the light source was lines selected from a G. E. H–3 mercury vapor lamp by the use of filters. This permitted readings over the range 420–660 mμ. More precise determinations were made using the monochrometer of the Beckman spectrophotometer as the light source. This arrangement gave a greater and more precise selection of wavelengths, but the intensity of the source was such that no readings could be obtained below 440 mμ.

The results are shown in figure 19 which gives the absorption spectra of Co^{++} and cobaltodihistidine and the specific rotation of histidine and cobaltodihistidine as a function of wavelength. Histidine exhibits a constant rotation throughout

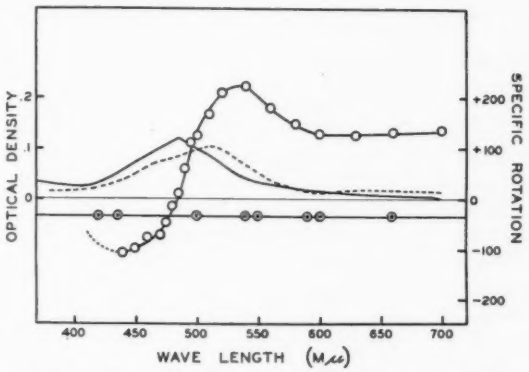

FIGURE 19.—The optical rotation of cobaltodihistidine:
——— Absorption spectrum of cobaltodihistidine 0.005 M, l=1.28 cm., pH=7.9
– – – Absorption spectrum of Co^{++} (chloride) 0.02 M, l=1.00
○——○ Specific rotation of cobaltodihistidine 0.01 M, pH=7.9, tube length=1 dm.
◉——◉ Specific rotation of L-histidine 0.02 M, pH=7.9, tube length=4.0 dm. T=25° C.

the visible region, the value of which is in good accord with values in the literature (*37*). The rotation of cobaltodihistidine, on the other hand, is a marked function of wavelength, increasing to a maximum at about 540 mμ, passing through zero at 484 mμ, essentially at the center of the absorption maximum. The data obtained below 440 mμ, using filters, indicate that a minimum occurs at about 440 mμ; this is indicated by the dotted portion of the curve. This relation between rotary dispersion and absorption spectrum (the Cotton effect) occurs when the electronic system responsible for the absorption band is also a major contributor to the optical activity.

Sufficiently numerous and accurate values were obtained on a very dilute solution of the irreversible complex, 0.002M with respect to Co^{++}, to indicate that the rotation of the complex behaves in a different manner from that of cobaltodihistidine. The values are shown in the following tabulation and are to be regarded as only approximate. The point is clear, however, that the dispersion is markedly different from cobaltodihistidine and that the rotation passes through zero twice, once in the neighborhood of the absorption maximum and once at 590 mμ.

Optical rotation of the irreversible oxygen complex

Specific rotation (degrees)	Wavelength ($m\mu$)
+516	420
−280	500
−320	550
±0.00	590
+169	600
+212	660

T°=28° C., l=1 dm., pH=7.9, C.=0.0738 gm./100 ml.=0.002 N cobalt. Wavelength selected from mercury lamp with filters.

MAGNETIC PROPERTIES

The theory of directed covalence (*24*) makes possible the assignation of configuration and state of co-ordination complexes from knowledge of the magnetic moments. Certain rather definite conclusions could be drawn from the stoichiometry of the reactions leading to the formation of cobaltodihistidine and oxy-bis(cobaltodihistidine) and from the fact that the oxygenated complex did not become autoxidized to the cobaltic state (*17*). From this information and from theory, a rather limited number of possibilities may be delineated. The number of choices arises largely from the fact that the complexes may be ionic or covalent. Also it would be of very great interest to compare the magnetic properties of the cobaltodihistidine-oxy-bis(cobaltodihistidine) system to the unusual properties (*38*) of the hemoglobin-oxyhemoglobin system. In view of the foregoing statements, it was desirable to have determinations of the magnetic susceptibility of the various cobalt complexes. We acquainted Dr. L. Michaelis, of the Rockefeller Institute for Medical Research, with our discovery of the reversible formation of oxy-bis(cobaltodihistidine) and the foregoing implications fully detailed in (*17*), and he kindly consented to carry out measurements jointly on materials which we prepared. Determinations of the magnetic susceptibility of cobaltodihistidine, oxy-bis(cobaltodihistidine) and the irreversible complex were carried out.

A solution of cobaltodihistidine was prepared from 0.4M histidine and 1.0 M $CoCl_2$. The histidine had been neutralized with equivalent NaOH. Ten milliliters of histidine and 2 milliliters of cobalt were placed in separate compartments of a Thunberg tube and, after thorough evacuation, mixed. The resulting solution was 0.1 M with respect to cobaltodihistidine and the pH 7.8. The tube was filled with N_2 which had been purified over hot Cu and pyrogallol. The top of the Thunberg tube was carefully removed and solution from the bottom of the tube was immediately transferred to the calibrated cylindrical glass tube in which the measurements were made. Oxy-bis(cobaltodihistidine) was prepared from the foregoing solution by aeration at ice-bath temperature. The resulting solution, which was 0.05 M with respect to oxy-bis(cobaltodihistidine), was transferred to the calibrated measuring tube which was completely filled with the solution and closed. The irreversible complex was prepared from equal volumes of 0.4 M histidine and 0.2 M $CoCl_2$ by shaking in air for 24 hours at 40° C. The measurements were made at 23° on the Gouy balance. The results under these conditions were as follows: cobaltodihistidine, 4.44 Bohr magnetons; oxy-bis(cobaltodihistidine), 0.139 Bohr magnetons; and the irreversible complex was diamagnetic. The diamagnetic solution of the irreversible complex was used as the reference material in applying the correction for diamagnetism to the susceptibility of the first two complexes. The moment of cobaltodihistidine is taken to indicate the presence of three unpaired electrons per molecule. We have concluded that the oxygenated complex is actually diamagnetic. It is possible that the small moment observed was due to incomplete oxygenation due to dissociation when the solution and tube came to the temperature of the balance. In any event, such a value may not be interpreted as any integral number of unpaired electrons. These results are fully interpreted in a previous paper (*17*). It is simply noted here that the cobalt-nitrogen bonds in cobaltodihistidine are essentially ionic, whereas those in the two oxygenated complexes are strictly covalent.

Dr. Michaelis has since repeated the measurements with slight modifications without significant change in result or conclusion (*14, 15, 16, 39*).

SUMMARY

Presented are the results of a study of the reactions involved in the formation of complexes of cobalt with histidine and cobaltodihistidine with molecular oxygen, and related reactions with other metals and amino compounds.

It was shown titrimetrically that histidine (ϕH) and Co^{++} combine to form the chelate compound, cobaltodihistidine, according to the reaction

$$2\phi H + Co^{++} \rightleftharpoons \phi_2Co + 2H^+.$$

From potentiometric data, the equilibrium constant of the reaction was determined at temperatures from 15° to 40° C. The value at 25° was 2.0×10^{-7}; the ΔH of the reaction was 19.1 k cal mol^{-1}.

The foregoing reaction was shown to consist of the component reactions

$$2\phi H \rightleftharpoons 2\phi + 2H^+$$
$$\phi^- + Co^{++} \rightleftharpoons \phi Co^+$$
$$\phi^- + \phi Co^+ \rightleftharpoons \phi_2Co.$$

At 25° the equilibrium constant for the formation of ϕCo^+ was found to be 1.98×10^7 l. mol^{-1} and that for the formation of ϕ_2Co from ϕCo^+ to be 2.12×10^4 l. mol^{-1}. The equilibrium constant for the over-all reaction

$$2\phi^- + Co^{++} \rightleftharpoons \phi_2Co$$

was 4.11×10^{11} l^2mol^{-2} and the ΔH was zero.

The complex cobaltodihistidine was shown to combine reversibly and covalently with molecular oxygen. From manometric data the reaction was established as

$$2\phi_2Co + O_2 \rightleftharpoons (\phi_2Co)_2O_2.$$

The equilibrium constant was 4.16×10^6 l^2mol^{-2} at 25°. From determinations of the equilibrium constant at temperatures from 14°–45°, the ΔH was shown to be -38.2 k cal mol^{-1}. From the equilibrium expression, curves for the oxygenation of cobaltodihistidine are presented and similarities and differences between the curves and analogous hemoglobin oxygenation curves discussed.

It was shown that the slow, irreversible oxygen uptake which occurs when cobaltodihistidine is exposed to oxygen does not involve the oxidation of the metal, Co^{++}, to the higher valence state, Co^{+++}. Various aspects of the irreversible reaction are discussed. CO_2 and hydroxyl ion may be produced in some instances.

The histidine complexes of Cu^{++}, Ni^{++}, Fe^{++}, and Cu^+ were studied with respect to their possible oxygen-carrying ability. The complexes of Cu^{++} and Ni^{++} did not react with O_2; those of Fe^{++} and Cu^+ were irreversibly oxidized.

Cobaltodihistidine did not take up carbon monoxide at 1 atmosphere. It was shown that the CN^- ion competes with histidine for Co^{++} and thereby converts the $\phi_2Co \rightleftharpoons (\phi_2Co)_2O_2$ system to $Co(CN)_6^{- - - -}$ and eventually to $Co(CN)_6^{- - -}$.

The complexes of Co^{++} and various histidine derivatives are compared with cobaltodihistidine with respect to reversible oxygenation and irreversible oxidation, and the results are discussed on the basis of the probable structures of the complexes.

The visible absorption spectra of Co^{++}, cobaltodihistidine, oxy-bis(cobaltodihistidine) and the final irreversible complex are presented and discussed. The optical rotation of cobaltodihistidine as a function of wavelength was investigated, and the occurrence of the Cotton effect was demonstrated.

The magnetic moments of cobaltodihistidine, oxy-bis(cobaltodihistidine) and the irreversible complex are presented. It was concluded that the nitrogen-cobalt bonds in cobaltodihistidine are essentially ionic, that those in oxy-bis(cobaltodihistidine) are essentially covalent, and that the cobalt in all three complexes is in the cobaltous state. This last-mentioned conclusion in regard to the irreversible complex is in complete accord with the chemical and manometric data discussed.

A large number of amino acids and ammonium hydroxide were shown to yield reversibly oxygenated, yellow-brown complexes with Co^{++} and O_2, and to undergo further oxidation to irreversible pink complexes just as histidine and various histidine derivatives do.

These studies form a basic for further understanding of the rare phenomenon of reversible oxygenation (as of hemoglobin and hemocyanin), of essential cobalt function in growth and hematopoiesis, and of respiratory inhibition of bacteria and tumors.

REFERENCES

(1) Hellerman, L., and Perkins, M. E.: Activation of enzymes. III. The role of metal ions in the activation of arginase. The hydrolysis of arginine induced by certain metal ions with urease. J. Biol. Chem. 112: 175–194 (1935).

(2) Lohmann, K., and Kossel, A. J.: The effect of zinc and other metals on carboxylase. Naturwissenschaften 27: 595–596 (1939).

(3) Punt, A.: The influence of temperature and electrolytes on muscle contracture provoked by acetylcholine. Arch. neerl. de physiol. 26: 212–221 (1942).

(4) Cori, G. T., Colowick, S. P., and Cori, C. F.: Enzymatic conversion of glucose-l-phosphoric ester to 6-ester in tissue extracts. J. Biol. Chem. 124: 543–555 (1938).

(5) Gill, P. M., and Lehmann, H.: Some factors influencing the formation of Robison ester from glycogen and inorganic phosphate in muscle extract. Biochem. J. 33: 1151–1170 (1939).

(6) Barron, A. G., and Barron, E. S. G.: Mechanism of cobalt polycythemia: effect of ascorbic acid. Proc. Soc. Exper. Biol. & Med. 35: 407–409 (1936).

(7) Dickens, F.: The toxic effects of oxygen on brain metabolism and on tissue enzymes. 1. Brain metabolism. Biochem. J. 40: 145–171 (1946).

(8) Marks, H. P.: Report Royal Naval Personnel Research Committee. Med. Research Council 101 (1944).

(9) Burk, D., Hesselbach, M. L., Fischer, C., Hearon, J., and Schade, A. L.: Interrelationships between biotin, carbon dioxide and heavy metals (Co, Cu) in tumor glycolysis, fermentation and dehydrogenation. Cancer Research 6: 497–498 (1946).

(10) Burk, D., duBuy, H., Fischer, C., Hearon, J., Hesselbach, M. L., James, W., Levy, H., Olson, B., Piggott, W. R., Schade, A. L., and Vinson, S.: Metabolic inhibitions of microorganisms and animal tissues and tumors by penicillin, penicillin impurity, streptomycin, and cobalt, and some applications to metabolic identification, assay, and mode of action. A report to the Antibiotics Study Section, National Institute of Health, May 2, 1947.

(11) Burk D., Schade, A. L., Hesselbach, M. L., and Fischer, C.: Cobalt inhibition of tissue respiration, glycolysis and growth. Fed. Proc. 5: 126–127 (1946).

(12) Hearon, J., Schade, A. L., Levy, H., and Burk, D.: Cobalt inhibition of tumor respiration and protection by histidine. Cancer Research 7: 713 (1947).

(13) Burk, D., Hearon, J., Caroline, L., and Schade, A. L.: Reversible complexes of cobalt, histidine, and oxygen gas. J. Biol. Chem. 165: 723–724 (1947).

(14) Burk, D., Hearon, J., Levy, H., and Schade, A. L.: Reversible oxygenation of cobaltodihistidine to oxy-bis(cobaltodihistidine) and comparison with other metal-amino acids, oxyhemoglobin and oxyhemocyanin. Fed. Proc. 6: 242 (1947).

(15) Hearon, J.: The tetrahedral configurations of cobaltodihistidine. Fed. Proc. 6: 259–260 (1947).

(16) Hearon, J.: The configuration of oxy-bis(cobaltodihistidine). Fed. Proc. 6: 260 (1947).

(17) Hearon, J. Z.: The configuration of cobaltodihistidine and oxy-bis(cobaltodihistidine). J. Nat. Cancer Inst. 9: 1–11 (1948).

(18) Cohn, E. J., and Edsall, J. T.: Proteins, amino acids and peptides as ions and dipolar ions. Reinhold, New York (1943).

(19) Nims, L. F., and Smith, P. K.: The ionization of *dl*-alanine from twenty to forty-five degrees. J. Biol. Chem. 101: 401–412 (1933).

(20) Greenstein, J. P.: Studies of the peptides of trivalent amino acids. III. The apparent dissociation constants, free energy changes, and heats of ionization of peptides involving arginine, histidine, lysine, tryosine, and aspartic and glutamic acids and the behavior of lysine peptides toward nitrous acid. J. Biol. Chem. 101: 603–621 (1933).

(21) Keefer, R. M.: Polarographic determination of cupric glycinate and cupric alaninate complex ions. J. Am. Chem. Soc. 68: 2329–2331 (1946).

(22) Calvin, M., and Wilson, K. W.: Stability of chelate compounds. J. Am. Chem. Soc. 67: 2003–2007 (1945).

(23) Michaelis, L.: Oxidation-reduction systems of biological significance; mechanism of catalytic effect of iron on oxidation of cysteine. J. Biol. Chem. 84: 777–787 (1929).

(24) Pauling, L.: The nature of the chemical bond. Cornell Univ. Press, Ithaca, N. Y., and Humphry Mifford, London, Oxford Univ. Press (1940).

(25) Hill, R.: Perspectives in biochemistry. Edited by J. Needham and D. E. Green. Cambridge Univ. Press (1939).

(26) Neill, J. M., and Hastings, A. B.: The influence of the tension of molecular oxygen upon certain oxidations of hemoglobin. J. Biol. Chem. 63: 479–492 (1925).

(27) Brooks, J.: The oxidation of haemoglobin to methaemoglobin by oxygen; II. The relation between the rate of oxidation and the partial pressure of oxygen. Proc. Roy. Soc., London, s. B 118: 560–577 (1935).

(28) Levy, M.: A note on the titration constants of imidazole derivatives. J. Biol. Chem. 109: 361–363 (1935).

(29) Gordy, W., and Stanford, S. C.: Spectroscopic evidence for hydrogen bonds: comparison of proton attracting properties of liquids. II. J. Chem. Phys. 8: 170–177 (1940).

(30) LATIMER, W. M., and HILDEBRAND, J. H.: Reference book of inorganic chemistry, p. 107. Macmillan Co., N. Y. (1940).

(31) SMYTHE, C. V.: The mechanism of iron catalysis in certain oxidations. J. Biol. Chem. 90: 251–265 (1931).

(32) CONANT, J. B., CHOW, B. F., and SCHOENBACH, E. B.: The oxidation of hemocyanin. J. Biol. Chem. 101: 463–473 (1933).

(33) RAWLINSON, W. A., JR.: The effects of oxidizing agents on hemocyanin. Australian J. Exper. Biol. & M. Sc. 19: 137–141 (1941).

(34) ———: Crystalline hemocyanin: Some physical and chemical constants. Australian J. Exper. Biol. & M. Sc. 18: 131–140 (1940).

(35) CALVIN, J., BAILES, R. H., and WILMARTH, W. K.: The oxygen carrying synthetic chelate compounds I. J. Am. Chem. Soc. 68: 2254–2256 (1946).

(36) PAULING, L., and CORYELL, C. D.: The magnetic properties of the hemochromogens and related substances. Proc. Nat. Acad. Sc. 22: 159–163 (1936).

(37) SCHMIDT, C. L. A., editor: The chemistry of the amino acids and proteins, p. 581. Charles C. Thomas, Springfield, Ill. (1938).

(38) PAULING, L., and CORYELL, C. D.: The magnetic properties and structure of hemoglobin, oxyhemoglobin and carbomonoxyhemoglobin. Proc. Nat. Acad. Sc. 22: 210–216 (1936).

(39) MICHAELIS, L.: The magnetic properties of the cobalto-histidine complex before and after oxygenation. Arch. Biochem. 14: 17–21 (1947).

APPENDIX I

THE EXPRESSION K_2

It is proposed to develop here the exact expression for K_2 and to show that by ignoring certain negligible terms the expression that has been employed in calculating K_2 is obtained. The notation, except for constants defined herein is that used in the text.

Consider the reactions:

$$\phi H_2^+ \rightleftharpoons \phi H + H^+, \qquad K_i = \frac{[H^+][\phi H]}{[\phi H^+]};$$

$$\phi H \rightleftharpoons \phi^- + H^+, \qquad K_a = \frac{[H^+][\phi^-]}{[\phi H]};$$

$$\phi_2^- + Co^{++} \rightleftharpoons \phi_2 Co, \qquad K_2 = \frac{[H^+]^2[\phi_2 Co]}{[\phi H]^2[Co^{++}]}.$$

The relation sought is that for K_2. There are six species involved, viz, ϕH_2^+, ϕH, ϕ^-, Co^{++}, $\phi_2 Co$, and H^+. We may consider $[H^+]$ known. In order that the system be determinant, five relations among the remaining species are required. These are: K_i, K_a, the material balance (1) and (2)

$$b = [Co^{++}] + [\phi_2 Co] \tag{1}$$

$$c = [\phi H_2^+] + [\phi H] + [\phi^-] + 2[\phi_2 Co] \tag{2}$$

and the set (3) definining electroneutrality,

$$\left.\begin{aligned} &[Na^+] + [H^+] + 2[Co^{++}] + [\phi H_2^+] = \\ &[\phi^-] + [OH^-] + [Cl^-] \\ &[Na^+] = t + c \\ &[Cl^-] = 2b + c \\ &K_w = [H^+][OH^-]. \end{aligned}\right\} \tag{3}$$

Combining the relations in (3), solving for $[Co^{++}]$, and eliminating $[\phi H_2^+]$ we obtain

$$[Co^{++}] = (b - t/2) + \frac{[\phi^-]}{2}\left\{1 - \frac{[H^+]^2}{\overline{K}}\right\} + \frac{1}{2}\left\{\frac{K_w}{[H^+]} - [H^+]\right\} \tag{4}$$

where $\overline{K} = K_i \cdot K_a$. Equation (4) gives $[Co^{++}]$ if $[\phi^-]$ is determined. From (1) and (2), after eliminating $[\phi H_2^+]$ and $[\phi H]$ we see that

$$c - 2b = [\phi^-]\left\{\frac{[H^+]^2}{\overline{K}} + \frac{[H^+]}{K_a} + 1\right\} - 2[Co^{++}]. \tag{5}$$

Equations (4) and (5) solved for $[\phi^-]$ give

$$[\phi^-] = \frac{\left\{(c - t) + \frac{K_w}{[H^+]} - [H^+]\right\}\frac{K_a}{[H^+]}}{\left(\frac{2[H^+]}{K_i} + 1\right)}. \tag{6}$$

It follows directly from (6) and K_a that

$$[\phi H] = \frac{\left\{(c - t) + \frac{K_w}{[H^+]} - [H^+]\right\}}{\left(\frac{2[H^+]}{K_i} + 1\right)}. \tag{7}$$

From a rearrangement of (2)

$$[\phi_2 Co] = \frac{1}{2}(c - [\phi H_2^+] - [\phi H] - [\phi^-])$$

Eliminating $[\phi H_2^+]$ through $\overline{K}$ and introducing $[\phi H]$ from (7)

$$[\phi_2\mathrm{Co}]=\frac{1}{2}\left[c-\frac{(c-t)+\frac{K_w}{[H^+]}-[H^+]}{\left(\frac{2[H^+]}{K_a}+1\right)}-[\phi^-]\left\{\frac{[H^+]^2}{\overline{K}}+1\right\}\right]. \quad (8)$$

$$[Co^{++}]=(b-t/2)+\frac{1}{2}\left\{[\phi^-]\left(1-\frac{[H^+]^2}{\overline{K}}\right)+\frac{K_w}{[H^+]}-[H^+]\right\} \quad (4')$$

Equations 4, 7, and 8 with 6 give the required concentration terms for determining K_2 if $[H^+]$ be known. Writing these as

$$[\phi H]=\frac{(c-t)}{\frac{2[H^+]}{K_1}+1}+\left\{\frac{\frac{K_w}{[H^+]}-[H^+]}{\frac{2[H^+]}{K_1}+1}\right\} \quad (7')$$

$$[\phi_2\mathrm{Co}]=\frac{t}{2\left(\frac{2[H^+]}{K_1}+1\right)}+\left\{\frac{c}{2}-\frac{c}{2\left(\frac{2[H^+]}{K_1}+1\right)}-\frac{\frac{K_w}{[H^+]}-[H^+]}{2\left(\frac{2[H^+]}{K_1}+1\right)}-\frac{[\phi^-]}{2}\left(\frac{[H^+]^2}{\overline{K}}+1\right)\right\}, \quad (8')$$

it may be shown that the terms in braces are negligible under the conditions employed. At the isoelectric pH, $[H^+]^2/\overline{K}=1$, and $2[H^+]^2/K_1+1\sim 1$. These conditions reduce the right-hand members of the equations to $(b-t/2)$, $(c-t)$, and $t/2$, respectively, provided the terms $K_w/[H^+]-[H^+]$ and $[\phi^-]$ may be neglected. At the isoelectric point of histidine the term $K_w/[H^+]-[H^+]$ varies from $\sim 6 \times 10^{-7}$ at 15° C. to $\sim 1 \times 10^{-7}$ at 40° C. The term $[\phi^-]$ from (6), is $\sim 10^{-6}$ when $(c-t)$ is $\sim 10^{-4}$. In general $(c-t)$ fell in the range $10^{-4}-10^{-5}$. Thus (4′), (7′) and (8′) become $[Co^{++}]=(b-t/2)$, $[\phi H]=(c-t)$ and $[\phi_2\mathrm{Co}]=t/2$, which were the relations to be derived. The validity of these approximations depends in an obvious manner upon the assumption that $pH\sim pH_I$. It is also to be noted that when, as is usually true, histidine is present in excess of Co^{++}, since the value of $t/2\geqq b$, the magnitude of $(c-t)$ may become so great as to make $[\phi^-]$ significant at any pH. Thus the use of the approximation formula also depends on histidine and Co^{++} being initially present in a ratio not markedly different from 2/1. Since the order of the reaction, i. e., the stoichiometry, has been independently ascertained, and the formulation used was employed merely to determine the numerical magnitude of K_2, the limitation is not serious.

APPENDIX II

The Relative Propagated Error in K_2 as a Function of β

While it is certainly obvious that the relative uncertainty in any equilibrium constant is large when the reaction is virtually complete, and also when practically no reaction has occurred, the region of minimum error is not always an obvious choice, nor is the manner of increase in error clear without a detailed analysis. It is shown here that the region of minimum error in K_2 lies in the region $\beta\sim 0.37$, and the increase in the error is shown from a graphical examination of the function here derived.

As in the text (p. 342), let

$$K_2=[H^+]^2\frac{[z]}{[c-2z]^2[b-z]}.$$

Then $\ln K_2=\ln z-2\ln(c-2z)-\ln(b-z)-\frac{2}{2.3}\,\mathrm{pH}$.

For small errors, neglecting errors in pH, the relative error in K_2 is given by

$$\frac{dK_2}{K_2}=\frac{dz}{z}+\frac{4dz}{c-2z}+\frac{dz}{b-z}. \quad (1)$$

It is evident here that $\frac{dz}{z}$ is the relative error in the titration, t. We define, as before, β as z/b and make the simplifying assumption that $c=2b$. This assumption is clearly not necessary but is introduced for simplicity; although it makes the treatment less general, it closely approximates actual conditions experimentally employed. Equation 1 becomes

$$\frac{dK_2}{K_2}=\frac{dz}{b}\left\{\frac{1}{\beta}+\frac{3}{1-\beta}\right\}. \quad (2)$$

From equation 2 we learn that $\frac{dK_2}{K_2}$ is a minimum when

$$3\beta^2-(1-\beta)^2=0, \text{ or } \beta=\frac{\sqrt{12}-2}{4}\sim 0.37.$$

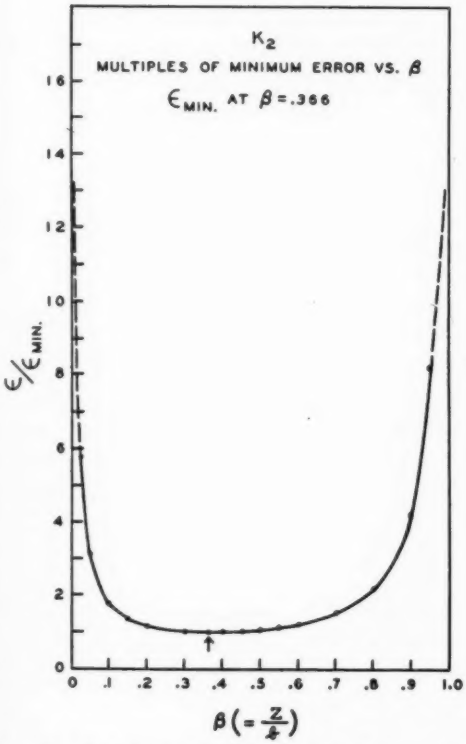

Figure 20.—Relative propagated error in K_2 as a function of β.

This result is quite independent of the value of $\frac{dz}{b}$. From equation 2 we may now plot $\frac{dK_2}{K_2}$ vs. β and determine the behavior in every region. In order that the results again be independent of $\frac{dz}{b}$, the values of $\frac{dK_2}{K_2}$ are plotted as multiples of the minimum value. Figure 20 shows the results. It is evident that for $0.18 \leqq \beta \leqq 0.60$, the error is less than 1.2 times the minimum.

While discussing the subject of error, we show here, in an entirely analogous manner, that the region of minimum error in K_{O_2} lies in the region $r \sim 0.42$.

The value of K_{O_2} is given by

$$K_{O_2} = \frac{x}{(a-2x)^2 P_{O_2}\alpha'}$$

whence

$$\frac{dK_{O_2}}{K_{O_2}} = \frac{dx}{x} + \frac{4dx}{a-2x} - \frac{d(P_{O_2}\alpha')}{P_{O_2}\alpha'}. \qquad (3)$$

Here $\frac{dx}{x}$ is the relative error in the observed oxygen uptake. Neglecting the uncertainty in $P_{O_2}\alpha'$ and defining r as $\frac{2x}{a}$, (3) becomes

$$\frac{dK_{O_2}}{K_{O_2}} = \frac{2dx}{a}\left\{\frac{1}{r} + \frac{2}{1-r}\right\}. \qquad (4)$$

From (4) it is seen that $\frac{dK_{O_2}}{K_{O_2}}$ is a minimum when $r = \sqrt{2} - 1 \sim 0.42$.

The plot of $\frac{dK_{O_2}}{K_{O_2}}$ as multiples of the minimum is given in figure 21. When $0.21 \leqq r \leqq 0.66$, the error is less than 1.2 times the minimum. Note that in both cases (K_2 and K_{O_2}) the error increases faster

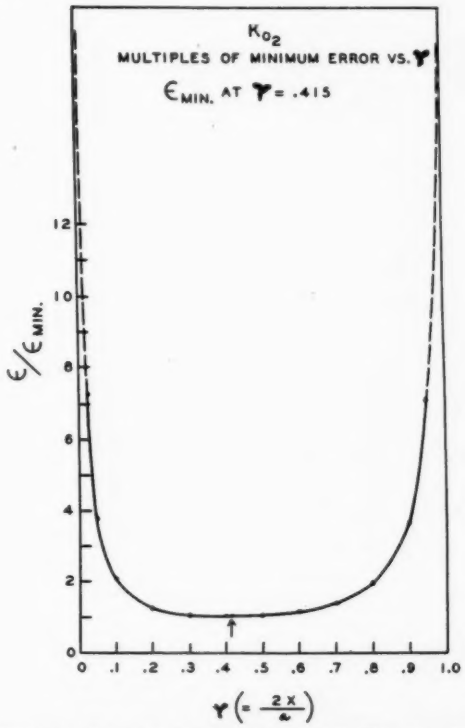

FIGURE 21.—Relative propogated error in K_O as a function of r.

on the lower side of the minimum, i. e., r, or β may be decreased below the minimum value with less error than it may be raised above the minimum value. The curve will be symmetrical about the minimum only for a reaction first order with respect to two components when the minimum occurs at 50-percent completion.

APPENDIX III

Derivation of Relations Used in Computing K_3

As in the text, the reactions are:

$$\phi H_2^+ \rightleftharpoons \phi H + H^+$$

$$\phi H \rightleftharpoons \phi^- + H^+$$

$$\phi^- + Co^{++} \rightleftharpoons \phi Co^+$$

$$\phi^- + \phi Co^+ \rightleftharpoons \phi_2 Co.$$

The corresponding equilibrium constants are:

$$K_1 = \frac{[H^+][\phi H]}{[\phi H_2^+]},\ K_a = \frac{[H^+][\phi^-]}{[\phi H]},\ K_3 = \frac{[\phi Co^+]}{[\phi^-][Co^{++}]},$$

$$K_4 = \frac{[\phi_2 Co]}{[\phi^-][\phi Co^+]},$$

and for use below:

$$\overline{K} = K_1 K_a = \frac{[H^+]^2[\phi^-]}{[\phi H_2^+]},\ K_{\phi^-} = K_3 K_4 = \frac{[\phi_2 Co]}{[\phi^-]^2[Co^{++}]}.$$

Of the species present in the system the concentrations of H^+, Na^+, Cl^-, and OH^- are known; those of ϕH_2^+, ϕH, ϕ^-, ϕCo^+, $\phi_2 Co$, and Co^{++} must be computed. The necessary relations are furnished by K_1, K_a, and K_{ϕ^-}, and the material balance equations 1, 2, and the condition of electroneutrality 3,

$$b = [Co^{++}] + [\phi Co^+] + [\phi_2 Co] \quad (1)$$

$$c = [\phi H_2^+] + [\phi H] + [\phi^-] + [\phi Co^+] + 2[\phi_2 Co] \quad (2)$$

$$\left.\begin{aligned} &[Na^+] + [H^+] + 2[Co^{++}] + [\phi H_2^+] + [\phi Co^+] = \\ &[\phi^-] + [OH^-] + [Cl^-] \qquad [Na^+] = t \\ &[Cl^-] = 2b + c \qquad K_w = [H^+][OH^-]. \end{aligned}\right\} \quad (3)$$

Combining the separate relations of (3), and solving for $2[Co^{++}]$ gives, after eliminating $[\phi H_2^+]$ through $\overline{K}$,

$$2[Co^{++}] = [\phi^-]\left\{1 + \frac{[H^+]^2}{\overline{K}}\right\} + \frac{K_w}{[H^+]} - [H^+] - [\phi Co^+] + (2b + c - t). \quad (4)$$

From (1) and (2), after eliminating $[\phi H_2^+]$ and $[\phi H]$ through $\overline{K}$ and K_a respectively, is obtained

$$2[Co^{++}] = [\phi^-]\left\{\frac{[H^+]^2}{\overline{K}} + \frac{[H^+]}{K_a} + 1\right\} - [\phi Co^+] - (c - 2b). \quad (5)$$

By subtracting (5) from (4) and solving for $[\phi^-]$ we see that

$$[\phi^-] = \frac{(2c - t) + \frac{K_w}{[H^+]} - [H^+]}{\frac{2[H^+]^2}{\overline{K}} + \frac{[H^+]}{K_a}}. \quad (6)$$

From (1) and K_{ϕ^-}

$$b = [Co^{++}] + [\phi Co^+] + K_{\phi^-}[\phi^-]^2 =$$

$$[Co^{++}]\{1 + K_{\phi^-}[\phi^-]^2\} + [\phi Co^+]. \quad (7)$$

Equations 5 and 7 may be solved for $[Co^{++}]$ and $[\phi Co^+]$. The solution for $[Co^{++}]$ is

$$[Co^{++}] = \frac{(c - b) - [\phi^-]\left\{\frac{[H^+]^2}{\overline{K}} + \frac{[H^+]}{K_a} + 1\right\}}{K_{\phi^-}[\phi^-]^2 - 1},\ K_{\phi^-}[\phi^-]^2 \neq 1 \quad (8)$$

Since $[\phi^-]$ and $[Co^{++}]$ may be determined from (6) and (8), $[\phi Co^+]$ is given from (7) by

$$[\phi Co^+] = b - [Co^{++}]\{1 + K_{\phi^-}[\phi^-]^2\}. \quad (7a)$$

Equations 6, 8, and 7a give the required concentration terms for calculating K_3. It is clear that the remaining species may at once be determined, if desired, from the proper equilibrium constant since both $[\phi^-]$ and $[Co^{++}]$ have been determined, viz, $[\phi_2 Co]$ is obtained from K_{ϕ^-}, $[\phi H_2^+]$ from $\overline{K}$, and $[\phi H]$ from K_a.

It is of some interest to examine equation 8 in detail. Experimentally the arrangement may be such that $(c - b)$ is positive, negative, or zero. We may inquire as to the sign of $[Co^{++}]$ under these various conditions, since from physical considera-

tions it is inherently positive. This point is best handled by substituting for the second term in the denominator of (8) the equivalent expression $c-[\phi Co^+]-2[\phi_2Co]$ obtained from (2). The right-hand member of equation 8 then becomes

$$\frac{[\phi Co^+]+2[\phi_2Co]-b}{K_{\phi^-}[\phi^-]^2-1}.$$

Substituting for b its value from (1) there results

$$\frac{[\phi Co^+]+2[\phi_2Co]-[Co^{++}]-[\phi Co^+]-[\phi_2Co]}{K_{\phi^-}[\phi^-]^2-1}=$$

$$\frac{[\phi_2Co]-[Co^{++}]}{K_{\phi^-}[\phi^-]^2-1}.$$

Finally, by substituting for $K_{\phi^-}[\phi^-]^2$ the expression $\frac{[\phi_2Co]}{[Co^{++}]}$, the right-hand member of equation 8 may be written as

$$\frac{[\phi_2Co]-[Co^{++}]}{\frac{[\phi_2Co]}{[Co^{++}]}-1}. \qquad (8a)$$

When $[\phi_2Co]>[Co^{++}]$, the expression is positive. When $[\phi_2Co]<[Co^{++}]$, the numerator is negative but at the same time $\frac{[\phi_2Co]}{[Co^{++}]}>1$ and the entire expression is positive. Thus the numerator and denominator must change signs at the same point, and $[Co^{++}]$ is always positive. It is clear, however, that at the point at which the signs of numerator and denominator change, the expression is indeterminate. The question of the location of the indeterminate point, if it occurs, may be discussed as three cases.

When $c<b$ the numerator of equation 8 is negative under all conditions. It is seen from equation 8a that the denominator is also negative. The indeterminate point does not occur.

When $c=b$ the numerator of equation 8 is negative provided $[\phi^-]\neq 0$. The denominator is also negative, from equation 8a, until all of the histidine is completely bound as ϕ_2Co; then $\left[\frac{\phi_2Co}{Co^{++}}\right]=1$ and $[\phi^-]=0$. This may be seen by considering that (equations 1 and 2) $[\phi_2Co]\leqq c/2$ and $[Co^{++}]\geqq b-c/2$. In this case, the expression does not "pass through" the indeterminate point, for the conditions for the occurrence of the point are such that no further shift in equilibrium may take place.

When $c>b$ the expression must pass through the indeterminate point when $[\phi_2Co]=[Co^{++}]$ and this will occur when $[\phi^-]$ has the fixed value $K_{\phi^-}^{-\frac{1}{2}}$.